



Université
de Toulouse

THÈSE

En vue de l'obtention du

DOCTORAT DE L'UNIVERSITÉ DE TOULOUSE

Délivré par :

Institut Supérieur de l'Aéronautique et de l'Espace (ISAE)

Présentée et soutenue par :

Francesco FICHERA

le vendredi 11 octobre 2013

Titre :

Techniques Lyapunov pour une classe de systèmes hybrides et synthèses de
contrôleurs à réinitialisation

Lyapunov techniques for a class of hybrid systems and reset controller
syntheses for continuous-time plants

École doctorale et discipline ou spécialité :

EDSYS : Automatique et Robotique

Unité de recherche :

LAAS

Directeur(s) de Thèse :

Mme Sophie TARBOURIECH (directrice de thèse)

M. Christophe PRIEUR (co-directeur de thèse)

Jury :

M. Claudio DE PERSIS - Rapporteur

M. Marc JUNGERS - Rapporteur

M. Jean-Marc BIANNIC - Examineur

M. Lorenzo MARCONI - Examineur

M. Ricardo SANFELICE - Examineur

M. Luca ZACCARIAN - Examineur

This page was intentionally left blank

Lyapunov techniques for a class of
hybrid systems and reset controller
syntheses for continuous-time plants.

Francesco FICHERA

Contents

List of Symbols	iii
Introduction	1
1 Preliminary concepts of the hybrid systems framework	5
1.1 Some preliminary definitions	5
1.2 The modeling framework	6
1.3 Hybrid time domain, solutions and their basic properties	6
1.4 Asymptotic and Exponential Stability	8
1.5 Dwell-time logic	9
1.6 t -decay rate	10
1.7 t - \mathcal{L}_2 norm and t - \mathcal{L}_2 stability	10
2 Analysis for a class of hybrid systems	13
2.1 Introduction	13
2.2 A homogeneous class of hybrid systems	13
2.2.1 Relaxed jump region and its ϵ -inflated set	16
2.3 \mathcal{L}_2 stability	19
2.3.1 LMI-based statement	25
3 Hybrid controller architectures	27
3.1 Introduction	27
3.2 Overview	28
3.3 Resets from the plant state	30
3.3.1 First controller architecture	31
3.3.2 Second controller architecture	33
3.4 Comments and remarks	38
3.5 Simulations	39
3.5.1 A double integrator	39
3.5.2 A servo motor	41
3.5.3 A DC motor	44
4 Hybrid controller architectures with plant state estimation	47
4.1 Introduction	47
4.2 Overview	48
4.3 Hybrid output feedback with dwell-time logic	50
4.3.1 Problem statement	50
4.3.2 First controller architecture	52
4.3.3 Second controller architecture	57
4.3.4 Comments and remarks	60
4.3.5 Simulations	62
4.4 Hybrid output feedback without dwell-time logic	66
4.4.1 Problem statement	66
4.4.2 Practical asymptotic stability	69

4.4.3	Simulations	74
4.5	Comparisons	75
5	Multi-objective hybrid controller synthesis	77
5.1	Introduction	77
5.2	Convex hybrid controller synthesis	79
5.2.1	Overview and synthesis problem	79
5.2.2	Multi-objective convex synthesis	80
5.3	Comments on the convex hybrid output feedback synthesis	86
5.4	Simulations	87
5.4.1	A DC motor	88
5.4.2	The F-8 aircraft	92
	Conclusion	97
	Appendix A	99
	Appendix B	101
	Appendix C	103

List of Symbols

\dot{x}	the derivative, with respect to time, of the state of a hybrid system
x^+	the state of a hybrid system after a jump
x^\top	denotes the transpose of x
$x^{+\top}$	denotes the transpose of x^+
(x, y)	equivalent notation for the vector $[x^\top \ y^\top]^\top$
M^{-1}	the inverse of the squared matrix M
$M^{-\top}$	the transpose of M^{-1}
\mathbb{R}	denotes the set of real numbers
\mathbb{R}^n	denotes the n -dimensional Euclidean space
$\mathbb{R}_{\geq n}$	denotes the set of real numbers greater than or equal to $n \in \mathbb{R}$
\mathbb{Z}	denotes the set of integer numbers
$\mathbb{Z}_{\geq n}$	denotes the set of integer numbers greater than or equal to $n \in \mathbb{Z}$
$M \in \mathbb{R}^{m \times n}$	real matrix with m rows and n columns, $m, n \in \mathbb{Z}_{\geq 1}$
I	the identity matrix of appropriate dimensions
$\partial \mathcal{A}$	denotes the boundary of set \mathcal{A}
$\bar{\mathcal{A}}$	the closure of set \mathcal{A}
$\text{int}(\mathcal{A})$	denotes the interior of set \mathcal{A} (see Definition 1.2)
$\mathcal{A} \equiv \mathcal{B}$	denotes the fact that $x \in \mathcal{A}$ implies $x \in \mathcal{B}$ and vice versa
$\mathcal{A} \setminus \mathcal{B}$	denotes the set of points in \mathcal{A} that are not in \mathcal{B}
$\mathcal{A} \subset \mathcal{B}$	denotes the fact that $x \in \mathcal{A}$ implies $x \in \mathcal{B}$
$\bar{\partial} W(x)$	denotes the generalized gradient in the Clarke sense of a function $x \mapsto W(x)$ at x
$\text{dom}(\xi)$	denotes the hybrid time domain of ξ (see Definition 1.5)
$\text{dz}(s)$	the unitary deadzone of $s \in \mathbb{R}$ (see Definition 1.4)
\emptyset	denotes the empty set
$\text{He}(M)$	$M + M^\top$
\mathcal{K}_∞	the class of functions from $\mathbb{R}_{\geq 0}$ to $\mathbb{R}_{\geq 0}$ that are continuous, zero at zero, strictly increasing and unbounded (see Definition 1.1)
$\lambda_{\max}(M)$	the maximum eigenvalue of matrix M

$\lambda_{min}(M)$	the minimum eigenvalue of matrix M
$ x $	the Euclidean norm of a vector $x \in \mathbb{R}^n$
$ x _{\mathcal{A}}$	the minimum distance of vector $x \in \mathbb{R}^n$ to a compact set \mathcal{A} (see Definition 1.3)
$\ w[t_i, t_j]\ _2$	denotes $\left(\int_{t_i}^{t_j} w(s, i) ^2 ds\right)^{\frac{1}{2}}$
$\text{sgn}(s)$	the sign function of $s \in \mathbb{R}$
$f: \mathbb{R}^m \rightarrow \mathbb{R}^n$	denotes a function from \mathbb{R}^m to \mathbb{R}^n
FORE	First Order Reset Element
GAS	Globally Asymptotically Stable
GES	Globally Exponentially Stable
LMI	Linear Matrix Inequality
LTI	Linear Time-Invariant

Introduction

Technological development and always more sophisticated applications continue to demand numerical tools and control techniques to design and validate controllers able to guarantee the desired specifications. In the attempt to satisfy these challenging exigences, research tries to provide solutions to overcome the limits of the classical theory. The introduction of the hybrid systems framework sheds light on new frontiers of control theory and offers promising results useful for all sort of applications [39, 40].

It is from the 1940's that research is aware of intrinsic limitations of classical control. Already [9] gave some hints on integral constraints on sensitivity functions applied to electrical networks. However, not much interest has been showed in these questions, at first. Lately, such an interest has been renewed (see [2, 34, 36, 37, 60]). In particular, [2] analyses control properties of minimum and non-minimum phase systems and provides some guidelines to preliminary assess the feasibility of a design problem by means of a continuous-time (linear and nonlinear) control. [60] emphasizes fundamental constraints on achievable performance in linear control loops and characterizes the overshoot in non-minimum phase systems. Note that control limitations might go beyond the best possible trade-off of specifications. In [12, 25, 76], systems for which there is no smooth feedback are deeply investigated. For a clear survey on the usefulness of investigating fundamental limitations the reader is referred to [81].

In parallel with limitations in control, also limitations in modeling represent an important issue to consider in many applications. For instance, satellite applications cannot validate a control on-board before the launch, therefore a massive amount of simulations for design and (mostly) validation and certification needs to be accomplished, requiring very precise models to reduce the risks. Moreover, in certain domains of control, the usual dynamical representations do not provide enough flexibility for analysis and synthesis purposes. For instance, in some applications with impulsive problems, only dynamic model with differential inclusions provide good precision accounting also for robustness (see [80]).

In the attempt to solve some of the issues listed above, research proposes several control schemes (see for instance [47, 55, 56, 85, 86] and references therein). In [23, Section 7.1], for instance, an example is shown where the impulsive control reaches the global optimum whereas any control as a function of time cannot attain it. Also switching systems try to solve both modeling issues and trade-off limitations [51]. In [66, 82], the plant to control is modeled with a switching system to account for failures or output quantizations. On the other hand, [48, 68] propose multiple controllers for the same plant which are suitably switched to meet all the design specifications.

The hybrid systems framework [39, 40] unifies all these branches of control research and enlarges the frontiers of modeling and control. Combining both continuous and discrete dynamics, hybrid systems are able to model with better precision mechanical systems where impacts are involved or electronic devices where switches repeatedly occur or with logical modes. Moreover the hybrid controller architecture offers insights which only recently started to be investigated. For instance, a hybrid control can guarantee robust stability in nonlinear systems not stabilizable by smooth feedback [46, 69], overcome some intrinsic limitations of linear control systems whenever a trade-off between the specifications has to be found [7] and establish global results where only local ones

can be achieved with a smooth control law.

In the recent years, particular attention has been devoted to the study of optimal hybrid controllers for continuous-time plants with the intent of achieving better trade-offs of performance. The desirable closed-loop behavior may be induced by resetting the controller state according to an optimal reset law [68]. Only a few hybrid controller architectures have been proposed. The main one is the FORE controller, on which several performance studies have been conducted [63, 65, 87, 88]. In [70], a new architecture has been proposed where the resets are triggered by suitable Lyapunov-like conditions and in [71], an optimal convex synthesis to maximize the decay-rate for such new architecture has been proposed. Furthermore in [72], also an optimal synthesis for the overshoot reduction is presented.

Although hybrid systems represent a breakthrough in the domain of control theory, the growth of complexity in the dynamics requires new mathematical tools and methods for the analysis and the design problem. Lyapunov theory comes in handy to describe the trajectories of hybrid systems without analytically calculating the actual solutions [58]. This allows to establish useful results on \mathcal{L}_p stability [65], equivalence between robust stability and existence of a smooth Lyapunov function [15, 16] and, for certain classes of hybrid controllers, leads to LMI formulations both for analysis and synthesis.

In this context, our work aims at developing systematic techniques for the design of a hybrid controller for a continuous-time plant. The hybrid controller architecture represents the first issue because each architecture presents its own characteristics and degrees of freedom, therefore optimal design techniques are specific for a particular type of hybrid controller. Moreover, to be able to state performance in a classical sense and allow comparison with classical solutions, the hybrid controller has to satisfy certain conditions, to avoid behavior which are unknown in the continuous-time domain and to avoid inaccurate performance estimations. The final objective is to investigate hybrid controller architectures whose analysis and synthesis, in eventual presence of input saturation, can be held through LMI conditions solvable with SDP tools [10].

This dissertation is structured as follows. First, some fundamental definitions that will be used in the sequel, are presented in Chapter 1. In Chapter 2, we present a class of hybrid systems of interest for our purposes. In particular, we focus on a class of hybrid systems which embeds several control schemes in the literature and we provide some general results for the analysis of the stability and the performance. We make some examples to show that particular care has to be taken whenever a classical performance index is selected to evaluate a hybrid system performance. By using a hybrid system framework, a Lyapunov function is used to represent all the trajectories of the hybrid model and to establish performance bounds. We first provide results based on a generic Lyapunov function, then we focus on the case where the Lyapunov function is quadratic, yielding convex LMI formulations, which can be handled via SDP.

In Chapter 3, two hybrid controller architectures for linear continuous-time plants are proposed. Due to the complexity of the problem, only the hybrid state feedback case is considered, where the plant state measurements are used to design flow set, jump set and hybrid map. Although this strong simplifications, some insights on the potential of these schemes are given, especially in terms of overshoot reduction and guaranteed exponential decay rate.

In Chapter 4, the hybrid state feedback schemes introduced in Chapter 3 are generalized to the hybrid output feedback case. The idea is to introduce an observer to obtain the estimation of the plant state. First, we introduce some issues related to the introduction of the observer. Then, two

main approaches are discussed, all of them allowing overshoot reduction.

In Chapter 5, a convex multi-objective synthesis of the control scheme in Chapter 3 is presented. By combining a change of coordinates and the LMI-based results in Chapters 2 and 3, we provide sufficient conditions to completely design an multi-objective hybrid controller with respect to the decay rate and the classical \mathcal{L}_2 gain. The hybrid output feedback case and its intrinsic difficulties are also discussed. Promising results in the attainable performance trade-offs and comparisons with the corresponding linear case are showed in the simulations.

Finally, some comments on the presented results and a glimpse on the perspectives for the future works complete this document. All the results in this dissertation are based on the following publications:

- F. Fichera, C. Prieur, S. Tarbouriech, L. Zaccarian, “Improving the Performance of Linear Systems by Adding a Hybrid Loop: the Output Feedback Case”. In *Proceedings of the 2012 American Control Conference*, pages 3192–3197, Montreal, Canada, 2012;
- F. Fichera, C. Prieur, S. Tarbouriech, L. Zaccarian, “On Hybrid State-feedback Loops Based on a Dwell-time Logic”. In *4th IFAC Conference on Analysis and Design of Hybrid Systems*, pages 388–393, Eindhoven, The Netherlands, 2012;
- F. Fichera, C. Prieur, S. Tarbouriech, L. Zaccarian, “A Convex Hybrid \mathcal{H}_∞ Synthesis with Guaranteed Convergence Rate”. In *Proceedings of the 51st Conference on Decision and Control*, pages 4217–4222, Maui (HI), USA, 2012;
- F. Fichera, C. Prieur, S. Tarbouriech, L. Zaccarian, “Using Luenberger Observers and Dwell-time Logic for Feedback Hybrid Loops in Continuous-time Control Systems”. *International Journal of Nonlinear and Control*, 23:1065–1086, 2013;
- F. Fichera, C. Prieur, S. Tarbouriech, L. Zaccarian, “Static Anti-windup Scheme for a Class of Homogeneous Dwell-time Hybrid Controllers”. *Proceedings of the 2013 European Control Conference*, Zürich, Switzerland, 2013.

Preliminary concepts of the hybrid systems framework

Contents

1.1	Some preliminary definitions	5
1.2	The modeling framework	6
1.3	Hybrid time domain, solutions and their basic properties	6
1.4	Asymptotic and Exponential Stability	8
1.5	Dwell-time logic	9
1.6	t-decay rate	10
1.7	t-\mathcal{L}_2 norm and t-\mathcal{L}_2 stability	10

Some fundamental notions useful to understand the content of this dissertation are introduced. From Section 1.1 to Section 1.4 the definitions are standard and can be found more detailed in [40]. In Sections 1.5, 1.6 and 1.7, some notions particularized for our purposes are presented.

1.1 Some preliminary definitions

In this dissertation we will use the following useful definitions (further details may be found in [53, 74]).

Definition 1.1. (*Class- \mathcal{K}_∞ functions*) A function $\alpha : \mathbb{R}_{\geq 0} \mapsto \mathbb{R}_{\geq 0}$ is a class- \mathcal{K}_∞ function, also written $\alpha \in \mathcal{K}_\infty$, if α is zero at zero, continuous, strictly increasing and unbounded. \diamond

An interesting property of \mathcal{K}_∞ functions is that if $\alpha \in \mathcal{K}_\infty$ then also $\alpha^{-1} \in \mathcal{K}_\infty$.

Definition 1.2. (*Interior of a set*) Given a set $\mathcal{A} \subset \mathbb{R}^n$, we say

$$\text{int}(\mathcal{A}) = \{x \in \mathbb{R}^n : \exists \lambda > 0, \quad x + \lambda \mathbb{B} \subset \mathcal{A}\}, \quad (1.1)$$

where $\lambda \mathbb{B} = \{x \in \mathbb{R}^n : |x| < \lambda\}$. \diamond

We need also to define the distance of a vector $x \in \mathbb{R}^n$ to a compact set $\mathcal{A} \subset \mathbb{R}^n$.

Definition 1.3. (*Distance to a closed set*) Given a vector $x \in \mathbb{R}^n$ and a compact set $\mathcal{A} \subset \mathbb{R}^n$, the distance of x to \mathcal{A} is denoted $|x|_{\mathcal{A}}$ and is defined by $|x|_{\mathcal{A}} := \min\{|x - y| : y \in \mathcal{A}\}$. \diamond

Finally, we need to define the unitary deadzone.

Definition 1.4. (*Unitary deadzone*) For any $s \in \mathbb{R}$, the function $\text{dz} : \mathbb{R} \rightarrow \mathbb{R}$ is defined by

$$\text{dz}(s) = \begin{cases} 0 & \text{if } |s| \leq 1 \\ \text{sgn}(s)(|s| - 1) & \text{if } |s| \geq 1 \end{cases} . \quad (1.2)$$

◇

1.2 The modeling framework

A hybrid system can be represented as¹

$$\begin{cases} \dot{x} = f(x, w) & (x, w) \in \mathcal{C} \\ x^+ = g(x, w) & (x, w) \in \mathcal{D} \end{cases} \quad (1.3)$$

where $x \in \mathbb{R}^n$ is the state space of the hybrid system, $w \in \mathbb{R}^{n_w}$ is an exogenous signal, $\mathcal{C} \subset \mathbb{R}^n \times \mathbb{R}^{n_w}$ is the *flow set*, $\mathcal{D} \subset \mathbb{R}^n \times \mathbb{R}^{n_w}$ is the *jump set*, while $f : \mathcal{C} \mapsto \mathbb{R}^n$ and $g : \mathcal{D} \mapsto \mathbb{R}^n$ are single-valued mappings, called the *flow map* and the *jump map*, respectively. Note that \mathcal{C} and \mathcal{D} make a *regional separation* of the (x, w) -space on which the dynamics depends.

To shorten the terminology, the behavior of a dynamical system described by the flow map is referred to as *flow*. The behavior of a dynamical system described by the jump map is referred to as *jump* (or *reset*).

The model (1.3) can represent dynamical systems which have been modeled in different frameworks. Trivial examples consist in the representation of purely continuous-time systems (represented by (1.3) with $\mathcal{C} \equiv \mathbb{R}^n \times \mathbb{R}^{n_w}$ and $\mathcal{D} = \emptyset$) or purely discrete-time systems (represented by (1.3) with $\mathcal{C} = \emptyset$ and $\mathcal{D} \equiv \mathbb{R}^n \times \mathbb{R}^{n_w}$). Further and more consistent examples of frameworks which can be modeled as a hybrid systems include systems with logical modes, hybrid automata, impulsive control and switching systems.

1.3 Hybrid time domain, solutions and their basic properties

For a hybrid system (1.3), it seems natural to parameterize the solutions by both the ordinary time t which considers the amount of flow, and a discrete variable i related to the jumps. The next definition clarifies this concept.

Definition 1.5. (*Hybrid time domain*) A subset E of $\mathbb{R}_{\geq 0} \times \mathbb{Z}_{\geq 0}$ is a compact hybrid time domain if

$$E = \bigcup_{i=0}^{J-1} ([t_i, t_{i+1}], i) \quad (1.4)$$

for some finite sequence of times $0 = t_0 \leq t_1 \leq t_2 \leq \dots \leq t_J$. It is a hybrid time domain if for all $(T, J) \in E$, $E \cap ([0, T] \times \{0, 1, \dots, J\})$ is a compact hybrid time domain. ◇

Note that given $(t, j), (\bar{t}, \bar{j}) \in E$, if $t \leq \bar{t}$ or $t = \bar{t}$ and $j \leq \bar{j}$, namely $(t, j) \leq (\bar{t}, \bar{j})$, we can use the equivalent condition $t + j \leq \bar{t} + \bar{j}$. Moreover, it is important to stress that the hybrid time domain $\text{dom}(\phi)$ is determined by the hybrid arc ϕ and it is not appropriate to select a hybrid time

¹System (1.3) comes from [62], where also exogenous signals are considered. Note also that more general representations of a hybrid system can be found in [40].

domain E first, and then to find a solution ϕ such that $E = \text{dom}(\phi)$.

On the concept of hybrid time domain, we can build the concept of hybrid arc, as stated in the next definition.

Definition 1.6. (*Hybrid arc*) A function $\phi : E \mapsto \mathbb{R}^n$ is a hybrid arc if E is a hybrid time domain and if for each $j \in \mathbb{Z}_{\geq 0}$, the function $t \mapsto \phi(t, j)$ is locally absolutely continuous on the interval $I^j = \{t : (t, j) \in E\}$. \diamond

For the definition of absolutely continuous functions, the reader is referred to [75, pag. 119]. Note that the requirement of absolute continuity is important only for the intervals I^j with nonempty interiors.

Given a hybrid arc ϕ , we denote its hybrid time domain as $\text{dom}(\phi)$.

It is useful to distinguish some types of hybrid arcs based on their domains.

Definition 1.7. (*Types of hybrid arcs*) A hybrid arc ϕ is called:

- **nontrivial** if $\text{dom}(\phi)$ contains at least two points;
- **complete** if $\text{dom}(\phi)$ is unbounded;
- **Zeno** if it is complete and $\sup_t \text{dom}(\phi) < \infty$;
- **eventually discrete** if $T = \sup_t \text{dom}(\phi) < \infty$ and $\text{dom}(\phi) \cap (\{T\} \times \mathbb{Z}_{\geq 0})$ contains at least two points;
- **discrete** if nontrivial and $\text{dom}(\phi) \subset \{0\} \times \mathbb{Z}_{\geq 0}$;
- **eventually continuous** if $J = \sup_j \text{dom}(\phi) < \infty$ and $\text{dom}(\phi) \cap (\mathbb{R}_{\geq 0} \times \{J\})$ contains at least two points;
- **continuous** if nontrivial and $\text{dom}(\phi) \subset \mathbb{R}_{\geq 0} \times \{0\}$;
- **compact** if $\text{dom}(\phi)$ is compact.

\diamond

Note that a hybrid arc may satisfy more items of the previous list. For instance, continuous hybrid arcs or Zeno hybrid arcs may be complete. Every discrete hybrid arc is also eventually discrete.

The Zeno-type hybrid arcs are a very general class and we will refer to Zeno arcs which are not eventually discrete nor both complete and discrete as “genuinely Zeno”, while Zeno arcs which are complete and discrete are referred to as “instantaneously Zeno”.

We need to define the closeness of hybrid arcs.

Definition 1.8. (*(T, J, ε) -close and ε -close arcs*) The hybrid arcs $x : \text{dom}(x) \mapsto \mathbb{R}^n$, $y : \text{dom}(y) \mapsto \mathbb{R}^n$ are (T, J, ε) -close if:

- (a) for all $(t, j) \in \text{dom}(x)$ with $t \leq T$, $j \leq J$ there exists s such that $(s, j) \in \text{dom}(y)$, $|t - s| < \varepsilon$, and

$$|x(t, j) - y(s, j)| < \varepsilon; \quad (1.5)$$

(b) for all $(t, j) \in \text{dom}(y)$ with $t \leq T$, $j \leq J$ there exists s such that $(s, j) \in \text{dom}(x)$, $|t - s| < \varepsilon$, and

$$|y(t, j) - x(s, j)| < \varepsilon. \quad (1.6)$$

Moreover if the conditions above hold for any T, J , the hybrid arcs x, y are said to be ε -close.

◇

Given a hybrid system (1.3), its solutions are hybrid arcs which satisfy certain conditions, as clarified in the next definition.

Definition 1.9. (*Solution to a hybrid system*) A hybrid arc ϕ is a solution to the hybrid system (1.3), if $\phi(0, 0) \in \overline{\mathcal{C}} \cup \mathcal{D}$ and²:

(S1) for all $j \in \mathbb{Z}_{\geq 0}$ such that $I^j = \{t : (t, j) \in \text{dom}(\phi)\}$ has nonempty interior

$$\begin{aligned} \phi(t, j) &\in \mathcal{C} && \text{for all } t \in \text{int}(I^j), \\ \dot{\phi}(t, j) &= f(\phi(t, j)) && \text{for almost all } t \in \text{dom}(\phi); \end{aligned} \quad (1.7)$$

(S2) for all $(t, j) \in \text{dom}(\phi)$ such that $(t, j + 1) \in \text{dom}(\phi)$,

$$\begin{aligned} \phi(t, j) &\in \mathcal{D}, \\ \phi(t, j + 1) &= g(\phi(t, j)). \end{aligned} \quad (1.8)$$

◇

1.4 Asymptotic and Exponential Stability

In general, a system (1.3) converges to a set rather than to an equilibrium point. For simplicity, we will consider only compact sets (for more generalized definitions the reader is referred to [40]).

Let us mention that a hybrid system may exhibit also a type of solution which is said to be maximal and not complete (see [39, 40]). Nevertheless in this dissertation all the hybrid systems present only complete solutions and therefore we can rely on the following stability and attractivity definitions.

Definition 1.10. (*Global asymptotic stability*) Given the hybrid system (1.3) with $w = 0$, a compact set $\mathcal{A} \subset \mathbb{R}^n$ is said to be

- *stable for (1.3):* if for each $\varepsilon > 0$ there exists $\delta > 0$ such that each solution x to (1.3) with $|x(0, 0)|_{\mathcal{A}} \leq \delta$ satisfies $|x(t, j)|_{\mathcal{A}} \leq \varepsilon$ for all $(t, j) \in \text{dom}(x)$;
- *attractive for (1.3):* if every solution x to (1.3) satisfies $\lim_{t+j \rightarrow \infty} |x(t, j)|_{\mathcal{A}} = 0$, where $(t, j) \in \text{dom}(x)$;
- *globally asymptotically stable (GAS) for (1.3):* if it is both stable and attractive for (1.3).

◇

Additionally to Definition 1.10, we give the definition of global exponential stability. For further details the reader is referred to [84].

²Note that since $\phi = (x, w)$, we are implicitly requiring that $\text{dom}(x) = \text{dom}(w)$, according to [62].

Definition 1.11. (*Global exponential stability*) Given the hybrid system (1.3) with $w = 0$, a compact set $\mathcal{A} \subset \mathbb{R}^n$ is said to be globally exponentially stable (GES) if there exist strictly positive real numbers k and λ such that each solution x satisfies

$$|x(t, j)|_{\mathcal{A}} \leq k \exp(-\lambda(t + j)) |x(0, 0)|_{\mathcal{A}}, \quad (1.9)$$

for all $(t, j) \in \text{dom}(x)$. \diamond

1.5 Dwell-time logic

Roughly speaking, the dwell-time logic (also called temporal regularization) is a dynamic component which allows a nonzero amount of flow of the solutions after each jump, and the hybrid system (1.3) satisfies a *dwell-time condition* if all its solutions are such that $t_{i+1} - t_i \geq \rho$, for all $i \in \mathbb{Z}_{\geq 1}$, with $\rho > 0$.

In the following chapters, we use a dwell-time logic represented by the hybrid dynamics

$$\begin{aligned} \dot{\tau} &= 1 - \text{dz}\left(\frac{\tau}{\rho}\right) & \tau \in [0, \rho] \\ \tau^+ &= 0 & \tau \in [\rho, 2\rho], \end{aligned} \quad (1.10)$$

where $\text{dz}(\cdot)$ is defined in (1.2) and $\rho > 0$. Note that the flow map of (1.10) satisfies the following useful properties that will be used in the sequel

$$\begin{aligned} \dot{\tau} &= 1 & \tau \in [0, \rho] \\ \dot{\tau} &\leq 1 & \tau \in [\rho, 2\rho] \end{aligned}, \quad (1.11)$$

where in particular, $\dot{\tau} = 0$ for $\tau = 2\rho$. We also stress that the set $[0, 2\rho]$ is forward invariant.

Definition 1.12. (*Dwell-time condition*) The dwell-time logic (1.10) ensures

$$\rho + t - s \geq \rho(j - k), \quad (1.12)$$

for any pair of hybrid times $(t, j), (s, k) \in \text{dom}(\tau)$, $(t, j) \geq (s, k)$. \diamond

Condition (1.12) (also referred to as dwell-time property) comes from [17, Proposition 1.1]. Notice that if (1.3) satisfies (1.12) then each maximal solution (x, w) to (1.3) (see [40] for the definition) has a hybrid domain $E = \text{dom}(x)$ which is unbounded in the ordinary time t direction. Therefore no Zeno solutions may occur when a dwell-time condition is satisfied.

We finally observe that whenever the dwell time is initialized outside its forward invariant set, the solution of (1.10) stops.

Remark 1.1. In this dissertation we rely on the dwell-time logic architecture in (1.10). However, all the results here presented hold whenever (1.10) is replaced by any other dwell-time dynamics which satisfies (1.12), with the caveat that the forward invariant set in the τ -direction change accordingly. \star

1.6 t -decay rate

To be able to perform comparisons with the classical (continuous-time) exponential decay rate, we introduce the following definition, used also in [26, 65, 78].

Definition 1.13. (*t*-decay rate) *Given a compact set $\mathcal{A} \subset \mathbb{R}^n$ and $w = 0$, the hybrid system (1.3) has t -decay rate $\lambda > 0$ if there exists a strictly positive real number k such that each solution x satisfies*

$$|x(t, j)|_{\mathcal{A}} \leq k \exp(-\lambda t) |x(0, 0)|_{\mathcal{A}}, \quad (1.13)$$

for all $(t, j) \in \text{dom}(x)$. \diamond

Note that whenever the solutions to system (1.3) satisfy (1.12), the t -decay rate property (1.13) implies global exponential stability of the x component of (1.3) in the hybrid sense, namely (1.9). To see this, consider (1.12) with $(s, k) = (0, 0)$ and multiply both sides by $-\lambda$, by adding and subtracting $\frac{\lambda}{2}t$ and rearranging the terms, we get

$$\begin{aligned} -\lambda t &\leq -\frac{2}{3}\lambda\rho j - \frac{\lambda}{3}t + \frac{2}{3}\lambda\rho \\ &\leq -\frac{1}{3} \min\{2\lambda\rho, \lambda\}(t + j) + \frac{2}{3}\lambda\rho. \end{aligned}$$

Therefore from (1.13), we get

$$\begin{aligned} |x(t, j)|_{\mathcal{A}} &\leq k \exp(-\lambda t) |x(0, 0)|_{\mathcal{A}} \\ &\leq \bar{k} \exp(-\alpha(t + j)) |x(0, 0)|_{\mathcal{A}}, \end{aligned}$$

which corresponds to (1.9), where $\alpha := \frac{1}{3} \min\{2\lambda\rho, \lambda\}$ and $\bar{k} := k \exp(\frac{2}{3}\lambda\rho)$.

1.7 t - \mathcal{L}_2 norm and t - \mathcal{L}_2 stability

Paralleling the previous section, we want to introduce a performance index which allows us to make comparisons with the classical continuous-time framework. Consider the following definitions, used also in [33, 65, 88].

Definition 1.14. *For a hybrid signal w , with domain $\text{dom}(w) \subset \mathbb{R}_{\geq 0} \times \mathbb{Z}_{\geq 0}$, the t - \mathcal{L}_2 norm of w is given by*

$$\|w\|_{2t} = \left(\sum_{j \in \text{dom}_j(w)} \int_{t_j}^{t_{j+1}} |w(t, j)|^2 dt \right)^{\frac{1}{2}}, \quad (1.14)$$

with t_{j+1} possibly being ∞ if $(j + 1) \notin \text{dom}_j(w)$, where $\text{dom}_j(w) = \{j \in \mathbb{Z}_{\geq 0} : (t, j) \in \text{dom}(w) \text{ for some } t \geq 0\}$. \diamond

The definition in (1.14) essentially corresponds to the continuous-time \mathcal{L}_2 norm of the continuous-time signal $t \mapsto w_t(t)$ obtained by projecting on the ordinary time the hybrid signal $(t, j) \mapsto w(t, j)$. Note that when the hybrid signal w only flows, that is $\text{dom}(w) = [0, +\infty) \times \{0\}$, then (1.14) corresponds to the standard continuous-time \mathcal{L}_2 norm. Note also that (1.14) is not a norm because, for example, a solution w starting at a nonzero value and jumping to zero at

$(t, j + 1) = (0, 1)$ would satisfy $\|w\|_{2t} = 0$ (this is not the case for the hybrid norms in [14, 61])³. Nevertheless we call it norm due to the intuition that it generalizes the continuous-time norm. In the sequel, we will also use the following definition.

Definition 1.15. For a hybrid signal w , with domain $\text{dom}(w) \subset \mathbb{R}_{\geq 0} \times \mathbb{Z}_{\geq 0}$, we say $w \in t\text{-}\mathcal{L}_2$ whenever $\|w\|_{2t} < \infty$. \diamond

These definitions lead us to a performance index for dynamical systems related to the mapping from a finite-energy input w and an output signal of interest. More precisely, we defined the $t\text{-}\mathcal{L}_2$ gain of system (1.3) as follows.

Definition 1.16. Consider a set $\mathcal{A} \subset \mathbb{R}^n$ globally asymptotically stable for system (1.3) and $z = h(x, w)$ with $h(\cdot, \cdot)$ continuous in both arguments. System (1.3) is finite $t\text{-}\mathcal{L}_2$ gain from w to z with gain (upper bounded by) $\gamma > 0$ if any solution to (1.3) starting from \mathcal{A} satisfies

$$\|z\|_{2t} \leq \gamma \|w\|_{2t} \quad (1.15)$$

for all $w \in t\text{-}\mathcal{L}_2$. \diamond

According to the definition above, we consider z as the *performance output* of system (1.3).

Note that all the definitions in this section consider only the projection of hybrid signals on the ordinary time domain, neglecting their discrete component. Therefore due to the loss of information, particular care must be taken in general cases where hybrid signals might exhibit consecutive jumps or Zeno solutions, and in some cases this performance index cannot even be established. However, in the sequel we will deal with hybrid systems where these definitions can be directly employed without issues.

³Similarly, if a solution w is such that (t, j) and $(t, j + n) \in \text{dom}(w)$ with $n > 0$ (namely, w jumps n times consecutively at the ordinary instant time t), Definition 1.14 will consider only the values of w at (t, j) and $(t, j + n)$, neglecting all the intermediate values (namely, $w(t, j + 1), w(t, j + 2), \dots, w(t, j + n - 1)$).

Analysis for a class of hybrid systems

Contents

2.1	Introduction	13
2.2	A homogeneous class of hybrid systems	13
2.2.1	Relaxed jump region and its ϵ -inflated set	16
2.3	\mathcal{L}_2 stability	19
2.3.1	LMI-based statement	25

In this chapter a class of hybrid systems of interest is presented. The motivation and the interests in the results we are going to present, are detailed in Section 2.1. In Section 2.2 the general model and its properties are introduced. Section 2.2.1 states the problem we want to solve and introduces the idea behind the solution we propose. Finally, in Section 2.3 the main result based on a generic Lyapunov function is presented and in Section 2.3.1 an LMI version of the solution is provided.

2.1 Introduction

Hybrid dynamical systems exhibit characteristics of both continuous-time and discrete-time dynamical systems and their solutions can cover a wide range of behavior. In [40], powerful tools based on Lyapunov conditions are provided to accomplish stability analysis and the fact that Lyapunov functions do not guarantee existence or completeness of solutions is deeply and clearly investigated and explained. Nevertheless, the problem of accounting for all the solutions to a hybrid system becomes even more challenging whenever a performance bound has to be established. In this context we mention a good work in [65], where Lyapunov-based conditions for verifying \mathcal{L}_2 stability for a certain class of hybrid systems are presented. Also in [88], a rigorous study on hybrid control schemes embedding a FORE controller is clearly provided.

In this chapter, we address the same class of hybrid systems in [65], which is a particular case of (1.3), and we relax the Lyapunov conditions in [65]. We emphasize that most of the hybrid closed-loop scheme in the literature arising from the interconnection of a linear plant with a hybrid controller are included in the class of hybrid systems addressed in [65] and in this chapter. Finally, we anticipate that most of the hybrid control schemes in this dissertation fit such a class of interest.

2.2 A homogeneous class of hybrid systems

In Chapter 1, general notions and a general hybrid system representation were given. Now, we want to focus on a particular class of hybrid systems with the goal to provide LMI-based tools

to establish stability and performance analysis. To this aim, the class under consideration has features which allow us to use LMI tools and moreover as motivation, we also show that such a class is wide and embeds several promising hybrid control systems frequently occurring in the literature (see, for instance, [6, 28, 64, 70, 78]).

The analysis results that we present in this chapter are referred to a certain class of hybrid systems that can be represented as

$$\begin{cases} \dot{x} = Ax + Bw \\ \dot{\tau} = 1 - dz\left(\frac{\tau}{\rho}\right) & (x, \tau) \in \mathcal{C} \\ \begin{cases} x^+ = Gx \\ \tau^+ = 0 \end{cases} & (x, \tau) \in \mathcal{D} \\ z = C_z x + D_{zw} w \\ y = Cx + D_w w \end{cases} \quad (2.1a)$$

where $x \in \mathbb{R}^n$ is the state, $\tau \in [0, 2\rho]$ with $\rho > 0$ is a dwell-time logic, $w \in \mathbb{R}^{n_w}$ is an exogenous signal, $z \in \mathbb{R}^{n_z}$ is the performance output, $y \in \mathbb{R}^{n_y}$ is the measured output and \mathcal{C} and \mathcal{D} are

$$\mathcal{C} = \{(x, \tau) : x \in \mathcal{F} \text{ or } \tau \in [0, \rho]\} = \{(x, \tau) : x \in \mathcal{F}\} \cup \{(x, \tau) : \tau \in [0, \rho]\}, \quad (2.1b)$$

$$\mathcal{D} = \{(x, \tau) : x \in \mathcal{J} \text{ and } \tau \in [\rho, 2\rho]\} = \{(x, \tau) : x \in \mathcal{J}\} \cap \{(x, \tau) : \tau \in [\rho, 2\rho]\}, \quad (2.1c)$$

with \mathcal{F} and \mathcal{J} symmetric cones defined by the matrix $M = M^\top$ as

$$\mathcal{F} = \left\{x \in \mathbb{R}^n : x^\top M x \leq 0\right\}, \quad (2.1d)$$

$$\mathcal{J} = \left\{x \in \mathbb{R}^n : x^\top M x \geq 0\right\}. \quad (2.1e)$$

Since $\mathcal{C} \cup \mathcal{D}$ is forward invariant and no finite escape times are possible due to the linear flow map, it follows that all maximal solutions are complete and we will refer to asymptotic stability rather than pre-asymptotic stability (see [39, 40] for details)¹. In the sequel we denote the flow intervals as $[t_i, t_{i+1}]$ with $i \in \mathbb{Z}_{\geq 0}$, where t_i and t_{i+1} are the instants in which a jump occurs (see Chapter 1 for more details on the hybrid time domain).

Note that (2.1) is less general than (1.3). First, the flow and jump map of (2.1) are linear in the x -dimension and the exogenous signal w is injected *only* into the flow map. Moreover, the flow and jump sets are conic in the x subspace and a dwell-time logic is embedded. The next section has the purpose of listing some interesting properties related to system (2.1).

The dwell-time logic τ presents the same autonomous dynamics described in Chapter 1, and the state space (x, τ) is divided into flow and jump sets, respectively \mathcal{C} and \mathcal{D} (note that no exogenous signal w is injected here). In particular, the τ -component of \mathcal{C} and \mathcal{D} ensures that the *dwell-time condition* (1.12) is satisfied, whereas the x -component of \mathcal{C} and \mathcal{D} is projected into the flow set \mathcal{F} and the jump set \mathcal{J} . Figure 2.1 shows that sets \mathcal{F} and \mathcal{J} are conic subsets of \mathbb{R}^n and $\mathcal{F} \cap \mathcal{J}$ (represented with a dash dot dotted line) is non empty.

Remark 2.1. It is important to stress the following facts:

- if $M = 0$, then we have $\mathcal{F} \equiv \mathcal{J} \equiv \mathbb{R}^n$, namely both \mathcal{F} and \mathcal{J} correspond to the entire state space on the x -direction;

¹Notice also that (2.1a) and $\mathcal{C} \cup \mathcal{D} = \mathbb{R}^n \times [0, 2\rho]$ satisfy the Basic Assumptions of [39, 40] so that solutions exist for all initial conditions of x and for all initial values in $[0, 2\rho]$ of the dwell time τ .

- if $M < 0$ (namely, M negative definite since $M = M^\top$), we have $\mathcal{F} \equiv \mathbb{R}^n$, namely \mathcal{F} corresponds to the entire state space on the x -direction, whereas \mathcal{J} contains only the origin;
- if $M > 0$ (namely, M positive definite since $M = M^\top$), we have $\mathcal{J} \equiv \mathbb{R}^n$, namely \mathcal{J} corresponds to the entire state space on the x -direction, whereas \mathcal{F} contains only the origin.

★

Despite the particular cases listed in Remark 2.1, matrix M in (2.1d) and (2.1e) is, in general, indefinite (see [50, p. 397]), giving a more standard conic shape similar to the one illustrated in Figure 2.1.

Sets \mathcal{F} and \mathcal{J} make a *regional separation* of the x -state space and the general desired property is that the x -component of all the trajectories flow when $x \in \mathcal{F}$ and jump when $x \in \mathcal{J}$. Nevertheless due to the dwell time, the solutions² $\xi = (x, \tau)$ to (2.1) might behave differently. The next remark states some properties related to the trajectories ξ of (2.1).

Remark 2.2. It is important to stress that system (2.1) satisfies the following properties:

- $t_{i+1} - t_i \geq \rho$, for all $i \in \mathbb{Z}_{\geq 1}$. In particular, if $t_{i+1} - t_i > \rho$, $i \in \mathbb{Z}_{\geq 1}$, then $x(t, i) \in \mathcal{F}$ for all $t \in [t_i + \rho, t_{i+1}]$;
- only in the interval $[t_0, t_1]$, we have $t_1 - t_0 \geq \rho - \tau(t_0, 0)$ and so it might happen that $t_1 - t_0 < \rho$ (note that this might also imply that $t_1 = t_0$ if $\tau(t_0, 0) \geq \rho$). Nevertheless, $x(t, 0) \in \mathcal{F}$ for all $t \in [\max\{t_0, t_0 + \rho - \tau(t_0, 0)\}, t_1]$;
- flow may occur in \mathcal{J} due to the dwell-time logic:
 - $x \in \mathcal{J}$ and $\tau < \rho$, thus the system must flow. Among all the cases that may occur, we mention:
 - 1. Initial Condition.** For instance, we might have $\xi(t_0, 0) = (x(t_0, 0), \tau(t_0, 0)) \in \mathcal{J} \times [0, \rho)$, so that $x(t, 0) \in \mathcal{J}$ for some $t \in [t_0, \max\{t_0, t_0 + \rho - \tau(t_0, 0)\}]$;

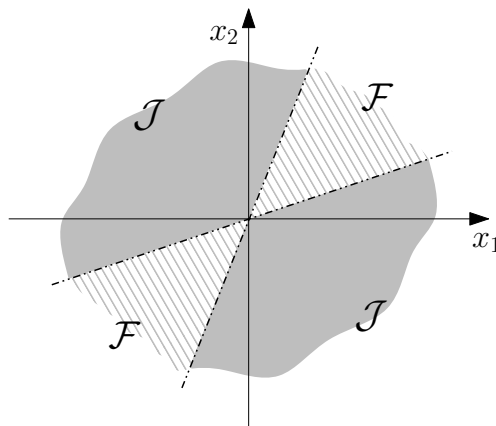


Figure 2.1: Flow and jump sets, \mathcal{F} and \mathcal{J} .

²Unlike Chapter 1, we denote the solutions to (2.1) with the compact notation $\xi = (x, \tau)$ instead of $\xi = (x, \tau, w)$. Note that the two notations are equivalent, due to the dwell time and to the fact that w enters only in the flow map.

2. Jump into \mathcal{J} . If $\xi(t_i, i) = (x(t_i, i), \tau(t_i, i)) = (Gx(t_i, i - 1), 0)$ with $i \in \mathbb{Z}_{\geq 1}$, then according to item i, flow occurs for at least an interval ρ , independently of where $x(t, i)$ lies.

- $x \in \mathcal{F}$ and $\tau < \rho$, thus the system must flow and eventually reaches \mathcal{J} before $\tau \geq \rho$.

iv. whenever $x \in \mathcal{F} \cap \mathcal{J}$ and $\tau = \rho$, the solution may either jump or flow;

v. the linearity of the mappings in (2.1a) and the conic shape of the sets \mathcal{F} and \mathcal{J} allow us to conclude the homogeneity of the substate x of the hybrid system (2.1).

★

In particular items i and ii of Remark 2.2 come from the dwell-time property (1.12).

2.2.1 Relaxed jump region and its ϵ -inflated set

In this chapter, we want to provide sufficient conditions to establish performance t - \mathcal{L}_2 bounds for system (2.1) relying on a Lyapunov function defined only in the x -state space. By proceedings similarly to [65], we want to establish if there exists a non-empty set of possible dwell-time parameter ρ that guarantees the stability property of system (2.1), as formally stated in the following problem.

Problem 2.1. Consider system (2.1) with $A, B, G, M, C_z, D_{zw}, C$ and D_w given. Provide sufficient conditions based on a Lyapunov function $x \mapsto V(x)$ to establish if there exists a dwell-time parameter $\rho > 0$ such that:

- the set $\mathcal{A} := \{0\} \times [0, 2\rho] \subset \mathbb{R}^n \times [0, 2\rho]$ is globally asymptotically stable for (2.1) with $w = 0$;
- an estimation of the t - \mathcal{L}_2 gain of (2.1) from w to z is assessed.

○

Due to the fact that the dwell time affects the x -component of the trajectories only through the sets \mathcal{C} and \mathcal{D} , we want to describe the x -component of the trajectories of system (2.1) via a Lyapunov function $x \mapsto V(x)$ (instead of $(x, \tau) \mapsto W(x, \tau)$), taking into account the dwell-time effects upon the trajectories. In particular, we want to certify the existence of a dwell-time parameter $\rho > 0$ to system (2.1), which guarantees the performance t - \mathcal{L}_2 bound. The motivation of this approach (carried out also in [65]) is in the fact that we want to provide convex conditions to be checked with SDP tools. Whenever the conditions are expressed only through a function $x \mapsto V(x)$, convex conditions can be obtained by selecting $V(x)$ quadratic. This is not possible if the trajectories $\xi = (x, \tau)$ of (2.1) are studied via a Lyapunov function $(x, \tau) \mapsto W(x, \tau)$, because the dwell time is in general injected through an exponential function³.

To establish stability property for system (2.1) via a function $x \mapsto V(x)$, we need to consider the effects induced by the dwell time upon the trajectories of (2.1). The next remark highlights a few aspects in this sense.

Remark 2.3. Although the dwell time allows us to use performance indexes in a continuous-time sense, Remark 2.2 shows that the dwell time can also be considered as a perturbation upon the trajectories. In particular, according to item iii of Remark 2.2, the x -component of a generic solution

³As a matter of fact, the stability results presented in Chapter 4 rely on Lyapunov functions which cannot be easily handled with SDP tools (see also [32]).

$\xi = (x, \tau)$ to (2.1) can flow on the set \mathcal{J} enforced by the dwell time, removing the desired regional separation of the x -state space induced by set \mathcal{F} (where only flow should occur) and set \mathcal{J} (where only jump should occur). The larger is ρ , the longer the trajectories might flow on the set \mathcal{J} . For this reason, to assess the simple stability property, a Lyapunov function $x \mapsto V(x)$ has to maintain a good decrease property to all these solutions. By selecting ρ too large, flow might be enforced on set \mathcal{J} where only jumps should occur, compromising the stability or the performance t - \mathcal{L}_2 bound of the system. On the other hand, by selecting ρ too small, not enough flow would be allowed and the function $(t, j) \mapsto V(x(t, j))$ might not compensate increase at jumps by decreasing at flows. \star

To cope with the effects of the dwell time upon the trajectories described in Remark 2.3, we introduce relaxed conditions based on different conic sets defined as

$$\tilde{\mathcal{F}} = \left\{ x \in \mathbb{R}^n : x^\top \tilde{M} x \leq 0 \right\}, \quad (2.2)$$

$$\tilde{\mathcal{F}}_\epsilon = \left\{ x \in \mathbb{R}^n : x^\top \tilde{M} x - \epsilon x^\top x \leq 0 \right\}, \quad (2.3)$$

with $\tilde{M} = \tilde{M}^\top \in \mathbb{R}^{n \times n}$ and $\epsilon > 0$. Note that (2.3) is the ϵ -inflated version of (2.2), therefore we have always that $\tilde{\mathcal{F}} \subset \tilde{\mathcal{F}}_\epsilon$.

Although system (2.1) uses sets \mathcal{F} and \mathcal{J} , we use the definitions in (2.2) and (2.3) to give more flexibility to our approach, solving Problem 2.1. Indeed in [65], stability conditions based on the inflated set of \mathcal{F} were given (namely, $\tilde{\mathcal{F}} \equiv \mathcal{F}$ and so $\tilde{\mathcal{F}}_\epsilon \equiv \mathcal{F}_\epsilon = \{x \in \mathbb{R}^n : x^\top M x - \epsilon x^\top x \leq 0\}$). Here instead, we introduce a new set $\tilde{\mathcal{F}}$ and its ϵ -inflation, $\tilde{\mathcal{F}}_\epsilon$, and we allow only certain relations between \mathcal{F} , $\tilde{\mathcal{F}}$ and $\tilde{\mathcal{F}}_\epsilon$.

In the results we are going to present, we require $\mathcal{F} \subset \tilde{\mathcal{F}}_\epsilon$ so that, given the structural $\tilde{\mathcal{F}} \subset \tilde{\mathcal{F}}_\epsilon$, the only possible inclusions between \mathcal{F} , $\tilde{\mathcal{F}}$ and $\tilde{\mathcal{F}}_\epsilon$ are:

- $\mathcal{F} \subset \tilde{\mathcal{F}} \subset \tilde{\mathcal{F}}_\epsilon$ (see Figure 2.2(a));
- $\tilde{\mathcal{F}} \subset \mathcal{F} \subset \tilde{\mathcal{F}}_\epsilon$ (see Figure 2.2(b)).

Notice that since $\mathcal{F} \cap \mathcal{J} \neq \emptyset$ and $\mathcal{F} \subset \tilde{\mathcal{F}}_\epsilon$, we have always $\tilde{\mathcal{F}}_\epsilon \cap \mathcal{J} \neq \emptyset$.

Notice that we are not excluding trivial cases like (see also Remark 2.1):

- $\tilde{M} = 0$, which corresponds to have $\tilde{\mathcal{F}} \equiv \tilde{\mathcal{F}}_\epsilon \equiv \mathbb{R}^n$;
- $\epsilon = \infty$, which corresponds to have $\tilde{\mathcal{F}}_\epsilon \equiv \mathbb{R}^n$;
- $\tilde{M} = M$, which corresponds to have $\mathcal{F} \equiv \tilde{\mathcal{F}}$;
- $\tilde{M} - \epsilon I = M$, which corresponds to have $\mathcal{F} \equiv \tilde{\mathcal{F}}_\epsilon$.

The rationale behind the introduction of these sets stands in establishing t - \mathcal{L}_2 bounds for system (2.1) only in the region where the trajectories of the solutions flow. Indeed in [65], the idea is to use the fact that jumps lead into the flow set \mathcal{F} and that the dwell time was sufficiently small, to guarantee all the trajectories within an ϵ -inflation of set \mathcal{F} . Here by introducing sets (2.2) and (2.3), we generalize the same approach and we allow jumps in the set $\tilde{\mathcal{F}}$ which can be larger than \mathcal{F} .

To better explain this, we introduce the following claim, whose proof is in Appendix 5.4.2.

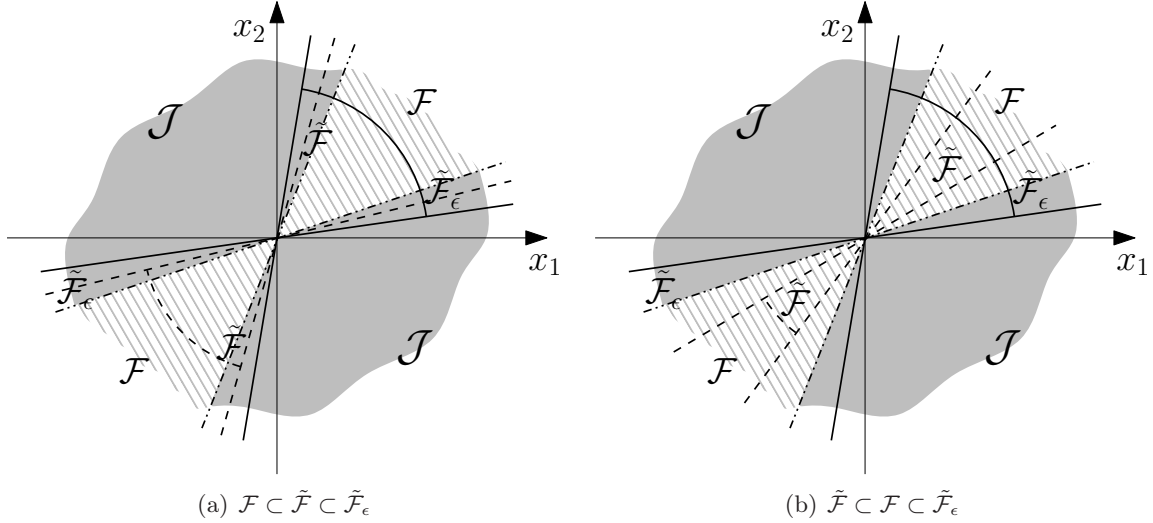


Figure 2.2: The only possible relative positions of \mathcal{F} , $\tilde{\mathcal{F}}$ and $\tilde{\mathcal{F}}_\epsilon$: $\tilde{\mathcal{F}}$ is the conic region delimited by dashed lines; $\tilde{\mathcal{F}}_\epsilon$ is the conic region delimited by bold lines.

Claim 2.1. Consider system (2.1) with $w = 0$ and sets (2.2) and (2.3). If

$$Gx \in \tilde{\mathcal{F}}, \quad \forall x \in \mathcal{J}, \quad (2.4)$$

then for any $\rho \in (0, \bar{\rho})$ with $\bar{\rho} := \varphi^{-1}\left(\frac{\epsilon}{|2(M-\epsilon I)A|}\right)$, where $\varphi(s) := s \exp(2|A|s)$, we have

$$x(t_i, i) \in \tilde{\mathcal{F}} \implies x(t, i) \in \tilde{\mathcal{F}}_\epsilon, \quad (2.5)$$

for all $t \in [t_i, t_{i+1}]$, $i \in \mathbb{Z}_{\geq 1}$. ◦

Claim 2.1 states that (2.4) implies the existence of a dwell-time parameter $\rho > 0$ such that (2.5) holds. In particular, (2.5) guarantees that all the trajectories do not exit set $\tilde{\mathcal{F}}_\epsilon$ (that is, the ϵ -inflation of $\tilde{\mathcal{F}}$) after the first jump. Note that Claim 2.1 does not draw any conclusion on the stability property of (2.1), but states only that all the trajectories lie on set $\tilde{\mathcal{F}}_\epsilon$ after the first jump. Notice that Claim 2.1 considers only the case with $w = 0$, nevertheless the same mechanism can be applied to the case where $w \in t\mathcal{L}_2$.

The main advantage of (2.5) is that bound of performance indexes coming from the classic theory can be evaluated only where the flow occurs (namely in $\tilde{\mathcal{F}}_\epsilon$), with the caveat to consider also the initial part of the trajectory in the interval $[t_0, t_1]$ (see item 1 of Remark 2.2).

Claim 2.1 and the property of the trajectories in (2.5) draw inspiration from [65]. Nevertheless here we introduced sets (2.2) and (2.3), which combined with (2.4) provide more flexibility in the analysis of system (2.1). Indeed, [65] requires $Gx \in \mathcal{F}$, for all $x \in \mathcal{J}$ and therefore for the simple analysis the system has to satisfy this requirement. Here instead for a given system (and therefore given jump map G and flow and jump sets \mathcal{F} and \mathcal{J}), the analysis is tackled by selecting the extra set $\tilde{\mathcal{F}}$ satisfying (2.4). The next example show that this approach enlarges the hybrid systems we can address with these relaxed conditions.

Example 2.1. Consider system (2.1) with

$$A = \begin{bmatrix} 0 & 1 \\ 0 & 0 \end{bmatrix}, \quad B = \begin{bmatrix} 0 \\ 0 \end{bmatrix}, \quad G = \begin{bmatrix} \frac{1}{2} & 0 \\ 0 & \frac{1}{2} \end{bmatrix}, \quad M = \begin{bmatrix} 1 & 0 \\ 0 & -1 \end{bmatrix},$$

$C_z = C = [1 \ 0]$ and $D_{zw} = D_w = 0$, which is globally asymptotically stable⁴ for some $\rho > 0$. Since $G^\top MG$ is not negative definite, we have $Gx \notin \mathcal{F}$ for all $x \in \mathcal{J}$ so that the results in [65] cannot be applied. Indeed, by selecting $\tilde{M} = \begin{bmatrix} -1 & 0 \\ 0 & -1 \end{bmatrix}$, (2.4) holds and the results in the next section can be used to accomplish the analysis of system (2.1). ■

A few more words are needed to stress that system (2.1) is very generic. Most of the hybrid closed-loop systems considered in the sequel can be represented by (2.1). Note also that the hybrid closed loop arising from the interconnection of a FORE architecture with a linear plant can be represented by (2.1), by defining A , G , C and M in (2.1) as in [88, eqs. (5a) and (5b)]. Moreover, the jump map of system (2.1) might represent the case where all the state x can jump, overcoming the case considered in the sequel in which a hybrid controller is used to control a linear plant.

In the next section we will provide some sufficient conditions to carry out the analysis of (2.1) with respect to t - \mathcal{L}_2 stability and asymptotic stability. The results will be stated first considering a generic Lyapunov function $x \mapsto V(x)$ and afterwards considering a quadratic Lyapunov function to provide LMI-based tools. The reason for this approach is that in [88], an example of a stable hybrid systems for which does not exist a quadratic Lyapunov function, has been given.

2.3 \mathcal{L}_2 stability

A common performance index for dynamical systems consists in the estimate of the mapping from a finite-energy input w and an output signals of interest z . More precisely, we want to estimate the finite t - \mathcal{L}_2 gain of system (2.1).

Notice that we are assuming $w \in t$ - \mathcal{L}_2 according to Definition 1.14. Moreover, due to the dwell-time logic in (2.1), (1.15) corresponds to the continuous-time quadratic performance of the continuous-time signals $\xi_t(t)$, $w_t(t)$ and $z_t(t)$ obtained by projecting on the ordinary time the hybrid signals $\xi(t, j)$, $w(t, j)$ and $z(t, j)$, respectively (see Definition 1.15).

We are now ready for the following result.

Theorem 2.1. Consider system (2.1) and the definitions in (2.2) and (2.3). If there exist a continuously differentiable function $V : \mathbb{R}^n \rightarrow \mathbb{R}_{\geq 0}$, a matrix \tilde{M} and a positive scalar ϵ such that set $\tilde{\mathcal{F}}_\epsilon$ in (2.3) satisfies $\mathcal{F} \subset \tilde{\mathcal{F}}_\epsilon$ and positive real scalars $a_1, a_2, a_3, a_4, a_5, \bar{\gamma}$ and a nonnegative scalar $\underline{\rho}$ satisfying

$$a_1|x|^2 \leq V(x) \leq a_2|x|^2, \quad \forall x \in \mathbb{R}^n, \quad (2.6a)$$

$$\langle \nabla V(x), Ax + Bw \rangle + a_3V(x) + \frac{1}{\bar{\gamma}}z^\top z - \bar{\gamma}w^\top w < 0, \quad \forall x \in \tilde{\mathcal{F}}_\epsilon, \forall w \in \mathbb{R}^{n_w}, x \neq 0, \quad (2.6b)$$

$$V(Gx) \leq \exp(a_3\underline{\rho})V(x), \quad \forall x \in \mathcal{J} \quad (2.6c)$$

$$Gx \in \tilde{\mathcal{F}}, \quad \forall x \in \mathcal{J} \quad (2.6d)$$

$$\langle \nabla V(x), Ax + Bw \rangle \leq a_4V(x) + a_5|x||w|, \quad \forall x \in \mathbb{R}^n, \forall w \in \mathbb{R}^{n_w}, \quad (2.6e)$$

⁴The proof is carried out by using $W(x, \tau) = x^\top P x \varphi(\tau)$, with $\varphi(\tau) = \exp(\lambda(2\rho - \tau))$, $\lambda > 0$ and [39, Theorem 20].

then for any γ satisfying

$$\gamma \geq \bar{\gamma} \exp\left(\frac{a_3 \rho}{2}\right), \quad \gamma > \sqrt{2}|D_{zw}|, \quad (2.7)$$

there exists $\bar{\rho} > 0$ such that for any $\rho \in (\underline{\rho}, \bar{\rho})$:

1) the set $\mathcal{A} = \{0\} \times [0, 2\rho]$ is globally asymptotically stable for the hybrid closed-loop system (2.1) with $w = 0$.

In particular, there exists $\rho_1^* := \varphi_e^{-1}\left(\frac{\epsilon}{|2(\tilde{M} - \epsilon I)A|}\right)$ where \tilde{M} comes from $\tilde{\mathcal{F}}$ in (2.2) and $\varphi_e(s) := s \exp(2|A|s)$, such that $\bar{\rho}$ can be selected as $\bar{\rho} := \rho_1^*$ to guarantee the stability property of \mathcal{A} ;

2) the finite t - \mathcal{L}_2 gain from w to z is less than or equal to γ , namely (1.15) holds for any solution to (2.1) from an initial condition $\xi(0, 0) = (x(0, 0), \tau(0, 0)) \in \{0\} \times [0, 2\rho]$ and with $w \in t$ - \mathcal{L}_2 .

In particular, $\bar{\rho}$ can be selected as $\bar{\rho} := \min\{\rho_2^*, \rho_3^*\}$, where ρ_2^* and ρ_3^* are defined as

$$\rho_2^* := \varphi_1^{-1}(\gamma^2 - 2|D_{zw}|^2), \quad \rho_3^* := \varphi_2^{-1}\left(\frac{\epsilon}{a_2}\right) \quad (2.8a)$$

$$\varphi_1(s) := \kappa_1(s) + \kappa_2(s) + \frac{2|C_z|^2 s}{a_1}(1 + \kappa_1(s) + \kappa_2(s)) \quad (2.8b)$$

$$\varphi_2(s) := L_1 \frac{s}{a_1}(1 + \kappa_1(s) + \kappa_2(s)) + L_2 \sqrt{\frac{s}{a_1}(1 + \kappa_1(s) + \kappa_2(s))} \quad (2.8c)$$

$$\kappa_1(s) := \exp\left(\frac{\bar{a}_4}{2}s\right) \kappa(s) + \frac{4a_1 \bar{a}_4}{\bar{a}_5^2} \kappa^2(s) \quad (2.8d)$$

$$\kappa_2(s) := \exp\left(\frac{\bar{a}_4}{2}s\right) \kappa(s) + \kappa^2(s) \quad (2.8e)$$

$$\kappa(s) := \frac{\bar{a}_5}{2} \sqrt{\frac{\exp(\bar{a}_4 s) - 1}{a_1 \bar{a}_4}} \quad (2.8f)$$

$$L_1 := 2|(\tilde{M} - \epsilon I)A|, \quad L_2 := 2|(\tilde{M} - \epsilon I)B| \quad (2.8g)$$

$$\bar{a}_4 := a_4 + a_3, \quad \bar{a}_5 := a_5 \exp(a_3 \rho) \quad (2.8h)$$

where \tilde{M} comes from $\tilde{\mathcal{F}}$ in (2.2).

Therefore by selecting $\bar{\rho} := \min\{\rho_1^*, \rho_2^*, \rho_3^*\}$, both items are guaranteed. \square

Proof of Theorem 2.1. First, notice that $\mathcal{F} \subset \tilde{\mathcal{F}}_\epsilon$, that $\xi(0, 0) = (x(0, 0), \tau(0, 0)) \in \{0\} \times [0, 2\rho]$ implies $x(0, 0) \in \mathcal{F} \subset \tilde{\mathcal{F}}_\epsilon$ and that $V(x(0, 0)) = 0$. Moreover due to (2.6d), we have $x(t_i, i) \in \tilde{\mathcal{F}}$ for all $i \in \mathbb{Z}_{\geq 1}$.

Define $W(x, \tau) := \varphi(\tau)V(x)$, with $\varphi(\tau) := \exp(a_3 \min\{\tau, \underline{\rho}\})$. Note that for all $\tau \in [0, 2\rho]$, we can write⁵

$$1 \leq \varphi(\tau) \leq \exp(a_3 \underline{\rho}), \quad (2.9a)$$

$$\dot{\varphi}(\tau) = a_3 \varphi(\tau) \dot{\tau} \leq a_3 \varphi(\tau), \quad (2.9b)$$

where in the last inequality we used the fact that $\dot{\tau} \leq 1$ (see (1.11)).

From (2.6a) and (2.9a), we have

$$a_1 |x|^2 \leq V(x) \leq W(x, \tau) \leq W(x, 2\rho) \leq \exp(a_3 \underline{\rho}) a_2 |x|^2, \quad (2.10)$$

⁵Note that due to the definition of φ we should use the generalized gradient as in [63]. Nevertheless to keep the proof simple and without loss of generality we do not use such an expedient, but we consider only the upper bound of $\dot{\varphi}(\tau)$ as in (2.9b).

for all $(x, \tau) \in \mathbb{R}^n \times [0, 2\rho]$.

Consider W along flow. From (2.6b) and (2.9b), we have

$$\begin{aligned}\dot{W}(x, \tau) &= \dot{\varphi}(\tau)V(x) + \varphi(\tau)\dot{V}(x) \\ &< a_3\varphi(\tau)V(x) + \varphi(\tau)(-a_3V(x) - \frac{1}{\bar{\gamma}}z^\top z + \bar{\gamma}w^\top w) \\ &\leq -\frac{1}{\bar{\gamma}}z^\top z + \bar{\gamma}\exp(a_3\underline{\rho})w^\top w,\end{aligned}\tag{2.11}$$

for all $(x, \tau) \in \tilde{\mathcal{F}}_\epsilon \times [0, 2\rho]$, $x \neq 0$. Which implies $\dot{W}(x, \tau) < 0$, for all $(x, \tau) \in \tilde{\mathcal{F}}_\epsilon \times [0, 2\rho]$, $x \neq 0$ and $w = 0$.

Consider now W across jumps. From (2.6c) and (2.9a), we have

$$\begin{aligned}\Delta W(x, \tau) &= W(Gx, 0) - W(x, \tau) \\ &= V(Gx) - \varphi(\tau)V(x) \\ &\leq (\exp(a_3\underline{\rho}) - \exp(a_3\underline{\rho}))V(x) = 0,\end{aligned}\tag{2.12}$$

for all $(x, \tau) \in \mathcal{J} \times [\rho, 2\rho]$, $x \neq 0$, where in the last line we used the fact that $\rho > \underline{\rho}$ and that jumps occur only if $\tau \in [\rho, 2\rho]$, namely only when $\varphi(\tau) = \underline{\rho}$.

Let us now prove item 1 and note that Claim 2.1 holds (in particular (2.4) is equivalent to (2.6d)). Therefore (2.5) holds and due to (2.11), we have that

$$\dot{W}(x(t, i), \tau(t, i)) < 0,\tag{2.13}$$

for all $t \in [t_i, t_{i+1}]$, $i \in \mathbb{Z}_{\geq 1}$ and $x(t, i) \neq 0$, whenever $\rho \in (0, \rho_1^*)$ with ρ_1^* defined in the statement and coming directly from Claim 2.1. Moreover for all $t \in [t_0, t_1]$, we have two subcases: i. $t \in [t_0, t_0 + \rho]$ and ii. $t \in (t_0 + \rho, t_1]$.

Consider **Case i**. Since $|\dot{x}| \leq |A||x|$ (see also proof of Claim 2.1 in Appendix 5.4.2) and using (2.6a), we have

$$W(x(t, 0), \tau(t, 0)) \leq \frac{a_2}{a_1} \exp(2|A|\rho)W(x(t_0, 0), \tau(t_0, 0)),\tag{2.14}$$

for all $t \in [t_0, t_0 + \rho]$.

Consider **Case ii**. By Remark 2.2 item ii, we have $x(t, 0) \in \mathcal{F} \subset \tilde{\mathcal{F}}_\epsilon$ for all $t \in (t_0 + \rho, t_1]$, therefore also (2.13) holds for all $t \in (t_0 + \rho, t_1]$.

Therefore by combining (2.12), (2.13) and (2.14), for any initial condition function $(t, i) \mapsto W(x(t, i), \tau(t, i))$ might grows only in the interval $t \in [t_0, t_0 + \rho]$, and it is strictly decreasing along flow and not increasing at jumps. Recalling that after each jump the system flows yields the result.

To prove item 2, we use the following lemma, which is a generalization of [65, Lemma 1] and whose proof is reported next.

Lemma 2.1. Suppose that the conditions in Theorem 2.1 hold. Then for any γ in (2.7), there exists $\bar{\rho} > 0$ such that for all $\rho \in (\underline{\rho}, \bar{\rho})$, we have that if $x(t_i, i) \in \tilde{\mathcal{F}}$ and $w \in t\text{-}\mathcal{L}_2$ then for all $t \in [t_i, t_{i+1}]$, $i \in \mathbb{Z}_{\geq 0}$,

$$\int_{t_i}^t |z(s, i)|^2 ds \leq W(x(t_i, i), \tau(t_i, i)) - W(x(t, i), \tau(t, i)) + \gamma^2 \int_{t_i}^t |w(s, i)|^2 ds,\tag{2.15}$$

with $W(x, \tau) := \varphi(\tau)V(x)$ and $\varphi(\tau) := \exp(a_3 \min\{\tau, \rho\})$. \square

Consider any solution ξ to (2.1) starting from $\xi(0, 0) \in \{0\} \times [0, 2\rho]$. For each $(t, j) \in \text{dom}(\xi)$, denote $t_0 = 0$ and $t_{j+1} = t$. Then using (2.12) and (2.15), we have

$$\begin{aligned} \|z\|_{2t}^2 &= \sum_{i=0}^j \int_{t_i}^{t_{i+1}} |z(s, i)|^2 ds \leq \sum_{i=0}^j (W(x(t_i, i), \tau(t_i, i)) - W(x(t_{i+1}, i), \tau(t_{i+1}, i)) + \gamma^2 \|w[t_i, t_{i+1}]\|_2^2) \\ &\leq W(x(t_0, 0), \tau(t_0, 0)) - W(x(t_{j+1}, j), \tau(t_{j+1}, j)) + \gamma^2 \sum_{i=0}^j \|w[t_i, t_{i+1}]\|_2^2 \\ &= -W(x(t, j), \tau(t, j)) + \gamma^2 \|w[t_0, t]\|_2^2 \\ &\leq \gamma^2 \|w\|_{2t}^2, \end{aligned}$$

for all $(t, j) \in \text{dom}(\xi)$ with $x(t_0, 0) = 0$. This completes the proof. \blacksquare

Proof of Lemma 2.1. The proof heavily relies on the calculations in the proof of [65, Lemma 1]. Therefore we emphasize here only the different steps.

First, by definition of z in (2.1), we have

$$\begin{aligned} |z|^2 &\leq (|C_z||x| + |D_{zw}||w|)^2 \\ &\leq 2|C_z|^2|x|^2 + 2|D_{zw}|^2|w|^2. \end{aligned} \quad (2.16)$$

Notice also that from (2.6e), we can write

$$\begin{aligned} \langle \nabla V(x), Ax + Bw \rangle &\leq a_4 V(x) + a_5 |x||w| \\ &= (a_4 + a_3)V(x) + a_5 |x||w| - a_3 V(x) \\ &:= (\bar{a}_4 - a_3)V(x) + a_5 |x||w|, \quad \forall x \in \mathbb{R}^n. \end{aligned} \quad (2.17)$$

Therefore from (2.9a) and (2.17), we get

$$\begin{aligned} \dot{W}(x, \tau) &= \dot{\varphi}(\tau)V(x) + \varphi(\tau)\dot{V}(x) \\ &\leq a_3 \varphi(\tau)V(x) + \varphi(\tau)((\bar{a}_4 - a_3)V(x) + a_5 |x||w|) \\ &\leq \bar{a}_4 W(x, \tau) + \exp(a_3 \rho) a_5 |x||w| \\ &:= \bar{a}_4 W(x, \tau) + \bar{a}_5 |x||w|. \end{aligned} \quad (2.18)$$

Now, following the same steps as in the proof of [65, Lemma 1], we consider two cases: $t \in [t_i, t_i + \rho]$ and $t \in (t_i + \rho, t_{i+1}]$, with $\rho \in (\underline{\rho}, \bar{\rho})$, $\bar{\rho} := \min\{\rho_2^*, \rho_3^*\}$ and ρ_2^* and ρ_3^* defined in (2.8a).

Case 1: suppose that $t \in [t_i, t_i + \rho]$. From (2.10), (2.18) and using exactly the same calculations as in [65, Lemma 1] we get,

$$W(x(t, i), \tau(t, i)) \leq (1 + \kappa_1(t - t_i))W(x(t_i, i), \tau(t_i, i)) + \kappa_2(t - t_i)\|w[t_i, t]\|_2^2, \quad (2.19)$$

which is similar to the one in [65, eq. (29)]. By using (2.10) and (2.16), we have

$$|z(t, i)|^2 \leq \frac{2|C_z|^2}{a_1} ((1 + \kappa_1(t - t_i))W(x(t_i, i), \tau(t_i, i)) + \kappa_2(t - t_i)\|w[t_i, t]\|_2^2) + 2|D_{zw}|^2|w(t, i)|^2. \quad (2.20)$$

Note that $\kappa_1(s)$ and $\kappa_2(s)$ are non-decreasing functions, hence we can integrate (2.20) in the fol-

lowing way

$$\begin{aligned}
\int_{t_i}^t |z(s, i)|^2 ds &\leq \frac{2|C_z|^2(t-t_i)}{a_1} \left((1 + \kappa_1(t-t_i))W(x(t_i, i), \tau(t_i, i)) + \kappa_2(t-t_i)\|w[t_i, t]\|_2^2 \right) \\
&\quad + 2|D_{zw}|^2 \int_{t_i}^t |w(s, i)|^2 ds \\
&= \frac{2|C_z|^2(t-t_i)}{a_1} \left((1 + \kappa_1(t-t_i))W(x(t_i, i), \tau(t_i, i)) + \kappa_2(t-t_i)\|w[t_i, t]\|_2^2 \right) \\
&\quad + 2|D_{zw}|^2\|w[t_i, t]\|_2^2. \tag{2.21}
\end{aligned}$$

Since we are considering the case where $t - t_i \leq \rho$ and both expressions in (2.19) and (2.21) are non-decreasing, we can write

$$W(x(t, i), \tau(t, i)) \leq (1 + \kappa_1(\rho))W(x(t_i, i), \tau(t_i, i)) + \kappa_2(\rho)\|w[t_i, t]\|_2^2, \tag{2.22a}$$

$$\int_{t_i}^t |z(s, i)|^2 ds \leq \frac{2|C_z|^2\rho}{a_1}(1 + \kappa_1(\rho))W(x(t_i, i), \tau(t_i, i)) + \left(\frac{2|C_z|^2\rho}{a_1}\kappa_2(\rho) + 2|D_{zw}|^2 \right) \|w[t_i, t]\|_2^2, \tag{2.22b}$$

which are similar to [65, eqs. (31)].

Now, we distinguish two subcases: **A.** $\|w[t_i, t]\|_2^2 \geq W(x(t_i, i), \tau(t_i, i))$ and **B.** $\|w[t_i, t]\|_2^2 \leq W(x(t_i, i), \tau(t_i, i))$.

Subcase A: by proceeding with the same calculations as in the proof of [65, Lemma 1], we may add and subtract $\frac{2|C_z|^2\rho}{a_1}(1 + \kappa_1(\rho))W(x(t_i, i), \tau(t_i, i))$ to the right-hand side of (2.22a), rearrange and combine with (2.22b) to get

$$\begin{aligned}
\int_{t_i}^t |z(s, i)|^2 ds &\leq W(x(t_i, i), \tau(t_i, i)) - W(x(t, i), \tau(t, i)) \\
&\quad + \left(\kappa_1(\rho) + \kappa_2(\rho) + \frac{2|C_z|^2\rho(1 + \kappa_1(\rho) + \kappa_2(\rho))}{a_1} + 2|D_{zw}|^2 \right) \|w[t_i, t]\|_2^2 \\
&= W(x(t_i, i), \tau(t_i, i)) - W(x(t, i), \tau(t, i)) + (\varphi_1(\rho) + 2|D_{zw}|^2)\|w[t_i, t]\|_2^2 \\
&\leq W(x(t_i, i), \tau(t_i, i)) - W(x(t, i), \tau(t, i)) + (\varphi_1(\rho_2^*) + 2|D_{zw}|^2)\|w[t_i, t]\|_2^2 \\
&= W(x(t_i, i), \tau(t_i, i)) - W(x(t, i), \tau(t, i)) + \gamma^2\|w[t_i, t]\|_2^2, \tag{2.23}
\end{aligned}$$

where we used the fact that $\rho < \rho_2^*$ and in the last line we applied the definition of ρ_2^* in (2.8a).

Subcase B: it follows exactly the same calculations as in the proof of [65, eqs. (35)-(39)]. In particular, the fact that $x(t_i, i) \in \tilde{\mathcal{F}} \setminus \{0\}$ implies that $x(t, i) \in \tilde{\mathcal{F}}_\epsilon$ for all $t \in [t_i, t_i + \rho]$ with $\rho < \rho_3^*$. Therefore, by integrating (2.11), we get

$$\int_{t_i}^t |z(s, i)|^2 ds \leq W(x(t_i, i), \tau(t_i, i)) - W(x(t, i), \tau(t, i)) + \bar{\gamma}^2 \exp(a_3\rho) \int_{t_i}^t |w(s, i)|^2 ds, \tag{2.24}$$

for all $t \in [t_i, t_i + \rho]$. This completes Case 1.

Case 2: suppose that $t \in [t_i + \rho, t_{i+1}]$. Indeed, in the exact same way as in [65, eq. (40)], if $t_{i+1} - t_i > \rho$, then $x(t, i) \in \mathcal{F} \subset \tilde{\mathcal{F}}_\epsilon$ for all $t \in [t_i + \rho, t_{i+1}]$ by definition of the flow set. Therefore, by integrating (2.11) as above, we get (2.24) for all $t \in [t_i + \rho, t_{i+1}]$. This completes the proof. ■

Theorem 2.1 generalizes the results in [65] by introducing the following novelties:

- the gain D_{zw} is allowed, by means of condition (2.7). In particular, condition (2.7) guarantees that ρ_2^* exists, whenever $D_{zw} \neq 0$. In [65, 78] such a gain has to be selected equal to zero;
- increase at jumps of the Lyapunov function $x \mapsto V(x)$ is allowed. By selecting a strictly positive $\underline{\rho}$ in (2.6c), we allow growth at jumps balanced by a suitable decrease during flow (see [40, Proposition 3.29]);
- [65, Assumption 1] is replaced by the introduction of set $\tilde{\mathcal{F}}$ and its ϵ -inflation, $\tilde{\mathcal{F}}_\epsilon$, in (2.2) and (2.3) respectively, which allow more flexibility (see Example 2.1).

Remark 2.4. Theorem 2.1 does not guarantee that the set of suitable ρ (namely, $(\underline{\rho}, \bar{\rho})$) is non empty. In particular, whenever $\underline{\rho}$ is strictly positive (namely, a growth at jumps is admitted) there is no guarantee a priori that $\underline{\rho} < \bar{\rho}$. Therefore, whenever $\underline{\rho} > \bar{\rho}$, the set $(\underline{\rho}, \bar{\rho})$ is empty. On the other hand, since ρ_1^* , ρ_2^* and ρ_3^* are strictly positive, then $\bar{\rho} > 0$ and whenever $\underline{\rho} = 0$, the set of suitable ρ is certainly non empty. Moreover, we emphasize that $\varphi_\epsilon(\cdot)$, $\varphi_1(\cdot)$ and $\varphi(\cdot)$ are class \mathcal{K}_∞ functions and so also their inverses, which in particular, depend either on γ or on ϵ . Therefore, since $\bar{\rho}$ is the minimum of these last class \mathcal{K}_∞ functions, it might be possible to enlarge ϵ and/or γ in order to guarantee $\underline{\rho} < \bar{\rho}$. Notice that only enforcing larger values of ϵ the feasibility of the conditions in Theorem 2.1 might be compromised, whereas γ can be selected slightly larger a posteriori (accordingly to (2.7) and (2.8a)). ★

Conditions in (2.7) are needed in item 2 of Theorem 2.1 to guarantee that ρ_2^* exists strictly positive. Although it may look complicated at first sight, it is enough to compare a posteriori $\bar{\gamma}$ with the square root in the second hand term of the latter in (2.7). If $\bar{\gamma}$ is larger, then we can select $\gamma = \bar{\gamma}$, otherwise we select γ larger but arbitrarily close to the value of the square root in the second condition in (2.7) according also to the value of $\underline{\rho}$ to guarantee (if possible) that the set $(\underline{\rho}, \bar{\rho})$ is non empty (see Remark 2.4).

Remark 2.5. Let us now list some important properties of Theorem 2.1:

1. if $\tilde{\mathcal{F}} \equiv \mathcal{F}$, $\underline{\rho} = 0$ and $D_{zw} = 0$, item 2 of Theorem 2.1 recovers the statement in [65, Theorem 1]. In this sense, [65, Theorem 1] can be considered as a corollary of item 2 of Theorem 2.1;
2. if $D_{zw} = 0$ then from (2.7) we have trivially $\gamma = \bar{\gamma}$;
3. consider $\tilde{\mathcal{F}}_\epsilon$ with $\epsilon = \infty$ (namely, $\tilde{\mathcal{F}}_\epsilon \equiv \mathbb{R}^n$), then (2.6b) holds globally and therefore even though $D_{zw} \neq 0$, condition (2.7) is not needed and $\gamma = \bar{\gamma}$. In particular, the fact that (2.6b) holds globally, makes conditions (2.6d) and (2.6e) useless for both items of Theorem 2.1. Moreover, the set $(\underline{\rho}, \bar{\rho})$ can always be selected non empty and the proof of Lemma 2.1 changes so that the analysis in Case 1 can be carried out as in Case 2;
4. item 1 of Theorem 2.1 establishes global asymptotic stability of set $\{0\} \times [0, 2\rho]$. Indeed to achieve global *exponential* stability, we should require a further decrease term in (2.6b). In particular, the term $a_3V(x)$ in (2.6b) is needed to compensate the eventual growth at jumps due to $\underline{\rho}$. Nevertheless whenever in (2.6b), due to the strict inequality, we can require a term $(a_3 + \zeta)V(x)$ with $\zeta > 0$ (see [53, Lemma 4.3]), then global exponential stability of set $\{0\} \times [0, 2\rho]$ can be established even when $\underline{\rho} \neq 0$. On the other hand, whenever $\underline{\rho} = 0$, item 1 of Theorem 2.1 establishes global exponential stability of set $\{0\} \times [0, 2\rho]$. ★

2.3.1 LMI-based statement

By selecting a quadratic Lyapunov function, Theorem 2.1 can be reformulated in the following LMI-based version.

Proposition 2.1. Consider system (2.1). If there exist matrices $P = P^\top > 0$, $\tilde{M} = \tilde{M}^\top$, non-negative scalars $\underline{\rho}$, τ_F , τ_C , $\tau_R \in \mathbb{R}_{\geq 0}$ and positive scalars ϵ , $\bar{\gamma}$, a_3 such that

$$\begin{pmatrix} A^\top P + PA + a_3 P - (\tilde{M} - \epsilon I) & PB & C_z^\top \\ B^\top P & -\bar{\gamma} I & D_{zw}^\top \\ C_z & D_{zw} & -\bar{\gamma} I \end{pmatrix} < 0, \quad (2.25a)$$

$$G^\top P G - \exp(a_3 \underline{\rho}) P + \tau_R M \leq 0, \quad (2.25b)$$

$$\tilde{M} - \tau_F M \leq \epsilon I, \quad (2.25c)$$

$$G^\top \tilde{M} G + \tau_C M \leq 0. \quad (2.25d)$$

Then for any γ satisfying (2.7), there exists $\bar{\rho} > 0$ such that for any $\rho \in (\underline{\rho}, \bar{\rho})$:

- 1) the set $\mathcal{A} = \{0\} \times [0, 2\rho]$ is globally exponentially stable for the hybrid system (2.1) with $w = 0$;
- 2) the t - \mathcal{L}_2 gain from w to z is less than or equal to γ , for all $w \in t\text{-}\mathcal{L}_2$.

□

Proof of Proposition 2.1. The proof is carried out by showing that all the conditions in Theorem 2.1 are satisfied. First consider the Lyapunov function $V(x) = x^\top P x$, which is continuously differentiable and note that (2.6a) holds with $a_1 = \lambda_{\min}(P)$, $a_2 = \lambda_{\max}(P)$ and (2.6e) follows from $\nabla V(x) = 2P x$, selecting large enough a_4 and a_5 .

Now note that from the S-procedure, (2.25c) implies $x^\top (\tilde{M} - \epsilon I) x \leq 0$ for all x such that $x^\top M x \leq 0$, namely $x \in \mathcal{F} \Rightarrow x \in \tilde{\mathcal{F}}_\epsilon$ or equivalently $\mathcal{F} \subset \tilde{\mathcal{F}}_\epsilon$.

Consider now (2.25a). Due to the strict inequality, there always exists a small enough $\epsilon > 0$ such that

$$\begin{bmatrix} A^\top P + PA + a_3 P - (\tilde{M} - \epsilon I) + \epsilon I & PB \\ B^\top P & 0 \end{bmatrix} + \begin{bmatrix} C_z & D_{zw} \\ 0 & I \end{bmatrix}^\top \begin{bmatrix} \frac{1}{\bar{\gamma}} I & 0 \\ 0 & -\bar{\gamma} I \end{bmatrix} \begin{bmatrix} C_z & D_{zw} \\ 0 & I \end{bmatrix} < 0. \quad (2.26)$$

By pre- and post-multiplying (2.26) by $[x^\top w^\top]$ and its transpose, respectively, and using the definition of z in (2.1), we have

$$\langle \nabla V(x), Ax + Bw \rangle + a_3 P + \frac{\epsilon}{2} |x|^2 + \begin{bmatrix} z \\ w \end{bmatrix}^\top \begin{bmatrix} \frac{1}{\bar{\gamma}} I & 0 \\ 0 & -\bar{\gamma} I \end{bmatrix} \begin{bmatrix} z \\ w \end{bmatrix} - x^\top (\tilde{M} - \epsilon I - \frac{\epsilon}{2} I) x < 0, \quad (2.27)$$

which, by applying S-procedure, implies (2.6b).

Consider (2.25b). By applying the S-procedure it is trivial to see that is equivalent to (2.6c).

Finally, (2.25d) guarantees (2.6d). In particular by applying S-procedure, (2.25d) is equivalent to

$$x^\top G^\top \tilde{M} G x = x^{+\top} \tilde{M} x^+ \leq 0, \quad \forall x \in \mathcal{J},$$

which is equivalent to (2.6d). This completes the proof. ■

Proposition 2.1 particularizes Theorem 2.1 for the case where the Lyapunov function $x \mapsto V(x)$ is quadratic. Notice that Remark 2.4 still holds, and so the non-emptiness of set $(\underline{\rho}, \bar{\rho})$ needs to be verified whenever $\underline{\rho} \neq 0$. Nevertheless, recall also that $\bar{\rho}$ is the minimum of class \mathcal{K}_∞ functions which depend on ϵ and γ , so that larger values of $\bar{\rho}$ might be enforced.

For the analysis of a given system (2.1) (see Problem 2.1), conditions (2.25) are linear in all the variables except for a_3 and $\underline{\rho}$. In particular, the term $a_3 P$ in (2.25a) and the exponential term in (2.25b) require a guess a priori upon a_3 and $\underline{\rho}$. Nevertheless the pursuit of the minimum of $\bar{\gamma}$ or of the maximum of ϵ can always be carried out. Moreover, a few more tips are given in the next remark.

Remark 2.6. Paralleling the fact that [65, Theorem 1] is a corollary of item 2 of Theorem 2.1, [65, Proposition 1] is a corollary of Proposition 2.1. In particular, by selecting $\tilde{M} = \tau_F M$ and $\underline{\rho} = 0$ (namely, no growth at jumps occurs, which implies that set $(\underline{\rho}, \bar{\rho}) = (0, \bar{\rho})$ is always non-empty (see Remark 2.4)), then:

- due to the quadratic nature of $V(x)$ and the strict inequality in (2.25a), there exists a strictly positive scalar which implies (2.6b) (see, for instance, the terms in ϵ in (2.27));
- in (2.25b), $\underline{\rho} = 0$ implies $\exp(a_3 \underline{\rho}) = 1$ for any a_3 ;
- (2.25c) is satisfied for any $\epsilon > 0$;
- (2.25d) replaces [65, Assumption 1].

Therefore whenever $\tilde{M} \leq \tau_F M$ and $\underline{\rho} = 0$, (2.25) can be linearly solved with $a_3 = \epsilon = 0$ (namely, neglecting the terms $a_3 P$ and ϵI), because those required terms are recovered from the strict inequality in (2.25a) and the quadratic nature of $V(x)$, which allow the introduction of a strictly positive term, as shown in (2.27) with $\epsilon > 0$. *

Remark 2.7. 1. If $\tilde{M} = 0$, then (2.25a) (and so (2.6b)) holds globally. Therefore according to item 3 in Remark 2.5, condition (2.7) is not needed, as well as (2.25c) and (2.25d);

2. Notice also that Proposition 2.1 establishes global exponential stability for any choice of $\underline{\rho} \geq 0$. Unlike Theorem 2.1, the strict inequality in (2.25a) and the quadratic Lyapunov function $V(x)$ implies a further strictly positive term which allows us to conclude a good decay property, establishing global exponential stability (see item 4 in Remark 2.5 and [53, Lemma 4.3], for further details). *

Hybrid controller architectures

Contents

3.1	Introduction	27
3.2	Overview	28
3.3	Resets from the plant state	30
3.3.1	First controller architecture	31
3.3.2	Second controller architecture	33
3.4	Comments and remarks	38
3.5	Simulations	39
3.5.1	A double integrator	39
3.5.2	A servo motor	41
3.5.3	A DC motor	44

In this chapter two hybrid control schemes are presented. In Section 3.1 some perspectives with respect to the scientific literature are given. In Section 3.2, the hybrid controller architecture is presented. In Section 3.3, we state the problem we want to solve. In Sections 3.3.1 and 3.3.2, two different solutions are presented, which have been proposed in [28]. Finally in Section 3.5, some numerical examples are presented combined with an optimal synthesis from [72].

3.1 Introduction

In the last decade one of the main strands of control research was focused on the design of hybrid controllers for linear continuous-time plants. In particular, we focus on hybrid controllers where the state can be reset and in the sequel, we will not consider hybrid control schemes obtained by means of switching systems techniques. In this context, [6, 7] show that a controller whose state can be reset might simultaneously guarantee several specifications which are not possible to satisfy with a classical linear controller.

One of the main hybrid controller architectures in the literature is the FORE controller. Nevertheless, no methodical design techniques have been proposed, even though we mention the works in [63, 65, 88] which provided useful analysis tools and some synthesis strategies. Beside the FORE controller, [43, 70] present different hybrid controller architectures. In particular, [43] proposes a hybrid controller architecture with time-based reset rules to establish stability and reduce the overshoot of the plant output. Nevertheless, the technique is not very simple and does not provide a convex tuning of the parameters. On the other hand, [70] proposed two new hybrid

controller architectures for which useful optimal design tools are available (see [71, 72]), making them suitable for control applications.

In this chapter, we extend the hybrid controller architectures in [70] in order to deal with hybrid control systems, which fit the representation in (2.1). In this way we will be able to use the results presented in Chapter 2 to lead stability analysis and to investigate new optimal synthesis strategies.

3.2 Overview

In this chapter, the control problem of a plant via a hybrid controller is tackled. In particular, we focus on continuous-time linear plant \mathcal{P} as

$$\begin{aligned} \dot{x}_p &= \bar{A}_p x_p + \bar{B}_p u \\ y &= \bar{C}_p x_p + \bar{D}_p u \end{aligned} \quad (3.1)$$

where $x_p \in \mathbb{R}^{n_p}$ is the state of the system, $u \in \mathbb{R}^{n_u}$ is the control input, $y \in \mathbb{R}^{n_y}$ is the output. Note that \mathcal{P} evolves *only* according to a differential equation and no resets occur on x_p .

To ease out the introduction of the control schemes, we make the following assumption on plant (3.1).

Assumption 3.1. The state x_p and the output y of \mathcal{P} are available through measurements at any time¹. ◦

Although Assumption 3.1 is restrictive, it allows to simplify the introduction of our hybrid controller architecture and to better emphasize some properties without loss of generality. Note that the same assumption has been made in [70, 71, 78].

Figure 3.1 shows the hybrid closed-loop system we consider, arisen from the interconnection of plant (3.1) and a hybrid controller \mathcal{H}_c (to be defined). In particular, we distinguish between *continuous feedback* (in particular we will consider *linear feedback*), represented with a plain line

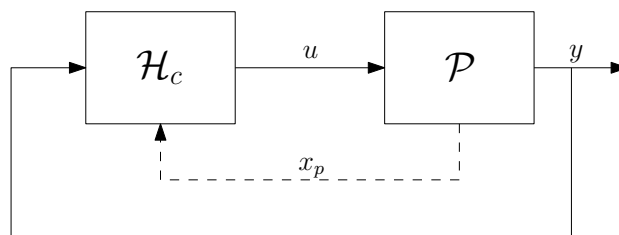


Figure 3.1: Hybrid state feedback.

and *hybrid feedback* (or equivalently *hybrid loop*), represented with a dashed line. According to the definitions in Chapter 1, the flow map of the hybrid closed-loop system arises from the continuous feedback, whereas the jump map comes from the hybrid feedback. Due to Assumption 3.1, from now on we will denote by *hybrid state feedback* the interconnection in Figure 3.1, where the state of the plant x_p is used in the jump map. Note also that, in this case, the continuous feedback is a classic output feedback.

¹Note that we are not imposing that $y = x_p$ (namely, $\bar{C}_p = I$ and $\bar{D}_p = 0$ in (3.1)). We are rather requiring that both signals x_p and y are available through measurements. The same approach has been considered in [70–72].

Let us now introduce the architecture of the hybrid controller \mathcal{H}_c . Figure 3.2 shows a scheme containing:

- a dynamic controller and a dwell-time logic, whose respective states $x_c \in \mathbb{R}^{n_c}$ and $\tau \in [0, 2\rho]$ can be reset;
- a supervisor, which decides whether to jump or flow and enforces jumps induced by the hybrid loop.

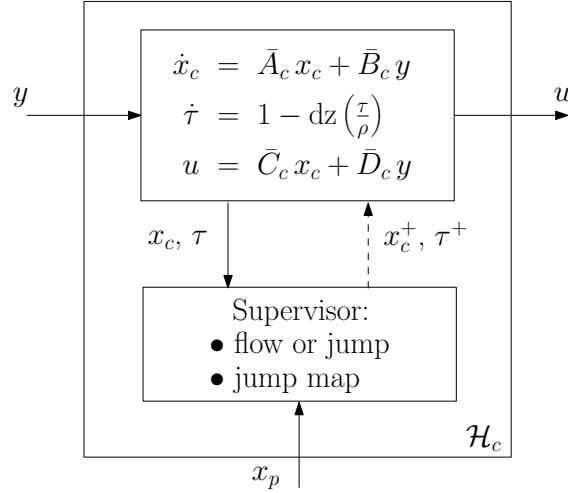


Figure 3.2: Scheme of the hybrid controller with resets from the plant state.

Note that in this case, the control u depends on a continuous feedback, which is *linear* and depends on the output of the plant y . On the other hand, the supervisor receives continuously the information of the states x_p , x_c and τ (see plain lines in Figure 3.2) and enforces the hybrid loop by resetting x_c and τ (see the dashed line in Figure 3.2). Therefore, for the schemes in the sequel we will say that the hybrid loop is composed by: flow and jump sets and the jump map.

The use of the block supervisor is not new in the control domain. In the event-triggered and switching systems domain, a block supervisor is a logic-based component that orchestrates the switching between a family of controllers for a given plant [45]. Here we adopt the same idea to denote a component which controls the resets of a state of a single continuous-time controller.

As a matter of fact there are several ways to design the supervisor. In our case, we choose to deal with linear jump maps and conic flow and jump sets which yield the following hybrid controller architecture

$$\begin{cases} \dot{x}_c = \bar{A}_c x_c + \bar{B}_c y \\ \dot{\tau} = 1 - \text{dz}\left(\frac{\tau}{\rho}\right) \\ x_c^+ = K_p x_p \\ \tau^+ = 0 \\ u = \bar{C}_c x_c + \bar{D}_c y \end{cases} \quad \begin{array}{l} (x_p, x_c, \tau) \in \mathcal{C} \\ (x_p, x_c, \tau) \in \mathcal{D} \end{array} \quad (3.2a)$$

with $x_c \in \mathbb{R}^{n_c}$ is the state, $\tau \in [0, 2\rho]$ is the dwell-time logic and \mathcal{C} and \mathcal{D} are

$$\begin{aligned} \mathcal{C} &= \{(x_p, x_c, \tau) : (x_p, x_c) \in \mathcal{F} \text{ or } \tau \in [0, \rho]\} \\ &= \{(x_p, x_c, \tau) : (x_p, x_c) \in \mathcal{F}\} \cup \{(x_p, x_c, \tau) : \tau \in [0, \rho]\}, \end{aligned} \quad (3.2b)$$

$$\begin{aligned} \mathcal{D} &= \{(x_p, x_c, \tau) : (x_p, x_c) \in \mathcal{J} \text{ and } \tau \in [\rho, 2\rho]\} \\ &= \{(x_p, x_c, \tau) : (x_p, x_c) \in \mathcal{J}\} \cap \{(\tau) : \tau \in [\rho, 2\rho]\}, \end{aligned} \quad (3.2c)$$

with \mathcal{F} and \mathcal{J} symmetric cones defined by the matrix $M = M^\top$ as

$$\mathcal{F} = \left\{ (x_p, x_c) : \begin{bmatrix} x_p \\ x_c \end{bmatrix}^\top M \begin{bmatrix} x_p \\ x_c \end{bmatrix} \leq 0 \right\}, \quad (3.2d)$$

$$\mathcal{J} = \left\{ (x_p, x_c) : \begin{bmatrix} x_p \\ x_c \end{bmatrix}^\top M \begin{bmatrix} x_p \\ x_c \end{bmatrix} \geq 0 \right\}. \quad (3.2e)$$

Notice that the dynamics of the state x_c is linear, as well as the control law u . In this sense, we can intend \mathcal{H}_c as a linear continuous-time controller (in linear feedback with the plant) augmented with a dwell-time logic and a supervisor, similarly to the approach used in [70, 71].

Let us now introduce the following assumption that will be used in the sequel.

Assumption 3.2. The interconnection (3.1), (3.2) is well-posed (in a classic sense), namely the matrix $(I - \bar{D}_p \bar{D}_c)$ is non singular. \circ

Under Assumption 3.2, the interconnection (3.1) and (3.2) yields the hybrid closed-loop system

$$\begin{cases} \begin{cases} \dot{x}_p \\ \dot{x}_c \end{cases} = \begin{bmatrix} A_p & B_p \\ B_c & A_c \end{bmatrix} x := Ax & (x, \tau) \in \mathcal{C} \\ \dot{\tau} = 1 - dz\left(\frac{\tau}{\rho}\right) \end{cases} \\ \begin{cases} x^+ = \begin{bmatrix} I & 0 \\ K_p & 0 \end{bmatrix} x := Gx & (x, \tau) \in \mathcal{D} \\ \tau^+ = 0 \\ y = [C_p \ C_c] x := Cx \end{cases} \end{cases} \quad (3.3)$$

with $x := [x_p^\top \ x_c^\top]^\top \in \mathbb{R}^{n:=n_p+n_c}$ and

$$\left(\begin{array}{cc} A_p & B_p \\ B_c & A_c \\ \hline C_p & C_c \end{array} \right) := \left(\begin{array}{cc} \bar{A}_p + \bar{B}_p \bar{D}_c (I - \bar{D}_p \bar{D}_c)^{-1} \bar{C}_p & \bar{B}_p \bar{C}_c + \bar{B}_p \bar{D}_c (I - \bar{D}_p \bar{D}_c)^{-1} \bar{D}_p \bar{C}_c \\ \bar{B}_c (I - \bar{D}_p \bar{D}_c)^{-1} \bar{C}_p & \bar{A}_c + \bar{B}_c (I - \bar{D}_p \bar{D}_c)^{-1} \bar{D}_p \bar{C}_c \\ \hline (I - \bar{D}_p \bar{D}_c)^{-1} \bar{C}_p & (I - \bar{D}_p \bar{D}_c)^{-1} \bar{D}_p \bar{C}_c \end{array} \right). \quad (3.4)$$

The hybrid system (3.3) represents the hybrid closed-loop system in Figure 3.1 and retrieves the same structure as (2.1) in the previous chapter (with $B = 0$, $C_z = 0$, $D_{zw} = 0$ and $D_w = 0$).

3.3 Resets from the plant state

The purpose of this section is to establish sufficient conditions under which controller \mathcal{H}_c stabilizes the plant \mathcal{P} . We do not impose the stability of the linear feedback, but similarly to [70, 71], we want to achieve stability through jumps, without imposing any structure to the flow map of system (3.3). In other words, for a given linear feedback not necessarily stabilizing in a classic sense (namely, matrix A is non Hurwitz), we want to design a hybrid loop (namely, flow and jump sets and a jump map) in order to stabilize the plant. The goal is to achieve global exponential stability of the origin through suitable resets.

Now we are ready to state the problem we want to solve in a formal way.

Problem 3.1. *Given a plant (3.1) under Assumption 3.1 and matrices \bar{A}_c , \bar{B}_c , \bar{C}_c and \bar{D}_c of controller (3.2) such that Assumption 3.2 is satisfied. Design matrix $M = M^\top \in \mathbb{R}^{n \times n}$, gain $K_p \in \mathbb{R}^{n_c \times n_p}$, $\rho > 0$ such that the set $\mathcal{A} := \{0\} \times [0, 2\rho] \subset \mathbb{R}^n \times [0, 2\rho]$ is globally exponentially stable for system (3.3)-(3.4). \circ*

3.3.1 First controller architecture

Theorem 3.1. Consider a plant-controller pair (3.1), (3.2) under Assumptions 3.1 and 3.2 and assume that $P = P^\top := \begin{bmatrix} P_p & P_{pc} \\ P_{pc}^\top & P_c \end{bmatrix} > 0$ satisfies

$$\Xi := \text{He} \left(\bar{P}_p (A_p + B_p K_p) + \frac{\alpha}{2} \bar{P}_p \right) < 0, \quad (3.5)$$

with

$$\bar{P}_p := P_p - P_{pc} P_c^{-1} P_{pc}^\top > 0, \quad K_p := -P_c^{-1} P_{pc}^\top, \quad (3.6)$$

for some $\alpha > 0$. Then there exists $\bar{\rho} > 0$ such that for all $\rho \in (0, \bar{\rho})$, and $\tilde{\alpha} \in (0, \alpha]$, the hybrid controller (3.2) with

$$M := \text{He} \left(PA + \frac{\tilde{\alpha}}{2} P \right), \quad (3.7)$$

solves Problem 3.1, namely the set $\mathcal{A} := \{0\} \times [0, 2\rho]$ is globally exponentially stable for system (3.3)-(3.4) with M in (3.7). \square

Proof of Theorem 3.1 The proof is carried out by using item 1 of Proposition 2.1. In particular, we show that for a particular choice of \tilde{M} , conditions (2.25) holds. Note that since we are considering only the stability, then according to (2.1) $w = 0$ and z is neglected, therefore in (2.25a) only the entry (1,1) needs to be considered.

Consider $V(x) = x^\top P x$ with $P = P^\top > 0$ satisfying conditions (3.5) and (3.6) and let us select $\tilde{M} = M + \epsilon I$, namely $\mathcal{F} \equiv \tilde{\mathcal{F}}_\epsilon$, which implies (2.25c) with $\tau_F = 1$.

Consider function $x \mapsto V(x)$ across jumps. By using (3.6), we have $V(x^+) = V(Gx) = x^\top G^\top P G x = x_p^\top \bar{P}_p x_p$. Thus we get

$$\begin{aligned} \Delta V(x) &= V(x^+) - V(x) = x_p^\top \bar{P}_p x_p - x_p^\top P_p x_p - 2x_p^\top P_{pc} x_c - x_c^\top P_c x_c \\ &= x_p^\top \bar{P}_p x_p - x_p^\top (\bar{P}_p + P_{pc} P_c^{-1} P_{pc}^\top) x_p - 2x_p^\top P_{pc} x_c - x_c^\top P_c x_c \\ &= \begin{bmatrix} x_p \\ x_c \end{bmatrix}^\top \begin{bmatrix} -P_{pc} P_c^{-1} P_{pc}^\top & -P_{pc} \\ -P_{pc}^\top & -P_c \end{bmatrix} \begin{bmatrix} x_p \\ x_c \end{bmatrix}, \end{aligned}$$

which, by applying a Schur complement, leads us to conclude

$$\Delta V(x) \leq 0, \quad \forall x \in \mathbb{R}^n, \quad (3.8)$$

which implies (2.25b), with $\underline{\rho} = 0$.

Consider now function $x \mapsto V(x)$ during flow. Note that we have $\langle \nabla V(x), Ax \rangle = x^\top \text{He}(PA)x$, thus by using (3.7), we get $\mathcal{F} := \{x : x^\top M x \leq 0\} = \{x : x^\top (\text{He}(PA) + \tilde{\alpha} P)x \leq 0\} = \{x : \langle \nabla V(x), Ax \rangle + \tilde{\alpha} V(x) \leq 0\}$. Therefore we can conclude

$$\langle \nabla V(x), Ax \rangle \leq -\tilde{\alpha} V(x), \quad \forall x \in \mathcal{F} \equiv \tilde{\mathcal{F}}_\epsilon, \quad (3.9)$$

which implies (2.25a) (note that only the entry (1, 1) of (2.25a) matters for the exponential stability) for any $a_3 \in (0, \tilde{\alpha})$.

Recall that $x = (x_p, x_c)$ and $x^+ = (x_p, K_p x_p)$ and notice that $|Gx|^2 = x_p^\top (I + K_p^\top K_p) x_p \leq |I + K_p^\top K_p| |x_p|^2$. From (3.7) and using (3.5) and (3.6), we have

$$\begin{aligned} x^\top G^\top \tilde{M} G x &= x^\top (G^\top M G + \epsilon G^\top G) x \\ &= \begin{bmatrix} x_p \\ x_c \end{bmatrix}^\top \begin{bmatrix} \Xi + \epsilon(I + K_p^\top K_p) & 0 \\ 0 & 0 \end{bmatrix} \begin{bmatrix} x_p \\ x_c \end{bmatrix} \\ &\leq \begin{bmatrix} x_p \\ x_c \end{bmatrix}^\top \begin{bmatrix} (\lambda_{\max}(\Xi) + \epsilon|I + K_p^\top K_p|)I & 0 \\ 0 & 0 \end{bmatrix} \begin{bmatrix} x_p \\ x_c \end{bmatrix} \\ &< \begin{bmatrix} x_p \\ x_c \end{bmatrix}^\top \begin{bmatrix} (\lambda_{\max}(\Xi) + \epsilon^*|I + K_p^\top K_p|)I & 0 \\ 0 & 0 \end{bmatrix} \begin{bmatrix} x_p \\ x_c \end{bmatrix} = 0, \end{aligned} \quad (3.10)$$

$\forall x \in \mathcal{J}$, $x_p \neq 0$, where the strict inequality in the last line holds for all $\epsilon \in (0, \epsilon^*)$ with $\epsilon^* := -\frac{\lambda_{\max}(\Xi)}{|I + K_p^\top K_p|}$. Note that (3.10) implies (2.25d) with $\tau_C = 0$.

Therefore all conditions (2.25) are satisfied and this concludes the proof. \blacksquare

Theorem 3.1 is an extension of the results in [70]. In particular, [70] presents a hybrid controller without dwell-time logic for a continuous-time plant \mathcal{P} and under the same conditions of Theorem 3.1, establishes global asymptotic stability of the origin. Here instead, the hybrid controller in [70] is augmented with a dwell-time logic arising controller (3.2) with sets \mathcal{F} and \mathcal{J} defined by M in (3.7) and establishes, with no extra conditions, global exponential stability of the origin rather than global asymptotic stability.

The introduction of a dwell time into the controller in [70] returns a hybrid closed loop which can be represented as (2.1), so that the results in Chapter 2 can be used to establish global exponential stability of the origin.

Both controllers in [70] and (3.2) with M defined in (3.7), share the same x_c dynamics and flow and jump sets \mathcal{F} and \mathcal{J} . In particular, the rationale behind the results in [70] and Theorem 3.1 (see also its proof) is to use a quadratic Lyapunov function $V(x_p, x_c)$ which admits a sufficiently smooth minimizer $\phi(x_p) = \operatorname{argmin}_{x_c} V(x_p, x_c)$ satisfying for all $x_p \in \mathbb{R}^{n_p}$

$$V(x_p, \phi(x_p)) \leq V(x_p, x_c), \quad \forall x_c \in \mathbb{R}^{n_c}. \quad (3.11)$$

Moreover, (3.9) shows that (3.7) allows the flow whenever such a Lyapunov function satisfies a desired decay rate imposed via $\tilde{\alpha}$. Otherwise, a jump occurs in the interior of the flow set, where a good decay condition is satisfied again and with no increase of function $(x_p, x_c) \mapsto V(x_p, x_c)$.

From a geometric point of view, the tuning of $\tilde{\alpha}$ corresponds to enlarge or shrink the conic set \mathcal{F} where flow occurs. In particular, when $\tilde{\alpha}$ tends to α , set \mathcal{F} shrinks toward the region where jumps are mapped, because flow is enforced only where the fastest decay rate is possible, which is only a narrow neighborhood of the points where the system jumps according to (3.5). On the other hand, when $\tilde{\alpha}$ tends to zero, we are not imposing a decay rate anymore and the flow region is the largest possible, therefore flow is allowed as long as the energy of the system decreases. Due to this dependence of M on $\tilde{\alpha}$, the smaller value for $\tilde{\alpha}$ is selected and the smaller the maximum

eigenvalue of M will be, which allows a larger value for $\bar{\rho}$.

We stress that stability is achieved across jumps. Indeed no particular conditions are required on the flow map A which, in general, can also be non Hurwitz. Indeed for a given flow map A , it is enough to define a matrix P satisfying (3.5) and (3.6), so that the hybrid loop (composed by a jump map and sets \mathcal{F} and \mathcal{J}) establishes global exponential stability of the origin.

Theorem 3.1 draws inspiration from the fact that, in some cases, the dwell time can be selected small enough in order that only Zeno solutions are removed (see also Claim 2.1) with respect to the controller architecture presented in [70], where no dwell time was used. This last property is better established in the next proposition, whose proof is reported next.

Proposition 3.1. Consider the *hybrid state feedback* of [70, Proposition 1] and the one of Theorem 3.1. There exists $\rho^* > 0$ such that for all $\rho \in (0, \rho^*]$ any solution of the *hybrid state feedback* of [70, Proposition 1], starting from $(x_p(0, 0), x_c(0, 0)) = (x_{p0}, x_{c0})$, with $x_{p0} \neq 0$, is also a solution of the *hybrid state feedback* (3.3), (3.4) of Theorem 3.1 starting from $(x_p(0, 0), x_c(0, 0), \tau(0, 0)) = (x_{p0}, x_{c0}, \tau_0)$ with $\tau_0 \geq \rho$. \square

Proof of Proposition 3.1 It is sufficient to show that there exists $\rho^* > 0$ such that all the solutions to the state-feedback hybrid closed loop without dwell-time logic (that is corresponding to [70, Proposition 1]) automatically satisfy a dwell time of at least ρ^* as long as $x_p(0, 0) \neq 0$, so that the dwell-time condition does not prevent any jump of the original state-feedback scheme.

To prove this fact, we will use the fact that $x_p(0, 0) \neq 0$ implies $x_p(t, j) \neq 0$ for all $(t, j) \in \text{dom}(x)$, indeed during flows x_p asymptotically converges to zero and during jumps it remains unchanged. Once we know that x_p is different from zero, then it is easy to see that whenever a jump occurs, so that $(x_p, x_c) \in \mathcal{J}$, we have that $(x_p^+, x_c^+) = (x_p, K_p x_p)$ belongs to the interior of \mathcal{F} (mainly due to the fact that $\tilde{\alpha} \leq \alpha$ and by the strict inequality in (3.5)). Therefore from continuity the system necessarily flows for some time $t_f(x_p)$, which depends on the plant state x_p before the jump. Since the dynamics is homogeneous and the flow and jump sets are symmetric cones, then each response can be written as a scaled version of the response starting from the initial condition with unit norm $\frac{x_p}{|x_p|}$, $x_p \neq 0$. Due to this fact, we can compute

$$\min_{x_p \neq 0} t_f(x_p) = \min_{x_p: |x_p|=1} t_f(x_p) = t_{fm},$$

where we have $t_{fm} > 0$ because the minimum is carried out over a compact set and $t_f(x_p) > 0$ for all $x_p \neq 0$. Finally, it is sufficient to pick $\rho^* \leq t_{fm}$ to obtain the result. \blacksquare

Some solutions in [70, Proposition 1] starting from the origin are removed from the dwell-time based scheme presented in Theorem 3.1. Indeed, Proposition 3.1 establishes the equivalence of solutions which do not originate at the origin, whenever a small enough dwell-time parameter $\rho > 0$ is selected.

3.3.2 Second controller architecture

Let us focus on the second hybrid controller. Although such a hybrid controller guarantees global exponential stability in all the x -direction, its peculiarity is to return an exponential bound for the x_p -direction, which makes it interesting for the results that we are going to present.

Consider the following statement whose proof is reported next.

Theorem 3.2. Consider a plant-controller pair (3.1), (3.2) under Assumptions 3.1 and 3.2 and assume that $\bar{P}_p = \bar{P}_p^\top > 0$, $K_p \in \mathbb{R}^{n_c \times n_p}$ satisfy (3.5) for some $\alpha > 0$. Then for each $\tilde{\alpha} \in (0, \alpha]$, there exists $\mu > 0$ such that

$$\chi := \text{He} \left(\bar{P}_p(A_p + B_p K_p) + \frac{\tilde{\alpha}}{2} \bar{P}_p + \frac{\mu}{2} K_p^\top K_p \right) < 0, \quad (3.12)$$

and for each μ satisfying (3.12), there exists $\bar{\rho} > 0$ such that for all $\rho \in (0, \bar{\rho})$ the hybrid controller (3.2) with

$$M := \text{He} \left(\begin{bmatrix} \bar{P}_p A_p + \frac{\tilde{\alpha}}{2} \bar{P}_p & \bar{P}_p B_p \\ 0 & \frac{\mu}{2} I \end{bmatrix} \right), \quad (3.13)$$

solves Problem 3.1, namely the set $\mathcal{A} := \{0\} \times [0, 2\rho]$ is globally exponentially stable for system (3.3)-(3.4) with M in (3.13). Moreover, any solution $\xi = (x_p, x_c, \tau)$ to (3.3), (3.4) with M in (3.13), starting from $\xi(0, 0) = (x_p(0, 0), x_c(0, 0), \tau(0, 0)) \in \mathbb{R}^{n_p} \times \{0\} \times [0, 2\rho]$, satisfies

$$|x_p(t, j)| \leq K \exp\left(-\frac{\tilde{\alpha}}{2} t\right) |x_p(0, 0)|, \quad \forall (t, j) \in \text{dom}(\xi), \quad (3.14)$$

where $K := \frac{\lambda_{\max}(\bar{P}_p)}{\lambda_{\min}(\bar{P}_p)} \exp((\tilde{\alpha} + 2|A|)\frac{\rho}{2})$ and $\bar{\rho} := \varphi^{-1}\left(-\frac{\lambda_{\max}(\chi)}{|2MA| + K_p^\top K_p}\right)$, where $\varphi(s) := s \exp(2|A|s)$. \square

Proof of Theorem 3.2. Consider the function $V_p(x_p) := x_p^\top \bar{P}_p x_p$ and note that by using (3.13), the sets in (3.2d) and (3.2e) can be written as

$$\mathcal{F} = \{x : \langle \nabla V_p(x_p), A_p x_p + B_p x_c \rangle \leq -\tilde{\alpha} V_p(x_p) - \mu |x_c|^2\}, \quad (3.15a)$$

$$\mathcal{J} = \{x : \langle \nabla V_p(x_p), A_p x_p + B_p x_c \rangle \geq -\tilde{\alpha} V_p(x_p) - \mu |x_c|^2\}. \quad (3.15b)$$

Moreover, since $\bar{P}_p = \bar{P}_p^\top > 0$, V_p is positive definite.

The proof is split in two parts: first we show the global exponential stability of the origin by means of Proposition 2.1, then we show the bound (3.14). Note that since we are considering only the stability, then according to (2.1) $w = 0$ and z is neglected, therefore in (2.25a) only the entry (1, 1) needs to be considered.

First we show that (3.5) implies (3.12). In particular, the strict inequality in (3.5) implies that there exists $\mu > 0$ such that

$$\text{He}(\bar{P}_p(A_p + B_p K_p)) < -\alpha \bar{P}_p - \mu K_p^\top K_p \quad (3.16)$$

$$\leq -\tilde{\alpha} \bar{P}_p - \mu K_p^\top K_p \quad (3.17)$$

$$< 0. \quad (3.18)$$

Consider now $V(x) := x^\top P x := V_p(x_p) + \lambda(x_c - K_p x_p)^\top (x_c - K_p x_p)$, where $\lambda > 0$ will be selected later and let us select $\tilde{M} = M + \epsilon I$, namely $\mathcal{F} \equiv \tilde{\mathcal{F}}_\epsilon$ which implies (2.25c) with $\tau_F = 1$.

Consider function $x \mapsto V(x)$ across jumps. Since $(x_p^+, x_c^+) = (x_p, K_p x_p)$, it is easy to check that

$$V(x^+) - V(x) = -\lambda(x_c - K_p x_p)^\top (x_c - K_p x_p) < 0, \quad \forall x \in \mathbb{R}^n, \quad (3.19)$$

which implies (2.25b), with $\underline{\rho} = 0$ (note that (3.19) holds for any $\lambda > 0$).

Consider now function $x \mapsto V(x)$ during flow. Then from (3.15), for all $x \in \mathcal{F} \equiv \tilde{\mathcal{F}}_\epsilon$, $x \neq 0$ we

have

$$\begin{aligned}
\langle \nabla V(x), Ax \rangle &= \langle \nabla V_p(x_p), \dot{x}_p \rangle + 2\lambda(x_c - K_p x_p)^\top (\dot{x}_c - K_p \dot{x}_p) \\
&\leq -\tilde{\alpha} V_p(x_p) - \mu |x_c|^2 + 2\lambda \begin{bmatrix} x_p \\ x_c \end{bmatrix}^\top \begin{bmatrix} K_p^\top \\ -I \end{bmatrix} \begin{bmatrix} A_p & B_p \\ B_c & A_c \end{bmatrix} \begin{bmatrix} x_p \\ x_c \end{bmatrix} \\
&< 0
\end{aligned} \tag{3.20}$$

where the last inequality holds for a small enough selection of $\lambda > 0$ because the good negative terms dominate over the bad terms by completion of squares. Therefore, due to the strict inequality in (3.20) and the quadratic nature of $V(x)$, for any $\lambda > 0$ satisfying (3.20) there exists a small enough $a_3 > 0$ such that a term $-a_3 V(x)$ can be injected in the right-hand side of (3.20), implying (2.25a) (note that only the entry (1, 1) of (2.25a) matters for the exponential stability).

Recall that $x = (x_p, x_c)$ and $x^+ = (x_p, K_p x_p)$ and notice that $|Gx|^2 = x_p^\top (I + K_p^\top K_p) x_p \leq |I + K_p^\top K_p| |x_p|^2$. From (3.13), we have

$$\begin{aligned}
x^\top G^\top \tilde{M} G x &= x^\top (G^\top M G + \epsilon G^\top G) x \\
&= \begin{bmatrix} x_p \\ x_c \end{bmatrix}^\top \begin{bmatrix} \chi + \epsilon(I + K_p^\top K_p) & 0 \\ 0 & 0 \end{bmatrix} \begin{bmatrix} x_p \\ x_c \end{bmatrix} \\
&\leq \begin{bmatrix} x_p \\ x_c \end{bmatrix}^\top \begin{bmatrix} (\lambda_{\max}(\chi) + \epsilon |I + K_p^\top K_p|) I & 0 \\ 0 & 0 \end{bmatrix} \begin{bmatrix} x_p \\ x_c \end{bmatrix} \\
&< \begin{bmatrix} x_p \\ x_c \end{bmatrix}^\top \begin{bmatrix} (\lambda_{\max}(\chi) + \epsilon^* |I + K_p^\top K_p|) I & 0 \\ 0 & 0 \end{bmatrix} \begin{bmatrix} x_p \\ x_c \end{bmatrix} = 0,
\end{aligned} \tag{3.21}$$

$\forall x \in \mathcal{J}$, $x_p \neq 0$, where the strict inequality in the last line holds for all $\epsilon \in (0, \epsilon^*)$ with $\epsilon^* := -\frac{\lambda_{\max}(\chi)}{|I + K_p^\top K_p|}$. Note that (3.21) implies (2.25d) with $\tau_C = 0$.

Therefore conditions (2.25) are satisfied and the first part of the proof is completed.

Consider now the bound (3.14). By applying Claim 2.1 (note that (2.4) is equivalent to (2.25d), which is implied by (3.21)), there exists a $\bar{\rho} > 0$ such that for all $\rho \in (0, \bar{\rho})$, $x(t, i) \in \tilde{\mathcal{F}}_\epsilon$ for all $t \in [t_i, t_{i+1}]$, $i \in \mathbb{Z}_{\geq 1}$. Therefore from the definition in (3.15a), we have $\dot{V}_p(x_p) \leq -\tilde{\alpha} V_p(x_p) - \mu |x_c|^2 \leq -\tilde{\alpha} V_p(x_p)$, which yields

$$V_p(x_p(t, i)) \leq \exp(-\tilde{\alpha}(t - t_i)) V_p(x_p(t_i, i)), \tag{3.22}$$

for all $t \in [t_i, t_{i+1}]$, $i \in \mathbb{Z}_{\geq 1}$. Regarding the interval $[t_0, t_1]$, we proceed similarly to Theorem 2.1 and we consider two subcases: $t \in [t_0, t_0 + \rho]$ and $t \in (t_0 + \rho, t_1]$.

Case i: $t \in [t_0, t_0 + \rho]$. From $|\dot{x}| \leq |A||x|$, one has $|x(t, i)|^2 \leq \exp(2|A|(t - t_i)) |x(t_i, i)|^2$ for all $t \in [t_i, t_{i+1}]$, $i \in \mathbb{Z}_{\geq 0}$ and so also in the interval of interest. Therefore recalling that $x_c(t_0, 0) = 0$, we get

$$V_p(x_p(t, 0)) \leq \frac{a_2}{a_1} \exp(2|A|(t - t_0)) V_p(x_p(t_0, 0)),$$

where $x_p(t_0, 0)$ is the plant initial condition, $a_1 := \lambda_{\min}(\bar{P}_p)$ and $a_2 := \lambda_{\max}(\bar{P}_p)$.

Case ii: $t \in (t_0 + \rho, t_1]$. By Remark 2.2 item ii, we have $x(t, 0) \in \mathcal{F} \equiv \tilde{\mathcal{F}}_\epsilon$ for all $t \in (t_0 + \rho, t_1]$, therefore also (3.22) holds.

By combining the two subcases, one has

$$V_p(x_p(t, 0)) \leq \exp(-\tilde{\alpha}(t - t_0 - \rho)) V_p(x_p(t_0 + \rho, 0))$$

$$\begin{aligned}
&\leq \frac{a_2}{a_1} \exp(2|A|\rho) \exp(-\tilde{\alpha}(t - t_0 - \rho)) V_p(x_p(t_0, 0)) \\
&= \frac{a_2}{a_1} \exp((2|A| + \tilde{\alpha})\rho) \exp(-\tilde{\alpha}(t - t_0)) V_p(x_p(t_0, 0)) \\
&= \frac{a_1}{a_2} K^2 \exp(-\tilde{\alpha}(t - t_0)) V_p(x_p(t_0, 0)),
\end{aligned} \tag{3.23}$$

for all $t \in [t_0, t_1]$.

Finally, by combining (3.19), (3.22) and (3.23), we have

$$V_p(x_p(t, j)) \leq \frac{a_1}{a_2} K^2 \exp(-\tilde{\alpha}(t - t_0)) V_p(x_p(t_0, 0)), \tag{3.24}$$

for all $(t, j) \in \text{dom}(\xi)$. Therefore from (3.24) and using the fact that $a_1|x_p|^2 \leq V_p(x_p) \leq a_2|x_p|^2$, we get (3.14). This concludes the proof. \blacksquare

Remark 3.1. Theorem 3.2 establishes global exponential stability of set \mathcal{A} . Nevertheless bound (3.14) holds for all the solutions $\xi = (x_p, x_c, \tau)$ to (3.3)-(3.4) with M in (3.13), starting from $\xi(0, 0) = (x_p(0, 0), x_c(0, 0), \tau(0, 0))$, with $x_c(0, 0) = 0$. Although this is not very restrictive, for solutions starting from points where $x_c(0, 0) \neq 0$, global exponential stability of set \mathcal{A} is still maintained but (3.14) is not guaranteed. The reason is that bound (3.14) is established by exploiting the definition in (3.13) (see also (3.15)), which considers the dynamic of a Lyapunov-like function only in the x_p -direction. Moreover, the proof relies on Claim 2.1, to ensure that despite the dwell time, after the first interval the trajectories do not leave set \mathcal{F} where bound (3.14) is established (this was presented as property of the trajectories in Section 2.2.1, see also (2.5)). Note that bound (3.14) implies that the control scheme has t -decay rate $\tilde{\alpha}/2$ in the x_p direction. \star

Remark 3.2. The gain K in bound (3.14) takes into account the increase of the Lyapunov function that may occur in the first interval due to the dwell time (see Remark 2.2 for further details). Indeed bound (3.14) can be tightened by expressing the dependence of K on $\tau(0, 0)$. Although we preferred to keep the proof of Theorem 3.2 simple, we can modify the proof technique to replace K in bound (3.14) by $\tilde{K}(\tau(0, 0))$ defined as

$$\tilde{K}(\tau(0, 0)) := \frac{\lambda_{\max}(\bar{P}_p)}{\lambda_{\min}(\bar{P}_p)} \exp\left(\left(\tilde{\alpha} + 2|A|\right) \frac{\max\{0, \rho - \tau(0, 0)\}}{2}\right), \tag{3.25}$$

with $\tau(0, 0) \in [0, 2\rho]$. Notice that this new $\tilde{K}(\tau(0, 0))$ takes into account that whenever $\tau(0, 0) \in [0, 2\rho]$, system (2.1) is ready to jump if $x \notin \mathcal{F}$ and in that case the exponential term in (3.25) disappears, making the accuracy of bound (3.14) depend on the condition number of matrix \bar{P}_p (see [13]). Finally, we have $\tilde{K}(\tau(0, 0)) \leq K$. \star

Remark 3.3. We stress that the exponential decay rate in (3.14) depends on $\tilde{\alpha} > 0$, which is selected in the flow and jump sets, \mathcal{F} and \mathcal{J} , through M in (3.13). Recall also that $\tilde{\alpha} \in (0, \alpha]$, with $\alpha > 0$ selected in (3.5). \star

Theorem 3.2 generalizes the state feedback solution proposed in [71, Theorem 1] (see also [70, Proposition 2]). However, an extra x_c -dependent term is added to allow the insertion of the dwell-time logic in the scheme without compromising the stability property. While the flow and

jump sets \mathcal{F} and \mathcal{J} , coming from (3.7) in Theorem 3.1, coincide with those of [70, Proposition 1], it is not true that the flow and jump sets coming from the matrix M in (3.13) in Theorem 3.2 coincide with those of [70, Proposition 2] and [71]. The difference stands in the term $-\mu|x_c|^2$ introduced here to provide a sufficient level of robustness. Such a robustness is required to tolerate the inevitable perturbations introduced by the dwell-time logic, which forces the system to flow even though x belongs to \mathcal{J} when the timer τ is too small².

Although we do not have a formal proof of fragility of the scheme in [70, Proposition 2], we should emphasize that the proofs of stability in [70, Proposition 2] were based on the invariance principle because Lyapunov arguments only allowed to establish negative semidefiniteness of our candidate Lyapunov functions. It turns out that the term $-\mu|x_c|^2$ provides the missing decrease and significantly simplifies the proof of exponential stability for both Theorem 3.2 and [28, Theorem 2]. Moreover the strict decrease arising from this term allows us to introduce the dwell-time logic without compromising the exponential stability of the closed loop. It should also be emphasized that the dwell-time parameter $\bar{\rho}$ shrinks to zero as μ becomes smaller. To illustrate the effect of the new term $-\mu|x_c|^2$ in (3.13), consider the following example.

Example 3.1. Consider the system (3.3) defined by the following data

$$A = \begin{bmatrix} A_p & B_p \\ B_c & A_c \end{bmatrix} = \begin{bmatrix} -1 & 0 \\ 1 & 0 \end{bmatrix}, \quad \bar{P}_p = 1,$$

which, regardless of K_p , satisfies (3.5) for any $\alpha < 1$ (because $B_p = 0$). This example does not satisfy the detectability condition in [71, Theorem 1] and indeed one can see that setting $\mu = 0$ in (3.13) (thus recovering the definitions in [71]) the system starting from $(x_p, x_c) = (0, a)$ for any $a \neq 0$ can flow indefinitely so that $x_c(t, j) = a \neq 0$ for all times, implying no convergence (even with dwell time). Consider now the flow and jump sets coming from the definition of matrix M in (3.13) with $\mu \neq 0$ and notice that $(x_p, x_c) = (0, a) \notin \mathcal{F}$ because $-\mu|x_c|^2 = -\mu|a|^2 < 0$. Then x_c is instantaneously forced to jump to $x_c^+ = K_p x_p = 0$, regardless of K_p , and this shows convergence. In other words, the extra term $-\mu|x_c|^2$ appearing in (3.13) (combined with the dwell-time logic) ensures that, upon convergence to zero of x_p , if $x_c \neq 0$, the controller can eventually be forced to jump (as x_p gets small enough) and the x_c substate is stabilized through jumps regardless of the detectability of (B_p, A_c) required in [71, Theorem 1]. ■

Remark 3.4. It is not possible to prove an equivalent statement to Proposition 3.1 with reference to the hybrid controller in Theorem 3.2 and the hybrid controller in [70, Proposition 2] and [71]. Indeed, as emphasized earlier, the jump and flow sets \mathcal{F} and \mathcal{J} considered in [70, 71] correspond to the ones defined in (3.2d) and (3.2e) coming from the definition of M in (3.13) with $\mu = 0$. Due to this fact, since we require $\mu > 0$ here, we cannot say that the solutions to (3.3), (3.4) satisfying Theorem 3.2, graphically converge to those of the corresponding hybrid state-feedback loops of [70, 71]. Nevertheless, since the system with a small $\mu > 0$ corresponds to a perturbation of the system with $\mu = 0$, we can state by relying on the results of [41] that the arising trajectories can be made arbitrarily close to those of [70, Proposition 2] and [71] by choosing μ arbitrarily small.

★

²For Theorem 3.2, this might still happen in the interval $[t_0, t_1]$.

3.4 Comments and remarks

Remark 3.5. Theorems 3.1 and 3.2 are a generalization of the results in [70, 71]. Among the similarities between Theorems 3.1 and 3.2 and the results in [70, 71], we have:

- a. the flow and jump sets \mathcal{F} and \mathcal{J} are defined according to Lyapunov-like functions. Indeed, Theorem 3.1 shares the same sets as [70, Proposition 1], whereas Theorem 3.2 slightly modifies the sets from [71, Theorem 1] (see also [70, Proposition 2]).
- b. the jump map is built in order to:
 - i. guarantee non-increase at jumps of the Lyapunov-like functions used in \mathcal{F} and \mathcal{J} ;
 - ii. ensure a good decrease condition of the Lyapunov-like functions used in \mathcal{F} and \mathcal{J} , after each jump.
- c. all the results rely on condition (3.5);
- d. the stability of the origin of the schemes is achieved through resets.

Among the differences between Theorems 3.1 and 3.2 and the results in [70, 71], we have:

- e. Theorems 3.1 and 3.2 establish global exponential stability of set \mathcal{A} and moreover Theorem 3.2 guarantees the t -decay rate in the x_p -direction. On the other hand, [70, 71] establish global asymptotic stability of set \mathcal{A} ;
- f. Theorems 3.1 and 3.2 refer to the hybrid controller architecture (3.2), which presents a dwell-time logic, whereas results in [70, 71] do not rely on dwell-time logic;
- g. both Theorems 3.1 and 3.2 are proved by using smooth Lyapunov functions which allow us to conclude robustness according to [16].

★

As already mentioned, the key element for both techniques in Theorems 3.1 and 3.2 is condition (3.5), which, roughly speaking, resembles to the condition of the classic static state feedback, [3, 10, 19, 38]. Indeed, (3.5) can be considered either as the classic formulation for the static state feedback control for the pair (A_p, B_p) for a given α , or as the generalized eigenvalue problem in case also α is considered as a variable (see [11] and Section 3.5 for further details).

Note that whenever α is selected small enough, (3.5) admits a solution only if the pair (A_p, B_p) is controllable in a classic sense (see [8, 44, 67]). Nevertheless for the hybrid case addressed here, matrices A_p and B_p do depend on the plant but also on the flow map of the hybrid controller (3.2a) (see also (3.4)). Therefore in order to solve (3.5), the flow map of the cascade of the plant and the hybrid controller has to be at least controllable.

Finally, not much on the comparison between Theorem 3.1 and Theorem 3.2 can be said yet. Both techniques shares similarities in their mappings but not in their sets. In particular, Theorem 3.1 seems to have more parameters to tune with respect to Theorem 3.2 and we cannot exclude that this may be an advantage for certain applications. On the other hand, Theorem 3.2 has a simpler implementation and returns an exponential bound for the plant direction which is useful. Nevertheless, further investigations are needed to clarify what schemes is the best and under which circumstances and no further space will be dedicated to this issue in this document.

3.5 Simulations

We are now ready to introduce how to design the hybrid loops presented in this chapter. Following Problem 3.1, we assume that the matrix A of (3.3) is given and not necessarily stable and we want to augment the existing linear feedback with a hybrid loop from the state of the plant. Moreover for illustrative purposes, we assume also that $\alpha > 0$ is given as a performance parameter. Therefore the following procedure can be used to solve both Theorems 3.1 and 3.2.

Procedure.

Step 1: Given $\alpha > 0$, solve in Y and Q the following linear condition

$$\text{He} \left(A_p Y + B_p Q + \frac{\alpha}{2} Y \right) < 0, \quad Y = Y^\top > 0. \quad (3.26)$$

Step 2: Calculate $\bar{P}_p = Y^{-1}$ and $K_p = Q\bar{P}_p$.

Step 3: Select any $P_c = P_c^\top > 0$.

Step 4: Calculate $P_{pc} = -K_p P_c$ and $P_p = \bar{P}_p + P_{pc} P_c^{-1} P_{pc}^\top$. ■

Note that Theorem 3.1 requires that all the steps of the procedure above be solved, whereas for Theorem 3.2 the procedure stops after completing step 2 and solving (3.12) which is linear in the only variable μ . In particular, (3.26) is equivalent to (3.5) by pre- and post-multiplying it by $Y = \bar{P}_p^{-1}$ (which always exists) and defining the new variable $Q := K_p Y$. On the other hand for the case of Theorem 3.1, the identities (3.6) have to be satisfied to define matrix P (which is used in the flow and jump sets defined by M in (3.7)). Therefore the last two steps of the procedure ensure the satisfaction of these further constraints. Notice that the procedure above does not try to minimize any performance index, therefore in step 3 a guess is required and no optimal choice is available at the moment.

The similarities emphasized in items a and c of Remark 3.5 (see also Proposition 3.1 for Theorem 3.1 and Remark 3.4 for Theorem 3.2) allow us to use the optimal synthesis introduced in [71] to design an optimal hybrid controller with respect to the maximum decay rate and the one in [72] to reduce the overshoot of the plant output. In what follows, we will use the approach in [72] whose basic idea, roughly speaking, is to approximate the Lyapunov-like function, used to define the flow and jump sets \mathcal{F} and \mathcal{J} , to the norm of the plant output. In Appendix 5.4.2, we briefly report the conditions of such a technique.

3.5.1 A double integrator

As a first example, we propose a double integrator represented by

$$\left[\begin{array}{c|c} \bar{A}_p & \bar{B}_p \\ \hline \bar{C}_p & \bar{D}_p \end{array} \right] = \left[\begin{array}{cc|c} 0 & 1 & 0 \\ 0 & 0 & 1 \\ \hline 1 & 0 & 0 \end{array} \right].$$

According to Problem 3.1, the flow map of the controller is given by

$$\left[\begin{array}{c|c} \bar{A}_c & \bar{B}_c \\ \hline \bar{C}_c & \bar{D}_c \end{array} \right] = \left[\begin{array}{c|c} -1 & -1 \\ \hline 1 & 0 \end{array} \right].$$

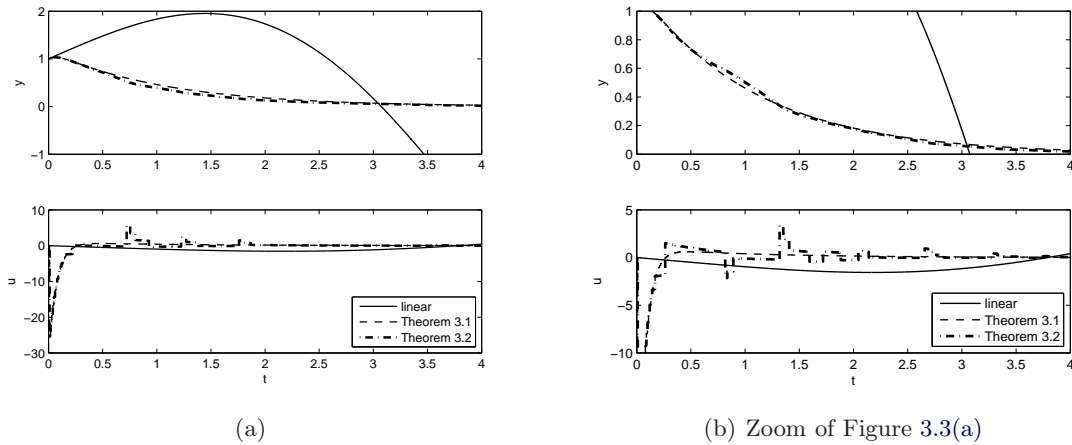


Figure 3.3: Double integrator controlled through the techniques in Theorems 3.1 and 3.2.

Note that the flow map A of the arising hybrid closed loop (3.3) is not Hurwitz, so that stability has to be enforced through the hybrid loop. Moreover, as control specification is required that $\alpha = 1$ in (3.5).

We want to solve Problem 3.1 by using both techniques presented in Theorems 3.1 and 3.2. Consider first Theorem 3.1. By applying the procedure in Section 3.5, after step 2 we obtain³:

$$K_p = \begin{bmatrix} -11.8598221 & -13.6571764 \end{bmatrix},$$

$$\bar{P}_p = \begin{bmatrix} 0.0555172 & 0.0195509 \\ 0.0195509 & 0.0245409 \end{bmatrix}.$$

By choosing $P_c = 1$, we can complete the procedure obtaining

$$P = \begin{bmatrix} 140.7108971 & 161.9912328 & 11.8598221 \\ 161.9912328 & 186.5430073 & 13.6571764 \\ 11.8598221 & 13.6571764 & 1 \end{bmatrix},$$

and by selecting $\tilde{\alpha} = \alpha$, we design the flow and jump sets, \mathcal{F} and \mathcal{J} with

$$M = \begin{bmatrix} 116.9912529 & 289.0449536 & 160.9912328 \\ 289.0449536 & 510.5254729 & 198.4028294 \\ 160.9912328 & 198.4028294 & 26.31435274 \end{bmatrix}.$$

Therefore the design of hybrid controller (3.2) satisfying conditions in Theorem 3.1 is complete. In the rest of the paragraph, we will refer to this hybrid controller as $\mathcal{H}_{thm3.1}$.

Consider now Theorem 3.2. By applying the procedure in Section 3.5, after step 2 we obtain the same gain K_p and \bar{P}_p as above. Therefore to be able of selecting the correct matrix M in (3.13), we need to select $\mu > 0$ in order to satisfy (3.12), which is linear in the only variable μ . By solving (3.12) as a convex optimization problem maximizing μ , we obtain $\mu = 0.0028689$, and therefore by

³Condition (3.26) has been solved with two further conditions. In particular, to avoid fast exponential trends involving numerical problems in the simulations, we added the constraint $\text{He}(A_p Y + B_p Q + 50Y/2) > 0$ (see also [10, 22]). Moreover, to have a good condition number of matrix Y , we added the constraint $\lambda I \leq Y \leq k_1 \lambda I$ where $\lambda \geq k_2$, with $k_1 = 10^8$ and $k_2 = 10^{-6}$ and minimizing λ .

selecting again $\tilde{\alpha} = \alpha = 1$, we design the flow and jump sets, \mathcal{F} and \mathcal{J} with

$$M = \begin{bmatrix} 0.0555172 & 0.0750681 & 0.0195509 \\ 0.0750681 & 0.0636428 & 0.0245409 \\ 0.0195509 & 0.0245409 & 0.0028689 \end{bmatrix},$$

completing the design of hybrid controller (3.2) satisfying conditions in Theorem 3.1. We will refer to this hybrid controller as $\mathcal{H}_{thm3.2}$. Notice that the t -decay rate $\tilde{\alpha}/2$ is guaranteed by selecting the dwell-time parameter small enough.

Figure 3.3 shows a simulation starting from $\xi(0,0) = (x(0,0), \tau(0,0)) = (1, 1, 0)$ with $\rho = 0.01$. The linear controller without hybrid loop is unstable since A is not Hurwitz, whereas the two hybrid loops return comparable trend for the output y , although $\mathcal{H}_{thm3.1}$ tends to generate a control u that jumps more often than the one of $\mathcal{H}_{thm3.2}$. On the other hand controller $\mathcal{H}_{thm3.2}$ generates a control u with more peaks than the scheme with $\mathcal{H}_{thm3.1}$.

3.5.2 A servo motor

To show the effectiveness of the technique in Theorem 3.1, we consider an experimental example used in [20, 49], in which all the controller specifications cannot be guaranteed by a linear controller (see [49]). The system consists in a series of three flywheels connected via a flexible shaft. A servo motor drives the first flywheel and the speed of the third one is measured via a tachometer. The system obtained by the union of the servo motor, the three flywheels and the filtered tachometer output was identified from frequency-response data as:

$$P(s) = \frac{46083950}{(s + 1.524)(s^2 + 3.1s + 2820)(s^2 + 3.62 + 9846)}.$$

In the sequel, its state (for the state space form) will be denoted by $x_{p1} \in \mathbb{R}^5$. For this system, five specifications are required:

- i) bandwidth constraint;
- ii) disturbance rejection;
- iii) sensor-noise suppression;
- iv) asymptotic performance;
- v) overshoot reduction.

[49] proved that it is not possible to meet all the specifications above with a linear time-invariant controller. In particular, in [49] two LTI controllers are designed: one that achieves all the specifications without obtaining the required noise rejection and another one guaranteeing all the specifications above, except for the overshoot reduction.

As in [49], we decide to keep this second controller

$$C(s) = \frac{-1075460(s + 7)(s^2 + 3.662s + 2798)(s^2 + 5.419s + 9876)}{s(s + 209.6)(s + 35.8)(s^2 + 132.8s + 12050)(s^2 + 375.9s + 66930)},$$

whose state is denoted by $x_{p2} \in \mathbb{R}^7$. Moreover according to [49], we also add a further first order reset controller, as illustrated in Figure 3.4. The goal is to exploit the controller $C(s)$ for the

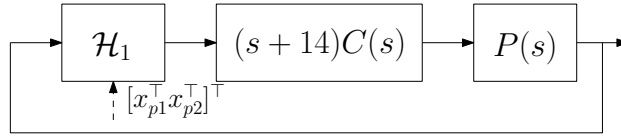


Figure 3.4: Scheme of the closed-loop system proposed by [49].

guaranteed specifications and to add a reset controller to reduce the overshoot, thus achieving all the desired specifications with a reset closed-loop system. In particular, [49] proposes to add a FORE controller with a pole in -14 and a further zero to cancel the pole of the reset controller without affecting the steady-state properties, see Figure 3.4.

We now compare the FORE controller proposed by [49] with the hybrid controller \mathcal{H}_1 illustrated in Figure 3.2 and presented in Theorem 3.1. Note that the aim of the hybrid controller \mathcal{H}_1 (and of the FORE in [49]) is to reduce the overshoot, which is the only property not guaranteed by the LTI controller $C(s)$. To this aim we use the optimal technique for overshoot reduction presented in [71] to tune the hybrid controller \mathcal{H}_1 .

We point out that to reset the hybrid controller \mathcal{H}_1 we need to assume that the state of the plant is available. In this case such a state consists in the series of the controller $C(s)$ (slightly modified by an extra zero) and $P(s)$ (that is $x_p = [x_{p1}^T x_{p2}^T]^T \in \mathbb{R}^{12}$). The assumption of the knowledge of the plant state through measurements is restrictive because the plant state is, in general, not completely measurable and because often the state (or a subpart of it) does not have a physical meaning (due for instance, to the adopted identification methods as in this case for x_{p1}). Note that for this problem setting we might also consider the hybrid output feedback scheme of [27, 29]. When using our state feedback scheme, a possible strategy to avoid the use of the measurement of x_p is to approximate the twelve order state x_p by a second order state \bar{x}_p and use what we will refer to as the *reduced hybrid controller* \mathcal{H}_1 . In particular, we will consider a first order approximation for the plant $P(s)$ and a first order approximation for $(s + 14)C(s)$ (using the Gramian-based balancing of state-space realizations and a reduction of the system preserving the static gain). In this way by measuring the input and output of each system, it is possible to recover the state $\bar{x}_p := [\bar{x}_{p1}^T \bar{x}_{p2}^T]^T$.

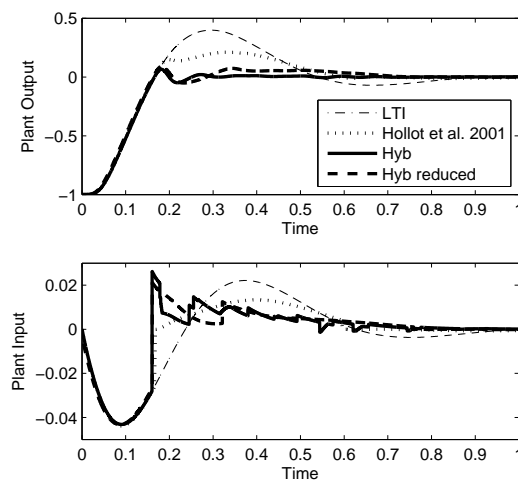


Figure 3.5: Comparison between a FORE by [49], the LTI control and the hybrid controller \mathcal{H}_1 in full order and reduced form.

Table 3.1: Hybrid controller settings.

\bar{P}_p	K_p^\top	κ_M	ρ_y	ρ
★	★	2.3	0.827	$6 \cdot 10^{-4}$
$\begin{bmatrix} 0.0072497 & 0.0071644 \\ 0.0071644 & 0.99994 \end{bmatrix}$	$\begin{bmatrix} -0.0074407 \\ 25.35 \end{bmatrix}$	2.5	0.007	0.16

Figure 3.5 compares the LTI control, the FORE solution from [49] and the hybrid controller \mathcal{H}_1 reset both with the full-order plant state feedback and with the output feedback scheme arising from the approximate technique discussed above. The continuous-time part of the reset controller \mathcal{H}_1 (like for the FORE proposed by [49]) is

$$\left[\begin{array}{c|c} \bar{A}_c & \bar{B}_c \\ \hline C_c & D_c \end{array} \right] = \left[\begin{array}{c|c} -14 & 1 \\ \hline 1 & 0 \end{array} \right].$$

The settings for the full and reduced order controllers \mathcal{H}_1 are in Table 3.1 and have been obtained with the optimal overshoot reduction technique in [71] by selecting κ_M and minimizing ρ_y (using the nomenclature in [71]). For reason of space, the matrices $K_p \in \mathbb{R}^{1 \times 12}$ and $\bar{P}_p \in \mathbb{R}^{12 \times 12}$ for the full-order case are detailed in Appendix 5.4.2 (we fill the corresponding fields in Table 3.1 with a ★). The remaining parameters are the same for both controllers: $P_c = 0.2$ and $\tilde{\alpha} = 10^{-6}$. All the simulations start from the initial conditions $x_{p2}(0,0) = (0,0,0,0,0,0,-0.91)$, $x_{p1}(0,0) = (0,0,0,0,1)$, $x_c(0,0) = 0$ and $\tau(0,0) = \frac{3\rho}{2}$. Note that by selecting $\tau \in (\rho, 2\rho]$ the hybrid controller (3.2) is ready to jump also at the time $(0,0)$. Figure 3.5 illustrates that the hybrid controller based on the full-order plant state for the reset reduces the overshoot better than the FORE. Anyway the approximated and feasible solution with the hybrid controller based on the reduced state for the reset still behaves better than the FORE and the LTI controller.

In Table 3.1, it is possible to note that the solution with the reduced state for resets uses a higher dwell-time parameter ρ . In this way, it is possible to force the system to flow (since the continuous-time feedback is stabilizing) between jumps obtaining a suitable trend of the output (dashed line). Using the techniques in [70, 71] the solution with the reduced order state for the reset would not have been feasible since the approximation errors and the feedforward matrix (namely, D) in the state space approximated model, would have triggered a very large amount of resets. This example is only illustrative but it suggests some further robustness properties given by the addition of the dwell-time logic.

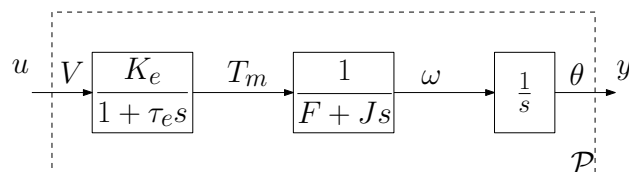


Figure 3.6: Plant block scheme.

3.5.3 A DC motor

For illustrating the technique in Theorem 3.2, we consider a positioning system comprising an electrical DC motor. In particular, let us use a DC motor to place a load in a desired position (namely, the origin). Figure 3.6 represents the series of the DC motor and the load that we are considering, where $K_e = 10$ and $\tau_e = 0.05$ are the electrical gain and time constant of the motor, $F = 1.2$ and $J = 0.5$ are the friction and inertia of the load. Note that $J = 0.5$ corresponds, for example, to the inertia of a cylindric load with radius $R = 0.25\text{m}$ and mass $m = 16\text{Kg}$.

With these parameters, the plant in observer canonical form is

$$\left[\begin{array}{c|c} \bar{A}_p & \bar{B}_p \\ \hline \bar{C}_p & \bar{D}_p \end{array} \right] = \left[\begin{array}{ccc|c} -22.4 & -6 & 0 & 50 \\ 8 & 0 & 0 & 0 \\ 0 & 1 & 0 & 0 \\ \hline 0 & 0 & 1 & 0 \end{array} \right], \quad (3.27)$$

which can be stabilized by the following PI controller whose parameters have been tuned following a typical PI design procedure (see, *e.g.*, [35, Chapter 4.3.4])

$$\left[\begin{array}{c|c} \bar{A}_c & \bar{B}_c \\ \hline \bar{C}_c & \bar{D}_c \end{array} \right] = \left[\begin{array}{c|c} 0 & 0.1250 \\ \hline -0.08 & -0.05 \end{array} \right]. \quad (3.28)$$

Now let us introduce the hybrid loop tuned in such a way to reduce the overshoot induced by the integral action, through the optimization technique in [71, Theorem 3]. For $\kappa_M = 0.1$ (with the notation of [71]) we get

$$\begin{aligned} K_p &= [0.00803345 \quad 0.02347159 \quad 0.09657843], \\ \rho_y &= 0.280961, \\ \bar{P}_p &= \begin{bmatrix} 0.02290376 & 0.06418020 & 0.06227308 \\ 0.06418020 & 0.19173178 & 0.18092975 \\ 0.06227308 & 0.18092975 & 0.95345625 \end{bmatrix}, \end{aligned}$$

where ρ_y is the quantity to be minimized (according to [71]). Then, by selecting $\tilde{\alpha} = 10^{-9}$ (the optimization returns $\alpha = 1.421 \cdot 10^{-8}$), we verify that (3.12) is satisfied by choosing $\mu = 10^{-6}$. Therefore the hybrid controller (3.2) satisfying conditions in Theorem 3.2 is ready with

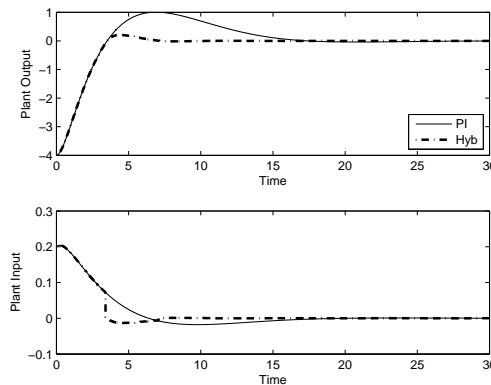


Figure 3.7: DC motor controlled with the technique in Theorem 3.2.

M as in (3.13) and $\rho = 0.004$. Notice that by selecting $\tilde{\alpha}$ the bound in (3.14) is not very performing.

Figure 4.5(a) compares the behavior of the linear closed-loop system with the PI and the arisen hybrid closed-loop system (3.3) obtained by augmenting the PI with the hybrid loop for overshoot reduction. The plant and controller initial conditions are $x_p(0,0) = (0.7, 0, -4)$, $x_c(0,0) = 0$ and $\tau(0,0) = \frac{3\rho}{2}$. Note that by selecting $\tau \in (\rho, 2\rho]$, bound (3.14) can be tightened according to Remark 3.2.

Hybrid controller architectures with plant state estimation

Contents

4.1	Introduction	47
4.2	Overview	48
4.3	Hybrid output feedback with dwell-time logic	50
4.3.1	Problem statement	50
4.3.2	First controller architecture	52
4.3.3	Second controller architecture	57
4.3.4	Comments and remarks	60
4.3.5	Simulations	62
4.4	Hybrid output feedback without dwell-time logic	66
4.4.1	Problem statement	66
4.4.2	Practical asymptotic stability	69
4.4.3	Simulations	74
4.5	Comparisons	75

In this chapter some hybrid output feedback schemes by means of a Luenberger observer are presented. The motivations and the difficulties related to the observer are introduced in Sections 4.1 and 4.2. In Section 4.3, we extend the results of Section 3.3, where a dwell-time logic was used. In Section 4.4, the results of [70] are extended to the output feedback without relying on a dwell-time logic, leading to a new class of hybrid systems. Finally Section 4.5 compares the two proposed solutions and concludes the chapter. All the results here presented have been published in [27, 29].

4.1 Introduction

The results in Chapter 3 can guarantee some desirable control properties like exponential stability and overshoot reduction. Nevertheless as also in [70–72], the hybrid state feedback strongly limits the field of application due to the fact that the plant state is rarely available. This disadvantage makes the FORE controller a preferable choice in the domain of hybrid controllers, although the hybrid architecture in Chapter 3 is easier to design, thanks to the available convex optimal syntheses.

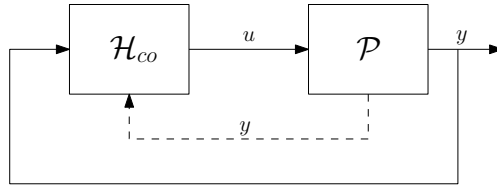


Figure 4.1: Hybrid output feedback.

For this reason, the results in this chapter aim to extend the results in Chapter 3 to the hybrid output feedback (or simply output feedback) case in order to enlarge its field of application. In the next section, the main difficulties arising from the hybrid output scheme are deeply discussed.

4.2 Overview

We want to unleash the schemes in Chapter 3 (and in [70, 71]) from the dependence on the measurement of the plant state, x_p . The idea is to rely on a classical Luenberger observer to get the estimation of the plant state, and to use this estimation to build the hybrid loop (namely, the flow and jump sets and the jump map). As well as before, we focus on hybrid controllers for a continuous-time linear plant \mathcal{P} as

$$\begin{aligned}\dot{x}_p &= \bar{A}_p x_p + \bar{B}_p u \\ y &= \bar{C}_p x_p + \bar{D}_p u\end{aligned}\quad (4.1)$$

where $x_p \in \mathbb{R}^{n_p}$ is the state of the system, $u \in \mathbb{R}^{n_u}$ is the control input, $y \in \mathbb{R}^{n_y}$ is the measured output. Note that \mathcal{P} evolves only according to a differential equation and no resets occur on x_p .

Unlike Chapter 3, no assumption is made on the availability through measurements of the plant state x_p , due to the introduction of a Luenberger observer \mathcal{O} (see [57]), represented as

$$\begin{aligned}\dot{\hat{x}}_p &= \bar{A}_p \hat{x}_p + \bar{B}_p u + L(y - \hat{y}) := A_e \hat{x}_p + B_e u + Ly \\ \hat{y} &= \bar{C}_p \hat{x}_p + \bar{D}_p u\end{aligned}\quad (4.2)$$

where $\hat{x}_p \in \mathbb{R}^{n_p}$ is the estimated state, $u \in \mathbb{R}^{n_u}$ is the control input, $\hat{y} \in \mathbb{R}^{n_y}$ is the estimated output, $A_e := \bar{A}_p - L\bar{C}_p$ and $B_e := \bar{B}_p - L\bar{D}_p$.

In the sequel we will make the following assumption.

Assumption 4.1. The gain L is such that matrix $A_e := \bar{A}_p - L\bar{C}_p$ is Hurwitz. \circ

Figure 4.1 shows the very general idea behind the *hybrid output feedback* that will be presented in this chapter. In particular, the hybrid controller \mathcal{H}_{co} is completely in output feedback with the plant (4.1) and both the *continuous* (represented with a plain line) and the *hybrid feedback* (or equivalently *hybrid loop* and represented by a dashed line) depend only on the plant output, y .

Getting more into details, the hybrid controller \mathcal{H}_{co} we consider, is composed by:

- a continuous-time controller \mathcal{G} , whose state can be reset;
- a supervisor, which decides whether to jump or flow and enforces the resets (see also Section 3.2);

- a linear observer \mathcal{O} .

In particular, Figure 4.2 shows that all the elements of controller \mathcal{H}_{co} depend on the plant output. The plain lines denote continuous flow of information among the blocks, whereas the dashed line denotes the information transmitted only at jumps. Similarly to Chapter 3, the

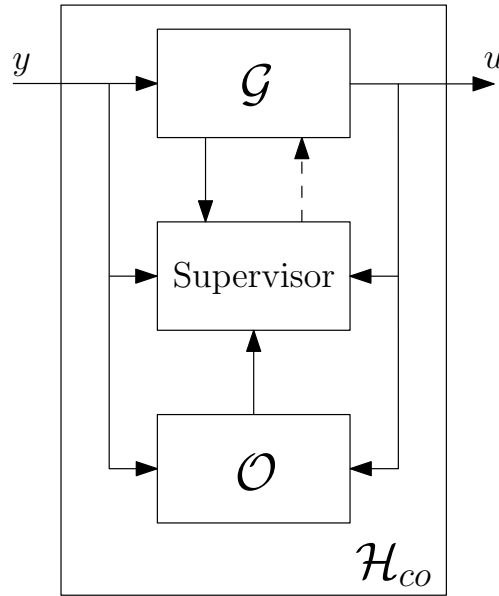


Figure 4.2: Scheme of the hybrid controller with observer, \mathcal{H}_{co} .

controller \mathcal{G} into \mathcal{H}_{co} we consider, is in *linear feedback* with the plant \mathcal{P} . Moreover, the supervisor receives continuous information from the other block and enforces the hybrid loop by resetting the state of \mathcal{G} (dashed line). Nevertheless unlike Chapter 3, the observer \mathcal{O} into \mathcal{H}_{co} transmits the information only to the supervisor. Therefore the observer does not affect directly the linear feedback between \mathcal{G} and \mathcal{P} but contributes to the hybrid loop.

As for the plant \mathcal{P} , the dynamics of \mathcal{O} , and so of the estimated state, \hat{x}_p , evolves only according to a differential equation and no change occurs across jumps. This is an important issue that needs to be taken into account when designing a hybrid controller. The following remark clarifies this fact.

Remark 4.1. Consider the estimation error $e := x_p - \hat{x}_p$ (which is unknown since x_p is not available through measurements), then since $x_p^+ = x_p$ and $\hat{x}_p^+ = \hat{x}_p$, it comes straightforward that $e^+ = e$ and after some calculations one has $\dot{e} = A_e e$. Moreover from Assumption 4.1, A_e is Hurwitz, which guarantees the convergence to zero when flowing. Therefore to guarantee the convergence of e to the origin, Zeno solutions must be removed and in particular in the control schemes presented in this chapter (and similarly to those presented previously), flow after each jump will be ensured so that both Zeno solutions and also consecutive jumps do not occur. \star

In this chapter, two different ways to remove Zeno solutions and guarantee the convergence of e to the origin are presented. As an extension of the results in Chapter 3, Section 4.3 will use a dwell-time logic. On the other hand, in Section 4.4 a modification of the conic flow and jump sets is made to remove Zeno solutions without introducing a dwell time.

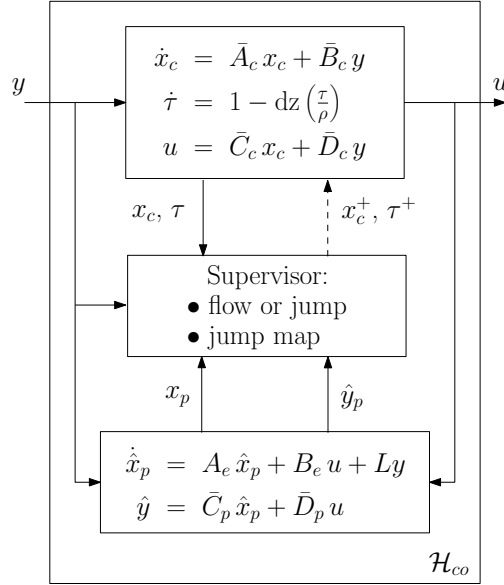


Figure 4.3: Scheme of the hybrid controller with resets from the plant estimation.

The presence of the observer into the control scheme might have the side effect of introducing undesirable behavior during the transient time. To compensate this effect the flow set, jump set and the jump map will be suitably modified (with respect to Chapter 3 and [70]) by using the available but partial information about the estimation error, e , as stated next.

Remark 4.2. The hybrid loops rely on the new available information $\eta := y - \hat{y}$, which returns some information on the estimation error e and, in absence of noise, can be expressed as its linear combination, namely $\eta = \bar{C}_p e$. This information might turn out to be useful to reduce undesired transient time behavior coming from the observer, due to its relation with the subspace, e . In particular, note that whenever $e \rightarrow 0$ then also $\eta \rightarrow 0$ whereas $\eta = 0$ does not imply $e = 0$. Finally, since noise is not taken into account (and according to the dynamics in Remark 4.1), whenever $e(\bar{t}, \bar{j}) = x_p(\bar{t}, \bar{j}) - \hat{x}_p(\bar{t}, \bar{j}) = 0$, then $e(t, j) = 0$ and $\hat{x}_p(t, j) = x_p(t, j)$ for all $(t, j) \in \text{dom}(e)$ with $t \geq \bar{t}$ and $j \geq \bar{j}$. ★

4.3 Hybrid output feedback with dwell-time logic

4.3.1 Problem statement

In this section, we generalize the control techniques stated in Theorems 3.1 and 3.2 to the output feedback case. Figure 4.3 particularizes Figure 4.2 to this case and shows the augmentation of the scheme in Figure 3.2 with the observer. Notice that block \mathcal{G} in Figure 4.2 is replaced here with a linear dynamics with state x_c and a dwell time, as in Chapter 3.

The supervisor accomplishes the same tasks as before, although now the output signal y and estimated output signal \hat{y} enter into the supervisor block due to modifications on the flow and jump sets and the jump map anticipated in Remark 4.2, to mitigate the undesired effects induced by the observer.

The hybrid controller architecture \mathcal{H}_{co} is represented as

$$\begin{cases} \begin{cases} \begin{bmatrix} \dot{\hat{x}}_p \\ \dot{x}_c \end{bmatrix} = \begin{bmatrix} A_e & B_e \bar{C}_c \\ 0 & \bar{A}_c \end{bmatrix} \begin{bmatrix} \hat{x}_p \\ x_c \end{bmatrix} + \begin{bmatrix} B_e \bar{D}_c + L \\ \bar{B}_c \end{bmatrix} y \\ \dot{\tau} = 1 - \text{dz} \left(\frac{\tau}{\rho} \right) \end{cases} & (\hat{x}_p, x_c, e, \tau) \in \mathcal{C} \\ \begin{cases} \begin{bmatrix} \hat{x}_p^+ \\ x_c^+ \end{bmatrix} = \begin{bmatrix} I & 0 \\ K_p & 0 \end{bmatrix} \begin{bmatrix} \hat{x}_p \\ x_c \end{bmatrix} + \begin{bmatrix} 0 \\ K_y \end{bmatrix} \eta \\ \tau^+ = 0 \end{cases} & (\hat{x}_p, x_c, e, \tau) \in \mathcal{D} \\ u = [0 \ \bar{C}_c] \begin{bmatrix} \hat{x}_p \\ x_c \end{bmatrix} + \bar{D}_c y \end{cases} \end{cases} \quad (4.3a)$$

where $\hat{x}_p \in \mathbb{R}^{n_p}$ is the state of the observer, $x_c \in \mathbb{R}^{n_c}$ is the state to reset, $\tau \in [0, 2\rho]$ is the dwell-time logic, A_e and B_e are defined in (4.2) (see also Assumption 4.1) and $\eta \in \mathbb{R}^{n_y}$ is defined in Remark 4.2, the sets \mathcal{C} and \mathcal{D} are

$$\begin{aligned} \mathcal{C} &= \{(\hat{x}_p, x_c, e, \tau) : (\hat{x}_p, x_c, e) \in \mathcal{F} \text{ or } \tau \in [0, \rho]\} \\ &= \{(\hat{x}_p, x_c, e, \tau) : (\hat{x}_p, x_c, e) \in \mathcal{F}\} \cup \{(\hat{x}_p, x_c, e, \tau) : \tau \in [0, \rho]\}, \end{aligned} \quad (4.3b)$$

$$\begin{aligned} \mathcal{D} &= \{(\hat{x}_p, x_c, e, \tau) : (\hat{x}_p, x_c, e) \in \mathcal{J} \text{ and } \tau \in [\rho, 2\rho]\} \\ &= \{(\hat{x}_p, x_c, e, \tau) : (\hat{x}_p, x_c, e) \in \mathcal{J}\} \cap \{(\hat{x}_p, x_c, e, \tau) : \tau \in [\rho, 2\rho]\}, \end{aligned} \quad (4.3c)$$

with \mathcal{F} and \mathcal{J} symmetric cones defined by the matrix $\bar{M} = \bar{M}^\top$ as

$$\mathcal{F} = \left\{ (\hat{x}_p, x_c, e) \in \mathbb{R}^n : \begin{bmatrix} \hat{x}_p \\ x_c \\ e \end{bmatrix}^\top \underbrace{\begin{bmatrix} I & 0 & 0 \\ 0 & I & 0 \\ 0 & 0 & \bar{C}_p \end{bmatrix}^\top \bar{M} \begin{bmatrix} I & 0 & 0 \\ 0 & I & 0 \\ 0 & 0 & \bar{C}_p \end{bmatrix}}_M \begin{bmatrix} \hat{x}_p \\ x_c \\ e \end{bmatrix} \leq 0 \right\}, \quad (4.3d)$$

$$\mathcal{J} = \left\{ (\hat{x}_p, x_c, e) \in \mathbb{R}^n : \begin{bmatrix} \hat{x}_p \\ x_c \\ e \end{bmatrix}^\top \underbrace{\begin{bmatrix} I & 0 & 0 \\ 0 & I & 0 \\ 0 & 0 & \bar{C}_p \end{bmatrix}^\top \bar{M} \begin{bmatrix} I & 0 & 0 \\ 0 & I & 0 \\ 0 & 0 & \bar{C}_p \end{bmatrix}}_M \begin{bmatrix} \hat{x}_p \\ x_c \\ e \end{bmatrix} \geq 0 \right\}, \quad (4.3e)$$

where as stated in Remark 4.1, the state e is unknown, nevertheless according to Remark 4.2, the linear combination $\bar{C}_p e$ is known through the signal η and it can be used to define matrix \bar{M} (and so also M) in the flow and jump sets¹.

Notice that the observer estimation affects the control law u and the continuous-time dynamics of x_c only at jumps. During flow, the observer estimation does not affect directly the dynamics of x_c nor the control signal u , and only the supervisor uses its information to evaluate if the trajectory is in \mathcal{F} or \mathcal{J} .

Let us now introduce the following assumption that will be used in the sequel.

Assumption 4.2. The interconnection (4.1), (4.3) is well-posed, namely the matrix $(I - \bar{D}_p \bar{D}_c)$ is non singular. \circ

¹Matrix \bar{M} is introduced to emphasize the fact that the e -projection of the state space can be used only through the element $\bar{C}_p e$, adding a further constraint on matrix M .

Under Assumption 4.2, the interconnection (4.1) and (4.3) yields the hybrid closed-loop system

$$\begin{cases} \begin{cases} \begin{bmatrix} \dot{\hat{x}}_p \\ \dot{x}_c \\ \dot{e} \end{bmatrix} = \begin{bmatrix} A_p & B_p & B_o \\ B_c & A_c & B_c \\ 0 & 0 & A_e \end{bmatrix} x := Ax \\ \dot{\tau} = 1 - \text{dz}\left(\frac{\tau}{\rho}\right) \end{cases} & (x, \tau) \in \mathcal{C} \\ \begin{cases} x^+ = \begin{bmatrix} I & 0 & 0 \\ K_p & 0 & K_y \bar{C}_p \\ 0 & 0 & I \end{bmatrix} x := Gx \\ \tau^+ = 0 \\ y = [C_p \ C_c \ C_p] x := Cx \end{cases} & (x, \tau) \in \mathcal{D} \end{cases} \quad (4.4)$$

with $x := [\hat{x}_p^\top \ x_c^\top \ e^\top]^\top \in \mathbb{R}^{n:=2n_p+n_c}$, $B_o := L\bar{C}_p + \bar{B}_p\bar{D}_c(I - \bar{D}_p\bar{D}_c)^{-1}\bar{C}_p$ and A_p, B_p, A_c, B_c, C_p and C_c are defined in (3.4) and the flow and jump sets are in (4.3b) and (4.3c).

The hybrid system (4.4) represents the hybrid closed loop in Figure 4.1, whenever the hybrid controller (4.3) is used and moreover, recalls the same structure as (2.1). Moreover, the dwell time removes Zeno solutions and, according to Remark 4.1, this is important to guarantee the convergence of e to the origin. We better explain this phenomenon and particularize it to this control scheme by using the following example.

Example 4.1. Consider (4.4) and the initial condition $x(0,0) := (\hat{x}_p(0,0), x_c(0,0), e(0,0)) = (0,0,a)$, with $a > 0$ and suppose $\eta = \bar{C}_p a = 0$. According to the flow and jump sets² \mathcal{F} and \mathcal{J} , a supervisor without dwell-time logic, may either decide to flow or to jump, and according to the jump map we would have $x^+ = (0,0,a)$, which again belongs both to \mathcal{F} and \mathcal{J} . Therefore without dwell time the system might only jump without that x converges to the origin. ■

Finally, we remark that the control techniques presented in this section are only an extension of the ones in Chapter 3 to the hybrid output feedback and whenever $e = 0$, the results in this section and in Chapter 3 perfectly match and are totally equivalent.

Now we are ready to state the problem we want to solve in this section.

Problem 4.1. Given plant (4.1) and matrices $\bar{A}_c, \bar{B}_c, \bar{C}_c, \bar{D}_c$ and L of controller (4.3) under Assumptions 4.1 and 4.2. Design matrix $\bar{M} = \bar{M}^\top \in \mathbb{R}^{(n_p+n_c+n_y) \times (n_p+n_c+n_y)}$, gains $K_p \in \mathbb{R}^{n_c \times n_p}$, $K_y \in \mathbb{R}^{n_c \times n_y}$ and $\rho > 0$ such that the set $\mathcal{A} := \{0\} \times [0, 2\rho] \subset \mathbb{R}^n \times [0, 2\rho]$ is globally exponentially stable for system (4.4). ◦

4.3.2 First controller architecture

Paralleling Section 3.3.1, we are now ready to present the first hybrid controller. Consider the following statement whose proof is reported next.

Theorem 4.1. Consider a plant-controller pair (4.1), (4.3) under Assumptions 4.1 and 4.2, four parameters K_y, K_x, K_c and K_η and assume that $P = P^\top := \begin{bmatrix} P_p & P_{pc} \\ P_{pc}^\top & P_c \end{bmatrix} > 0$ satisfies (3.5) and (3.6)

²Although we did not define yet the matrix \bar{M} , we have $x(0,0) := (\hat{x}_p(0,0), x_c(0,0), e(0,0)) = (0,0,a)$ and due to the fact that only the $\bar{C}_p e$ is used in \mathcal{F} and \mathcal{J} , we have $x(0,0)^\top M x(0,0) = 0 \in \mathcal{F} \cap \mathcal{J}$.

for some $\alpha > 0$. Then there exists $\bar{\rho} > 0$ such that for all $\rho \in (0, \bar{\rho})$ and $\tilde{\alpha} \in (0, \alpha]$, the hybrid controller (4.3) with

$$\bar{M} := \text{He} \left(\frac{P \begin{bmatrix} A_p & B_p \\ B_c & A_c \end{bmatrix} + \frac{\tilde{\alpha}}{2} P \begin{bmatrix} K_x \\ K_c \end{bmatrix}}{\begin{array}{cc|c} 0 & 0 & K_\eta \end{array}} \right), \quad (4.5)$$

solves Problem 4.1, namely the set $\mathcal{A} := 0 \times [0, 2\rho]$ is globally exponentially stable for the hybrid closed-loop system (4.4) with \bar{M} in (4.5). \square

Proof of Theorem 4.1. As a first step, consider the following change of coordinates: $x = [\hat{x}_p^\top \ x_c^\top \ e^\top]^\top \mapsto \bar{x} := [\hat{x}_p^\top \ \sigma^\top \ e^\top]^\top := [\hat{x}_p^\top (x_c - K_p \hat{x}_p - K_y \bar{C}_p e)^\top \ e^\top]^\top$. In this transformed set of coordinates, it can be verified that the flow dynamics in (4.4) corresponds to (see also (4.3)):

$$\begin{bmatrix} \dot{\hat{x}}_p \\ \dot{\sigma} \\ \dot{e} \end{bmatrix} = \begin{bmatrix} A_p + B_p K_p & A_{12} & A_{13} \\ A_{21} & A_{22} & A_{23} \\ 0 & 0 & A_e \end{bmatrix} \begin{bmatrix} \hat{x}_p \\ \sigma \\ e \end{bmatrix}, \quad (4.6)$$

where $A_{12} := B_p$, $A_{13} := B_o + B_p K_y \bar{C}_p$, $A_{21} := B_c - K_p(A_p + B_p K_p) + A_c K_p$, $A_{22} := A_c - K_p B_p$ and $A_{23} := A_c K_y \bar{C}_p - K_y \bar{C}_p A_e + B_c - K_p(B_o + B_p K_y \bar{C}_p)$ are constant matrices.

Now let us define $V(\hat{x}_p, x_c) := \begin{bmatrix} \hat{x}_p \\ x_c \end{bmatrix}^\top P \begin{bmatrix} \hat{x}_p \\ x_c \end{bmatrix}$, using the identities in (3.6), it can be verified after some calculations that

$$\begin{aligned} \hat{x}_p^\top \bar{P}_p \hat{x}_p + \sigma^\top P_c \sigma &= \begin{bmatrix} \hat{x}_p \\ x_c \end{bmatrix}^\top P \begin{bmatrix} \hat{x}_p \\ x_c \end{bmatrix} + 2 \begin{bmatrix} \hat{x}_p \\ x_c \\ e \end{bmatrix}^\top \begin{bmatrix} \Sigma_{13} \\ \Sigma_{23} \\ \Sigma_{33} \end{bmatrix} e \\ &= V(\hat{x}_p, x_c) + 2 \begin{bmatrix} \hat{x}_p \\ x_c \\ e \end{bmatrix}^\top \Sigma e, \end{aligned} \quad (4.7)$$

where $\Sigma_{13} := K_p^\top P_c K_y \bar{C}_p$, $\Sigma_{23} := -P_c K_y \bar{C}_p$ and $\Sigma_{33} := \frac{1}{2} \bar{C}_p^\top K_y^\top P_c K_y \bar{C}_p$ are constant matrices.

Let us now introduce the function $\varphi(\tau) := \exp((2\rho - \tau)\lambda)$, where $\lambda > 0$ is a scalar to be selected later and note that, for all $\tau \in [0, 2\rho]$, this function satisfies:

$$\begin{aligned} 1 &\leq \varphi(\tau) \leq \exp(2\lambda\rho) \\ \dot{\varphi}(\tau) &= -\lambda \dot{\tau} \varphi(\tau) \leq 0. \end{aligned} \quad (4.8)$$

Based on this equation, we consider the following positive definite and radially unbounded candidate Lyapunov function:

$$W_\xi(\bar{x}, \tau) := \hat{x}_p^\top \bar{P}_p \hat{x}_p + \varphi(\tau) \sigma^\top P_c \sigma + \xi e^\top P_e e, \quad (4.9)$$

where \bar{P}_p and P_c are defined in the statement, $\xi > 0$ is a scalar (to be selected later) and $P_e = P_e^\top > 0$ is the solution to the Lyapunov equation $A_e^\top P_e + P_e A_e = -I$. Note that P_e always exists because A_e is Hurwitz by Assumption 4.2. From (4.8) it follows that for all $\bar{x} \in \mathbb{R}^n$ and for all $\tau \in [0, 2\rho]$,

$$c_1 |\bar{x}|^2 \leq W_\xi(\bar{x}, \tau) \leq c_2 |\bar{x}|^2, \quad (4.10)$$

where $c_1 = \min\{\lambda_{\min}(\bar{P}_p), \lambda_{\min}(P_c), \xi \lambda_{\min}(P_e)\}$ and $c_2 = \max\{\lambda_{\max}(\bar{P}_p), \exp(2\lambda\rho) \lambda_{\max}(P_c), \xi \lambda_{\max}(P_e)\}$.

$\xi \lambda_{\max}(P_e)\}$.

To complete the proof of the theorem, we make use of the following claim, whose proof is reported next.

Claim 4.1. There exist a small enough $\bar{\rho}$ and a large enough ξ^* such that for all $\rho \leq \bar{\rho}$ and all $\xi \geq \xi^*$ the function W_ξ in (4.9) satisfies, for some $\gamma > 0$,

$$\dot{W}_\xi(\bar{x}, \tau) < -\gamma|\bar{x}|^2, \quad T_x \bar{x} \in \mathcal{F} \setminus \{0\} \text{ or } \tau \in [0, \rho] \quad (4.11a)$$

$$\Delta W_\xi(\bar{x}, \tau) \leq 0, \quad T_x \bar{x} \in \mathcal{J} \setminus \{0\} \text{ and } \tau \in [\rho, 2\rho], \quad (4.11b)$$

where $T_x := \begin{bmatrix} I & 0 & 0 \\ K_p & I & K_y \bar{C}_p \\ 0 & 0 & I \end{bmatrix}$ satisfies $x = T_x \bar{x}$. ◦

From the properties (4.10) and (4.11), we can apply [77, Theorem 7.6] to establish that the set \mathcal{A} is stable. Moreover, exponential stability of the set \mathcal{A} comes from [84, Theorem 2] where the nonstrict inequality in (4.11b) is dealt with by exploiting the dwell-time property of temporally regularized solutions. In particular, by decomposing the closed-loop state in its components \bar{x} and τ , conditions 1)-4) of [84, Assumption 1] are satisfied due to (4.10) and (4.11) and because the pair (I, A) (where A is defined in (4.4)) is trivially observable. Finally, condition 5) of [84, Assumption 1] is satisfied because the hybrid solutions obey the dwell-time constraint. Thus, \mathcal{A} is globally exponentially stable, which completes the proof. ■

Proof of Claim 4.1 Equation (4.11b) follows trivially from noticing that the jump rule in (4.4) can be written as $\bar{x}^+ = [\hat{x}_p^{+\top} \sigma^{+\top} e^{+\top}]^\top = [\hat{x}_p^\top 0^\top e^\top]^\top$ and due to the block diagonal structure of W_ξ in (4.9) we have $W_\xi^+ \leq W_\xi$ everywhere, because the second term becomes zero after the jump and the other terms remain unchanged.

To prove equation (4.11a) we separate the analysis in two cases, corresponding to the two flow conditions appearing in (4.11a).

Case 1: $\tau \in [0, \rho]$.

From the special structure of the dynamics in (4.6) and since equation (3.5) holds, then, also using the inequalities in (4.8) and the fact that $\dot{\tau} = 1$ whenever $\tau \in [0, \rho]$, the time-derivative of W_ξ in (4.9) satisfies

$$\begin{aligned} \dot{W}_\xi(\bar{x}, \tau) &= 2\hat{x}_p^\top \bar{P}_p (A_p + B_p K_p) \hat{x}_p + 2\hat{x}_p^\top \bar{P}_p (A_{12}\sigma + A_{13}e) - \lambda\varphi(\tau)\sigma^\top P_c \sigma \\ &\quad + 2\varphi(\tau)\sigma^\top P_c \dot{\sigma} + 2\xi e^\top P_e A_e e \\ &\leq -\tilde{\alpha}\hat{x}_p^\top \bar{P}_p \hat{x}_p - \lambda\sigma^\top P_c \sigma - \xi e^\top e \\ &\quad + 2 \begin{bmatrix} \hat{x}_p \\ \sigma \\ e \end{bmatrix}^\top \begin{bmatrix} 0 & \bar{P}_p A_{12} & \bar{P}_p A_{13} \\ \varphi(\tau)P_c A_{21} & \varphi(\tau)P_c A_{22} & \varphi(\tau)P_c A_{23} \\ 0 & 0 & 0 \end{bmatrix} \begin{bmatrix} \hat{x}_p \\ \sigma \\ e \end{bmatrix}, \end{aligned} \quad (4.12)$$

where A_{ij} , $i = 1, 2$, $j = 1, 2, 3$ are taken from (4.6). Note that the first three terms of the last inequality are negative definite quadratic terms and both ξ and λ can be selected arbitrarily large to complete squares with the mixed terms arising from the fourth term. Moreover, from the first equation in (4.8), $\varphi(\tau)$ is bounded from above and from below and, once λ has been fixed large enough, the upper bound on $\varphi(\tau)$ can be made arbitrarily close to 1 for all $\rho \leq \bar{\rho}_1$, as long as $\bar{\rho}_1 > 0$ is selected small enough. In this way, the terms in which $\varphi(\tau)$ figures can be maintained small. Then, there exist large enough selections of λ and ξ_1 and a small enough $\bar{\rho}_1$ such that for

all $\rho \in [0, \bar{\rho}_1]$ and all $\xi \geq \xi_1$, equation (4.12) implies

$$\dot{W}_\xi(\bar{x}, \tau) \leq -\frac{\tilde{\alpha}}{2}|\bar{x}|^2, \quad \forall \bar{x} \in \mathbb{R}^n \text{ and } \forall \tau \in [0, \rho].$$

Case 2: $T_x \bar{x} \in \mathcal{F}$.

Define $N := \text{He} \left(P \begin{bmatrix} A_p & B_p \\ B_c & A_c \end{bmatrix} \right)$ and note that from the definition of V in the proof of Theorem 4.1 and from (4.4), we get

$$\dot{V}(\hat{x}_p, x_c) = \begin{bmatrix} \hat{x}_p \\ x_c \end{bmatrix}^\top N \begin{bmatrix} \hat{x}_p \\ x_c \end{bmatrix} + 2 \begin{bmatrix} \hat{x}_p \\ x_c \end{bmatrix}^\top P \begin{bmatrix} B_o \\ B_c \end{bmatrix} e, \quad (4.13)$$

Using (4.7), we can rewrite the function W_ξ in (4.9) as follows

$$\begin{aligned} W_\xi(\bar{x}, \tau) &= \hat{x}_p^\top \bar{P}_p \hat{x}_p + \sigma^\top P_c \sigma + (\varphi(\tau) - 1) \sigma^\top P_c \sigma + \xi e^\top P_e e \\ &= V(\hat{x}_p, x_c) + 2 \begin{bmatrix} \hat{x}_p \\ x_c \\ e \end{bmatrix}^\top \Sigma e + (\varphi(\tau) - 1) \sigma^\top P_c \sigma + \xi e^\top P_e e. \end{aligned}$$

Therefore, from the flow set definition in (4.3d) where M depends on \bar{M} in (4.5), using (4.13) and (4.8), we get

$$\begin{aligned} \dot{W}_\xi(\bar{x}, \tau) &= \begin{bmatrix} \hat{x}_p \\ x_c \end{bmatrix}^\top N \begin{bmatrix} \hat{x}_p \\ x_c \end{bmatrix} + 2 \begin{bmatrix} \hat{x}_p \\ x_c \\ e \end{bmatrix}^\top \left(\Sigma A_e + \begin{bmatrix} P \begin{bmatrix} B_o \\ B_c \end{bmatrix} \\ 0 \end{bmatrix} + A^\top \Sigma \right) e \\ &\quad - \lambda \dot{\tau} \varphi(\tau) \sigma^\top P_c \sigma + 2(\varphi(\tau) - 1) \sigma^\top P_c \dot{\sigma} + 2\xi e^\top P_e \dot{e} \\ &\leq -\tilde{\alpha} \begin{bmatrix} \hat{x}_p \\ x_c \end{bmatrix}^\top P \begin{bmatrix} \hat{x}_p \\ x_c \end{bmatrix} + 2 \begin{bmatrix} \hat{x}_p \\ x_c \\ e \end{bmatrix}^\top \left(\Sigma A_e + \begin{bmatrix} P \begin{bmatrix} B_o \\ B_c \end{bmatrix} \\ 0 \end{bmatrix} + A^\top \Sigma + \begin{bmatrix} K_x \bar{C}_p \\ K_c \bar{C}_p \\ \bar{C}_p^\top K_\eta \bar{C}_p \end{bmatrix} \right) e \\ &\quad + 2(\varphi(\tau) - 1) \sigma^\top P_c \dot{\sigma} - \xi |e|^2 \\ &= -\tilde{\alpha} \begin{bmatrix} \hat{x}_p \\ x_c \end{bmatrix}^\top P \begin{bmatrix} \hat{x}_p \\ x_c \end{bmatrix} + 2 \begin{bmatrix} \hat{x}_p \\ x_c \\ e \end{bmatrix}^\top \begin{bmatrix} Z_{13} \\ Z_{23} \\ Z_{33} \end{bmatrix} e + \kappa(\tau, \rho) x^\top \Xi x - \xi |e|^2, \end{aligned} \quad (4.14)$$

where Z_{i3} , $i = 1, 2, 3$ are suitable matrices, $\Xi := \bar{T}^{-\top} \begin{bmatrix} P_c A_{21} & P_c A_{22} & P_c A_{23} \\ 0 & 0 & 0 \end{bmatrix} \bar{T}^{-1}$ is defined in such a way that $x^\top \Xi x = \sigma^\top P_c \dot{\sigma}$ and, from (4.8), $\kappa(\tau, \rho) = 2(\varphi(\tau) - 1)$ satisfies $0 \leq \kappa(\tau, \rho) \leq 2(\exp(2\rho\lambda) - 1)$, namely for any fixed value of λ , $\kappa(\tau, \rho)$ can be made arbitrarily small by selecting ρ sufficiently small. Due to this fact, it follows that, once λ has been fixed according to Case 1 above, it is possible to select $\bar{\rho}_2$ sufficiently small and ξ_2 sufficiently large such that for all $\rho \in [0, \bar{\rho}_2]$, and $\xi \geq \xi_2$, inequality (4.14) implies

$$\dot{W}_\xi(\bar{x}, \tau) \leq -\frac{\tilde{\alpha}}{2} \lambda_{\min}(P) |x|^2, \quad \forall T_x \bar{x} \in \mathcal{F}, \forall \tau \in [0, 2\rho].$$

Finally, combining the studies in Cases 1 and 2 above, the proof of (4.11a) follows from picking $\bar{\rho} = \min\{\bar{\rho}_1, \bar{\rho}_2\}$, $\xi^* = \max\{\xi_1, \xi_2\}$ and $\gamma = \frac{\tilde{\alpha}}{2} \min\{1, \lambda_{\min}(P) \lambda_{\min}(T_x^\top T_x)\}$. \blacksquare

Theorem 4.1 shares some similarities with Theorem 3.1. In particular, conditions (3.5) and (3.6) are required and moreover the entry (1,1) of matrix \bar{M} in (4.5) exactly corresponds to M in Theorem 3.1. On the other hand, Theorem 4.1 presents new gains due to the e -dimension of the state space. Although gain L (see Assumption 4.1) is the only one that guarantees convergence of the error to the origin, gains K_y, K_x, K_c, K_η might play an important role in reducing undesired transient time behavior due to the observer estimation (see also Remark 4.2).

Theorem 4.1 only establishes the stability properties of the *hybrid output feedback* solution proposed here, whereas it does not highlight its strong relation with the parallel *hybrid state feedback* of [70–72]. Such a relation is established in the next proposition. In the following statement we use the notion of solutions (T, J, ε) -close and ε -close, whose definition can be found in Definition 1.8, see also [41].

Proposition 4.1. Consider the *hybrid state feedback* of [70, Proposition 1] and the *hybrid output feedback* (4.4) of Theorem 4.1. There exists $\bar{\rho} > 0$ such that for all $\rho \in (0, \bar{\rho})$ the following hold:

1. any solution to the *hybrid state feedback* of [70, Proposition 1], starting from $(x_p(0,0), x_c(0,0)) = (x_{p0}, x_{c0})$, with $x_{p0} \neq 0$, is also the (x_p, x_c) -component of a solution to the *hybrid output feedback* (4.4) of Theorem 4.1, starting from $\xi(0,0) = (\hat{x}_p(0,0), x_c(0,0), e(0,0), \tau(0,0)) = (x_{p0}, x_{c0}, 0, \tau_0)$ with $\tau_0 \geq \rho$;
2. for each $\varepsilon > 0$, there exists $\delta > 0$ such that the (x_p, x_c) -component of any solution to the *hybrid output feedback* (4.4) of Theorem 4.1, starting from $\xi(0,0) = (\hat{x}_p(0,0), x_c(0,0), e(0,0), \tau(0,0)) = (x_{p0}, x_{c0}, e_0, \tau_0)$ with $x_{p0} \neq 0$, $\tau_0 \geq \rho$ and $|e_0| \leq \delta|(x_{p0}, x_{c0})|$ is $\varepsilon|(x_{p0}, x_{c0})|$ -close to a solution to the *hybrid state feedback* of [70, Proposition 1], starting from $(x_p(0,0), x_c(0,0)) = (x_{p0}, x_{c0})$.

□

Proof of Proposition 4.1 Let us consider item 1. First note that due to the cascaded structure of the system (4.4), if $e(0,0) = 0$, then $e(t,j) = 0$ for all $(t,j) \in \text{dom}(\xi)$. Therefore the observer dynamics does not affect the system and it is sufficient to show that there exists $\bar{\rho} > 0$ such that all the solutions to the hybrid state feedback corresponding to [70, Proposition 1], automatically satisfy a dwell time of at least $\bar{\rho}$, as long as $x_p(0,0) \neq 0$, so that the dwell-time condition does not prevent any jump of the original hybrid state feedback scheme.

To prove this property, note that $x_p(0,0) \neq 0$ implies $x_p(t,j) \neq 0$ for all $(t,j) \in \text{dom}(\xi)$, indeed during flows x_p asymptotically converges to zero and during jumps it remains unchanged. Since x_p is never zero, whenever a jump occurs, so that $(x_p, x_c, 0) \in \mathcal{J}$, then $(x_p^+, x_c^+, e^+) = (x_p, K_p x_p, 0)$ belongs to the interior of \mathcal{F} (due to the fact that $\bar{\alpha} \leq \alpha$ and by the strict inequality in (3.5)), therefore from continuity it necessarily flows for some time $t_f(x_p)$ which depends on the plant state x_p at the jump time. Since the dynamics is homogeneous and the flow and jump sets are symmetric cones, then each response can be written as a scaled version of the response starting from the initial condition with unit norm $\frac{x_p}{|x_p|}$. Due to this fact, we can compute

$$\min_{x_p \neq 0} t_f(x_p) = \min_{x_p: |x_p|=1} t_f(x_p) = t_{fm},$$

where we have $t_{fm} > 0$ because the minimum is carried out over a compact set and $t_f(x_p) > 0$ for all $x_p \neq 0$. Finally, it is sufficient to pick $\bar{\rho} \leq t_{fm}$ to obtain the result at item 1.

Consider now item 2 and note that, from item 1, any solution to the hybrid state feedback of [70] is a solution to (4.4) starting from $e(0,0) = 0$ and $\tau(0,0) \geq \rho$. Therefore we prove this item by only focusing on two solutions ξ_o and ξ_1 to (4.4), where $\xi_o(0,0) = (x_{p0}, x_{c0}, 0, \tau_0)$ and $\xi_1(0,0) = (x_{p0}, x_{c0}, e_0, \tau_0)$. To this aim, we first establish the result for the case $|(x_{p0}, x_{c0})| = 1$ and then apply homogeneity to extend it to the whole space.

First note that from global exponential stability of (4.4), uniform convergence implies that for each $\varepsilon > 0$, $\exists(T_\varepsilon, J_\varepsilon) \in \mathbb{R}_{\geq 0} \times \mathbb{Z}_{\geq 0}$ such that for all solutions $\xi := (x, \tau) := (\hat{x}_p, x_c, e, \tau)$ to (4.4)

$$\begin{aligned} \frac{|(x_{p0}, x_{c0})|}{|e_0|} &= 1 \Rightarrow |x(t, j)| \leq \frac{\varepsilon}{2}, \quad \forall(t, j) \geq (T_\varepsilon, J_\varepsilon), (t, j) \in \text{dom}(\xi). \end{aligned} \quad (4.15)$$

Moreover, since the hybrid system (4.4) satisfies the fundamental conditions (A0)-(A4) of [41] and are forward complete, given two solutions $\xi_o = (x_o, \tau_o)$, $\xi_1 = (x_1, \tau_1)$ starting from the compact set $|(x_{p0}, x_{c0})| = 1$, $|e_0| \leq 1$ and $\tau_0 \in [0, 2\rho]$ and given $\varepsilon, T_\varepsilon, J_\varepsilon$ in (4.15), from [41, Corollary 4.8], there exists $\delta_N > 0$ such that $|e_0| \leq \delta_N$ implies that ξ_o and ξ_1 are $(T_\varepsilon, J_\varepsilon, \varepsilon)$ -close. Outside the compact hybrid time domain $(T_\varepsilon, J_\varepsilon)$, from (4.15), we get

$$|x_o(t, j) - x_1(t, j)| \leq |x_o(t, j)| + |x_1(t, j)| \leq \varepsilon, \quad \forall(t, j) \geq (T_\varepsilon, J_\varepsilon).$$

Therefore, combining the two bounds above, we have

$$\begin{aligned} \frac{|(x_{p0}, x_{c0})|}{|e_0|} &= 1 \Rightarrow (x_o, x_1) \text{ are } \varepsilon\text{-close}, \end{aligned} \quad (4.16)$$

where $\delta := \min\{1, \delta_N\}$. The proof is completed by extending the result to the whole space by using the homogeneity of system (4.4). In particular, noticing that the x component of any solution $\xi = (x, \tau)$, starting from $\xi(0,0) = (x_{p0}, x_{c0}, e_0, \tau_0)$ with $x_{p0} \neq 0$, can be written as $\xi = (|(x_{p0}, x_{c0})|x_N, \tau)$, with $x_N := \frac{x}{|(x_{p0}, x_{c0})|} = (x_{pN}, x_{cN}, e_N)$ satisfying $|(x_{pN}(0,0), x_{cN}(0,0))| = \frac{|(x_{p0}, x_{c0})|}{|(x_{p0}, x_{c0})|} = 1$ and $|e_N(0,0)| = \frac{e_0}{|(x_{p0}, x_{c0})|}$, the bound in (4.16) implies that for any $|e_0| \leq |(x_{p0}, x_{c0})|\delta$, the components x_o, x_1 of ξ_o and ξ_1 (therefore, also their (\hat{x}_p, x_c) -components) are $\varepsilon|(x_{p0}, x_{c0})|$ -close. \blacksquare

As it will be clearer later in the sequel, the optimal selection of gains K_y, K_x, K_c and K_η is still unclear. Therefore to simplify the presentation of the results in the sequel, we introduce the following result which can be considered as a corollary of Theorem 4.1, where such gains are selected null.

Corollary 4.1. Consider a plant-controller pair (4.1), (4.3) under Assumptions 4.1 and 4.2, with K_y, K_x, K_c, K_η null matrices and assume that $P = P^\top := \begin{bmatrix} P_p & P_{pc} \\ P_{pc}^\top & P_c \end{bmatrix} > 0$ satisfies (3.5) and (3.6) for some $\alpha > 0$. Then there exists $\bar{\rho} > 0$ such that for all $\rho \in (0, \bar{\rho})$ and $\tilde{\alpha} \in (0, \alpha)$, the hybrid controller (4.3) with \bar{M} in (4.5) solves Problem 4.1, namely the set $\mathcal{A} := 0 \times [0, 2\rho]$ is globally exponentially stable for the hybrid closed-loop system (4.4) with \bar{M} in (4.5). \square

4.3.3 Second controller architecture

Paralleling Section 3.3.2, we focus now on the second hybrid output feedback scheme.

Theorem 4.2. Consider a plant-controller pair (4.1), (4.3) under Assumptions 4.1 and 4.2, five parameters $\mu > 0$, K_y , K_x , K_c , K_η and assume that $\bar{P}_p = \bar{P}_p^\top > 0$, $K_p \in \mathbb{R}^{n_c \times n_p}$ satisfy (3.5) for some $\alpha > 0$. Then there exists $\bar{\rho} > 0$ such that for all $\rho \in (0, \bar{\rho})$ and $\tilde{\alpha} \in (0, \alpha]$, the hybrid controller (4.3) with

$$\bar{M} := \text{He} \left(\left[\begin{array}{cc|c} \bar{P}_p A_p + \frac{\tilde{\alpha}}{2} \bar{P}_p & \bar{P}_p B_p & K_x \\ 0 & \frac{\mu}{2} I & K_c \\ \hline 0 & 0 & K_\eta \end{array} \right] \right), \quad (4.17)$$

solves Problem 4.1, namely the set $\mathcal{A} := 0 \times [0, 2\rho]$ is globally exponentially stable for the hybrid closed-loop system (4.4) with \bar{M} in (4.17). \square

Proof of Theorem 4.2. Consider (4.6) and (4.8) and the following positive definite and radially unbounded Lyapunov function candidate

$$\bar{W}_{\xi_\sigma, \xi_e}(\bar{x}, \tau) := \hat{x}_p^\top \bar{P}_p \hat{x}_p + \xi_\sigma \varphi(\tau) \sigma^\top \sigma + \xi_e e^\top P_e e \quad (4.18)$$

where $\xi_\sigma > 0$ and $\xi_e > 0$ are scalars (to be selected later) and $P_e = P_e^\top > 0$ is the solution to the Lyapunov equation $A_e^\top P_e + P_e A_e = -I$. P_e always exists by Assumption 4.2. Note that from (4.8), it follows that for all $\bar{x} \in \mathbb{R}^n$ and for all $\tau \in [0, 2\rho]$,

$$c_1 |\bar{x}|^2 \leq \bar{W}_{\xi_\sigma, \xi_e}(\bar{x}, \tau) \leq c_2 |\bar{x}|^2, \quad (4.19)$$

where $c_1 = \min\{\lambda_{\min}(\bar{P}_p), \xi_\sigma, \xi_e \lambda_{\min}(P_e)\}$ and $c_2 = \max\{\lambda_{\max}(\bar{P}_p), \xi_\sigma \exp(2\lambda\rho), \xi_e \lambda_{\max}(P_e)\}$.

The proof of the theorem is completed by following the same steps as those described at the end of the proof of Theorem 4.1, using the following claim, which corresponds to Claim 4.1 rewritten for the case addressed here.

Claim 4.2. There exist positive numbers λ , ξ_σ and ξ_e , and a small enough $\bar{\rho}$ such that for all $\rho \leq \bar{\rho}$ the function $\bar{W}_{\xi_\sigma, \xi_e}$ in (4.18) satisfies, for some $\gamma > 0$,

$$\dot{\bar{W}}_{\xi_\sigma, \xi_e}(\bar{x}, \tau) < -\gamma |\bar{x}|^2, \quad T_x \bar{x} \in \mathcal{F} \setminus \{0\} \text{ or } \tau \in [0, \rho] \quad (4.20a)$$

$$\Delta \bar{W}_{\xi_\sigma, \xi_e}(\bar{x}, \tau) \leq 0, \quad T_x \bar{x} \in \mathcal{J} \setminus \{0\} \text{ and } \tau \in [\rho, 2\rho], \quad (4.20b)$$

where $T_x := \begin{bmatrix} I & 0 & 0 \\ K_p & I & K_y \bar{C}_p \\ 0 & 0 & I \end{bmatrix}$ satisfies $x = T_x \bar{x}$. \circ

This completes the proof of Theorem 4.2. \blacksquare

Proof of Claim 4.2 Equation (4.20b) follows trivially from noticing that the jump rule in (4.4) can be written as $\bar{x}^+ = [\hat{x}_p^{+\top} \sigma^{+\top} e^{+\top}]^\top = [\hat{x}_p^\top 0^\top e^\top]^\top$ and due to the block diagonal structure of $\bar{W}_{\xi_\sigma, \xi_e}$ in (4.18) we have $\bar{W}_{\xi_\sigma, \xi_e}^+ \leq \bar{W}_{\xi_\sigma, \xi_e}$ everywhere, because the second term becomes zero after the jump and the other terms remain unchanged.

To prove equation (4.20a), we compute the time-derivative of $\bar{W}_{\xi_\sigma, \xi_e}$ in two cases, corresponding to the two flow conditions appearing in (4.20a). Then, we combine the analysis of such cases.

Case 1: $\tau \in [0, \rho]$.

From the special structure of the dynamics in (4.6) and since equation (3.5) holds, then, also using the inequalities in (4.8) and the fact that $\dot{\tau} = 1$ whenever $\tau \in [0, \rho]$, the time-derivative of $\bar{W}_{\xi_\sigma, \xi_e}$ in (4.18) satisfies

$$\dot{\bar{W}}_{\xi_\sigma, \xi_e}(\bar{x}, \tau) = 2\hat{x}_p^\top \bar{P}_p (A_p + B_p K_p) \hat{x}_p + 2\hat{x}_p^\top \bar{P}_p (A_{12} \sigma + A_{13} e) - \lambda \xi_\sigma \varphi(\tau) \sigma^\top \sigma$$

$$\begin{aligned}
& + 2\xi_\sigma\varphi(\tau)\sigma^\top\dot{\sigma} + 2\xi_e e^\top P_e A_e e \\
\leq & -\tilde{\alpha}\hat{x}_p^\top \bar{P}_p \hat{x}_p - \lambda\xi_\sigma\sigma^\top\sigma - \xi_e e^\top e \\
& + 2 \begin{bmatrix} \hat{x}_p \\ \sigma \\ e \end{bmatrix}^\top \begin{bmatrix} 0 & \bar{P}_p A_{12} & \bar{P}_p A_{13} \\ \varphi(\tau)\xi_\sigma A_{21} & \varphi(\tau)\xi_\sigma A_{22} & \varphi(\tau)\xi_\sigma A_{23} \\ 0 & 0 & 0 \end{bmatrix} \begin{bmatrix} \hat{x}_p \\ \sigma \\ e \end{bmatrix}, \quad (4.21)
\end{aligned}$$

where A_{ij} , $i = 1, 2$, $j = 1, 2, 3$ are taken from (4.6). Note that the first three terms of the last inequality are negative and that ξ_e , $\lambda\xi_\sigma$ can be adjusted by choosing ξ_σ , ξ_e and λ in (4.18). In particular, since from (4.8), $1 \leq \varphi(\tau) \leq \exp(2\lambda\rho)$, then there exist positive numbers $c_{\sigma 1}$, $c_{\rho 1}$ and ξ_{e1} such that

$$\lambda\xi_\sigma \geq c_{\sigma 1}, \quad \lambda\rho \leq c_{\rho 1}, \quad \xi_e \geq \xi_{e1}. \quad (4.22)$$

Then (4.21) implies:

$$\dot{\bar{W}}_{\xi_\sigma, \xi_e}(\bar{x}, \tau) \leq -\frac{\tilde{\alpha}}{2}|\bar{x}|^2, \quad \forall \bar{x} \in \mathbb{R}^n \text{ and } \forall \tau \in [0, \rho].$$

Case 2: $T_x \bar{x} \in \mathcal{F}$.

Using \mathcal{F} in (4.3d) defined by \bar{M} in (4.17) and the equations in (4.8), we get for all $T_x \bar{x} = x \in \mathcal{F}$,

$$\begin{aligned}
\dot{\bar{W}}_{\xi_\sigma, \xi_e}(\bar{x}, \tau) & = 2\hat{x}_p^\top \bar{P}_p (A_p \hat{x}_p + B_p x_c) + 2\hat{x}_p^\top \bar{P}_p B_o e - \dot{\tau} \lambda \xi_\sigma \varphi(\tau) \sigma^\top \sigma + 2\xi_\sigma \varphi(\tau) \sigma^\top \dot{\sigma} + 2\xi_e e^\top P_e A_e e \\
& \leq \begin{bmatrix} \hat{x}_p \\ x_c \end{bmatrix}^\top \begin{bmatrix} -\tilde{\alpha}\bar{P}_p & 0 \\ 0 & -\mu I \end{bmatrix} \begin{bmatrix} \hat{x}_p \\ x_c \end{bmatrix} + 2 \begin{bmatrix} \hat{x}_p \\ x_c \\ e \end{bmatrix}^\top \begin{bmatrix} K_x \bar{C}_p \\ K_c \bar{C}_p \\ \bar{C}_p^\top K_\eta \bar{C}_p \end{bmatrix} e + 2\hat{x}_p^\top \bar{P}_p B_o e \\
& \quad + 2\xi_\sigma \varphi(\tau) \sigma^\top \dot{\sigma} - \xi_e |e|^2 \\
& = \begin{bmatrix} \hat{x}_p \\ x_c \end{bmatrix}^\top \begin{bmatrix} -\tilde{\alpha}\bar{P}_p & 0 \\ 0 & -\mu I \end{bmatrix} \begin{bmatrix} \hat{x}_p \\ x_c \end{bmatrix} + 2\xi_\sigma \varphi(\tau) x^\top \Xi x + \begin{bmatrix} \hat{x}_p \\ x_c \\ e \end{bmatrix}^\top \begin{bmatrix} Z_{13} \\ Z_{23} \\ Z_{33} \end{bmatrix} e - \xi_e |e|^2, \quad (4.23)
\end{aligned}$$

where Z_{i3} $i = 1, 2, 3$ are suitable matrices, $\Xi := \bar{T}^{-\top} \begin{bmatrix} 0 & 0 & 0 \\ A_{21} & A_{22} & A_{23} \\ 0 & 0 & 0 \end{bmatrix} \bar{T}^{-1}$ is defined in such a way that $x^\top \Xi x = \sigma^\top \dot{\sigma}$. At the right hand side of (4.23) we find a first term providing good quadratic decrease in \hat{x}_p and x_c , followed by a second bad term which can be made arbitrarily small by choosing ξ_σ (and $\lambda\rho$ too, due to the term $\varphi(\tau)$ – see (4.8)) small enough, followed by two terms providing mixed and quadratic terms in e which can be dominated by selecting ξ_e large enough. In particular, since $\varphi(\cdot)$ is bounded (see (4.8)), there exist positive numbers $c_{\sigma 2}$, $c_{\rho 2}$ and ξ_{e2} such that if

$$\xi_\sigma \leq c_{\sigma 2}, \quad \lambda\rho \leq c_{\rho 2}, \quad \xi_e \geq \xi_{e2}, \quad (4.24)$$

then

$$\dot{\bar{W}}_{\xi_\sigma, \xi_e}(\bar{x}, \tau) \leq -\frac{1}{2} \min\{\tilde{\alpha}, \mu\} |\bar{x}|^2, \quad \forall T_x \bar{x} \in \mathcal{F} \text{ and } \forall \tau \in [0, 2\rho].$$

Now let us consider (4.22) and (4.24). To satisfy them both, so that the analysis in the two cases above holds, we can select $\xi_\sigma = c_{\sigma 2}$, $\lambda = \frac{c_{\sigma 1}}{c_{\sigma 2}}$, $\xi_e \geq \max\{\xi_{1e}, \xi_{2e}\}$ and $\bar{\rho} = \frac{c_{\rho 2}}{c_{\sigma 1}} \min\{c_{\rho 1}, c_{\rho 2}\}$.

Then for any $\rho \leq \bar{\rho}$, (4.22) and (4.24) hold and the proof of the claim holds too with $\gamma = \frac{1}{2} \min\{\tilde{\alpha}, \mu\} \min\{1, \lambda_{\min}(T_x^\top T_x)\}$. ■

Theorem 4.2 has some structural differences with respect to Theorem 3.2. In particular, condition (3.12) is not required and no exponential bound similar to (3.14) is established. Although Claim 2.1 was used in the proof of Theorem 3.2 to establish (3.14) (see also Remark 3.1), in Theorem 4.2 it is not possible to establish an exponential bound in the x_p -direction with the same tools, due to the presence of the observer.

As well as Theorem 4.1, Theorem 4.2 presents new gains with respect to Theorem 3.2, related to the introduction of the observer and, perhaps, able to reduce its undesired transient effects (see Remark 4.2).

We cannot establish an equivalent statement to Proposition 4.1 with reference to the scheme in Theorem 4.2 and the hybrid state feedback of [70, Proposition 2] and [71]. Indeed, as emphasized in Section 3.3.2, the flow and jump sets considered in [70–72] correspond to the ones in (4.3d) and (4.3e) with \bar{M} in (4.17) where $e = 0$ and $\mu = 0$. Due to this fact, since we require $\mu > 0$ here, we cannot say that the solutions to (4.4) defined in Theorem 4.2 graphically converge to those of the corresponding hybrid state feedback of [70–72]. Nevertheless, since the system with a small $\mu > 0$ corresponds to a perturbation of the system with $\mu = 0$, we can state by relying on the results of [41] that the arising trajectories can be made arbitrarily close to those of the hybrid state feedback law of [70, Proposition 2] and [71] by choosing μ arbitrarily small.

Similarly to Section 4.3.2, we state the following corollary of Theorem 4.2.

Corollary 4.2. Consider a plant-controller pair (4.1), (4.3) under Assumptions 4.1 and 4.2, a parameter $\mu > 0$ and K_y, K_x, K_c, K_η null matrices and assume that $\bar{P}_p = \bar{P}_p^\top > 0$, $K_p \in \mathbb{R}^{n_c \times n_p}$ satisfy (3.5) for some $\alpha > 0$. Then there exists $\bar{\rho} > 0$ such that for all $\rho \in (0, \bar{\rho})$ and $\tilde{\alpha} \in (0, \alpha]$, the hybrid controller (4.3) with \bar{M} in (4.17) solves Problem 4.1, namely the set $\mathcal{A} := 0 \times [0, 2\rho]$ is globally exponentially stable for the hybrid closed-loop system (4.4) with \bar{M} in (4.17). □

4.3.4 Comments and remarks

The results presented can be viewed as the output feedback version of the results in Chapter 3. In particular, under exactly the same conditions of Theorems 3.1 and 3.2, it is enough to add a Luenberger observer satisfying Assumption 4.1, to obtain the hybrid output feedback, with four extra free gains (*i.e.*, K_y, K_x, K_c, K_η) to reduce the undesired effects induced by the observer during the transient time.

In this section, we present some common features of Theorems 4.1 and 4.2. First, consider the results in Section 3.3. The next statement emphasizes a few similarities between the solutions to the *hybrid state feedback* and the *hybrid output feedback* schemes. The proof is omitted because it is identical to the proof of Proposition 4.1.

Proposition 4.2. Consider the *hybrid state feedback* of Theorems 3.1 and 3.2 and the *hybrid output feedback* (4.4) of Theorems 4.1 and 4.2. Then the following holds:

1. any solution to that *hybrid state feedback* of Theorem 3.1 (respectively Theorem 3.2) starting from $(x_p(0,0), x_c(0,0), \tau(0,0)) = (x_{p0}, x_{c0}, \tau_0)$ is also a solution to the *hybrid output feedback* (4.4) of Theorem 4.1 (respectively Theorem 4.2) starting from $\xi(0,0) = (\hat{x}_p(0,0), x_c(0,0), e(0,0), \tau(0,0)) = (x_{p0}, x_{c0}, 0, \tau_0)$;
2. for each $\varepsilon > 0$, there exists $\delta > 0$ such that the (x_p, x_c) -component of any solution to the *hybrid output feedback* (4.4) of Theorem 4.1 (respectively Theorem 4.2) starting from $\xi(0,0) = (\hat{x}_p(0,0), x_c(0,0), e(0,0), \tau(0,0)) = (x_{p0}, x_{c0}, e_0, \tau_0)$ with $x_{p0} \neq 0$ and $|e_0| \leq \delta |x_{p0}, x_{c0}|$ is $\varepsilon |x_{p0}, x_{c0}|$ -close to a solution to the *hybrid state feedback* of Theorem 3.1 (respectively Theorem 3.2) starting from $(x_p(0,0), x_c(0,0), \tau(0,0)) = (x_{p0}, x_{c0}, \tau_0)$.

□

The presented control schemes embed an observer to solve the hybrid output feedback case (see Problem 4.1). Nevertheless from the proof technique, it turns out that only the gain L (see Assumption 4.1) is responsible for the convergence of the error to the origin. Indeed, the remaining new gains related to the hybrid output feedback (that is K_y , K_x , K_c and K_η) do not affect the stability property of the schemes but they might play an important role in reducing the side effects coming from the observer (see Remark 4.2). Although it is still unclear how to select these gains, the following remark clarifies a bit these aspects.

Remark 4.3. According to the control schemes of Theorems 4.1 and 4.2, in (4.4) and in the sets defined by (4.5) and (4.17), the matrices K_y , K_x , K_c , K_η can be selected completely free. Notice that all these matrices are multiplied by η and that in particular, K_y appears into the jump map of (4.3) (see also (4.4)), whereas K_x , K_c , K_η shape sets \mathcal{F} and \mathcal{J} in the η -direction. In particular, since $\eta = \bar{C}_p e$ in absence of noise and since $\lim_{t+j \rightarrow \infty} e(t, j) = 0$ implies $\lim_{t+j \rightarrow \infty} \eta(t, j) = 0$ (see also Remark 4.2), these terms become ineffective once the error approaches zero. Nevertheless, during the observer estimation transient, when $e \neq 0$ and possibly $\eta = \bar{C}_p e \neq 0$ as well, nonzero selections of these parameters can beneficially modify the transient response. For example, it may be useful to choose K_η negative definite and possibly large as this will enlarge the flow set (see (4.5) or (4.17)) in the η -direction so that jumps are inhibited when $\eta = \bar{C}_p e$ is large. This is reasonable, because the jump map involves the estimated state, \hat{x}_p , and might (transiently) assign the controller state to an inaccurate value when the estimation error is large. On the other hand, the gain K_y may affect in a beneficial way the jump map when the output error is nonzero and may be manually tuned by inspecting the closed-loop response when the error is large (it is recalled that these gains essentially have no effect after the estimation error becomes small). The potential behind K_x , K_c remains unclear and no specific tuning rule is available. ★

Remark 3.5 still holds for Theorems 4.1 and 4.2 except for item b, which is true only whenever $e = 0$. In particular when $e = 0$, sets \mathcal{F} and \mathcal{J} of Theorem 4.1 (respectively, Theorem 4.2) match sets \mathcal{F} and \mathcal{J} of Theorem 3.1 (respectively, Theorem 3.2). Therefore since e tends to zero, the two pairs of sets always match after the observer transient time. Moreover, all the considerations in Section 3.4 on condition (3.5) still hold. This justifies the use of the optimal synthesis for overshoot reduction in [72].

We stress that the control schemes in this section match the representation (2.1), so that the framework in Chapter 2 can be used to prove the results here presented.

All the comments about Theorems 4.1 and 4.2 hold also for their corollaries. The interest in the corollaries is that they have a simpler implementation since the flow and jump sets are defined based on a smaller subset of parameters and simplify the illustration of the results through simulations.

4.3.5 Simulations

Due to the similarities of the control techniques so far presented, to accomplish the synthesis of the hybrid control schemes one can use the procedure presented in Section 3.5 (recall that Theorem 4.1 requires all the steps, whereas Theorem 4.2 requires only the first two) and add the two further steps:

- i. select a gain L satisfying Assumption 4.1;
- ii. manually select K_y , K_x , K_c and K_η to obtain a better transient behavior (note that this step is not necessary to Corollaries 4.1 and 4.2).

Moreover the optimal control synthesis for overshoot reduction in [72] (see also Appendix 5.4.2) can still be used, although the presence of the observer might reduce the efficiency of such synthesis technique.

According to Remark 4.3, the precise mechanism in which K_y , K_x , K_c and K_η affect the control schemes still needs to be investigated. Therefore no optimal synthesis is available to date in order to tune these parameters.

In this section, two simulation examples are presented to show the effectiveness of the proposed methods. For the techniques in Theorem 4.1 and Corollary 4.1, we use an historical example, appeared in several reset control papers. For the techniques in Theorem 4.2 and Corollary 4.2, we use the DC motor example already presented in Section 3.5.3. In all the cases, we use the optimal synthesis with respect to the overshoot reduction (see Appendix 5.4.2). Similarly to Section 3.5, we assume that the matrices \bar{A}_c , \bar{B}_c , \bar{C}_c and \bar{D}_c are given to better point out the attention on the hybrid loops.

4.3.5.1 A SISO plant with an integrator

Consider the plant $P(s) = \frac{s+1}{s(s+0.2)}$ introduced in [6] and discussed in [64, 72]. According to (4.1), a possible realization is

$$\left[\begin{array}{c|c} \bar{A}_p & \bar{B}_p \\ \hline \bar{C}_p & \bar{D}_p \end{array} \right] = \left[\begin{array}{cc|c} -0.6 & 0.6 & -1 \\ -0.4 & 0.4 & 1 \\ \hline 0 & 1 & 0 \end{array} \right]. \quad (4.25)$$

Notice that the pair (\bar{C}_p, \bar{A}_p) is observable. In this example we will use the hybrid controllers defined in Theorem 4.1 and Corollary 4.1. In particular, matrices \bar{A}_c , \bar{B}_c , \bar{C}_c and \bar{D}_c are already given from [6, 72] as

$$\left[\begin{array}{c|c} \bar{A}_c & \bar{B}_c \\ \hline \bar{C}_c & \bar{D}_c \end{array} \right] = \left[\begin{array}{c|c} -1 & -1 \\ \hline 1 & 0 \end{array} \right]. \quad (4.26)$$

For the hybrid part of our controllers, we exploit the optimal configuration presented for the static state feedback in [72] for the overshoot reduction (see also Appendix 5.4.2 for the notation). In particular, Table 4.1 shows the obtained values for gains \bar{P}_p and K_p . By selecting $P_c = 10^{-10}$ (namely the smallest P_c that satisfies all the conditions in Theorem 4.1), in order to reduce the contribution of the sub-state x_c into the flow and jump sets \mathcal{F} and \mathcal{J} , we obtain P , by using (3.6).

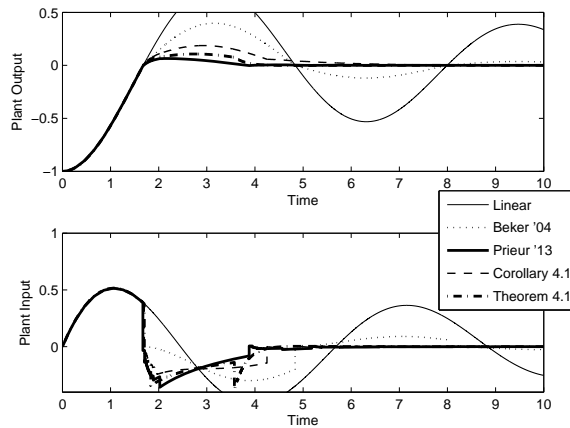


Figure 4.4: Hybrid controllers (4.3) of Corollary 4.1 and Theorem 4.1, compared to the linear case, to the FORE in [6] and to the optimal hybrid state feedback given in [72].

We also set $\tilde{\alpha} = 10^{-8}$ to enlarge as much as possible the flow set and $\rho = 2 \cdot 10^{-3}$. The observer gain is chosen as $L = [0.26 \ 1.37]^\top$. Moreover, only for the hybrid controller of Theorem 4.1 and following the technique of Remark 4.3, we choose $K_x = 0$, $K_c = 0$, and $K_\eta = 0$, whereas for K_y , the inspection of the transient response revealed that $K_y = -5$ leads to an improved transient, partially recovering the performance of the solid line obtained in [72] in which the knowledge of the state was assumed.

Figure 4.4 compares the input and output behavior between:

- the hybrid output feedback (4.4) of Corollary 4.1 (dashed line);
- the hybrid output feedback (4.4) of Theorem 4.1 (dash dotted line);
- the linear continuous-time output feedback;
- the hybrid feedback with a FORE controller in [6];
- the hybrid state feedback in [72].

All the controllers have zero initial conditions whereas the plant state starts from $x_p(0, 0) = -[1 \ 1]^\top$.

As expected, the undesired effects of the dynamics of the observer affect the controller (4.4) exhibiting a larger overshoot than the hybrid state feedback of [72]. This overshoot is caused by the observer transient. The control technique coming from Theorem 4.1 is capable to partially

Table 4.1: Hybrid controller setting proposed

\bar{P}_p	K_p^\top	α
$\begin{bmatrix} 0.0097785 & -0.0096375 \\ -0.0096375 & 0.99990 \end{bmatrix}$	$\begin{bmatrix} 0.0594992 \\ -4.83065 \end{bmatrix}$	$7.784 \cdot 10^{-6}$

compensate for this gap, recovering some performance for the output feedback case.

We remark that, although the FORE in [6] does not introduce further dynamics for the hybrid closed-loop system, it exhibits a larger overshoot than both control techniques in Theorem 4.1 and Corollary 4.1.

Finally we stress that K_y in the hybrid controller (4.3) of Theorem 4.1 has been selected through trial and error, from the simulation data.

4.3.5.2 A DC motor

Let us consider the example of a DC motor presented in Section 3.5.3. The plant in observer canonical form is in (3.27), which can be commonly controlled by the PI controller represented in (3.28).

We want to augment this controller with a hybrid loop tuned in order to reduce the overshoot induced by the integral action. Two different hybrid loops are presented:

- **Case 1:** with a *full order observer* (namely, the observer has the same order as the plant);
- **Case 2:** with a *reduced order observer* (designed based on a second order approximated model of the plant).

In both cases, the optimization technique in [72] for the overshoot reduction is used (see also Appendix 5.4.2 for the notation).

Another aspect taken into account is the robustness to parameters uncertainty. To this aim, we consider the case where the load has a mass 100% higher than expected, therefore the perturbed inertia value is $J = 1$ (see Figure 3.6) and the perturbed plant matrices become

$$\left[\begin{array}{c|c} \bar{A}_p & \bar{B}_p \\ \hline \bar{C}_p & \bar{D}_p \end{array} \right] = \left[\begin{array}{ccc|c} -21.2 & -6 & 0 & 50 \\ 4 & 0 & 0 & 0 \\ 0 & 1 & 0 & 0 \\ \hline 0 & 0 & 1 & 0 \end{array} \right]. \quad (4.27)$$

We denote with *nominal case* the one where the representation (3.27) of the plant is considered and with *perturbed case* the one where (4.27) is used instead.

Case 1. Let us consider the technique in [72] for $\kappa_M = 0.1$ (with the notation of Appendix 5.4.2). Then we get

$$\begin{aligned} K_p &= [0.00803345 \quad 0.02347159 \quad 0.09657843], \\ \rho_y &= 0.2809, \\ \bar{P}_p &= \begin{bmatrix} 0.02290376 & 0.06418020 & 0.06227308 \\ 0.06418020 & 0.19173178 & 0.18092975 \\ 0.06227308 & 0.18092975 & 0.95345625 \end{bmatrix}, \end{aligned}$$

where ρ_y is the minimized quantity (according to [72]). Moreover, we select an observer gain $L = [-0.0241 \ 0.0841 \ 1.0808]^\top$, $\tilde{\alpha} = 10^{-12}$, $\rho = 0.004$, $\mu = 0.01$. In Case 1, we design four hybrid controllers sharing the settings above:

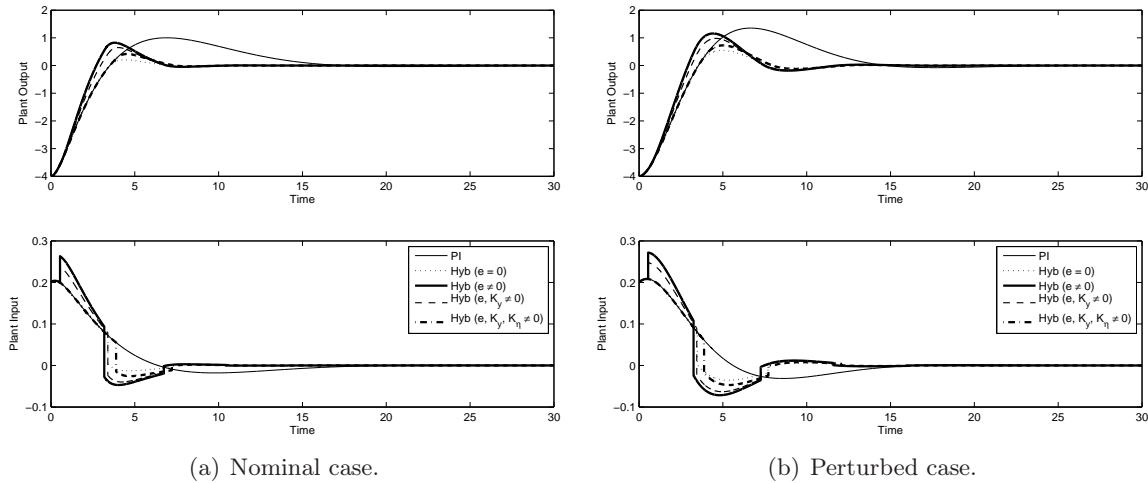


Figure 4.5: Full order observer, case 1.

- i. the hybrid controller (3.2) of Theorem 3.2 (note that this is a hybrid state feedback, namely $e = 0$);
- ii. the hybrid controller (4.3) of Corollary 4.2;
- iii. the hybrid controller (4.3) of Theorem 4.2 with $K_y = 0.06$ and K_x, K_c, K_η null;
- iv. the hybrid controller (4.3) of Theorem 4.2 with $K_y = 0.06, K_\eta = 0.1$ and K_x, K_c null.

In all of the next simulations, the plant and controller initial conditions are $x_p(0,0) = [0.7 \ 0 \ -4]^\top$, $x_c(0,0) = 0$ and $\tau(0,0) = \rho$, whereas the observer initial condition is also $\hat{x}_p(0,0) = 0$.

Figure 4.5(a) compares in the nominal case the four hybrid controllers defined above and the linear case. In particular, one can see that the linear case has the highest overshoot, whereas the hybrid state feedback of Theorem 3.2 has the lowest. In the meantime and according to Remark 4.3, the gains K_y and K_η are successfully used to bring the hybrid output feedback close to the hybrid state feedback (see the bold dash dotted line).

On the other hand, Figure 4.5(b) compares the behavior of the linear PI controller and the hybrid controllers with the perturbed plant. Also in this case, linear case shows the highest overshoot reduction, whereas the hybrid state feedback of Theorem 3.2 has the lowest. The gains K_y and K_η beneficially affect the control schemes and are successfully used to bring the hybrid output feedback close to the hybrid state feedback (see the bold dash dotted line). Note that in this perturbed case, all the overshoots are higher.

The faster rise time in the dashed and bold lines are not necessarily more desirable since it requires a larger control input (see lower plot).

Case 2. Let us consider the plant of Figure 3.6 neglecting the first block, related to the electrical dynamics of the DC motor. Then the remaining part is

$$\left[\begin{array}{c|c} \bar{A}_{pr} & \bar{B}_{pr} \\ \hline \bar{C}_{pr} & \bar{D}_{pr} \end{array} \right] = \left[\begin{array}{cc|c} -2.4 & 0 & 2 \\ 1 & 0 & 0 \\ \hline 0 & 1 & 0 \end{array} \right], \quad (4.28)$$

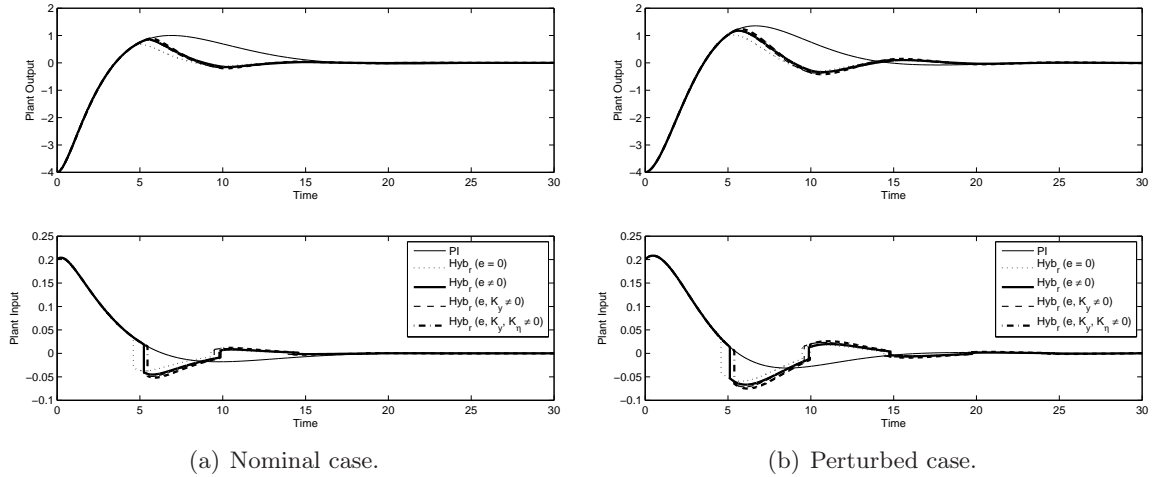


Figure 4.6: Reduced order observer, case 2.

and it can be exploited to define a reduced order observer (the subscript “r” stands for “reduced”). Since the goal is the overshoot reduction, we use the technique in [72], with $\kappa_M = 0.1$ (with the notation of Appendix 5.4.2), to get

$$\begin{aligned} K_p &= \begin{bmatrix} 0.03680221 & 0.09245721 \end{bmatrix}, \\ \rho_y &= 0.3435, \\ \bar{P}_p &= \begin{bmatrix} 0.41279516 & 0.24891952 \\ 0.24891952 & 0.89441164 \end{bmatrix}, \end{aligned}$$

where ρ_y is the minimized quantity (according to [72]). Then by selecting $L = [0.0063 \ 0.9015]^\top$, it is possible to define four hybrid controllers as in Case 1 with the same parameters.

Also in this case the simulations have the same initial condition as in Case 1, where in particular $x_p(0,0) = [0 \ -4]^\top$.

Figure 4.6 shows that the behavior does not change much as compared to Case 1. The overshoot reduction is achieved and no faster rise time or other considerable effects coming from the observer can be observed, even for very large initial estimate errors.

4.4 Hybrid output feedback without dwell-time logic

4.4.1 Problem statement

In this section, we extend [70, Proposition 1] to the hybrid output feedback case, without introducing a dwell-time logic.

Figure 4.7 particularizes Figure 4.2 to the case addressed here and shows the augmentation of the scheme in [70, Proposition 1], with the observer. Notice that block \mathcal{G} in Figure 4.2 is replaced here only with a linear dynamics with state x_c , similarly to [70].

The supervisor accomplishes the same tasks as in the previous section. Moreover, according to Remark 4.2, partial information on the error estimation is used to mitigate the undesired effects

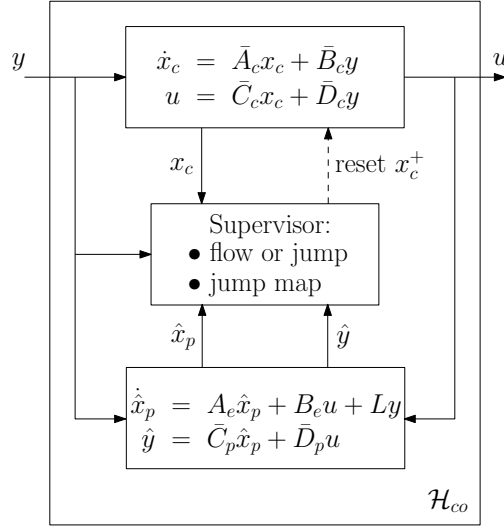


Figure 4.7: Scheme of the hybrid controller with resets from the plant estimation.

induced from the observer.

We are now ready to introduce our hybrid controller architecture, which can be represented as

$$\begin{cases} \begin{bmatrix} \dot{\hat{x}}_p \\ \dot{x}_c \end{bmatrix} = \begin{bmatrix} A_e & B_e \bar{C}_c \\ 0 & \bar{A}_c \end{bmatrix} \begin{bmatrix} \hat{x}_p \\ x_c \end{bmatrix} + \begin{bmatrix} B_e \bar{D}_c + L \\ \bar{B}_c \end{bmatrix} y & (\hat{x}_p, x_c, e) \in \mathcal{C} \\ \begin{bmatrix} \hat{x}_p^+ \\ x_c^+ \end{bmatrix} = \begin{bmatrix} I & 0 \\ K_p & 0 \end{bmatrix} \begin{bmatrix} \hat{x}_p \\ x_c \end{bmatrix} + \begin{bmatrix} 0 \\ K_y \end{bmatrix} \eta & (\hat{x}_p, x_c, e) \in \mathcal{D} \\ u = \begin{bmatrix} 0 & \bar{C}_c \end{bmatrix} \begin{bmatrix} \hat{x}_p \\ x_c \end{bmatrix} + \bar{D}_c y \end{cases} \quad (4.29a)$$

where $\hat{x}_p \in \mathbb{R}^{n_p}$ is the state of the observer, $x_c \in \mathbb{R}^{n_c}$ is the state to reset, A_e , B_e and $\eta \in \mathbb{R}^{n_y}$ are defined in Assumption 4.1 and in Remark 4.2, and \mathcal{C} and \mathcal{D} are

$$\begin{aligned} \mathcal{C} &= \{(\hat{x}_p, x_c, e) : (\hat{x}_p, x_c, e) \in \mathcal{F} \text{ or } (\hat{x}_p, x_c, e) \in \mathcal{F}_\rho\} \\ &= \{(\hat{x}_p, x_c, e) : (\hat{x}_p, x_c, e) \in \mathcal{F}\} \cup \{(\hat{x}_p, x_c, e) : (\hat{x}_p, x_c, e) \in \mathcal{F}_\rho\}, \end{aligned} \quad (4.29b)$$

$$\begin{aligned} \mathcal{D} &= \{(\hat{x}_p, x_c, e) : (\hat{x}_p, x_c, e) \in \mathcal{J} \text{ and } (\hat{x}_p, x_c, e) \in \mathcal{J}_\rho\} \\ &= \{(\hat{x}_p, x_c, e) : (\hat{x}_p, x_c, e) \in \mathcal{J}\} \cap \{(\hat{x}_p, x_c, e) : (\hat{x}_p, x_c, e) \in \mathcal{J}_\rho\}, \end{aligned} \quad (4.29c)$$

with

$$\mathcal{F}_\rho = \left\{ (\hat{x}_p, x_c, e) \in \mathbb{R}^n : \underbrace{\begin{bmatrix} \hat{x}_p \\ x_c \\ e \end{bmatrix}^\top \begin{bmatrix} I & 0 & 0 \\ 0 & I & 0 \\ 0 & 0 & \bar{C}_p \end{bmatrix}^\top \bar{M}_\rho \begin{bmatrix} I & 0 & 0 \\ 0 & I & 0 \\ 0 & 0 & \bar{C}_p \end{bmatrix} \begin{bmatrix} \hat{x}_p \\ x_c \\ e \end{bmatrix}}_{M_\rho} \leq \rho \right\}, \quad (4.29d)$$

$$\mathcal{J}_\rho = \left\{ (\hat{x}_p, x_c, e) \in \mathbb{R}^n : \underbrace{\begin{bmatrix} \hat{x}_p \\ x_c \\ e \end{bmatrix}^\top \begin{bmatrix} I & 0 & 0 \\ 0 & I & 0 \\ 0 & 0 & \bar{C}_p \end{bmatrix}^\top \bar{M}_\rho \begin{bmatrix} I & 0 & 0 \\ 0 & I & 0 \\ 0 & 0 & \bar{C}_p \end{bmatrix} \begin{bmatrix} \hat{x}_p \\ x_c \\ e \end{bmatrix}}_{M_\rho} \geq \rho \right\}, \quad (4.29e)$$

where $\bar{M}_\rho = \bar{M}_\rho^\top > 0$ (notice that $M_\rho = M_\rho^\top \geq 0$), $\rho > 0$ and \mathcal{F} and \mathcal{J} symmetric cones defined by the matrix $\bar{M} = \bar{M}^\top$ as

$$\mathcal{F} = \left\{ (\hat{x}_p, x_c, e) \in \mathbb{R}^n : \begin{bmatrix} \hat{x}_p \\ x_c \\ e \end{bmatrix}^\top \underbrace{\begin{bmatrix} I & 0 & 0 \\ 0 & I & 0 \\ 0 & 0 & \bar{C}_p \end{bmatrix}^\top \bar{M} \begin{bmatrix} I & 0 & 0 \\ 0 & I & 0 \\ 0 & 0 & \bar{C}_p \end{bmatrix}}_M \begin{bmatrix} \hat{x}_p \\ x_c \\ e \end{bmatrix} \leq 0 \right\}, \quad (4.29f)$$

$$\mathcal{J} = \left\{ (\hat{x}_p, x_c, e) \in \mathbb{R}^n : \begin{bmatrix} \hat{x}_p \\ x_c \\ e \end{bmatrix}^\top \underbrace{\begin{bmatrix} I & 0 & 0 \\ 0 & I & 0 \\ 0 & 0 & \bar{C}_p \end{bmatrix}^\top \bar{M} \begin{bmatrix} I & 0 & 0 \\ 0 & I & 0 \\ 0 & 0 & \bar{C}_p \end{bmatrix}}_M \begin{bmatrix} \hat{x}_p \\ x_c \\ e \end{bmatrix} \geq 0 \right\}, \quad (4.29g)$$

where as stated in Remark 4.2, the state e is not available through measurements, nevertheless following Remark 4.2, the linear combination $\bar{C}_p e$ is known through the signal η and it can be used to define matrix \bar{M} (and so also M) in the flow and jump sets³.

The mechanism with which the observer interacts with the control signal u and the dynamics of x_c is exactly the same as in Section 4.3.

Under Assumption 4.2, the interconnection (4.1) and (4.29) yields the hybrid closed-loop system

$$\begin{cases} \begin{bmatrix} \dot{\hat{x}}_p \\ \dot{x}_c \\ \dot{e} \end{bmatrix} = \begin{bmatrix} A_p & B_p & B_o \\ B_c & A_c & B_c \\ 0 & 0 & A_e \end{bmatrix} x := Ax & x \in \mathcal{C} \\ \begin{bmatrix} x^+ \\ y \end{bmatrix} = \begin{bmatrix} I & 0 & 0 \\ K_p & 0 & K_y \bar{C}_p \\ 0 & 0 & I \end{bmatrix} x := Gx & x \in \mathcal{D} \\ y = [C_p \ C_c \ C_p] x := Cx \end{cases} \quad (4.30)$$

with $x := [\hat{x}_p^\top \ x_c^\top \ e^\top]^\top \in \mathbb{R}^{n:=2n_p+n_c}$, $B_o := L\bar{C}_p + \bar{B}_p\bar{D}_c(I - \bar{D}_p\bar{D}_c)^{-1}\bar{C}_p$ and A_p, B_p, A_c, B_c, C_p and C_c are defined in (3.4) and the flow and jump sets are in (4.29b) and (4.29c).

The hybrid system (4.30) represents the hybrid closed loop in Figure 4.1, whenever the hybrid controller (4.29) is used. Moreover, we stress that due to the absence of the dwell time, the arisen hybrid system does not match the class of hybrid systems represented in (2.1), so that the framework in Chapter 2 cannot be applied.

The peculiarity of this new scheme is in the sets (4.29b) and (4.29c) where in particular, a neighborhood of the origin \mathcal{F}_ρ (defined by M_ρ and ρ) is removed from the jump set (a similar approach has been used also in [31]). According to Remark 4.1, this is important to guarantee the convergence of e to the origin. We better explain this phenomenon and particularize it to this control scheme by using the following example.

Example 4.2. Consider (4.30), the initial condition $x(0, 0) := (\hat{x}_p(0, 0), x_c(0, 0), e(0, 0)) = (0, 0, a)$,

³As before, matrix \bar{M} emphasizes the fact that the e -projection of the state space is not known, whereas $\bar{C}_p e$ can be obtained through signal η . The same holds for matrix \bar{M}_ρ .

with $a > 0$ and suppose $\eta = \bar{C}_p a = 0$. According to the flow and jump sets⁴ \mathcal{F} and \mathcal{J} , a supervisor without removing set \mathcal{F}_ρ from \mathcal{J} , may either decide to flow or to jump, and according to the jump map we would have $x^+ = (0, 0, a)$, which again belongs both to \mathcal{F} and \mathcal{J} . Therefore without set \mathcal{F}_ρ the system might only jump preventing x from converging to the origin. ■

Finally, although the control technique of this section draws inspiration from the hybrid state feedback in [70], whenever $e = 0$, the solutions of the two schemes are different, due to the modification of the flow and jump sets, so that no statement similar to Propositions 4.1 and 4.2 can be established with respect to any of the previous schemes.

Now we are ready to state the problem we want to solve.

Problem 4.2. *Given plant (4.1) and matrices $\bar{A}_c, \bar{B}_c, \bar{C}_c, \bar{D}_c$ and L of controller (4.29) under Assumptions 4.1 and 4.2. Design matrices $\bar{M} = \bar{M}^\top \in \mathbb{R}^{(n_p+n_c+n_y) \times (n_p+n_c+n_y)}$, $\bar{M}_\rho = \bar{M}_\rho^\top \in \mathbb{R}^{(n_p+n_c+n_y) \times (n_p+n_c+n_y)}$, gains $K_p \in \mathbb{R}^{n_c \times n_p}$, $K_y \in \mathbb{R}^{n_c \times n_y}$ and $\rho > 0$ such that the origin of system (4.30) is practically globally asymptotically stable, namely the set $\mathcal{A} := \{(\hat{x}_p, x_c) : [\hat{x}_p \atop x_c]^\top P [\hat{x}_p \atop x_c] \leq \rho\} \times \{0\} \subset \mathbb{R}^{n_p+n_c} \times \mathbb{R}^{n_p}$ is globally asymptotically stable for the closed-loop system (4.30), where ρ can be selected arbitrarily small (but different from zero). ◻*

In the sequel, we will use global *practical asymptotic stability* of the origin to denote the fact that a set \mathcal{A} is GAS and depends on ρ , with ρ being a free design parameter (see for instance [18]).

4.4.2 Practical asymptotic stability

We are now ready to present the main result of this section. Consider the following statement whose proof is reported next.

Theorem 4.3. Consider a plant-controller pair (4.1),(4.29) under Assumptions 4.1 and 4.2 and assume that $P = P^\top := \begin{bmatrix} P_p & P_{pc} \\ P_{pc}^\top & P_c \end{bmatrix} > 0$ satisfies (3.5) and (3.6) for some $\alpha > 0$. Then for any $\tilde{\alpha} \in (0, \alpha]$ and any $K_y \in \mathbb{R}^{n_c \times n_y}$, the hybrid controller (4.29) with $\rho > 0$ and

$$\bar{M} = \text{He} \left(\tilde{P} \begin{bmatrix} A_p & B_p & -B_p K_y \\ B_c & A_c & 0 \\ 0 & 0 & 0 \end{bmatrix} + \frac{\tilde{\alpha}}{2} \hat{P} \right), \quad (4.31a)$$

$$\bar{M}_\rho = \hat{P}, \quad (4.31b)$$

where

$$\hat{P} = \begin{bmatrix} I & 0 & 0 \\ 0 & I & -K_y \end{bmatrix}^\top P \begin{bmatrix} I & 0 & 0 \\ 0 & I & -K_y \end{bmatrix}, \quad (4.32)$$

solves Problem 4.2, namely the set $\mathcal{A} := \{(\hat{x}_p, x_c) : [\hat{x}_p \atop x_c]^\top P [\hat{x}_p \atop x_c] \leq \rho\} \times \{0\}$ is globally asymptotically stable for the closed-loop system (4.30), where ρ can be arbitrarily small. ◻

Proof of Theorem 4.3. First notice that according to \mathcal{F} and \mathcal{J} in (4.29f) and (4.29g), from

⁴Although we did not define yet matrix \bar{M} , we have $x(0, 0) := (\hat{x}_p(0, 0), x_c(0, 0), e(0, 0)) = (0, 0, a)$ and due to the fact that only the $\bar{C}_p e$ is used in \mathcal{F} and \mathcal{J} , we have $x(0, 0)^\top M x(0, 0) = 0 \in \mathcal{F} \cap \mathcal{J}$.

(4.31) and (4.32), we get

$$M = \text{He} \left(\tilde{P} \begin{bmatrix} A_p & B_p & -B_p K_y \bar{C}_p \\ B_c & A_c & 0 \\ 0 & 0 & 0 \end{bmatrix} + \frac{\tilde{\alpha}}{2} \tilde{P} \right), \quad (4.33a)$$

$$M_\rho = \tilde{P}, \quad (4.33b)$$

where

$$\tilde{P} = \begin{bmatrix} I & 0 & 0 \\ 0 & I & -K_y \bar{C}_p \end{bmatrix}^\top P \begin{bmatrix} I & 0 & 0 \\ 0 & I & -K_y \bar{C}_p \end{bmatrix}. \quad (4.34)$$

Consider now $\tilde{V}(x) := x^\top \tilde{P} x = x^\top \begin{bmatrix} P_p & P_{pc} & P_{pe} \\ * & P_c & P_{ce} \\ * & * & P_e \end{bmatrix} x$ and notice that $\tilde{P} \geq 0$. Since \tilde{V} is convex, to minimize $\tilde{V}(x)$ with respect to x_c , it is enough to calculate the gradient with respect to x_c and impose the condition for a minimum point. Therefore from (4.34), we get $\nabla_{x_c} \tilde{V}(x) = 2(P_{pc}^\top \hat{x}_p + P_c x_c - P_c K_y \bar{C}_p e) = 0$. Hence, solving this gradient condition with respect to x_c , we find the reset map in (4.29) (note that P_c is always invertible due to $P = P^\top > 0$).

Consider now the observer dynamics and introduce a function $e \mapsto V_e(e) = e^\top \bar{P}_e e$ such that $\bar{P}_e = \bar{P}_e^\top > 0$ and $A_e^\top \bar{P}_e + \bar{P}_e A_e < 0$. This matrix always exists because A_e is assumed to be Hurwitz. Note also that $V_e(e^+) = V_e(e)$.

From (3.6), one can see that $\tilde{V}(x) = V_p(\hat{x}_p) + (x_c - K_p \hat{x}_p - K_y \bar{C}_p e)^\top P_c (x_c - K_p \hat{x}_p - K_y \bar{C}_p e)$, with $V_p(\hat{x}_p) = \hat{x}_p^\top \bar{P}_p \hat{x}_p$ and it is easy to conclude that

$$\tilde{V}(Gx) \leq \tilde{V}(x), \quad \forall x \in \mathcal{D}.$$

Consider the following Lyapunov function candidate $W : \mathbb{R}^n \rightarrow \mathbb{R}_{\geq 0}$ defined for all $x \in \mathbb{R}^n$ by

$$W(x) = \max\{\xi V_e(e), \tilde{V}(x) + \xi V_e(e) - \rho\} \quad (4.35)$$

where $n = 2n_p + n_c$, ρ is a positive scalar (selected arbitrarily small) whereas ξ is a positive scalar selected large enough so that

$$-\tilde{\alpha} \tilde{P} + \text{He} \left(\begin{bmatrix} 0 & 0 & P_p B_o + P_{pc} B_c + P_{pe} A_e + P_p B_p K_y \bar{C}_p \\ 0 & 0 & P_{pc}^\top B_o + P_c B_c + P_{ce} A_e + P_{pc}^\top B_p K_y \bar{C}_p \\ 0 & 0 & P_{pe}^\top B_o + P_{ce}^\top B_c + P_e A_e + \xi \bar{P}_e A_e + P_{pe}^\top B_p K_y \bar{C}_p \end{bmatrix} \right) < 0. \quad (4.36)$$

Note first that denoting $W_1(x) := \xi V_e(e)$ and $W_2(x) := \tilde{V}(x) + \xi V_e(e) - \rho$ and defining the set $\bar{\mathcal{A}} = \{x : \tilde{V}(x) \leq \rho\}$, we may rewrite (4.35) as

$$W(x) = \begin{cases} W_1(x) & \text{if } x \in \bar{\mathcal{A}} \\ W_2(x) & \text{if } x \notin \bar{\mathcal{A}} \end{cases}. \quad (4.37)$$

The proof of Theorem 4.3 is carried out by showing that the Lyapunov function candidate W is decreasing along the solutions of (4.30) when it is either flowing or jumping. Note that the Lyapunov function candidate W is not continuously differentiable on \mathbb{R}^n , more precisely it is not differentiable in all the points $x = [\hat{x}_p^\top \ x_c^\top \ e^\top]^\top \in \mathbb{R}^n$ such that $(\hat{x}_p, x_c) \in \partial \bar{\mathcal{A}}$, and it is only continuous and locally Lipschitz on \mathbb{R}^n . Therefore this decreasing property when flowing is not written in terms of the usual gradient but should be solved in terms of the generalized gradient (in the sense of Clarke, see [24]) at any $x \in \mathcal{C}$. This generalized gradient is the set of the convex hull of all limits of sequence $\nabla W(x_i)$, where x_i is any sequence converging to x avoiding all the points

in which W is not differentiable (that is when $(\hat{x}_p, x_c) \in \partial\bar{\mathcal{A}}$). Thus the decreasing property along the solutions of (4.30) can be carried out by showing

$$\langle \nabla W_1(x), \dot{x} \rangle < 0, \forall x \in \mathcal{C} \setminus \mathcal{A}, x \in \bar{\mathcal{A}} \quad (4.38a)$$

$$\langle \nabla W_2(x), \dot{x} \rangle < 0, \forall x \in \mathcal{C} \setminus \mathcal{A}, x \notin \bar{\mathcal{A}} \quad (4.38b)$$

$$W(x^+) - W(x) \leq 0, \forall x \in \mathcal{D} \setminus \mathcal{A} \quad (4.38c)$$

where we have used (4.37) for the first two conditions.

We first prove (4.38a) by considering $x \in \mathcal{C} \setminus \mathcal{A}$ and $x \in \bar{\mathcal{A}}$. We have $\langle \nabla W_1(x), \dot{x} \rangle = e^\top \text{He}(\xi \bar{P}_e A_e) e < 0$. Thus (4.38a) holds.

To prove (4.38b), let us consider $x \in \mathcal{C} \setminus \mathcal{A}$ and $x \notin \bar{\mathcal{A}}$. By (4.36) and from \mathcal{F} (which holds because $\tilde{V}(x) > \rho$), we have

$$\begin{aligned} \langle \nabla W_2(x), \dot{x} \rangle &= x^\top \text{He} \left(\begin{bmatrix} P_p A_p + P_{pc} B_c & P_p B_p + P_{pc} A_c & P_p B_o + P_{pc} B_c + P_{pe} A_e \\ P_{pc}^\top A_p + P_c B_c & P_{pc}^\top B_p + P_c A_c & P_{pc}^\top B_o + P_c B_c + P_{ce} A_e \\ P_{pe}^\top A_p + P_{ce}^\top B_c & P_{pe}^\top B_p + P_{ce}^\top A_c & P_{pe}^\top B_o + P_{ce}^\top B_c + P_e A_e + \xi \bar{P}_e A_e \end{bmatrix} \right) x \\ &\leq x^\top \text{He} \left(-\frac{\tilde{\alpha}}{2} \tilde{P} + \begin{bmatrix} 0 & 0 & P_p B_o + P_{pc} B_c + P_{pe} A_e + P_p B_p K_y \bar{C}_p \\ 0 & 0 & P_{pc}^\top B_o + P_c B_c + P_{ce} A_e + P_{pc}^\top B_p K_y \bar{C}_p \\ 0 & 0 & P_{pe}^\top B_o + P_{ce}^\top B_c + P_e A_e + \xi \bar{P}_e A_e + P_{pe}^\top B_p K_y \bar{C}_p \end{bmatrix} \right) x \\ &< 0. \end{aligned}$$

This concludes the proof of (4.38b).

Consider now (4.38c). We need the following claim whose proof is reported next.

Claim 4.3. Under the conditions of Theorem 4.3, if $x \in \mathcal{D}$, then $x_c \neq K_p \hat{x}_p + K_y \bar{C}_p e$. \circ

Now, note that for all $x \notin \bar{\mathcal{A}}$, by (4.37) we have $W(x) = W_2(x)$. Moreover, since Claim 4.3 holds, we have that $x_c \neq K_p \hat{x}_p + K_y \bar{C}_p e$ for all $x \in \mathcal{D}$, therefore by definition of $\tilde{V}(x)$ we have

$$(x_c - K_p \hat{x}_p - K_y \bar{C}_p e)^\top P_c (x_c - K_p \hat{x}_p - K_y \bar{C}_p e) > 0, \quad \forall x \in \mathcal{D}. \quad (4.39)$$

To prove (4.38c), we need to consider only the following two situations:

1. if x is such that $x \in \bar{\mathcal{A}}$, then $W(x) = W_1(x)$ and we have $W_1(x^+) = W_1(x) = \xi V_e(e)$ (that is $\Delta W(x) = 0$).
2. if x is such that $x \notin \bar{\mathcal{A}}$, then $W(x) = W_2(x)$ and we have one of the two further cases:
 - 2a. x is such that $\tilde{V}(x^+) \geq \rho$. Using $\tilde{V}(x)$ definition in the second and third lines, and (4.39) in the next to last line, we have:

$$\begin{aligned} W(x^+) &= \tilde{V}(x^+) + \xi V_e(e^+) - \rho \\ &= \tilde{V}(\hat{x}_p, K_p \hat{x}_p + K_y \bar{C}_p e, e) + \xi V_e(e) - \rho \\ &= V_p(\hat{x}_p) + \xi V_e(e) - \rho \\ &< V_p(\hat{x}_p) + \xi V_e(e) - \rho + (x_c - K_p \hat{x}_p - K_y \bar{C}_p e)^\top P_c (x_c - K_p \hat{x}_p - K_y \bar{C}_p e) \\ &= W_2(x) = W(x) \end{aligned}$$

that is, $W(x^+) < W(x)$ (in particular $W_2(x^+) < W_2(x)$).

2b. x is such that $\tilde{V}(x^+) \leq \rho$. Using (4.39) in the next to last line, we have:

$$\begin{aligned} W(x^+) &= \xi V_e(e^+) \\ &= \xi V_e(e) \\ &< V_p(\hat{x}_p) + \xi V_e(e) - \rho + (x_c - K_p \hat{x}_p - K_y \bar{C}_p e)^\top P_c (x_c - K_p \hat{x}_p - K_y \bar{C}_p e) \\ &= W_2(x) = W(x) \end{aligned}$$

that is, $W(x^+) < W(x)$ (in particular $W_1(x^+) < W_2(x)$). This concludes the proof of (4.38c).

Finally, note that Claim 4.3 guarantees that $x \in \mathcal{D}$ implies $x^+ \in \mathcal{C} \setminus \mathcal{D}$.

To conclude the proof of Theorem 4.3 and deduce from (4.38) that \mathcal{A} is GAS for the system (4.30), we have to apply the LaSalle invariance principle. In particular, let us apply [77, Theorem 7.6], using the same nomenclature. First, note that the conditions (A0)-(A3) (defined in [77]) are satisfied, and the jump map in (4.30), that is $G := \begin{bmatrix} I & 0 & 0 \\ K_p & 0 & K_y \bar{C}_p \\ 0 & 0 & I \end{bmatrix}$, is locally bounded. Moreover, since $\mathcal{C} \cup \mathcal{D} = \mathbb{R}^n$, as remarked in the discussion after [41, Prop. 2.4], the viability conditions (VC) and (VD) (defined in [77] and [41]) are satisfied, and in particular each maximal solution of (4.30) is either complete or eventually leaves any compact subset of the state space. Note also that the condition (\star) of [77, Theorem 7.6] matches conditions in (4.38). Hence the set \mathcal{A} is stable for the system (4.30).

Let us define $\dot{W}^{-1}(0) := \{x \in \mathcal{C} : \dot{W}(x) = 0\}$ and $\Delta W^{-1}(0) := \{x \in \mathcal{D} : \Delta W(x) = 0\}$ to denote, respectively, all of the points of the flow set in which $\dot{W} := \langle \bar{\partial} W(x), \dot{x} \rangle = 0$ and all of the points of the jump set in which $\Delta W := W(x^+) - W(x) = 0$. Moreover, $W^{-1}(\epsilon)$ denotes the set level of W , that is, the set of all of the points x such that $W(x) = \epsilon$. Then, the condition $(\star\star)$ of [77, Theorem 7.6] states that the set \mathcal{A} is also locally asymptotically stable for the system (4.30) if for all $x \in \mathcal{U}$, with \mathcal{U} a neighborhood of \mathcal{A} , we have $\dot{W}(x) \leq 0$ and $\Delta W(x) \leq 0$, and the set

$$W^{-1}(r) \cap \mathcal{U} \cap [\dot{W}^{-1}(0) \cup (\Delta W^{-1}(0) \cap G(\Delta W^{-1}(0)))] \quad (4.40)$$

is empty for all $r \in (0, r^*)$ with $r^* > 0$ and $r \in W(\mathcal{U})$.

The proof that the set defined in (4.40) is empty is carried out by the fact that $[\dot{W}^{-1}(0) \cup (\Delta W^{-1}(0) \cap G(\Delta W^{-1}(0)))]$ is reduced to \mathcal{A} . If this holds, by (4.35) we have that $W(x) = 0$ for all $x \in \mathcal{A}$, hence the only possible r^* in (4.40) is zero, leading to a contradiction. In particular, the set $\dot{W}^{-1}(0)$ (*i.e.* all points x such that $\dot{W}(x) = 0$) is \mathcal{A} , because we showed with (4.38a) and (4.38b) that $\dot{W} < 0$ for all $x \in \mathcal{C} \setminus \mathcal{A}$ and zero otherwise. Looking $\Delta W^{-1}(0)$ (*i.e.* all points x such that $\Delta W(x) = 0$) and by (4.38c) we have that the only case in which $\Delta W(x) = 0$ is when x is such that $\tilde{V}(x) = \rho$. But for all such an x we have that x^+ is such that $\tilde{V}(x^+) < \tilde{V}(x) = \rho$. This means that $\Delta W^{-1}(0)$ and $G(\Delta W^{-1}(0))$ have no common points, and this concludes the proof that the term $[\dot{W}^{-1}(0) \cup (\Delta W^{-1}(0) \cap G(\Delta W^{-1}(0)))]$ is \mathcal{A} and that the set in (4.40) is empty, since $r > 0$.

Therefore, applying [77, Theorem 7.6], we get that the set \mathcal{A} is forward invariant and locally asymptotically stable for the hybrid closed-loop system (4.30) with sets (4.33). To show that such set is globally asymptotically stable, we notice that \mathcal{U} can be selected as the entire state space \mathbb{R}^n . Moreover, the practical attribute for the set \mathcal{A} comes by the fact that \mathcal{A} depends on ρ , that is a free positive design parameter. This concludes the proof of Theorem 4.3. \blacksquare

Proof of Claim 4.3. The proof is given by contradiction. Let us consider $x = [\hat{x}_p^\top (-P_c^{-1} P_{pc}^\top \hat{x}_p + K_y \bar{C}_p e)^\top e^\top]^\top$, then by (4.33), it can be verified that

$$x^\top M x = \hat{x}_p^\top \text{He}((P_p - P_{pc} P_c^{-1} P_{pc}^\top)(A_p - B_p P_c^{-1} P_{pc}^\top)) \hat{x}_p \quad (4.41a)$$

$$x^\top \tilde{P}x = \hat{x}_p^\top (P_p - P_{pc}P_c^{-1}P_{pc}^\top) \hat{x}_p. \quad (4.41b)$$

Hence using (3.5) for all $x \in \mathcal{D}$ such that $\hat{x}_p \neq 0$, we have

$$\alpha \hat{x}_p^\top (P_p - P_{pc}P_c^{-1}P_{pc}^\top) \hat{x}_p < -\hat{x}_p^\top \text{He}((P_p - P_{pc}P_c^{-1}P_{pc}^\top)(A_p - B_pP_c^{-1}P_{pc}^\top)) \hat{x}_p \quad (4.42)$$

but, by (4.41) and (4.29c), the right-side term is such that

$$\begin{aligned} -\hat{x}_p^\top \text{He}((P_p - P_{pc}P_c^{-1}P_{pc}^\top)(A_p - B_pP_c^{-1}P_{pc}^\top)) \hat{x}_p &= -x^\top Mx \\ &\leq \tilde{\alpha} x^\top \tilde{P}x \\ &= \tilde{\alpha} \hat{x}_p^\top (P_p - P_{pc}P_c^{-1}P_{pc}^\top) \hat{x}_p \\ &\leq \alpha \hat{x}_p^\top (P_p - P_{pc}P_c^{-1}P_{pc}^\top) \hat{x}_p \end{aligned} \quad (4.43)$$

which leads to a contradiction for all $\hat{x}_p \neq 0$ because the first term in (4.42) and the last term in (4.43) are the same. This proves that all $x = [\hat{x}_p^\top (-P_c^{-1}P_{pc}^\top \hat{x}_p + K_y \bar{C}_p e)^\top e^\top]^\top$ does not belong to \mathcal{D} when $\hat{x}_p \neq 0$. If $\hat{x}_p = 0$, then $x = [0^\top (K_y \bar{C}_p e)^\top e^\top]^\top$ and $\tilde{V}(x) = 0$, therefore x does not belong to \mathcal{D} because the second condition in (4.29c) does not hold. \blacksquare

For the linear case addressed here, the hybrid state feedback technique of [70] induces asymptotic stability of the origin. Theorem 4.3 only guarantees global practical asymptotic stability of the origin, namely GAS of set \mathcal{A} . The set \mathcal{A} shrinks to the origin as the free parameter $\rho > 0$ becomes arbitrarily small. The need for the set \mathcal{A} arises from the need to guarantee the convergence to zero of e , as explained in Example 4.2. Notice also that the set \mathcal{A} corresponds to \mathcal{F}_ρ in (4.29d) with M_ρ in (4.33b), whenever $e = 0$.

The control scheme of Theorem 4.3 guarantees the convergence of e to the origin, solving the issues in Remark 4.1, by ensuring a dwell-time condition (namely, the system flows after each jump for at least a minimum amount of time) even though there is no explicit dwell-time logic enforcing this property. Unlike Section 4.3, such dwell-time property is obtained by combining:

- i. linear mappings, so that finite escape times are not possible;
- ii. jumps into the flow set. In particular according to Claim 4.3, the hybrid loop guarantees that $Gx \in \mathcal{F} \setminus \mathcal{J}$, for all $x \in \mathcal{J}$;
- iii. suitable modification of the flow and jump sets around the origin. In particular the removal of a small neighborhood around the origin is obtained through sets \mathcal{F}_ρ and \mathcal{J}_ρ .

In this way, the hybrid control system does not exhibit Zeno solutions so that the estimation error converges to zero (see Remark 4.1).

According to Remark 4.2, it might be useful to exploit the signal $\eta = \bar{C}_p e$ to reduce the undesired effects coming from the observer. To this aim, the flow and jump sets in (4.29f) and (4.29g) are defined by \bar{M} in (4.31) (or equivalently M in (4.33)), where gain K_y can be manually tuned to reduce such undesired behavior.

Among the similarities with [70] (and also Theorem 4.1), we mention:

- a. the flow and jump sets \mathcal{F} and \mathcal{J} are defined according to a Lyapunov-like function. In particular, if $e = 0$ sets \mathcal{F} and \mathcal{J} in (4.29f) and (4.29g) are the same as in [70] (and also \mathcal{F} and \mathcal{J} in Theorem 4.1) except for an arbitrarily small neighborhood around the origin;

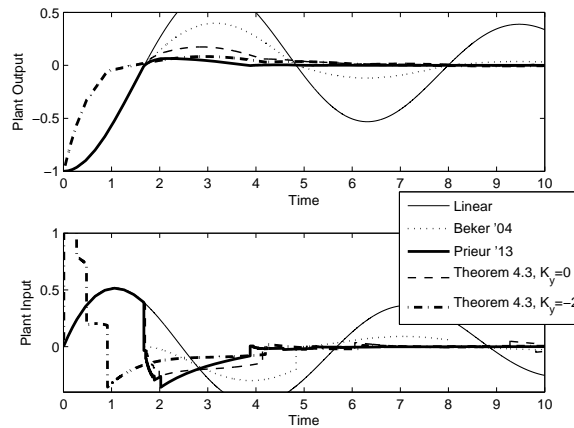


Figure 4.8: Hybrid controllers (4.29) of Theorem 4.3 with $K_y = 0$ and $K_y = -2$, respectively, compared to the linear case, to the FORE in [6] and to the optimal hybrid state feedback given in [72].

- b. the jump map is built in order to
 - i. guarantee non-increase at jumps of the Lyapunov-like function in \mathcal{F} and \mathcal{J} ;
 - ii. guarantee a good decrease condition of the Lyapunov-like function in \mathcal{F} and \mathcal{J} after each jump;
- c. if $e = 0$ the Lyapunov-like function is non-increasing along flow;
- d. the result relies on condition (3.5);
- e. the stability of the origin is achieved through resets.

4.4.3 Simulations

To show the effectiveness of this last control scheme and compare it with the control schemes in Section 4.3, we use the example presented in Section 4.3.5.1.

Note that due to the similarities with the control scheme in [70], the optimal syntheses for overshoot reduction in [72] can be applied also to this hybrid output feedback scheme (see also Appendix 5.4.2). In particular, we tune the parameters according to the optimal synthesis for overshoot reduction (which returns the same parameters obtained in Section 4.3.5.1). We observe that the mechanism behind K_y is still unclear and therefore an optimal technique to tune this parameter is not yet available and only a trial and error tuning is performed.

Consider (4.25) and (4.26), the optimal parameters in Table 4.1 and the observer gain L , matrix P_c and scalar $\tilde{\alpha}$ used in Section 4.3.5.1. Moreover, we select $\rho = 10^{-3}$.

Figure 4.8 compares the input and output behavior between:

- the hybrid output feedback (4.29) of Theorem 4.3 with the parameters above and $K_y = 0$ (dashed line);

- the hybrid output feedback (4.29) of Theorem 4.3 with the parameters above and $K_y = -2$ (dash-dotted line);
- the linear continuous-time output feedback;
- the hybrid feedback with a FORE controller [6];
- the hybrid state feedback in [72].

All the controllers have zero initial conditions whereas the plant state starts from $x_p(0,0) = -[1 \ 1]^\top$.

As expected, the undesired effects of the dynamics of the observer affect the controller (4.29) exhibiting a larger overshoot than the static state feedback of [72] caused by the observer transient. The controller (4.29) with $K_y = -2$ is capable to partially compensate for this gap reducing the overshoot for the output feedback case. Note that the faster rise time might misleadingly convey the idea that the dash dotted response is more desirable than the bold one. This is not the case because we are assessing overshoot reduction here and the shorter rise time is obtained by the dash dotted curve at the price of a larger control input (see the lower plot).

We remark that, although the FORE in [6] does not introduce further dynamics for the hybrid closed-loop system, it exhibits a larger overshoot than the two hybrid controllers proposed here for different values of K_y .

4.5 Comparisons

It is worth commenting on the difference between the dwell-time approach followed in Section 4.3 and the approach in Section 4.4 where no dwell time is used to address the extension of the result of [70] to the output feedback case. As already mentioned at the beginning of this chapter, the main difficulty arising from this output feedback extension corresponds to the fact that the results in [70–72] exhibit Zeno solutions at the origin which, when extending the scheme to a feedback from the observed state may become non-converging Zeno solutions (see Examples 4.1 and 4.2). In Section 4.3, we use a dwell-time logic to remove the Zeno solutions and global exponential stability is established. The approach in Section 4.4, instead, for suppressing the Zeno solutions is to remove a small ball around the origin (thereby resulting in global practical asymptotic stability of the origin). Note that a similar distinction can be made between the work in [31] which establishes global practical asymptotic stability and its revised version in [32] where global exponential stability is obtained with a dwell-time logic.

Theorems 4.1, 4.2 (their corollaries) and 4.3 have similar flow and jump sets \mathcal{F} and \mathcal{J} , based on Lyapunov-like functions and that allow the use of the optimal hybrid synthesis in [72]. Nevertheless, Theorems 4.1 and 4.2 have a larger set of parameters to tune, which might be useful to compensate the observer transient time (see Section 4.3.5). On the other hand, Theorem 4.3 has only the free gain K_y , which can be used to attenuate the same undesired effects. Indeed, by comparing Figures 4.4 and 4.8, one can see that for the case of overshoot reduction, the control scheme of Theorem 4.1 mitigates the observer effects without introducing further behavior, whereas the control scheme of Theorem 4.3 returns a (undesired) faster rise time when it reduces the overshoot. Perhaps, this suggests that Theorem 4.3 is less flexible than Theorem 4.1, although the less amount of parameters makes easier its implementation.

Note also that all the control schemes so far presented, guaranteed the global exponential stability of the origin at least in the e -direction (thanks to Assumption 4.1). Finally, notice that condition (3.5) remains the key point from which all the schemes are developed.

Multi-objective hybrid controller synthesis

Contents

5.1	Introduction	77
5.2	Convex hybrid controller synthesis	79
5.2.1	Overview and synthesis problem	79
5.2.2	Multi-objective convex synthesis	80
5.3	Comments on the convex hybrid output feedback synthesis	86
5.4	Simulations	87
5.4.1	A DC motor	88
5.4.2	The F-8 aircraft	92

In this chapter a convex synthesis of a multi-objective hybrid controller is proposed. Section 5.1 provides some motivation and literature context. In Section 5.2, the main result for the hybrid state feedback is presented. Section 5.3 makes a few remarks to the hybrid output feedback scheme. Finally, some simulations show the potential of our technique in Section 5.4. The main result of this chapter can be found in [26].

5.1 Introduction

In Chapters 3 and 4, we presented some hybrid control schemes arising from the interconnection of a hybrid controller with a linear plant, in order to guarantee the stability of the closed loop. We assumed that the flow map of the hybrid controller was given, so that only the hybrid loop needed to be designed to achieve the stability property. In particular, we presented simple convex procedures to design the hybrid loops and moreover, we linked our results to the optimal hybrid loop syntheses in [71, 72], which provide hybrid controllers (with given flow map) optimal with respect to overshoot reduction and maximum decay rate, respectively.

Although the results from the simulations are promising, the fact that the controller flow map was assumed as given, limits the potential of the hybrid control, because only a subsets of all its parameters (namely, the flow and jump sets and the jump map) are actually tuned. Note that this approach of augmenting a given flow map with a hybrid loop in the attempt to achieve stability and/or to improve performance has been widely used in hybrid control since the FORE architecture (see, for instance, [4, 7, 21]). Moreover in [5, 49], the design of the flow map and of

the hybrid loop was done separately. Decoupling the two syntheses in order to satisfy all the specifications. The problem of this approach is that, in general, there is no guarantee that the specifications obtained by means of the flow map are maintained, once that the hybrid loop is embedded in the control scheme. In other words, a separate optimal design of the continuous and the hybrid part of the controller might not return any guarantee of the specifications of the arisen hybrid closed-loop system if not done carefully. Therefore the method of decoupling the synthesis of the flow map from the hybrid part might return suitable behavior in the responses of the control schemes, but no certifications.

In this context, several convex tools have been proposed to make an analysis a posteriori with respect to some performance indexes (see for instance [65, 88]) and the most recent results introduced in Chapter 2. Nevertheless, the problem of designing an optimal hybrid controller in all its parts (namely, flow and jump sets and flow and jump maps) is complex. The main difficulty of the synthesis of a hybrid controller comes from matching the constraints between the Lyapunov function and the controller architecture in order to obtain convex conditions. To date, beside the result we present here, the only other attempt of optimal synthesis of a hybrid controller for a linear plant is in [78], which provides convex conditions (with a line-search) to design an optimal hybrid controller with linear mappings and conic sets, with respect to the t - \mathcal{L}_2 gain. Nevertheless, the preliminary results in [78] presents a few unclear aspects, which require further investigations.

In this chapter, we provide convex conditions to design a multi-objective hybrid controller for a linear continuous-time plant. In particular, we solve the synthesis problem with respect to the following performance indexes:

- the t -decay rate (see Definition 1.13);
- the t - \mathcal{L}_2 gain (see Definition 1.14).

Notice that we will propose convex synthesis strategies which do not minimize simultaneously both the performance indexes above. We will propose convex conditions in which we can minimize one of the two performance indexes with respect to the other one fixed a priori. In this sense we cannot speak of an optimal multi-objective hybrid controller, although the synthesis can return a hybrid controller optimal with respect to the requirements for these two performance indexes. The main idea is to combine the hybrid controller architecture presented in Section 3.3.2 and the results in Proposition 2.1 to obtain an convex formulation which will lead to the desired multi-objective hybrid controller. Recall that in Section 3.3.2, sufficient conditions are provided to return a hybrid controller guaranteeing a known exponential decay rate in the plant state direction. On the other hand, Proposition 2.1 provides sufficient conditions to estimate the t - \mathcal{L}_2 gain for a class of hybrid systems. As it will be clarified in the sequel, these last two results will be combined together via a particular change of coordinates, allowing to design simultaneously all the controller parameters.

Finally, we mention that in [54, 73], it has been proven that for linear plants there is no optimal nonlinear controller able to reduce the \mathcal{L}_2 gain more than the one associated to the optimal linear controller. Therefore [1] suggests that perhaps also optimal hybrid controllers might have the same bound like for nonlinear controllers. Although the conclusions in [1] are not definitive, since [54, 73] consider only continuous-time nonlinearities, the purpose of this chapter is to prove at least the significantly improvement that a hybrid controller can offer on a multi-objective context.

5.2 Convex hybrid controller synthesis

5.2.1 Overview and synthesis problem

Consider an LTI plant \mathcal{P} , represented by

$$\begin{aligned} \dot{x}_p &= \bar{A}_p x_p + \bar{B}_p u + \bar{B}_w w \\ z &= \bar{C}_z x_p + \bar{D}_z u + \bar{D}_{zw} w \\ y &= \bar{C}_p x_p + \bar{D}_p u + \bar{D}_w w \end{aligned} \quad (5.1)$$

where $x_p \in \mathbb{R}^{n_p}$ is the state of the system, $u \in \mathbb{R}^{n_u}$ is the control input, $y \in \mathbb{R}^{n_y}$ is the measured output, $w \in \mathbb{R}^{n_w}$ is an exogenous input (like disturbances, references) and $z \in \mathbb{R}^{n_z}$ is the performance output.

To keep the discussion simple, we make the following assumption.

Assumption 5.1. The plant (5.1) has $\bar{D}_p = 0$. ◦

Note that Assumption 5.1 is not very restrictive. In case system \mathcal{P} has $\bar{D}_p \neq 0$, we can always define $\bar{y} := y - \bar{D}_p u$ and use \bar{y} as new measured output.

The hybrid controller architecture \mathcal{H}_c we consider, is represented by

$$\begin{cases} \dot{x}_c = \bar{A}_c x_c + \bar{B}_c y \\ \dot{\tau} = 1 - \text{dz} \left(\frac{\tau}{\rho} \right) \\ x_c^+ = K_p x_p \\ \tau^+ = 0 \\ u = \bar{C}_c x_c + \bar{D}_c y \end{cases} \quad \begin{matrix} (x_p, x_c, \tau) \in \mathcal{C} \\ (x_p, x_c, \tau) \in \mathcal{D} \end{matrix} \quad (5.2a)$$

where $x_c \in \mathbb{R}^{n_c}$ is the state, $\tau \in [0, 2\rho]$ with $\rho > 0$ is the dwell-time logic and \mathcal{C} and \mathcal{D} are

$$\begin{aligned} \mathcal{C} &= \{(x_p, x_c, \tau) : (x_p, x_c) \in \mathcal{F} \text{ or } \tau \in [0, \rho]\} \\ &= \{(x_p, x_c, \tau) : (x_p, x_c) \in \mathcal{F}\} \cup \{(x_p, x_c, \tau) : \tau \in [0, \rho]\}, \end{aligned} \quad (5.2b)$$

$$\begin{aligned} \mathcal{D} &= \{(x_p, x_c, \tau) : (x_p, x_c) \in \mathcal{J} \text{ and } \tau \in [\rho, 2\rho]\} \\ &= \{(x_p, x_c, \tau) : (x_p, x_c) \in \mathcal{J}\} \cap \{(x_p, x_c, \tau) : \tau \in [\rho, 2\rho]\}, \end{aligned} \quad (5.2c)$$

with \mathcal{F} and \mathcal{J} symmetric cones defined as

$$\mathcal{F} = \left\{ (x_p, x_c) : \begin{bmatrix} x_p \\ x_c \end{bmatrix}^\top M \begin{bmatrix} x_p \\ x_c \end{bmatrix} \leq 0 \right\} \quad (5.2d)$$

$$= \left\{ (x_p, x_c) : \begin{bmatrix} x_p \\ x_c \end{bmatrix}^\top \text{He} \left(\begin{bmatrix} \bar{P}_p A_p + \frac{\alpha}{2} \bar{P}_p & \bar{P}_p B_p \\ 0 & \frac{\mu}{2} I \end{bmatrix} \right) \begin{bmatrix} x_p \\ x_c \end{bmatrix} \leq 0 \right\}, \quad (5.2e)$$

$$\mathcal{J} = \left\{ (x_p, x_c) : \begin{bmatrix} x_p \\ x_c \end{bmatrix}^\top M \begin{bmatrix} x_p \\ x_c \end{bmatrix} \geq 0 \right\} \quad (5.2f)$$

$$= \left\{ (x_p, x_c) : \begin{bmatrix} x_p \\ x_c \end{bmatrix}^\top \text{He} \left(\begin{bmatrix} \bar{P}_p A_p + \frac{\alpha}{2} \bar{P}_p & \bar{P}_p B_p \\ 0 & \frac{\mu}{2} I \end{bmatrix} \right) \begin{bmatrix} x_p \\ x_c \end{bmatrix} \geq 0 \right\}, \quad (5.2g)$$

where A_p and B_p will be defined next (see (5.3)).

Notice that (5.2) is exactly the same controller architecture used in Theorem 3.2. In particular, (5.2a) and sets (5.2b) and (5.2c) are the same as the ones defined in (3.2) and the flow and jump sets \mathcal{F} and \mathcal{J} are defined according to matrix (3.13), in Theorem 3.2.

Similarly to Chapter 3, due to the fact that we consider the hybrid state feedback (see Figure 3.1), the jump map and sets \mathcal{F} and \mathcal{J} depend on the knowledge of the plant state x_p . Therefore Assumption 3.1 is maintained. Note that also in [78], the optimal t - \mathcal{L}_2 synthesis of a controller in hybrid state feedback with the plant is considered.

The interconnection between (5.1) and (5.2) returns the hybrid system (2.1) with $x = [x_p^\top x_c^\top]^\top \in \mathbb{R}^{n:=n_p+n_c}$,

$$\left(\begin{array}{c|c} A & B \\ \hline G & - \\ \hline C_z & D_{zw} \\ \hline C_p & D_{pw} \end{array} \right) = \left(\begin{array}{cc|c} A_p & B_p & B_{pw} \\ \hline B_c & A_c & B_{cw} \\ \hline G & & - \\ \hline C_z & & D_{zw} \\ \hline C_p & & D_{pw} \end{array} \right) = \left(\begin{array}{cc|c} \bar{A}_p + \bar{B}_p \bar{D}_c \bar{C}_p & \bar{B}_p \bar{C}_c & \bar{B}_w + \bar{B}_p \bar{D}_c \bar{D}_w \\ \hline \bar{B}_c \bar{C}_p & \bar{A}_c & \bar{B}_c \bar{D}_w \\ \hline I & 0 & - \\ \hline K_p & 0 & - \\ \hline \bar{C}_z + \bar{D}_z \bar{D}_c \bar{C}_p & \bar{D}_z \bar{C}_c & \bar{D}_{zw} + \bar{D}_z \bar{D}_c \bar{D}_w \\ \hline \bar{C}_p & 0 & \bar{D}_w \end{array} \right) \quad (5.3)$$

and flow and jump sets \mathcal{F} and \mathcal{J} as in (5.2d) and (5.2f), respectively. In a more compact way, we will refer to this hybrid closed-loop system as (2.1), (5.3).

Now we are ready to state the problem we address here.

Problem 5.1. Consider the plant \mathcal{P} in (5.1) under Assumptions 3.1 and 5.1 and the hybrid controller \mathcal{H}_c in (5.2). Design the matrices \bar{A}_c , \bar{B}_c , \bar{C}_c , \bar{D}_c , K_p , \bar{P}_p , and the positive scalars $\tilde{\alpha}$ and μ such that, there exists $\bar{\rho} > 0$ such that for any $\rho \in (0, \bar{\rho})$ the following specifications are satisfied:

- i. **t -Decay rate:** the set $\{0\} \times [0, 2\rho]$ is globally exponentially stable for system (2.1), (5.3) with $w = 0$. Moreover, the t -decay rate is $\tilde{\alpha}/2$ of the x_p component of the solutions $\xi = (x, \tau)$ to (2.1), (5.3);
- ii. **\mathcal{H}_∞ specification:** for any $w \in t\text{-}\mathcal{L}_2$, the $t\text{-}\mathcal{L}_2$ gain of system (2.1), (5.3) from w to z is less than or equal to γ .

◦

We stress that Problem 5.1 relies on Definitions 1.16 and 1.13.

5.2.2 Multi-objective convex synthesis

Now we are ready for the following statement, whose proof is reported next.

Theorem 5.1. Given the plant (5.1) under Assumptions 3.1 and 5.1, assume that there exist $Y = Y^\top \in \mathbb{R}^{n_p \times n_p}$, $W = W^\top \in \mathbb{R}^{n_p \times n_p}$, $\hat{A} \in \mathbb{R}^{n_p \times n_p}$, $\hat{B} \in \mathbb{R}^{n_p \times n_y}$, $\hat{C} \in \mathbb{R}^{n_u \times n_p}$, $\hat{D} \in \mathbb{R}^{n_u \times n_y}$ and

positive scalars γ and α such that

$$\begin{bmatrix} Y & I \\ I & W \end{bmatrix} > 0, \quad (5.4a)$$

$$\text{He} \left(\begin{array}{cc|cc} \bar{A}_p Y + \bar{B}_p \hat{C} & \bar{A}_p + \bar{B}_p \hat{D} \bar{C}_p & \bar{B}_w + \bar{B}_p \hat{D} \bar{D}_w & Y \bar{C}_z^\top + \hat{C}^\top \bar{D}_z^\top \\ \hat{A} & W \bar{A}_p + \hat{B} \bar{C}_p & W \bar{B}_w + \hat{B} \bar{D}_w & \bar{C}_z^\top + \hat{C}_p^\top \hat{D}^\top \bar{D}_z^\top \\ \hline 0 & 0 & -\frac{\gamma}{2} I & \bar{D}_{zw}^\top + \bar{D}_w^\top \hat{D}^\top \bar{D}_z^\top \\ 0 & 0 & 0 & -\frac{\gamma}{2} I \end{array} \right) < 0, \quad (5.4b)$$

$$\text{He} \left(\bar{A}_p Y + \bar{B}_p \hat{C} + \frac{\alpha}{2} Y \right) < 0. \quad (5.4c)$$

Based on any solution to (5.4), define

$$\begin{aligned} \bar{D}_c &= \hat{D}, \\ \bar{C}_c &= (\hat{C} - \bar{D}_c \bar{C}_p Y)(Y - W^{-1})^{-1}, \\ \bar{B}_c &= -W^{-1} \hat{B} + \bar{B}_p \bar{D}_c, \\ \bar{A}_c &= -W^{-1} (\hat{A} + W \bar{B}_c \bar{C}_p Y - W \bar{B}_p \bar{C}_c (Y - W^{-1}) - W (\bar{A}_p + \bar{B}_p \bar{D}_c \bar{C}_p) Y)(Y - W^{-1})^{-1}, \\ \bar{P}_p &= Y^{-1}, \\ K_p &= (Y - W^{-1}) Y^{-1}. \end{aligned} \quad (5.5)$$

Then, for each $\tilde{\alpha}$ satisfying $0 < \tilde{\alpha} \leq \alpha$, there exists $\mu > 0$ such that (3.12) holds. Moreover, for each $\mu > 0$ satisfying (3.12), there exists a $\bar{\rho} > 0$ such that for any $\rho \in (0, \bar{\rho})$ the hybrid controller (5.2) guarantees that for the hybrid closed-loop system (2.1), (5.3):

- i. the set $\{0\} \times [0, 2\rho]$ is globally exponentially stable. Moreover, the t -decay rate of the x_p component of the solution ξ to (2.1), (5.3) is equal to $\tilde{\alpha}/2$ and in particular, (3.14) holds for all the solutions satisfying $x_c(0, 0) = 0$;
- ii. the t - \mathcal{L}_2 gain from w to z is smaller than or equal to γ , for all $w \in t$ - \mathcal{L}_2 .

□

Proof of Theorem 5.1. The proof is carried out by showing that conditions (5.4) and definitions (5.5) imply all the conditions of Theorem 3.2 and Proposition 2.1. Then from Theorem 3.2, we get item i and from Proposition 2.1, we get item ii.

Consider the following partitioned matrix $P = \begin{bmatrix} Y & Z \\ Z & Z \end{bmatrix}^{-1}$ (see also [59, 79]). By applying the matrix inversion lemma in [42], we get

$$P := \begin{bmatrix} Y & Z \\ Z & Z \end{bmatrix}^{-1} = \begin{bmatrix} (Y - Z)^{-1} & -(Y - Z)^{-1} \\ -(Y - Z)^{-1} & Z^{-1} + (Y - Z)^{-1} \end{bmatrix} = \begin{bmatrix} W & -W \\ -W & W + Z^{-1} \end{bmatrix}. \quad (5.6)$$

Notice that $Z = Y - W^{-1} \Leftrightarrow Y = Z + W^{-1}$. Moreover, by defining $R = W + Z^{-1}$ and by applying

again the matrix inversion lemma (see [42]), we can establish the following useful identities

$$\begin{aligned}
R^{-1} &= (W + Z^{-1})^{-1} \\
&= W^{-1} - W^{-1}(Z + W^{-1})^{-1}W^{-1} \\
&= (Y - Z) - (Y - Z)(Z + (Y - Z))^{-1}(Y - Z) \\
&= (Y - Z) - (Y - Z)Y^{-1}(Y - Z) \\
&= (I - (Y - Z)Y^{-1})(Y - Z) \\
&= (YY^{-1} - (Y - Z)Y^{-1})(Y - Z) \\
&= (Y - (Y - Z))Y^{-1}(Y - Z) \\
&= ZY^{-1}(Y - Z)
\end{aligned} \tag{5.7}$$

and since $I = RR^{-1}$, we have

$$I = (W + Z^{-1})ZY^{-1}(Y - Z). \tag{5.8}$$

Let us now show that all the conditions of Theorem 3.2 are satisfied. First notice that by applying a Schur complement (see [10, pag. 28]), (5.4a) is equivalent to

$$Y > 0 \tag{5.9a}$$

$$Y - W^{-1} = Z > 0 \tag{5.9b}$$

which imply $P = P^\top > 0$ and moreover, according to (5.5), also $\bar{P}_p = \bar{P}_p^\top > 0$. Furthermore, by multiplying (5.4c) on both sides by $\bar{P}_p = Y^{-1}$ and using (5.5), we get

$$\begin{aligned}
\text{He}(Y^{-1}(\bar{A}_p + \bar{B}_p\hat{C}Y^{-1})) &= \text{He}(Y^{-1}(\bar{A}_p + \bar{B}_p(\bar{C}_c(Y - W^{-1}) + \bar{D}_c\bar{C}_pY)Y^{-1})) \\
&= \text{He}(\bar{P}_p(A_p + B_pK_p)).
\end{aligned} \tag{5.10}$$

Therefore (3.5) is satisfied and Theorem 3.2 holds, this completes the proof of item i.

We want to prove now that (5.4) and (5.5) imply conditions (2.25) with $\tau_F = \tau_R = \tau_C = 0$, $\tilde{M} = 0$, $\underline{\rho} = 0$ and a_3 small enough, so that Proposition 2.1 holds. First, notice that according to Remark 2.7, condition (2.7) is not needed and therefore (2.25a) can hold with $\gamma = \bar{\gamma}$. Moreover, conditions (2.25c) and (2.25d) are automatically satisfied. Consider now condition (2.25a), where P is in (5.6), and the following definitions

$$\begin{aligned}
\hat{A} &:= W(-\bar{A}_cZ - \bar{B}_c\bar{C}_pY + \bar{B}_p\bar{C}_cZ + (\bar{A}_p + \bar{B}_p\bar{D}_c\bar{C}_p)Y), \\
\hat{B} &:= W(-\bar{B}_c + \bar{B}_p\bar{D}_c), \\
\hat{C} &:= \bar{C}_cZ + \bar{D}_c\bar{C}_pY, \\
\hat{D} &:= \bar{D}_c.
\end{aligned} \tag{5.11}$$

Notice that we retrieve (5.5) from (5.11) and vice versa. By pre- and post-multiplying (2.25a) by $T := \begin{bmatrix} \Pi & 0 & 0 \\ 0 & I & 0 \\ 0 & 0 & I \end{bmatrix}$ and its transpose, with $\Pi := \begin{bmatrix} Y & Z \\ I & 0 \end{bmatrix}$ (note that $\Pi P = \begin{bmatrix} I & 0 \\ W & -W \end{bmatrix}$), then (2.25a) is equivalent to

$$\text{He} \left(\left[\begin{array}{cc|cc} \bar{A}_pY + \bar{B}_p\hat{C} + a_3Y & \bar{A}_p + \bar{B}_p\hat{D}\bar{C}_p + a_3I & \bar{B}_w + \bar{B}_p\hat{D}\bar{D}_w & Y\bar{C}_z^\top + \hat{C}^\top\bar{D}_z^\top \\ \hat{A} + a_3I & W\bar{A}_p + \hat{B}\bar{C}_p + a_3W & W\bar{B}_w + \hat{B}\bar{D}_w & \bar{C}_z^\top + \bar{C}_p^\top\hat{D}^\top\bar{D}_z^\top \\ \hline 0 & 0 & -\frac{\gamma}{2}I & \bar{D}_{zw}^\top + \bar{D}_w^\top\hat{D}^\top\bar{D}_z^\top \\ 0 & 0 & 0 & -\frac{\gamma}{2}I \end{array} \right] \right) < 0, \tag{5.12}$$

which is implied by (5.4b), due to the strict inequality.

Now let us consider condition (2.25b). By using the definitions in (5.5) and the fact that $K_p = ZY^{-1}$, we have $G^\top PG = \begin{bmatrix} \Xi & 0 \\ 0 & 0 \end{bmatrix}$, where

$$\begin{aligned} \Xi &= W - WK_p - K_p^\top W + K_p^\top (W + Z^{-1})K_p \\ &= W - WZY^{-1} - Y^{-1}ZW + Y^{-1}Z(W + Z^{-1})ZY^{-1}. \end{aligned}$$

Then, since (5.8) implies $(W + Z^{-1})ZY^{-1} = (Y - Z)^{-1} = W$, we have

$$\Xi = W - WZY^{-1} = W - W(Y - W^{-1})Y^{-1} = Y^{-1}.$$

As a consequence, (2.25b) with $\tau_R = 0$ is equivalent to

$$G^\top PG - P = \begin{bmatrix} Y^{-1} - W & W \\ W & -(W + Z^{-1}) \end{bmatrix}. \quad (5.13)$$

By applying a Schur complement, we get

$$Y^{-1} - W \leq 0, \quad (5.14a)$$

$$Y^{-1} - W + W(W + Z^{-1})^{-1}W \leq 0. \quad (5.14b)$$

Notice that (5.14a) is implied by (5.9b) (to see this it is enough to pre- and post- multiplying (5.14a) by Y and W^{-1} , respectively). Regarding (5.14b), by using (5.7) and the definition of W , we get

$$\begin{aligned} Y^{-1} - W + W(W + Z^{-1})^{-1}W &= Y^{-1} - W + WZY^{-1}(Y - Z)(Y - Z)^{-1} \\ &= Y^{-1} - W + WZY^{-1} \\ &= Y^{-1} + W(-I + (Y - W^{-1})Y^{-1}) \\ &= Y^{-1} - Y^{-1} = 0. \end{aligned}$$

Therefore (2.25b) is satisfied, Proposition 2.1 holds and this completes the proof of item ii and hence of the theorem. ■

Theorem 5.1 provides a convex procedure to design a hybrid controller solving Problem 5.1. Indeed, conditions (5.4a) and (5.4b) are linear in the decision variables, whereas (5.4c) is a generalized eigenvalue problem (see [11]) whenever α is a variable and it becomes linear as soon as α is fixed. Notice also that the synthesis is in three steps:

1. solve (5.4) in the decision variables;
2. compute the controller gains in (5.5);
3. solve (3.12) in the only variable $\mu > 0$.

Notice that the synthesis returns a multi-objective controller with respect to t -decay rate and t - \mathcal{L}_2 gain. In particular, the t -decay rate is certified by (3.14) (see Remarks 3.1 and 3.2) and depends on α and $\tilde{\alpha}$ (see Remark 3.3). On the other hand, the t - \mathcal{L}_2 gain from w to z is less than or equal to the γ value in (5.4b).

The optimization in Theorem 5.1 can be done either by minimizing the t - \mathcal{L}_2 gain γ and fixing the parameter α , or maximizing α and solving the generalized eigenvalue problem. It is important to note that such a synthesis technique returns a controller whose order is the same as the plant, namely $n_p = n_c$.

By looking at the proof of Theorem 5.1, it is clear that the results strongly rely on Proposition 2.1 and Theorem 3.2. Indeed, the inequalities (5.4a) and (5.4b) imply the existence of a matrix $P = \begin{bmatrix} Y & Z \\ Z & Z \end{bmatrix}^{-1} = P^\top > 0$ satisfying (2.25) and then the t - \mathcal{L}_2 result follows from Proposition 2.1. In the meantime, (5.4a) and (5.4c) guarantee conditions in Theorem 3.2, so that the t -decay rate is assessed.

Notice that Proposition 2.1 guarantees the existence of $V(x) = x^\top P x$, which can be used as a disturbance attenuation Lyapunov function which does not increase at jumps, thus providing the t - \mathcal{L}_2 gain of the statement. On the other hand, Theorem 3.2 is based on a Lyapunov-like function $V_p(x_p) := x_p^\top \bar{P}_p x_p$ that under condition (3.12) guarantees global exponential stability of the hybrid closed-loop system with t -decay rate $\tilde{\alpha}/2$. Therefore the two performance indexes are guaranteed by two functions $x \mapsto V(x)$ and $x_p \mapsto V_p(x_p)$ and the main idea behind our construction is to define a reset map able to overlap these two functions without affecting each performance property. The next remark gives further details on this topic.

Remark 5.1. Under the hypotheses of Theorem 5.1 and according to Problem 5.1, the two functions $V(x)$ and $V_p(x_p)$ mentioned above are such that:

- V guarantees the t - \mathcal{L}_2 specification, arising from the flow map of the closed loop. Indeed, γ appears only in (5.4b), where only the flow map variables are involved;
- V_p guarantees the t -decay rate, by enforcing jumps whenever the decay rate condition would be violated. Indeed $\tilde{\alpha}$ depends on α which appears only in (5.4c), where only the hybrid loop variables are involved. Notice also that Theorem 3.2 does not require any assumption on the flow map (which can be given) and moreover V_p defines the flow and jump sets (see (3.15));
- both V and V_p do not increase across jumps;
- V and V_p match after each jump (namely, $V(x^+) = V_p(x_p^+) = V_p(x_p)$);
- at jumps both functions share the same dynamics (namely, $\dot{V}(x^+) = \dot{V}_p(x_p)$).

★

From Remark 5.1, we infer that through the resets we can keep all the trajectories in the region where V_p , therefore $|x_p|$, decreases at the desired rate. Therefore the hybrid loop guarantees the t -decay rate property. In the meantime, we can integrate V along flows and, since V does not increase at jumps, we can add all these integrals to obtain the t - \mathcal{L}_2 specification, which depends on the flow map of the hybrid controller. Therefore Theorem 5.1 provides a multi-objective synthesis which returns:

- an optimal flow map with respect to the t - \mathcal{L}_2 gain,
- an optimal jump map and flow and jump sets with respect to t -decay rate,

and suitably combines these two parts in a multi-objective hybrid controller which is optimal with respect to the minimized performance index subject to the other performance index given a priori

and selected with respect the requirements of the application.

Note that we are not claiming to use a different Lyapunov function for each objective, and the conservativeness discussed in [79, §IV.A] still holds. However, since the controller state can be reset (this is an extra degree of freedom), the flow and jump sets can be designed based on the Lyapunov-like function V_p that privileges the decrease in the x_p -direction. Moreover, such a function is built from the function V and shares with it some properties, as stated above.

We should mention that an interesting (and less conservative) key element of our synthesis is that the t -decay rate property is applied only to the x_p substate, whereas with linear techniques, one would need to focus on the whole state (x_p, x_c) which is more restrictive. Indeed in Appendix 5.4.2, the LMIs to perform the corresponding convex multi-objective synthesis in the linear case are reported. By comparing (5.4c) and (21), it is easy to see that our construction imposes the t -decay rate only in the x_p subspace, whereas (21) addresses it in all the state space.

Conditions (5.4) of Theorem 5.1 presents a convex synthesis which does not consider the sets \mathcal{F} , $\tilde{\mathcal{F}}$, $\tilde{\mathcal{F}}_\epsilon$ and \mathcal{J} namely, the conditions of Proposition 2.1 are satisfied with $\tau_F = \tau_R = \tau_C = 0$ and $\tilde{M} = 0$. This means that the regional separation due to the flow and jump sets is not taken into account (see Remark 2.7) and therefore, the estimated t - \mathcal{L}_2 gain established by V is guaranteed in all the state-space \mathbb{R}^{2np} . This is conservative because the trajectories of the hybrid closed loop are forced to evolve only in the flow set and less conservative conditions would be obtained by allowing $\tau_F \neq 0$ and $\tilde{M} = \tau_F M$ in (2.25a) (note that (2.25c) and (2.25d) would still be automatically satisfied, see also [88, Theorem 2]). Furthermore, $\tilde{M} = 0$ in (2.25a) implies that A in (5.3) is Hurwitz, namely the linear dynamics before resets is exponentially stable, allowing $\tau_F \neq 0$ would not necessarily imply this property and interesting closed-loop responses exhibiting exponentially diverging branches might be observed. However, with the change of coordinates used in the proof of Theorem 5.1, allowing $\tau_F \neq 0$ introduces nonlinear terms in our matrix inequalities, which destroy the desirable convex nature of our construction.

In spite of the fact that the t - \mathcal{L}_2 gain is estimated in all the state space, Theorem 5.1 relies on the regional separation of the state space to guarantee the other performance index, that is, the decay rate in (3.14). In particular, as explained in Chapter 3, the exponential bound comes from the fact that we do not leave \mathcal{F} , that is why we have an upper bound in the choice of ρ . Therefore for large enough ρ we might have exponential stability and the certified t - \mathcal{L}_2 gain, but we would not have the guarantee of bound (3.14) and so of a t -decay rate $\tilde{\alpha}/2$.

Finally, we stress that Theorem 5.1 is the only one in the literature to provide a multi-objective synthesis of a hybrid controller for a linear plant. As already mentioned, the only other optimal synthesis of a hybrid controller for a linear plant is [78]. Note that both [78] and Theorem 5.1 make Assumption 3.1, nevertheless Theorem 5.1 accomplishes a multi-objective synthesis whereas [78] focuses on the single-objective synthesis with respect to t - \mathcal{L}_2 gain. Furthermore, Theorem 5.1 relies on Theorem 2.1, which allows $\bar{D}_{zw} \neq 0$, whereas [78] relies on the results of [65, Theorem 1] (which is less generic than Theorem 2.1, see item 1 of Remark 2.5), which does not allow $\bar{D}_{zw} \neq 0$. However, it is unclear how [78] guarantees [65, Assumption 1] (which requires $Gx \in \mathcal{F}$, for all $x \in \mathcal{J}$) and the author does not provide further details on whether or not this assumption is guaranteed.

5.3 Comments on the convex hybrid output feedback synthesis

It is important to make some comments for the output feedback case. Indeed Section 5.2 presents a multi-objective synthesis with respect to t -decay rate and t - \mathcal{L}_2 gain, of a hybrid controller in hybrid state feedback with the plant. Therefore in the statement of Theorem 5.1, the restrictive Assumption 3.1 on the availability of x_p through measurements, is made.

In the meantime Chapter 4 provides hybrid output feedback schemes and in particular, Theorem 4.2 and Corollary 4.2 generalize the hybrid control scheme used in Theorem 3.2 (and so also the one in Theorem 5.1). Nevertheless the multi-objective synthesis here presented cannot at the moment, be immediately generalized successfully to the hybrid output feedback case as explained below.

First of all, the introduction of the observer does affect the guaranteed t -decay rate. The transient time induced by the observer presents undesired effects and the t -decay rate in the x_p -direction established in (3.14), cannot be guaranteed whenever an observer is introduced. It deserves to be mentioned the fact that preliminary studies show that by introducing an observer, a decay rate might still be guaranteed in the (\hat{x}_p, e) -direction, nevertheless more investigations are still needed and so we will not go any further on this topic, in this dissertation.

Due to the fact that by introducing an observer the t -decay rate is not guaranteed, the multi-objective synthesis for the hybrid output feedback becomes single-objective with respect to the t - \mathcal{L}_2 gain. As a direct consequence of the fact that Theorem 5.1 does not exploit the regional separation coming from \mathcal{F} and \mathcal{J} to assess the t - \mathcal{L}_2 gain, both Theorem 4.2 and Corollary 4.2 can be used to extend a posteriori the scheme in Theorem 5.1 to the output feedback case. In particular, Corollary 4.2 can be straightforwardly used, whereas for Theorem 4.2 depending on \bar{D}_w the following caveats need to be considered:

- a. if $\bar{D}_w = 0$: then in this case K_y , K_x , K_c and K_η can take any value;
- b. if $\bar{D}_w \neq 0$: then we need to select $K_y = 0$, $K_x = 0$, $K_c = 0$ and $K_\eta = 0$.

According to Remark 4.2, whenever $\bar{D}_w = 0$ (and under Assumption 5.1), $\eta := y - \hat{y} = \bar{C}_p e$ and item a comes from the fact that no noise is injected in the jump map of (4.3a) and moreover, η can be used into the sets (4.3d) and (4.3e) to exploit the $\bar{C}_p e$ component of the error. On the other hand, item b comes from the fact that if $\bar{D}_w \neq 0$, we have $\eta := y - \hat{y} = \bar{C}_p e + \bar{D}_w w$ with the consequence that $\bar{C}_p e$ is no longer available to be taken into account in sets (4.3d) and (4.3e) (through matrices K_x , K_c , K_η). Furthermore, $\bar{D}_w = 0$ would imply that the exogenous signal w is injected in the jump map and this is not admissible according to the framework in Chapter 2. This is why Theorem 4.2 needs some precautions which are not necessary for the simpler Corollary 4.2.

In spite of the cautions above, the two steps synthesis presented in Section 4.3.5 can be generalized to this case in the following way:

1. solve the convex hybrid state feedback synthesis;
2. according to items a and b above, design L satisfying Assumption 4.1 (and eventually K_y , K_x , K_c and K_η for the scheme in Theorem 4.2).

By following these two-steps synthesis, it is important to stress that the observer changes, in general, the estimated t - \mathcal{L}_2 gain obtained during the synthesis of the hybrid state feedback scheme.

Therefore the good way to proceed is to relaunch the analysis presented in Chapter 2 to estimate the t - \mathcal{L}_2 gain of the new arisen output feedback scheme. Note that the introduction of the observer, in general, deteriorates the t - \mathcal{L}_2 gain and the new estimation for the output feedback scheme might be several order of magnitude higher. Nevertheless, since the observer steps-in only at jumps, we will show in the simulations that although the certified t - \mathcal{L}_2 gain is worst for the output feedback case, the trend in the simulations does not change significantly from the hybrid state feedback case.

Finally we stress that preliminaries studies showed that a promising way to turn around the disadvantages induced by the observer for the t - \mathcal{L}_2 gain, looks to be a synthesis held by taking into account the sets information (namely, \tilde{M} , τ_F , τ_R and τ_C non zero in Proposition 2.1). The idea is to make an optimal synthesis of a hybrid state feedback controller with respect to the t - \mathcal{L}_2 gain γ and then, to augment such a controller to the output feedback scheme by designing L , K_y , K_x , K_c and K_η in order to maintain the same gain γ (if possible) to the hybrid output feedback case. Although this case presents several technical difficulties, it seems that the gains K_x , K_c and K_η may be used to attenuate the undesired effects of the observer, mitigating the deterioration of the t - \mathcal{L}_2 gain for output feedback scheme. Nevertheless in this dissertation, we will not consider any further this latter case.

Finally, we stress that although the observer augmentation looks promising, on the other hand the complete hybrid output feedback controller has order $n_c = 2n_p$, which is not suitable at the present time for large order plants.

5.4 Simulations

We want to show that the hybrid controller coming from our multi-objective synthesis has the capability to overcome some limitations of the corresponding linear multi-objective synthesis. In Appendix 5.4.2, the reader can find the condition for the synthesis of a multi-objective linear controller with respect to exponential decay rate and \mathcal{L}_2 gain. Note that we will use t -decay rate and t - \mathcal{L}_2 gain for the hybrid system and decay rate and \mathcal{L}_2 gain for the linear one. Recall that the t - \mathcal{L}_2 gain is obtained by projecting the hybrid signals on the ordinary time t and that, due to the dwell time in (2.1), we are allowed to make comparisons with the classical \mathcal{L}_2 gain.

We will perform the design syntheses by fixing α and α_L in order to cope only with LMI eigenvalue problems rather than generalized eigenvalue problems. Therefore, we compare controllers (linear and hybrid) guaranteeing the same convergence rate (namely $\alpha = \alpha_L$)¹.

In order to have good condition numbers for the simulations, both the linear and the hybrid syntheses we are going to present have been obtained with the following extra constraints (for details the reader is referred to [22])

$$\begin{aligned} \text{He} \left(\Sigma + \vartheta \begin{bmatrix} Y & I \\ I & W \end{bmatrix} \right) &> 0, \\ \begin{bmatrix} \sin(\theta)(\Sigma + \Sigma^\top) & -\cos(\theta)(\Sigma - \Sigma^\top) \\ \cos(\theta)(\Sigma - \Sigma^\top) & \sin(\theta)(\Sigma + \Sigma^\top) \end{bmatrix} &< 0, \end{aligned}$$

¹Note that the t -decay rate in Definition 1.13 allows us to make comparison with the classical exponential decay rate. On the other hand, recall that our hybrid synthesis returns an exponential bound only in the x_p subspace.

where

$$\Sigma = \begin{bmatrix} \bar{A}_p Y + \bar{B}_p \hat{C} & \bar{A}_p + \bar{B}_p \hat{D} \bar{C}_p \\ \hat{A} & W \bar{A}_p + \hat{B} \bar{C}_p \end{bmatrix},$$

$\vartheta = 50$ and $\theta = \pi/5$. Notice that the coefficients ϑ and θ imply that the eigenvalues of Σ lie in a cone of the complex left-hand plane in order to avoid numerical problems during the simulations. Moreover in order to build the flow and jump sets of the hybrid controller, we will select $\tilde{\alpha} = 99\% \alpha$ and μ is obtained by solving (3.12) and maximizing μ .

We propose also a hybrid output feedback augmentation by means of a Luenberger observer. We rely on Corollary 4.2 and the design is carried out by solving

$$\text{He} \left(P_e \bar{A}_p - Q_e \bar{C}_p + \frac{\alpha_o}{2} P_e \right) < 0,$$

with $P_e = P_e^\top > 0$, $\alpha_o > 0$ and followed by the extra condition

$$\text{He} \left(P_e \bar{A}_p - Q_e \bar{C}_p + \vartheta P_e / 2 \right) > 0.$$

The observer gain L is then obtained as $L = P_e^{-1} Q_e$. We stress that it is not available an optimal synthesis to design the observer in order to augment the hybrid controller to the output feedback case maintaining the t - \mathcal{L}_2 gain. Therefore we will only make the synthesis of the observer imposing α_o by trial and error.

We will denote state feedback with SF and output feedback with OF.

5.4.1 A DC motor

Let us consider the example of a DC motor presented in Sections 3.5.3 and 4.3.5.2. In particular, consider the reduced model presented in (4.28), which is reported next with also the gains related to the exogenous signal w (see (5.1))

$$\left[\begin{array}{c|c|c} \bar{A}_p & \bar{B}_p & \bar{B}_w \\ \hline \bar{C}_z & \bar{D}_z & \bar{D}_{zw} \\ \hline \bar{C}_p & \bar{D}_p & \bar{D}_w \end{array} \right] = \left[\begin{array}{cc|cc} -2.4 & 0 & 2 & 1 \\ 1 & 0 & 0 & 1 \\ \hline 0 & 1 & 10 & 0 \\ \hline 0 & 1 & 0 & 5 \end{array} \right].$$

Note that for the purpose of the simulation we decided to use a performance output z which penalizes the control input u coming from the controller and the plant output. The exogenous signal w can affect the state dynamics and the output y .

Figure 5.1 shows the γ values obtained with the linear and the hybrid syntheses as a function of the decay rate. To be fair with the linear \mathcal{L}_2 gain estimation, we applied the bounded real lemma (see [79]) to estimate the exact \mathcal{L}_2 gain. In this case, Figure 5.1 shows that the \mathcal{L}_2 gain returned from the linear synthesis matches the one obtained from the bounded real lemma². However, it is

²We emphasize that the bounded real lemma returns the exact \mathcal{L}_2 gain for the linear case and that due to the multi-objective nature of the linear synthesis the \mathcal{L}_2 gain obtained from the linear synthesis is not necessarily the exact \mathcal{L}_2 gain but only an upper bound.

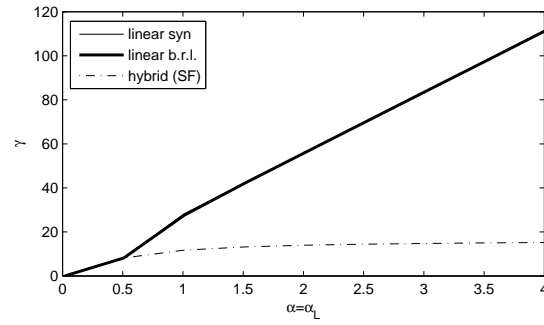


Figure 5.1: Trend of γ and $\alpha = \alpha_L$ for the linear and hybrid state feedback case.

easy to see that the hybrid case can induce a certain convergence rate without giving up too much on the achievable t - \mathcal{L}_2 gain. For decay rates larger than $\alpha = 0.5$, the linear synthesis returns larger \mathcal{L}_2 gains than the hybrid synthesis, whose t - \mathcal{L}_2 gains show a mild increase.

To show the effectiveness of our method, we propose two design syntheses with $\alpha = \alpha_L = 0.51$ and $\alpha = \alpha_L = 2.01$, respectively, and for each synthesis there will be two simulations corresponding to the items of Problem 5.1:

- **(no disturbance)** a simulation with $x_p(0,0) = [-0.7 \ -4]^\top$, $x_c(0,0) = 0$, $\tau(0,0) = \frac{3}{2}\rho$ and no disturbance;
- **(zero initial condition)** a simulation with $x(0) = 0$, $\tau(0,0) = 0$ and

$$w(t) = \begin{cases} \exp(-(t - 0.1)) & \text{if } t \geq 0.1 \\ 0 & \text{if } t < 0.1 \end{cases} .$$

The observer is always initialized at the origin whenever it is considered.

Once again, we point out that both linear and hybrid syntheses are obtained for a given speed of convergence, which is the same in both cases. Therefore, we do not expect, a priori, important differences in the speed of convergence between the linear and hybrid case.

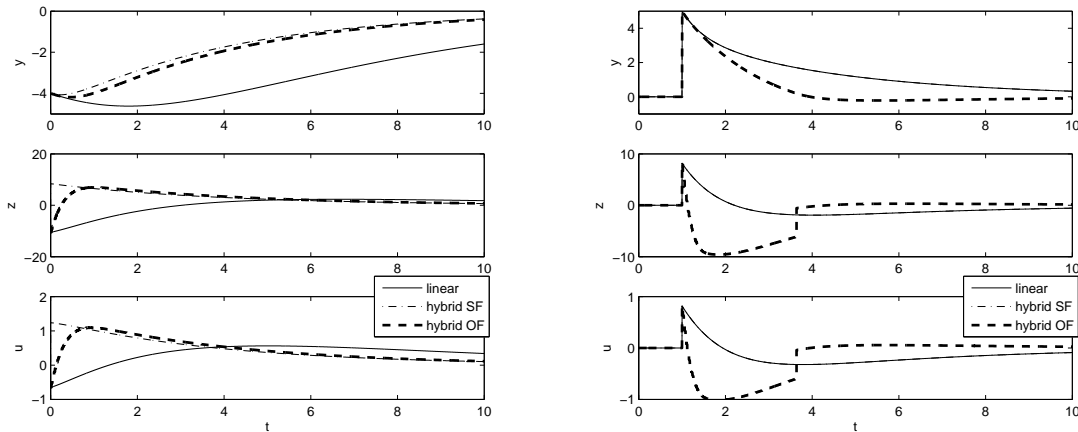
Case 1: Synthesis with $\alpha = \alpha_L = 0.5$. In this case, the syntheses return the linear controller

$$\left[\begin{array}{c|c} \bar{A}_\ell & \bar{B}_\ell \\ \hline \bar{C}_\ell & \bar{D}_\ell \end{array} \right] = \left[\begin{array}{cc|c} -2.56855 & -1.11709 & 0.52714 \\ 1 & -0.19999 & 0.19999 \\ \hline -0.08427 & -0.45854 & 0.16357 \end{array} \right],$$

and the hybrid controller

$$\left[\begin{array}{c|c} \bar{A}_c & \bar{B}_c \\ \hline \bar{C}_c & \bar{D}_c \end{array} \right] = \left[\begin{array}{cc|c} -2.56855 & -1.11709 & 0.52714 \\ 0.99999 & -0.2 & 0.2 \\ \hline -0.08427 & -0.45854 & 0.16357 \end{array} \right],$$

$$K_p = \begin{bmatrix} 0.99999 & -2.894 \cdot 10^{-8} \\ -6.06859 \cdot 10^{-7} & 0.99999 \end{bmatrix},$$



(a) Hybrid and linear controllers for $\alpha = \alpha_L = 0.5$ (**no disturbance**). (b) Hybrid and linear controllers for $\alpha = \alpha_L = 0.5$ (**zero initial condition**).

Figure 5.2: Linear output feedback, hybrid state feedback (SF) and hybrid output feedback (OF).

$$M = \begin{bmatrix} 0.05652 & 0.22055 & -0.0287 & -0.15616 \\ 0.22055 & 0.71794 & -0.0664 & -0.36129 \\ -0.0287 & -0.06640 & 6.32963 \cdot 10^{-6} & 0 \\ -0.15616 & -0.36129 & 0 & 6.32963 \cdot 10^{-6} \end{bmatrix}.$$

Furthermore the Luenberger observer for the hybrid output feedback is designed by imposing $\alpha_o = 10^{-2}$ and obtaining $L = [1.00565 \ 3.31903]^\top$. Finally, all the hybrid simulations are made selecting $\rho = 2 \cdot 10^{-2}$.

Note that in this case the hybrid synthesis returned a hybrid controller whose continuous-time part (that is $(\bar{A}_c, \bar{B}_c, \bar{C}_c, \bar{D}_c)$) matches the controller obtained through the linear synthesis.

As Figure 5.1 shows, for $\alpha = 0.5$ the linear and hybrid controllers guarantee the same $\gamma = 8.17855$. Unfortunately, the observer augmentation for the hybrid output feedback negatively affects the $t\text{-}\mathcal{L}_2$ gain for the hybrid state feedback. By applying the analysis in Proposition 2.1, we obtain that the new $t\text{-}\mathcal{L}_2$ gain is $\gamma_o = 283.16685$.

Looking at the transfer functions of both closed-loop systems (for the hybrid case we used the continuous-time part to compute it), it turns out that there is an unstable zero. It is surprising that the effects of the reset action on the reset controller somehow mitigates the negative effects of this bad zero on the transient response (see Figure 5.2(a) where the hybrid response shows a reduced undershoot). Note also that the hybrid output feedback still mitigates the undershoot³.

Figure 5.2(b) depicts the fact that in the presence of a disturbance $w \in \mathcal{L}_2$, the hybrid (state feedback) and linear controllers behave essentially in the same way, which is expected, since the γ is the same for both controllers. The hybrid output case shows a worst behavior, as expected.

³A hybrid system is nonlinear, thus the transfer function is not defined. Indeed all we are saying is that if we turn off the resets in the hybrid closed-loop system of Case 1, then the arising linear system would be a non-minimum phase and would present an undershoot in the output trend. In the meantime, with the resets turned on, the undershoot disappears (see y -plot in Figure 5.2(a)).

Case 2: Synthesis with $\alpha = \alpha_L = 2$. In this case, the syntheses return the linear controller

$$\left[\begin{array}{c|c} \bar{A}_\ell & \bar{B}_\ell \\ \hline \bar{C}_\ell & \bar{D}_\ell \end{array} \right] = \left[\begin{array}{cc|c} -26.80803 & -54.5639 & -2.10526 \\ -27.10017 & -65.92108 & 0.90999 \\ \hline -13.55108 & -30.33219 & -1.1189 \end{array} \right],$$

and the hybrid controller

$$\left[\begin{array}{c|c} \bar{A}_c & \bar{B}_c \\ \hline \bar{C}_c & \bar{D}_c \end{array} \right] = \left[\begin{array}{cc|c} -3.31857 & -3.0829 & 0.75773 \\ 0.99999 & -0.20001 & 0.2 \\ \hline -0.45928 & -1.44145 & 0.27886 \end{array} \right],$$

$$K_p = \begin{bmatrix} 0.99999 & -3.56778 \cdot 10^{-7} \\ -7.19699 \cdot 10^{-6} & 0.99998 \end{bmatrix},$$

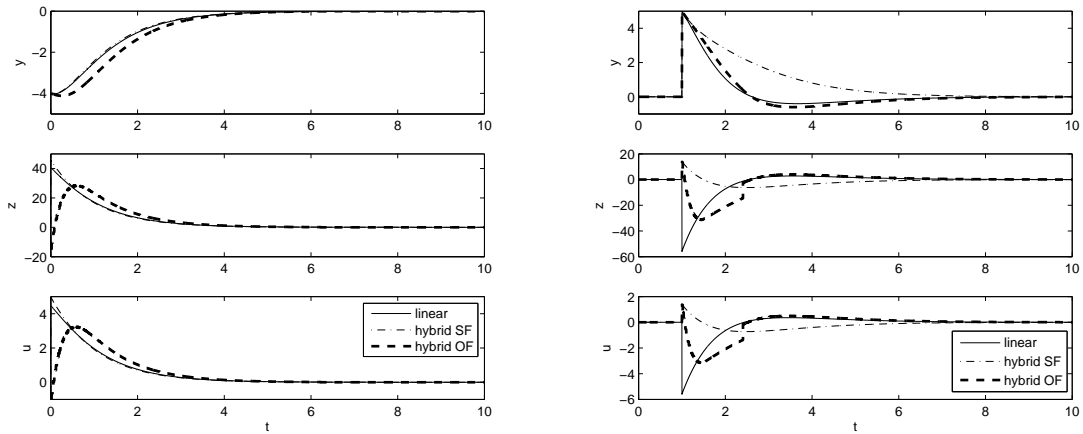
$$M = \begin{bmatrix} 1.36754 & 3.7342 & -0.69135 & -2.16979 \\ 3.7342 & 9.95868 & -1.59948 & -5.01991 \\ -0.69135 & -1.59948 & 4.94333 \cdot 10^{-6} & 0 \\ -2.16979 & -5.01991 & 0 & 4.94333 \cdot 10^{-6} \end{bmatrix}.$$

The Luenberger observer for the output feedback case is exactly as the one in the previous case. Finally the dwell-time parameter is $\rho = 2 \cdot 10^{-2}$.

The analysis of Proposition 2.1 returns that the hybrid output feedback case has a $t\text{-}\mathcal{L}_2$ gain smaller than or equal to 860.06616. Indeed, the $t\text{-}\mathcal{L}_2$ performance certification for the hybrid output feedback is more than one order of magnitude larger than the linear case ($\gamma = 55.9462$) and the hybrid (state feedback) case ($\gamma = 13.94329$).

Figure 5.3(a) shows that the hybrid (state feedback) controller induces a comparable decay rate to the linear one. Indeed both controllers induce decay rate $\alpha = 2.01$. The hybrid output feedback does not maintain the multi-objective origin of the hybrid controller and the trend is slower.

Figure 5.3(b) illustrates the γ gain improvement arisen from the use of the hybrid state feedback scheme. In particular, looking at the performance output z (middle plot), it is possible to see the improvement with the hybrid (state feedback) controller. Perhaps, the behavior of the hybrid output feedback may suggest that the $t\text{-}\mathcal{L}_2$ estimation coming from Proposition 2.1 is conservative due to the use of a quadratic Lyapunov function.



(a) Hybrid and linear controllers for $\alpha = \alpha_L = 2$ (**no disturbance**). (b) Hybrid and linear controllers for $\alpha = \alpha_L = 2$ (**zero initial condition**).

5.4.2 The F-8 aircraft

Consider now the following MIMO example used also in [52] representing the longitudinal dynamics of the F-8 aircraft. The system data is

$$\begin{bmatrix} \bar{A}_p & \bar{B}_p & \bar{B}_w \\ \bar{C}_z & \bar{D}_z & \bar{D}_{zw} \\ \bar{C}_p & \bar{D}_p & \bar{D}_w \end{bmatrix} = \begin{bmatrix} -0.8 & -0.0006 & -12 & 0 & -19 & -3 & -19 & -3 \\ 0 & -0.014 & -16.64 & -32.2 & -0.66 & -0.5 & -0.66 & -0.5 \\ 1 & -0.0001 & -1.5 & 0 & -0.16 & -0.5 & -0.16 & -0.5 \\ 1 & 0 & 0 & 0 & 0 & 0 & 0 & 0 \\ \hline 0 & 0 & 0 & 1 & 1 & 0 & 0 & 0 \\ 0 & 0 & -1 & 1 & 0 & 1 & 0 & 0 \\ \hline 0 & 0 & 0 & 1 & 0 & 0 & 0 & 0 \\ 0 & 0 & -1 & 1 & 0 & 0 & 0 & 0 \end{bmatrix}. \quad (5.15)$$

For the purpose of the simulation we selected a performance output which penalizes both the control u and the plant output y . Note that the system is a MIMO system with matrix \bar{A}_p Hurwitz. The state of this plant has state $x_p = [x_{p1} \ x_{p2} \ x_{p3} \ x_{p4}]^\top$ which represent, respectively: pitch rate (rad/sec), forward velocity (ft/sec), angle of attack (rad) and pitch angle (rad). The measured outputs $y = [y_1 \ y_2]^\top$ are, respectively: the pitch angle and the flight path angle. The control inputs $u = [u_1 \ u_2]^\top$ (supposed unconstrained) are, respectively: the aileron angle (deg) and the flaperon angle (deg).

Figure 5.3 shows the γ values obtained with the linear and the hybrid syntheses as a function of the decay rate. In this case the analysis with the bounded real lemma (see [79]) returned the exact \mathcal{L}_2 gains, which are lower than the one obtained from the linear synthesis. The hybrid (state feedback) controller induces a certain convergence rate without giving up on the achievable t - \mathcal{L}_2 gain, which shows a mild increase.

We propose a design synthesis with $\alpha = \alpha_L = 1.01$ and two simulations corresponding to the items of Problem 5.1:

- (**no disturbance**) a simulation with $x_p(0,0) = [0 \ 0 \ -1/2 \ -1/2]^\top$, $x_c(0,0) = 0$, $\tau(0,0) = \frac{3}{2}\rho$ and no disturbance;

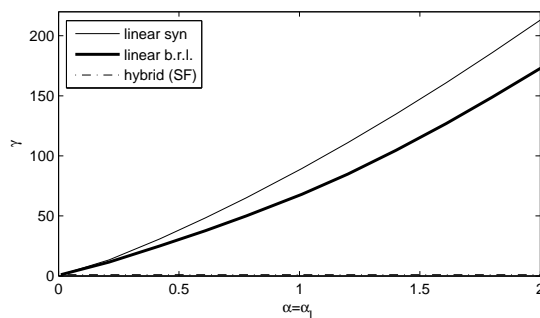


Figure 5.3: Trend of γ and $\alpha = \alpha_L$ for the linear and hybrid state feedback case.

- **(zero initial condition)** a simulation with $x(0,0) = 0$, $\tau(0,0) = 0$ and the exogenous signal $w = [w_1 \ w_2]^\top$ defined as

$$w_1(t) = \begin{cases} \exp(-10t) \sin(2t) & \text{if } t \geq 2 \\ 0 & \text{if } t < 2 \end{cases},$$

$$w_2(t) = \begin{cases} \exp(-5(t - 0.1)) & \text{if } t \geq 0.1 \\ 0 & \text{if } t < 0.1 \end{cases}.$$

The observer is always initialized at the origin whenever it is considered.

Similarly to the previous example the syntheses are obtained for a given speed of convergence, which is the same in both linear and hybrid (state feedback) case. Therefore, we do not expect, a priori, important differences in the speed of convergence between the linear and hybrid case.

By selecting $\alpha = \alpha_L = 1.01$, we get the linear controller and the hybrid controller in Appendix 5.4.2. The observer for the hybrid output feedback is designed by imposing $\alpha_o = 1$ and obtaining

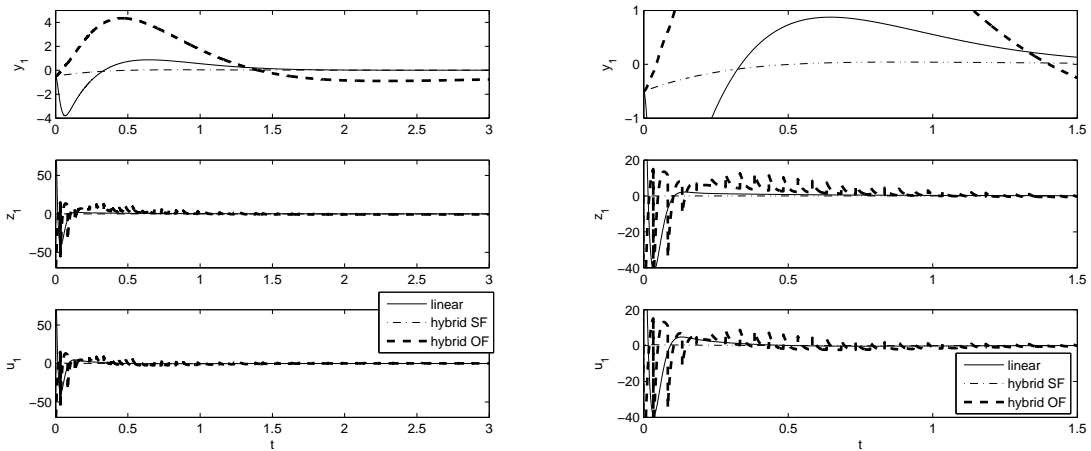
$$L = \begin{bmatrix} 10.19186 & 1.30772 \\ -28069.52978 & 13833.30767 \\ 15.32642 & -12.51867 \\ 9.16139 & 3.707 \end{bmatrix}.$$

All the hybrid simulations are made selecting $\rho = 5 \cdot 10^{-2}$.

As Figure 5.3 shows, for $\alpha = \alpha_L = 1$ the linear controller guarantees $\gamma = 68.00357$, whereas the hybrid (state feedback) controllers guarantees $\gamma = 1.07906$. Unfortunately, the analysis held by means of Proposition 2.1 certifies that the observer augmentation for the hybrid output feedback establishes the new t - \mathcal{L}_2 gain $\gamma_o = 2139.94263$.

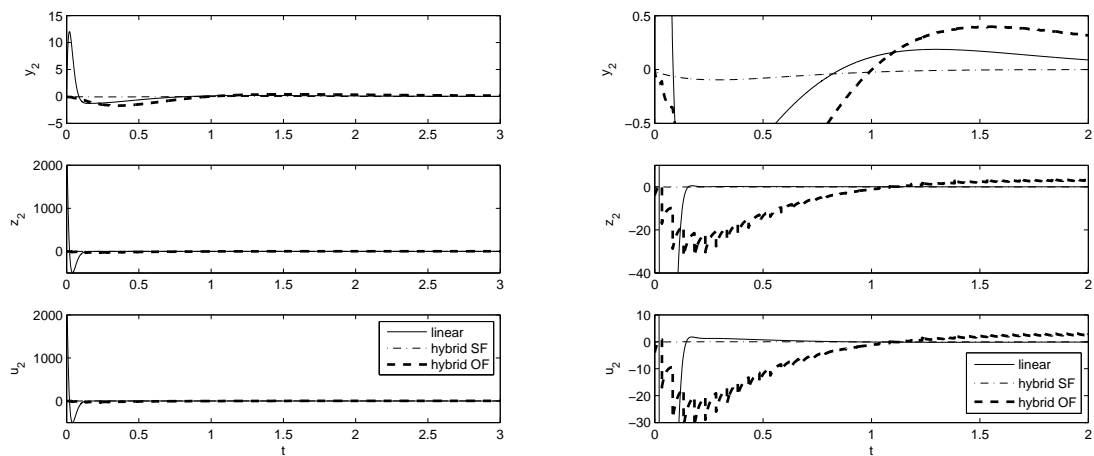
Figure 5.4(a) and its detail Figure 5.4(b) show that the linear and hybrid output feedback present some oscillations whereas the hybrid state feedback shows a very desirable behavior. Notice that for the case of u_2 and y_2 in Figure 5.5(a) and its detail Figure 5.5(b) the linear controller exhibits peaks higher even than the hybrid output feedback.

Figures 5.6(a) and 5.7(a) depict the fact that in the presence of a disturbance $w \in \mathcal{L}_2$, the hybrid output feedback presents lower peaks on the control u with respect to the linear controller. Again the hybrid state feedback exhibits the nicest trend which requires the zoom in Figures 5.6(b)



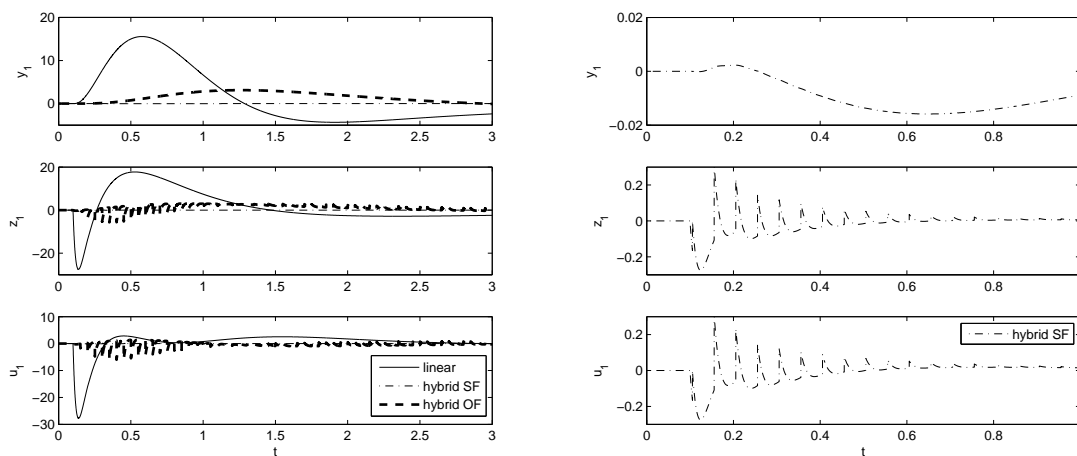
(a) Hybrid and linear controllers for $\alpha = \alpha_L = 1$ (no disturbance). (b) Zoom of Figure 5.4(a) (no disturbance).

Figure 5.4: Linear output feedback, hybrid state feedback (SF) and hybrid output feedback (OF). Only y_1 , z_1 and u_1 .



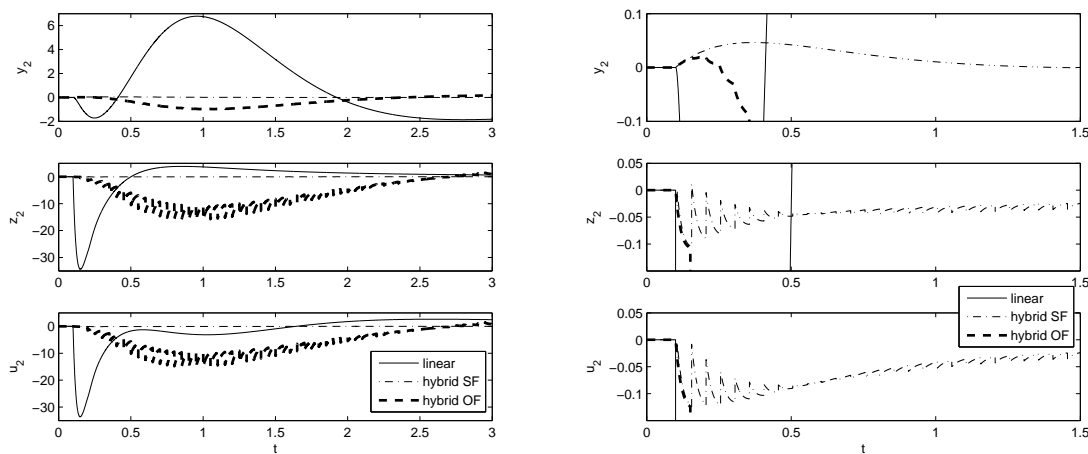
(a) Hybrid and linear controllers for $\alpha = \alpha_L = 1$ (no disturbance). (b) Zoom of Figure 5.5(a) (no disturbance).

Figure 5.5: Linear output feedback, hybrid state feedback (SF) and hybrid output feedback (OF). Only y_2 , z_2 and u_2 .



(a) Hybrid and linear controllers for $\alpha = \alpha_L = 1$ (zero initial condition). (b) Zoom of Figure 5.6(a) (zero initial condition).

Figure 5.6: Linear output feedback, hybrid state feedback (SF) and hybrid output feedback (OF). Only y_1 , z_1 and u_1 .



(a) Hybrid and linear controllers for $\alpha = \alpha_L = 1$ (zero initial condition). (b) Zoom of Figure 5.7(a) (zero initial condition).

Figure 5.7: Linear output feedback, hybrid state feedback (SF) and hybrid output feedback (OF). Only y_2 , z_2 and u_2 .

and 5.7(b) (in Figure 5.6(b) we removed the other signals to give visibility to the hybrid state feedback control u).

Conclusion

In this dissertation, we presented Lyapunov-based conditions to carry out performance analysis of a wide class of hybrid systems. These conditions based on a generic Lyapunov function V , returns LMI-based conditions whenever V is quadratic and generalize the results in [65]. Although quadratic Lyapunov functions may be conservative for hybrid systems, the advantage of having LMI conditions to solve with SDP tools allows us to easily establish performance bounds and to compare several control strategies. Moreover, convex analysis tools suggest the possibility to tackle the (more complicated) problem of synthesis, by means of suitable change of coordinates (see [79]).

Unfortunately, a change of coordinates able to return convex conditions for the synthesis of a hybrid controller for a linear continuous-time plant is not currently available. The main difficulty seems related to the fact that hybrid controller architectures are too general, even assuming conic sets and linear mappings. Then to simplify the problem, the hybrid controller need to be structured, yielding, for instance, the FORE controller. It is in this scenario that the hybrid controllers in Chapter 3 look more interesting. The fact that a quadratic Lyapunov-like function is used to define the sets, allows us to establish conditions in order to map the jumps, guaranteeing the decrease of such a function along the trajectories (and hence achieving stability). These conditions structure the synthesis problem and reduce the degrees of freedom, with the advantage of simplifying the development of convex synthesis strategies, as in [71, 72]. On the other hand, the controllers in Chapter 3 require the knowledge of the plant state, which is a strong limitation to their application.

Chapter 4 presents a way to overcome the drawback of measuring the plant state, by means of a Luenberger observer. The results seem to be useful in terms of overshoot reduction, although the price to pay is a controller of a higher order and no guarantees on the t -decay rate.

Chapter 5 has the merit to mix the general results in Chapter 2 with the structured hybrid controller in Chapter 3 and presents a multi-objective convex synthesis of a hybrid controller with respect to the t - \mathcal{L}_2 gain and t -decay rate. The insights coming from the results in Chapter 5 show that hybrid controllers may be a breakthrough of multi-objective control. Although the result concerns hybrid state feedback, this study allowed us to scratch the surface of the hybrid output feedback, which is more complicated.

Unfortunately, the results in Chapter 4 are not yet applicable to the multi-objective synthesis in Chapter 5. Indeed in the simulations of Chapter 5, we used only the simplest of our hybrid output feedback schemes, designed without any optimal strategy. In this case the analysis showed that both t - \mathcal{L}_2 gain and t -decay rate are very deteriorated. However, simulation data show that also the quasi-multi-objective⁴ hybrid output scheme may behave better than the multi-objective linear case.

As perspective for future works, the directions to investigate are many. The results in Chapter 2 can be extended to other performance indexes, with the effects that also new multi-objective syntheses involving different performance indexes may be developed. The hybrid output feedback in Chapter 4 deserves further investigations to establish whether or not the observer strongly bounds the performance. Preliminary studies are showing some difficulties in obtaining LMIs for the optimal synthesis. Indeed, the multi-objective synthesis of the structured hybrid controller in

⁴We use the attribute *quasi* to stress that the observer is selected a posteriori without any optimal criteria.

Chapter 4 leads to BMIs, due to the presence of the gains K_x , K_c , K_η in the flow set, which in turn is taken into account via S -procedure [10].

As ongoing works, we mention our studies accounting for actuator saturation. From simulation data, it is common to see that hybrid control has lower peaks than the classical linear ones (this is also true for our hybrid output schemes). Therefore it seems natural to wonder the implications of hybrid control in presence of actuator saturation. In this context, we developed stability analysis condition which lead to matrix inequalities whenever a quadratic Lyapunov function is considered. Nevertheless similarly to [83], we obtain LMIs for global results and BMIs for regional ones, due to the fact that the flow and jump sets have to be taken into account, preventing the use of common change of coordinates from the classical theory. Furthermore by structuring the Lyapunov-function, we developed sufficient conditions to design a static anti-windup compensator for a class of hybrid control schemes involving a hybrid controller and a linear plant with actuator saturation. The results are very preliminary and can be found in [30].

Appendix A

Proof of Claim 2.1 First recall that $t_{i+1} - t_i \geq \rho$ for all $i \in \mathbb{Z}_{\geq 1}$, due to the dwell time, and in particular $x(t, i) \in \mathcal{F}$ for all $t \in (t_i + \rho, t_{i+1}]$, $i \in \mathbb{Z}_{\geq 1}$ (see also Remark 2.2).

Now similarly to the proof of [65, Theorem 2], due to the fact that during flow $|\dot{x}| \leq |A||x|$, we have

$$|x(t, i)|^2 \leq \exp(2|A|(t - t_i))|x(t_i, i)|^2,$$

for all $t \in [t_i, t_{i+1}]$, $i \in \mathbb{Z}_{\geq 0}$, which by integrating implies

$$\begin{aligned} \|x[t_i, t]\|_2^2 &\leq (t - t_i) \exp(2|A|(t - t_i))|x(t_i, i)|^2 \\ &= \varphi(t - t_i)|x(t_i, i)|^2 \end{aligned} \quad (16)$$

for all $t \in [t_i, t_{i+1}]$, $i \in \mathbb{Z}_{\geq 0}$ and $\varphi(\cdot)$ defined in the statement.

Let us define $\chi(x) := x^\top \tilde{M}x - \epsilon x^\top x$. Thus, we have

$$\langle \nabla \chi, Ax \rangle \leq |2(\tilde{M} - \epsilon I)A||x|^2, \quad \forall x \in \mathbb{R}^n, \quad (17)$$

and due to (2.4), $x(t_i, i) \in \tilde{\mathcal{F}}$ for all $i \in \mathbb{Z}_{\geq 1}$, and since $\tilde{\mathcal{F}} \subset \tilde{\mathcal{F}}_\epsilon$, we have

$$\chi(x(t_i, i)) \leq -\epsilon|x(t_i, i)|^2, \quad \forall i \in \mathbb{Z}_{\geq 1}. \quad (18)$$

Then, by integrating (17) and using (16) and (18), for all $t \in [t_i, t_i + \rho]$, $i \in \mathbb{Z}_{\geq 1}$ and $|x(t_i, i)| \neq 0$, we have

$$\begin{aligned} \chi(x(t, i)) &\leq \chi(x(t_i, i)) + |2(\tilde{M} - \epsilon I)A|\|x[t_i, t]\|_2^2 \\ &\leq -(\epsilon - \varphi(t - t_i)|2(\tilde{M} - \epsilon I)A|)|x(t_i, i)|^2 \\ &< -(\epsilon - \varphi(\bar{\rho})|2(\tilde{M} - \epsilon I)A|)|x(t_i, i)|^2 = 0, \end{aligned} \quad (19)$$

where in the last line, we used the fact that $\rho \in (0, \bar{\rho})$ and the definition of $\bar{\rho}$. This concludes the proof. ■

Appendix B

Complements to Section 3.5.2

$$K_p = \begin{bmatrix} 0.0000116 \\ -0.0005687 \\ 0.0000143 \\ 0.0057060 \\ 0.0492531 \\ -0.1253410 \\ 0.0039875 \\ -0.0424092 \\ 0.0197270 \\ -0.0763948 \\ 0.0560231 \\ -0.5279079 \end{bmatrix},$$

$$\bar{P}_p = \begin{bmatrix} 0.0000016 & 0.0000105 & 0.0000137 & 0.0000768 & 0.0002319 & -0.0003181 \\ 0.0000105 & 0.0001218 & 0.0002113 & 0.0011626 & 0.0035532 & -0.0047534 \\ 0.0000137 & 0.0002113 & 0.0004823 & 0.0030136 & 0.0099310 & -0.0140680 \\ 0.0000768 & 0.0011626 & 0.0030136 & 0.0212743 & 0.0752808 & -0.1123512 \\ 0.0002319 & 0.0035532 & 0.0099310 & 0.0752808 & 0.2805448 & -0.4353699 \\ -0.0003181 & -0.0047534 & -0.0140680 & -0.1123512 & -0.4353699 & 0.6967520 \\ 0.0000122 & 0.0001841 & 0.0005324 & 0.0041673 & 0.0159177 & -0.0251964 \\ 0.0000496 & 0.0008302 & 0.0015540 & 0.0062958 & 0.0080622 & 0.0064265 \\ 0.0000175 & 0.0000184 & -0.0006059 & -0.0067500 & -0.0263212 & 0.0392753 \\ 0.0000677 & 0.0008638 & 0.0013054 & 0.0056083 & 0.0084086 & 0.0040072 \\ 0.0000289 & -0.0001299 & -0.0011416 & -0.0111090 & -0.0429308 & 0.0645609 \\ 0.0000919 & 0.0008866 & -0.0004615 & -0.0020113 & -0.0015240 & 0.0054357 \\ 0.0000122 & 0.0000496 & 0.0000175 & 0.0000677 & 0.0000289 & 0.0000919 \\ 0.0001841 & 0.0008302 & 0.0000184 & 0.0008638 & -0.0001299 & 0.0008866 \\ 0.0005324 & 0.0015540 & -0.0006059 & 0.0013054 & -0.0011416 & -0.0004615 \\ 0.0041673 & 0.0062958 & -0.0067500 & 0.0056083 & -0.0111090 & -0.0020113 \\ 0.0159177 & 0.0080622 & -0.0263212 & 0.0084086 & -0.0429308 & -0.0015240 \\ -0.0251964 & 0.0064265 & 0.0392753 & 0.0040072 & 0.0645609 & 0.0054357 \\ 0.0009147 & 0.0000139 & -0.0014505 & 0.0000702 & -0.0023778 & -0.0002114 \\ 0.0000139 & 0.0174043 & -0.0017262 & 0.0157849 & -0.0027044 & 0.0039945 \\ -0.0014505 & -0.0017262 & 0.0073748 & -0.0037478 & 0.0108487 & -0.0140637 \\ 0.0000702 & 0.0157849 & -0.0037478 & 0.0211570 & -0.0087528 & 0.0562713 \\ -0.0023778 & -0.0027044 & 0.0108487 & -0.0087528 & 0.0236907 & -0.0592855 \\ -0.0002114 & 0.0039945 & -0.0140637 & 0.0562713 & -0.0592855 & 0.9928438 \end{bmatrix}.$$

Complements to Section 5.4.2

Linear controller

$$\begin{bmatrix} \bar{A}_\ell & \bar{B}_\ell \\ \bar{C}_\ell & \bar{D}_\ell \end{bmatrix} = \left[\begin{array}{cccc|cc} -44.66133 & 10.10551 & 90904.29271 & -118026.24208 & 26900.45432 & 90971.10885 \\ -33.59083 & 7.7577 & 367184.22909 & -505132.47681 & 137724.8734 & 367241.63848 \\ -0.67799 & 0.42325 & 2618.09857 & -5843.35866 & 3214.94588 & 2622.75241 \\ 1.00122 & -0.00032 & -11.343 & -76.58293 & 87.9326 & -11.34527 \\ \hline 1.92272 & -0.43247 & -4174.8807 & 4489.43845 & -305.60814 & -4176.95944 \\ 2.76541 & -0.71469 & -4021.33963 & 10197.98804 & -6161.75083 & -4027.0238 \end{array} \right].$$

Hybrid controller

$$\begin{bmatrix} \bar{A}_c & \bar{B}_c \\ \bar{C}_c & \bar{D}_c \end{bmatrix} = \left[\begin{array}{cccc|cc} -20.70821 & 0.6617 & 31.35506 & 268.4008 & -371.60155 & -1.88858 \\ 0.16695 & 0.02843 & -29.06337 & 52.24756 & -71.00702 & -10.64126 \\ -6.17556 & 0.22419 & -35.4746 & -59.3947 & 65.20212 & -51.12682 \\ -7.25332 & 0.20065 & 0.45407 & -116.19095 & 83.51819 & -20.89777 \\ \hline -2.6964 & 0.07969 & -69.85215 & -124.9959 & 183.23244 & -76.56928 \\ 36.82637 & -0.99868 & 105.73428 & 242.02127 & 8.12775 & -13.35239 \end{array} \right],$$

$$K_p = \begin{bmatrix} 0.04195 & 0.03305 & 2.30003 & -6.10179 \\ -0.0288 & 1.00248 & 0.0418 & -0.16558 \\ -0.01436 & 0.00145 & 1.017 & -0.08008 \\ -0.01198 & -0.00044 & 0.04448 & 0.91341 \end{bmatrix},$$

$$M = \begin{bmatrix} 0.84872 & -0.02407 & -171.87061 & -228.88116 \\ -0.02407 & 0.00192 & 4.80313 & 6.09840 \\ -171.87061 & 4.80313 & 860.66119 & -511.73132 \\ -228.88116 & 6.0984 & -511.73132 & -2993.87728 \\ -1.47269 & 0.62911 & -7.03852 & -2.46935 \\ 0.02557 & -0.01667 & 0.22735 & -0.02582 \\ 173.73479 & -6.36768 & -410.26237 & 1102.05656 \\ 224.66781 & -2.17167 & -641.39219 & 1497.58611 \\ \hline -1.47269 & 0.02557 & 173.73479 & 224.66781 \\ 0.62911 & -0.01667 & -6.36768 & -2.17167 \\ -7.03852 & 0.22735 & -410.26237 & -641.39219 \\ -2.46935 & -0.02582 & 1102.05656 & 1497.58611 \\ 4.43571 \cdot 10^{-9} & 0 & 0 & 0 \\ 0 & 4.43571 \cdot 10^{-9} & 0 & 0 \\ 0 & 0 & 4.43571 \cdot 10^{-9} & 0 \\ 0 & 0 & 0 & 4.43571 \cdot 10^{-9} \end{bmatrix}.$$

Appendix C

Optimal synthesis for overshoot reduction

We present the convex synthesis for overshoot reduction by [72]. First, the dynamics (3.1) has to be written in observability canonical form, so that $x_p = \begin{bmatrix} x_1 \\ y \end{bmatrix}$, then we have to solve the following LMI eigenvalue problem

$$\begin{aligned} \min_{\bar{Q}_p = \bar{Q}_p^\top, \rho_x, \rho_y, X} \rho_y, \quad \text{s.t.} \quad \bar{Q}_p = \begin{bmatrix} Q_1 & q_{1y} \\ q_{1y}^\top & q_y \end{bmatrix} > I \\ 0 < \begin{bmatrix} \kappa_M I & X \\ X^\top & \kappa_M I \end{bmatrix}, \quad 0 > \text{He}(A_p \bar{Q}_p + B_p X) \\ 0 \leq \begin{bmatrix} \rho_x & 1 \\ 1 & \rho_y \end{bmatrix}, \quad \rho_x < Q_1, \quad q_y < 1 + \rho_y, \end{aligned} \quad (20)$$

where $\kappa_M > 0$ is given. The optimal solution to (20) leads to the gain $K_p = X \bar{Q}_p^{-1}$ and to $\bar{P}_p = \bar{Q}_p^{-1}$ satisfying (3.5) with a small enough $\tilde{\alpha}$ and such that $|K_p| \leq |X| |\bar{Q}_p^{-1}| \leq \kappa_M$. Moreover, the bounds given by the last three constraints can be shown to imply that smaller values of ρ_y lead to a function $V_p(x_p) = x_p^\top \bar{Q}_p^{-1} x_p$ closer to $|y|^2$.

Multi-objective synthesis of a linear controller

We present the equivalent multi-objective technique for the linear case. The reader is referred to [79, Theorem 2] and [22] for more details.

Consider the linear controller

$$\begin{aligned} \dot{x}_c &= \bar{A}_\ell x_c + \bar{B}_\ell y \\ u &= \bar{C}_\ell x_c + \bar{D}_\ell y \end{aligned}$$

with state $x_c \in \mathbb{R}^{n_c}$ (not resettable) and u and y interconnected with (5.1). Since the quadratic Lyapunov function in the transformed coordinates of (5.4b) is a quadratic form with the matrix $\begin{bmatrix} Y & I \\ I & W \end{bmatrix}$, then the multi-objective synthesis (optimal with respect to the \mathcal{L}_2 gain and decay rate α_L) for the linear (and continuous-time) case is given by solving (5.4a), (5.4b) and

$$\text{He} \left(\begin{bmatrix} \bar{A}_p Y + \bar{B}_p \hat{C} & \bar{A}_p + \bar{B}_p \hat{D} \bar{C}_p \\ \hat{A} & W \bar{A}_p + \hat{B} \bar{C}_p \end{bmatrix} \right) < -\alpha_L \begin{bmatrix} Y & I \\ I & W \end{bmatrix}, \quad (21)$$

and computing the linear controller $(\bar{A}_\ell, \bar{B}_\ell, \bar{C}_\ell, \bar{D}_\ell)$ by using (5.5) (where \bar{P}_p and K_p are not needed).

Note that inequality (21) is more restrictive than (5.4c) and allows us to conclude that the guaranteed decay rate by the continuous-time linear design is $\alpha_L/2$. We will use $\alpha_L/2$ to denote the decay rate for the linear case and to distinguish it from the hybrid decay rate $\tilde{\alpha}/2$ used in Theorem 5.1.

Bibliography

- [1] W.H.T.M. Aangenent, G. Witvoet, W.P.M.H. Heemels, M.J.G. van de Molengraft, and M. Steinbuch. Performance Analysis of Reset Control Systems. *International Journal of Robust and Nonlinear Control*, 20(11):1213–1233, 2010.
- [2] K.J. Åström. Limitations on Control System Performance. *European Journal of Control*, 6(1):2–20, 2000.
- [3] R. Bambang, E. Shimemura, and K. Uchida. Mixed $\mathcal{H}_2/\mathcal{H}_\infty$ control with pole placement: state feedback case. In *Proceedings of the 1993 American Control Conference*, pages 2777–2779, San Francisco, CA, 1993.
- [4] A. Banos, J. Carrasco, and A. Barreiro. Reset Times-Dependent Stability of Reset Control Systems. *IEEE Transactions on Automatic Control*, 56(1):217–223, 2011.
- [5] A. Banos and A. Vidal. Design of PI+CI Reset Compensators for Second Order Plants. In *Industrial Electronics, 2007. ISIE 2007. IEEE International Symposium on*, pages 118–123, 2007.
- [6] O. Beker, C. Hollot, and Y. Chait. Fundamental Properties of Reset Control Systems. *Automatica*, 40(6):905–915, 2004.
- [7] O. Beker, C.V. Hollot, and Y. Chait. Plant with an Integrator: an Example of Reset Control Overcoming Limitations of Linear Feedback. *IEEE Transactions on Automatic Control*, 46(11):1797–1799, November 2001.
- [8] V. Belevitch. *Classical Network Theory*, volume 36. Holden-Day, San Francisco, 1968.
- [9] H.W. Bode. *Network Analysis and Feedback Amplifier Design*. Van Nostrand, New York, NY, USA, 1945.
- [10] S.P. Boyd, L. El Ghaoui, E. Feron, and V. Balakrishnan. *Linear Matrix Inequalities in System and Control Theory*. Society for Industrial and Applied Mathematics, 1994.
- [11] S.P. Boyd and L. Vandenberghe. *Convex Optimization*. Cambridge University Press, New York, NY, USA, 2004.
- [12] R.W. Brockett. Asymptotic Stability and Feedback Stabilization. In *Differential Geometric Control Theory.*, volume 27 of *Progress in Mathematics.*, pages 181–191. Birkhäuser, 1983.
- [13] R.L. Burden and J.D. Faires. *Numerical Analysis*. Thomson Brooks/Cole, 2005.
- [14] C. Cai and A.R. Teel. Characterizations of Input-to-state Stability for Hybrid Systems. *Systems & Control Letters*, 58(1):47–53, 2009.
- [15] C. Cai, A.R. Teel, and R. Goebel. Converse Lyapunov Theorems and Robust Asymptotic Stability for Hybrid Systems. In *Proceedings of the 2005 American Control Conference*, pages 12–17, Portland (OR), USA, June 2005.
- [16] C. Cai, A.R. Teel, and R. Goebel. Smooth Lyapunov Functions for Hybrid Systems, Part I: Existence is Equivalent to Robustness. *IEEE Transactions on Automatic Control*, 52(7):1264–1277, 2007.

- [17] C. Cai, A.R. Teel, and R. Goebel. Smooth Lyapunov Functions for Hybrid Systems, Part II: (Pre)Asymptotically Stable Compact Sets. *IEEE Transactions on Automatic Control*, 53(3):734–748, 2008.
- [18] A. Chaillet and A. Loria. Uniform Semiglobal Practical Asymptotic Stability for Non-Autonomous Cascaded Systems and Applications. *Automatica*, 44(2):337–347, 2008.
- [19] B.M. Chen, Z. Lin, and Y. Shamash. *Linear Systems Theory: a Structural Decomposition Approach*. Birkhäuser, Boston, 2004.
- [20] Q. Chen. *Reset Control Systems: Stability, Performance and Application*. PhD thesis, University of Massachusetts, Amherst (MA), USA, 2000.
- [21] Q. Chen, Y. Chait, and C.V. Hollot. Analysis of Reset Control Systems Consisting of a FORE and Second Order Loop. *J. Dynamic Systems, Measurement and Control*, 123:279–283, 2001.
- [22] M. Chilali and P. Gahinet. H_∞ Design with Pole Placement Constraints: an LMI Approach. *IEEE Transactions on Automatic Control*, 41:358–367, 1996.
- [23] M. Claeys, D. Arzelier, D. Henrion, and J.-B. Lasserre. Moment LMI approach to LTV impulsive control. In *Proceedings of the 52nd IEEE Conference on Decision and Control*, December 2013, to appear.
- [24] F.H. Clarke, Y.S. Ledyaev, R.J. Stern, and P.R. Wolenski. *Nonsmooth Analysis and Control Theory*. New York: Springer-Verlag, 1998.
- [25] J.-M. Coron, L. Praly, and A.R. Teel. Feedback Stabilization of Nonlinear Systems: Sufficient Conditions and Lyapunov and Input-Output Techniques. In *Trends in Control: A European Perspective*, pages 293–348. Springer, 1995.
- [26] F. Fichera, C. Prieur, S. Tarbouriech, and L. Zaccarian. A Convex Hybrid \mathcal{H}_∞ Synthesis with Guaranteed Convergence Rate. In *Proceedings of the 51st Conference on Decision and Control*, pages 4217–4222, Maui (HI), USA, 2012.
- [27] F. Fichera, C. Prieur, S. Tarbouriech, and L. Zaccarian. Improving the Performance of Linear Systems by Adding a Hybrid Loop: the Output Feedback Case. In *Proceedings of the 2012 American Control Conference*, pages 3192–3197, Montreal, Canada, 2012.
- [28] F. Fichera, C. Prieur, S. Tarbouriech, and L. Zaccarian. On Hybrid State-feedback Loops Based on a Dwell-time Logic. In *4th IFAC Conference on Analysis and Design of Hybrid Systems*, pages 388–393, Eindhoven, The Netherlands, 2012.
- [29] F. Fichera, C. Prieur, S. Tarbouriech, and L. Zaccarian. Using Luenberger Observers and Dwell-time Logic for Feedback Hybrid Loops in Continuous-time Control Systems. *International Journal of Robust and Nonlinear Control*, 23:1065–1086, 2013.
- [30] F. Fichera, C. Prieur, S. Tarbouriech, and L. Zaccarian. In *Static Anti-windup Scheme for a Class of Homogeneous Dwell-time Hybrid Controllers.*, Zurich, Switzerland, 2013, to appear.
- [31] F. Forni, S. Galeani, D. Nešić, and L. Zaccarian. Lazy Sensors for the Scheduling of Measurements Samples Transmission in Linear Closed Loops Over Networks. In *Proceedings of the 49th IEEE Conference on Decision and Control*, pages 6469–6474, Atlanta (GA), USA, December 2010.

- [32] F. Forni, S. Galeani, D. Nešić, and L. Zaccarian. Lazy Sensors: Lyapunov-based Scheduling of Samples Transmission Over Networks. *Automatica*, 2012 submitted.
- [33] F. Forni, D. Nešić, and L. Zaccarian. Reset Passivation of Nonlinear Controllers via Suitable Time-regular Reset Map. *Automatica*, 47(9):2099–2106, 2011.
- [34] B.A. Francis. A Course in H_∞ Control Theory. 88, 1987.
- [35] G. Franklin, J.D. Powell, and A. Emami-Naeini. *Feedback Control of Dynamic Systems, 6Ed.* Prentice Hall, 2009.
- [36] J.S. Freudenberg and D.P. Looze. Right Half Plane Poles and Zeros and Design Trade-offs in Feedback Systems. *IEEE Transactions on Automatic Control*, 30(6):555–565, 1985.
- [37] J.S. Freudenberg and D.P. Looze. A Sensitivity Trade-off for Plants with Time Delay. *IEEE Transactions on Automatic Control*, 32(2):99–104, 1987.
- [38] J. Geromel, P. Peres, and J. Bernussou. On a Convex Parameter Space Method for Linear Control Design of Uncertain Systems. *SIAM Journal on Control and Optimization*, 29(2):381–402, 1991.
- [39] R. Goebel, R.G. Sanfelice, and A.R. Teel. Hybrid Dynamical Systems. *IEEE Control Systems Magazine*, 29(2):28–93, April 2009.
- [40] R. Goebel, R.G. Sanfelice, and A.R. Teel. *Hybrid Dynamical Systems: Modeling, Stability and Robustness.* Princeton University Press, 2012.
- [41] R. Goebel and A.R. Teel. Solutions to Hybrid Inclusions via Set and Graphical Convergence With Stability Theory Applications. *Automatica*, 42(4):573–587, 2006.
- [42] G.H. Golub and C.F. Van Loan. *Matrix Computations*, volume 3. Johns Hopkins University Press, 2012.
- [43] Y. Guo, W. Gui, C. Yang, and L. Xie. Stability analysis and design of reset control systems with discrete-time triggering conditions. *Automatica*, 48(3):528–535, 2012.
- [44] M.L.J. Hautus. Controllability and Observability Conditions of Linear Autonomous Systems. *Ned. Akad. Wetenschappen, Proc. Ser. A*, 72:443–448, 1969.
- [45] J.P. Hespanha. *Logic-Based Switching Algorithms in Control.* PhD thesis, Yale University, New Haven (CT), USA, 1998.
- [46] J.P. Hespanha, D. Liberzon, and A.S. Morse. Hysteresis-based Switching Algorithms for Supervisory. *Automatica*, 39(2):263–272, 2004.
- [47] J.P. Hespanha and A.S. Morse. Stabilization of Nonholonomic Integrators via Logic-based Switching. *Automatica*, 35(3):385–393, 1999.
- [48] J.P. Hespanha and A.S. Morse. Switching Between Stabilizing Controllers. *Automatica*, 38:1905–1971, 2002.
- [49] C. Hollot, O. Beker, Y. Chait, and Q. Chen. On Establishing Classic Performance Measures for Reset Control Systems. In *Perspectives in Robust Control.*, volume 268 of *Lecture Notes in Control and Information Sciences.*, pages 123–147. Springer London, 2001.

- [50] R.A. Horn and C.R. Johnson. *Matrix Analysis*. Cambridge University Press, Cambridge, UK, 1987.
- [51] M. Jungers and J. Daafouz. Guaranteed Cost Certification for Discrete-Time Linear Switched Systems With a Dwell Time. *IEEE Transactions on Automatic Control*, 58(3):768–772, 2013.
- [52] P. Kamasouris, M. Athans, and G. Stein. Design of Feedback Control Systems for Stable Plants with Saturating Actuators. In *Proceedings of the 27th IEEE Conference on Decision and Control*, pages 469–479, Austin, TX, 1988.
- [53] H.K. Khalil. *Nonlinear Systems*. Prentice Hall, PTR, 2002.
- [54] P. Khargonekar and K. Poolla. Uniformly Optimal Control of Linear Time-invariant Plants: Nonlinear Time-varying Controllers. *System & Control Letters*, 6(5):303–308, 1986.
- [55] M. Krstić, I. Kanellakopoulos, and P.V. Kokotović. *Nonlinear and Adaptive Control Design*, volume 8. John Wiley & Sons New York, 1995.
- [56] D. Liberzon. *Switching in Systems and Control*. Birkhäuser, 2003.
- [57] D.G. Luenberger. Observers for Multivariable Systems. *IEEE Transactions on Automatic Control*, 11(2):190–197, 1966.
- [58] A.M. Lyapunov. The General Problem of the Stability of Motion. *International Journal of Control*, 55(3):531–534, 1992.
- [59] I. Masubuchi, A. Ohara, and N. Suda. LMI-based Controller Synthesis: a Unified Formulation and Solution. *International Journal of Robust and Nonlinear Control*, 8(8):669–686, 1998.
- [60] R.H. Middleton. Trade-offs in Linear Control System Design. *Automatica*, 27(2):281–292, 1991.
- [61] D. Nešić, A.R. Teel, G. Valmorbida, and L. Zaccarian. On Finite Gain \mathcal{L}_p Stability for Hybrid Systems. In *4th IFAC Conference on Analysis and Design of Hybrid Systems (ADHS)*, pages 418–423, Eindhoven, The Netherlands, June 2012.
- [62] D. Nešić, A.R. Teel, G. Valmorbida, and L. Zaccarian. Finite-Gain \mathcal{L}_p Stability for Hybrid Dynamical Systems. *Automatica*, 2013, on-line.
- [63] D. Nešić, A.R. Teel, and L. Zaccarian. Stability and Performance of SISO Control Systems with First Order Reset Elements. *IEEE Transactions on Automatic Control*, 56(11):2567–2582, 2011.
- [64] D. Nešić, L. Zaccarian, and A.R. Teel. Stability Properties of Reset Systems. In *Proceedings of the 16th IFAC World Congress*, pages 67–72, Prague, Czech Republic, 2005.
- [65] D. Nešić, L. Zaccarian, and A.R. Teel. Stability Properties of Reset Systems. *Automatica*, 44(8):2019–2026, 2008.
- [66] C. De Persis and F. Mazenc. Stability of Quantized Time-delay Nonlinear Systems: a Lyapunov–Krasovskii-functional Approach. *Mathematics of Control, Signals, and Systems*, 21(4):337–370, 2010.
- [67] V.M. Popov. *Hyperstability of Control Systems*. Springer-Verlag New York, Inc., Secaucus, NJ, USA, 1973.

-
- [68] F.R. Poursafei, J.P. Hespanha, and G. Stewart. Quadratic Optimization for Controller Initialization in Multivariable Switching Systems. In *Proceedings of the 2010 American Control Conference*, pages 2511–2516, Baltimore, Maryland, USA, June 2010.
- [69] C. Prieur. Asymptotic Controllability and Robust Asymptotic Stabilizability. *SIAM Journal on Control and Optimization*, 43(5):1888–1912, 2005.
- [70] C. Prieur, S. Tarbouriech, and L. Zaccarian. Guaranteed Stability for Nonlinear Systems by Means of a Hybrid Loop. In *Proceedings of the 8th IFAC Symposium on Nonlinear Control Systems (NOLCOS)*, pages 72–77, Bologna, Italy, September 2010.
- [71] C. Prieur, S. Tarbouriech, and L. Zaccarian. Improving the Performance of Linear Systems by adding a Hybrid Loop. In *18th IFAC World Congress*, pages 6301–6306, Milano, Italy, September 2011.
- [72] C. Prieur, S. Tarbouriech, and L. Zaccarian. Lyapunov-based hybrid loops for stability and performance of continuous-time control systems. *Automatica*, 49(2):577–584, 2013.
- [73] S. Rangan. Multiobjective \mathcal{H}_∞ Problems: Linear and Nonlinear Control. *System & Control Letters*, 32(3):303–308, 1997.
- [74] R.T. Rockafellar and R.J-B Wets. *Variational Analysis*. Springer Verlag, 1998.
- [75] H.L. Royden and P. Fitzpatrick. *Real Analysis*, volume 4. Prentice Hall New York, 1988.
- [76] E.P. Ryan. On Brockett’s Condition for Smooth Stabilizability and its Necessity in a Context of Nonsmooth Feedback. *SIAM Journal on Control and Optimization*, 32(6):1597–1604, 1994.
- [77] R.G. Sanfelice, R. Goebel, and A.R. Teel. Invariance Principles for Hybrid Systems With Connections to Detectability and Asymptotic Stability. *IEEE Transactions on Automatic Control*, 52(12):2282–2297, 2007.
- [78] A. Satoh. State Feedback Synthesis of Linear Reset Control with \mathcal{L}_2 Performance Bound via LMI Approach. In *IFAC 18th World Congress*, pages 5860–5865, Milan, Italy, 2011.
- [79] C. Scherer, P. Gahinet, and M. Chilali. Multiobjective Output-feedback Control via LMI Optimization. *IEEE Transactions on Automatic Control*, 42(7):896–911, 1997.
- [80] G.N. Silva and R.B. Vinter. Measure Driven Differential Inclusions. *Journal of Mathematical Analysis and Applications*, 202(3):727–746, 1996.
- [81] G. Stein. Respect the Unstable. *IEEE Control Systems*, 23(4):12–25, 2003.
- [82] D.D. Swonder. Control of Systems Subject to Sudden Change in Character. *Proceedings of the IEEE*, 64(8):1219–1225, 1976.
- [83] S. Tarbouriech, T. Loquen, and C. Prieur. Anti-windup Strategy for Reset Control Systems. *International Journal of Robust and Nonlinear Control*, 21(10):1159–1177, 2011.
- [84] A.R. Teel, F. Forni, and L. Zaccarian. Lyapunov-based Sufficient Conditions for Exponential Stability in Hybrid Systems. *IEEE Transactions on Automatic Control*, 2013, on-line.
- [85] A.R. Teel, R.M. Murray, and G.C. Walsh. Non-holonomic Control Systems: from Steering to Stabilization with Sinusoids. *International Journal of Control*, 62(4):849–870, 1995.

-
- [86] T. Yang. *Impulsive Control Theory*, volume 272. Springer, 2001.
- [87] L. Zaccarian, D. Nešić, and A.R. Teel. First Order Reset Elements and the Clegg Integrator Revisited. In *Proceedings of the 2005 American Control Conference*, pages 563–568, vol. 1, Portland (OR), USA, June 2005.
- [88] L. Zaccarian, D. Nešić, and A.R. Teel. Analytical and Numerical Lyapunov Functions for SISO Linear Control Systems with First-order Reset Elements. *International Journal of Robust and Nonlinear Control*, 21:1134–1158, 2011.

Techniques Lyapunov pour une classe de systèmes hybrides et synthèses de contrôleurs à réinitialisation.

Francesco FICHERA

Table des matières

Symboles et acronymes	iii
Introduction	1
1 Concepts fondamentaux	5
1.1 Introduction	5
1.2 Modèle hybride	5
1.3 Le domaine temporel hybride et les solutions	6
1.4 Stabilité asymptotique et exponentielle	7
1.5 Temps de maintien	7
1.6 Taux de convergence en t	8
1.7 La norme $t\text{-}\mathcal{L}_2$ et la stabilité $t\text{-}\mathcal{L}_2$	8
1.8 Conclusion	9
2 Analyse d'une classe de systèmes hybrides	11
2.1 Introduction	11
2.2 Classe de systèmes hybrides	12
2.2.1 Relaxation de la région de saut et son inflation ϵ	13
2.3 Stabilité $t\text{-}\mathcal{L}_2$	13
2.3.1 Formulation LMI	15
2.4 Conclusion	16
3 Architectures des contrôleurs hybrides	17
3.1 Introduction	17
3.2 Aspects préliminaires	18
3.3 Boucles hybrides à retour d'état	19
3.3.1 Première architecture	19
3.3.2 Deuxième architecture	20
3.4 Commentaires et remarques	21
3.5 Simulations	21
3.5.1 Un servomoteur	22
3.5.2 Un moteur en CC	22
3.6 Conclusion	23
4 Architectures des contrôleurs hybrides avec estimation d'état	25
4.1 Introduction	25
4.2 Aspects préliminaires	26
4.3 Boucle hybride à retour de sortie avec temps de maintien	26
4.3.1 Définition du problème	26
4.3.2 Première architecture	28
4.3.3 Deuxième architecture	28
4.3.4 Commentaires et remarques	29
4.3.5 Simulations	30
4.4 Boucle hybride à retour de sortie sans temps de maintien	31

4.4.1	Définition du problème	31
4.4.2	Stabilité asymptotique pratique	33
4.4.3	Simulations	34
4.5	Conclusion	34
5	Synthèse d'un contrôleur hybride multi-objectif	35
5.1	Introduction	35
5.2	Synthèse convexe d'un contrôleur hybride	36
5.2.1	Aspects préliminaires et définition du problème	36
5.2.2	Synthèse convexe multi-objectif	37
5.3	Commentaires sur la boucle hybride à retour de sortie	39
5.4	Simulations	39
5.4.1	Un avion F-8	39
5.5	Conclusion	40
	Conclusion	43

Symboles et acronymes

\dot{x}	la dérivée par rapport au temps de l'état du système
x^+	l'état du système après un saut
x^\top	est la transposée de x
(x, y)	est équivalente à $[x^\top y^\top]^\top$
\mathbb{R}	est l'ensemble des nombres réels
\mathbb{R}^n	est l'espace Euclidien de dimension n
$\mathbb{R}_{\geq n}$	est l'ensemble des nombres plus grands ou égal que $n \in \mathbb{R}$
\mathbb{Z}	est l'ensemble des nombre entiers
$\mathbb{Z}_{\geq n}$	est l'ensemble des nombres entiers plus grands que ou égaux à $n \in \mathbb{Z}$
$M \in \mathbb{R}^{m \times n}$	est une matrice réelle avec m lignes et n colonnes, $m, n \in \mathbb{Z}_{\geq 1}$
I	est la matrice identité avec dimension appropriée
$\overline{\mathcal{A}}$	la clôture de l'ensemble \mathcal{A}
$\mathcal{A} \subset \mathcal{B}$	indique que $x \in \mathcal{A}$ implique $x \in \mathcal{B}$
$\text{dom}(\xi)$	est le domaine temporel hybride de ξ (voir Définition 1.1)
$ x $	la norme euclidienne d'un vecteur $x \in \mathbb{R}^n$
$\text{sgn}(s)$	est la fonction signe sur $s \in \mathbb{R}$
$\text{dz}(s)$	est une fonction égale à 0 si $ s \leq 1$ et $\text{sgn}(s)(s - 1)$ si $ s \geq 1$
FORE	First Order Reset Element
GES	Globalement Exponentiellement Stable
LMI	Linear Matrix Inequality

Introduction générale

Le développement technologique et les applications de plus en plus sophistiquées exigent des techniques de contrôle et des outils numériques pour concevoir et valider des contrôleurs qui garantissent les spécifications désirées. Les nouvelles spécifications demandent des solutions qui dépassent les limites de la théorie classique [26]. L'apparition de la théorie des systèmes hybrides a élargi les frontières de la théorie du contrôle, offrant des meilleures solutions pour une large gamme de problèmes [30, 31].

Dans les années 1940, les limites intrinsèques des lois de commande classiques commencent à être formalisées. Quelques indications sur les contraintes intégrales sur les fonctions de sensibilité appliquées aux réseaux électriques ont été présentées dans [5]. L'intérêt envers ces questions théoriques a été renouvelé dernièrement [1, 25, 27, 28, 44]. Les propriétés du contrôle des systèmes à phase minimale et non-minimale sont analysées dans [1]. Ces travaux fournissent les lignes directrices pour évaluer *a priori* les performances qui peuvent être obtenues avec une commande à temps continu (linéaire et non linéaire). [44] souligne les limites fondamentales des performances des boucles de régulation linéaires et caractérise le dépassement de la réponse temporelle des systèmes à non minimum de phase. Les conséquences de ces limitations de la commande à temps continu ne concernent pas seulement les performances de la boucle fermée par rapport aux spécifications données. Dans [8, 18, 56], des systèmes pour lesquels il n'existe pas de boucle de régulation continue garantissant leur stabilité sont étudiés en détail. L'importance de l'enquête concernant les limitations fondamentales de la commande est soulignée dans [60].

En parallèle avec les limites de la commande, les limites de la modélisation des systèmes représentent un problème important qui doit être pris en compte dans des nombreuses applications. Par exemple, pour les applications aérospatiales, le contrôleur à bord ne peut pas être testé directement avant le lancement. Une quantité massive de simulations est donc nécessaire pour le design et (surtout) pour la validation et la certification du contrôleur proposé. Ce processus exige un modèle très précis du système pour réduire les risques. Toutefois, il existe des cas où les représentations dynamiques habituelles n'offrent pas une flexibilité suffisante pour l'analyse et la synthèse des lois de commande qui respectent le cahier des charges. Par exemple, dans certaines applications ayant des propriétés impulsionnelles, seule un modèle dynamique avec inclusions différentielles peut assurer une précision suffisante, ayant des bonnes propriétés de robustesse [59].

Différentes solutions pour dépasser ces difficultés ont été proposées dans la littérature [34, 40, 41, 63, 64]. Dans [17, Section 7.1], un exemple est illustré où la commande impulsionnelle atteint l'optimum global, que toute commande en fonction du temps ne peut pas atteindre. Les systèmes à commutation s'intéressent à la fois au problème de la modélisation et au problème des performances atteignables [37]. Dans [49, 61], le système est modélisé comme un système à commutation pour tenir compte des défaillances ou des effets de numérisation de la sortie du système. D'autre part, [35, 50] proposent, pour le même système, multiples contrôleurs qui sont convenablement utilisés pour satisfaire les spécifications du cahier des charges.

La théorie des systèmes hybrides unifie toutes ces branches de la recherche et élargit les frontières de la modélisation et de la commande [30, 31]. Associant à la fois des dynamiques continues et des dynamiques discrètes, les systèmes hybrides peuvent modéliser avec une meilleure

précision les systèmes mécaniques qui présentent des impacts ou les appareils électroniques avec des commutations ou avec des modes logiques. De plus, l'architecture du contrôleur hybride offre plusieurs avantages qui ont récemment commencé à être étudiés. Par exemple, un contrôleur hybride peut garantir la stabilité robuste de systèmes non linéaires qui ne sont pas stabilisables par des boucles continues [33, 51] et peut surmonter certaines limitations intrinsèques à des systèmes de contrôle linéaires pour arriver à respecter les spécifications [4]. Une boucle de régulation hybride peut également fournir des résultats globaux au lieu des seuls résultats locaux qui peuvent être obtenus avec une loi de contrôle continue.

Dans les dernières années, une attention particulière a été consacrée à l'étude de contrôleurs hybrides optimaux pour les systèmes à temps continu, afin d'obtenir une solution garantissant le meilleur compromis entre les différentes spécifications. Le comportement en boucle fermée souhaité peut être induit à travers la réinitialisation de l'état du contrôleur selon une loi de réinitialisation optimale [50]. Dans ce cadre, peu d'architectures de contrôleurs hybrides ont été proposées, jusqu'à présent. La principale est celle du contrôleur FORE, sur laquelle plusieurs études de performance ont été menées [47, 48, 65, 66]. Une nouvelle architecture a été proposée dans [52] où la loi de réinitialisation est déclenchée par des conditions de Lyapunov appropriées et une synthèse convexe optimale pour maximiser le taux de convergence de cette nouvelle architecture a été présentée dans [53]. Une synthèse optimale pour un contrôleur hybride réduisant le dépassement du système a été donnée dans [54].

Bien que les systèmes hybrides représentent un verrou scientifique dans le domaine de la théorie du contrôle, l'augmentation de la complexité due à la dynamique nécessite des nouveaux outils mathématiques et des nouvelles méthodes pour l'analyse et la conception. La théorie de Lyapunov offre la possibilité de décrire les trajectoires des systèmes hybrides sans calculer les solutions de manière explicite [43]. Cela permet d'établir des résultats utiles sur la stabilité \mathcal{L}_p du système [48], l'équivalence entre la robustesse et l'existence de fonctions de Lyapunov lisses [10, 11] et, pour certaines catégories de contrôleurs hybrides, conduit à des formulations LMI à la fois pour l'analyse et pour la synthèse.

Dans ce contexte, notre travail cherche à développer des techniques systématiques pour la conception d'un contrôleur hybride pour des systèmes à temps continu. Le choix de l'architecture du contrôleur hybride représente un aspect important parce que chaque architecture présente différentes caractéristiques et degrés de liberté. Les différentes techniques de synthèse optimales sont spécifiques à un type particulier de contrôleur hybride. Pour pouvoir évaluer les performances et permettre la comparaison avec les solutions classiques, le contrôleur hybride doit satisfaire certaines conditions pour éviter les comportements qui sont inconnus dans le domaine en temps continu et les estimations de performance inexactes. L'objectif final est d'étudier des architectures de contrôleur hybride pour lesquelles l'analyse et la synthèse amènent à des conditions LMI, qui peuvent être résolues avec les outils numériques existantes [6].

Cette partie du manuscrit de thèse représente le résumé de la version en anglais intitulée "Lyapunov techniques for a class of hybrid systems and reset controller syntheses for continuous-time plants". Bien que cette partie du mémoire constitue un ensemble auto-suffisant, elle est structurée selon le même plan que la version anglaise pour simplifier la recherche des parties correspondantes, auxquelles le lecteur peut faire référence pour avoir plus de détails.

La thèse est structurée comme suit. Les notions fondamentales qui seront utilisées à travers le

manuscrit sont définies dans le Chapitre 1. Le Chapitre 2 présente une classe de systèmes hybrides d'intérêt pour nos études qui englobe plusieurs systèmes de contrôle présentés dans la littérature. Pour cette classe, nous donnons quelques résultats généraux pour l'analyse de la stabilité et des performances. En utilisant la théorie des systèmes hybrides, une fonction de Lyapunov est utilisée pour représenter toutes les trajectoires du modèle hybride et pour établir des bornes de performance. Nous présentons d'abord les résultats basés sur une fonction de Lyapunov générique, puis nous nous concentrons sur le cas où la fonction de Lyapunov est quadratique, ce qui mène à une formulation LMI.

Dans le Chapitre 3, deux architectures de contrôleur hybride pour des systèmes linéaires à temps continu sont proposées. Pour réduire la complexité du problème, seul le cas de retour d'état hybride est envisagé, où les mesures de l'état du système sont utilisées pour définir les ensembles du flux et du saut de la loi de commande hybride. Cela permet d'illustrer plus facilement le potentiel de ces architectures en termes de la réduction du dépassement et de le taux de convergence.

Les systèmes à retour d'état hybrides introduits dans le Chapitre 3 sont généralisées pour le cas de retour de sortie dans le Chapitre 4. L'idée est d'utiliser un observateur pour obtenir l'estimation de l'état du système. Nous traitons quelques questions liées aux effets de l'introduction de l'observateur dans la boucle hybride. Puis, deux approches principales sont discutées, chacune permettant la réduction du dépassement.

Dans le Chapitre 5, une synthèse convexe multi-objectif du système de contrôle décrit dans le Chapitre 3 est présentée. A travers un changement de coordonnées et en utilisant les résultats des Chapitres 2 et 3, nous fournissons des conditions suffisantes pour la conception d'un contrôleur hybride multi-objectif par rapport au taux de convergence et la norme \mathcal{L}_2 classique. Le cas du retour de sortie hybride et ses difficultés intrinsèques sont également abordés. Des résultats prometteurs par rapport aux compromis des performances et des comparaisons avec le cas linéaire correspondant sont montrés à travers des simulations.

Le manuscrit conclut avec des observations sur l'ensemble des résultats obtenus et décrit des possibles directions de recherche. Les résultats présentés dans ce mémoire peuvent être retrouvés dans les publications suivantes :

- F. Fichera, C. Prieur, S. Tarbouriech, L. Zaccarian, “Improving the Performance of Linear Systems by Adding a Hybrid Loop : the Output Feedback Case”. In *Proceedings of the 2012 American Control Conference*, pages 3192–3197, Montreal, Canada, 2012 ;
- F. Fichera, C. Prieur, S. Tarbouriech, L. Zaccarian, “On Hybrid State-feedback Loops Based on a Dwell-time Logic”. In *4th IFAC Conference on Analysis and Design of Hybrid Systems*, pages 388–393, Eindhoven, The Netherlands, 2012 ;
- F. Fichera, C. Prieur, S. Tarbouriech, L. Zaccarian, “A Convex Hybrid \mathcal{H}_∞ Synthesis with Guaranteed Convergence Rate”. In *Proceedings of the 51st Conference on Decision and Control*, pages 4217–4222, Maui (HI), USA, 2012 ;
- F. Fichera, C. Prieur, S. Tarbouriech, L. Zaccarian, “Using Luenberger Observers and Dwell-time Logic for Feedback Hybrid Loops in Continuous-time Control Systems”. *International Journal of Nonlinear and Control*, 23 :1065–1086, 2013 ;
- F. Fichera, C. Prieur, S. Tarbouriech, L. Zaccarian, “Static Anti-windup Scheme for a Class of Homogeneous Dwell-time Hybrid Controllers”. *Proceedings of the 2013 European Control Conference*, Zürich, Switzerland, 2013.

Concepts fondamentaux

Contents

1.1	Introduction	5
1.2	Modèle hybride	5
1.3	Le domaine temporel hybride et les solutions	6
1.4	Stabilité asymptotique et exponentielle	7
1.5	Temps de maintien	7
1.6	Taux de convergence en t	8
1.7	La norme t-\mathcal{L}_2 et la stabilité t-\mathcal{L}_2	8
1.8	Conclusion	9

Les Sections 1.1- 1.4 contiennent quelques définitions nécessaires pour la compréhension du document. Les Sections 1.5, 1.6 et 1.7 présentent plus en détail des notions sur lesquelles les développements des chapitres suivants vont s'appuyer.

1.1 Introduction

Ce chapitre est consacré à une synthèse des concepts fondamentaux nécessaires pour une bonne compréhension des outils présentés. Cependant, pour des raisons d'espace, certains détails sont omis et peuvent être trouvés dans [19, 31]. Il est difficile d'aborder les systèmes hybrides sans introduire les concepts de solutions et temps hybride. Nous introduisons donc ces notions, même si le texte ne se prétend pas exhaustif et les références choisies pourraient donner au lecteur intéressé une description plus détaillée du sujet. Le seul but de ce chapitre est de présenter des définitions connues dans la littérature qui seront utilisées dans les chapitres suivants.

1.2 Modèle hybride

Un système hybride peut être représenté sous la forme suivante :

$$\begin{cases} \dot{x} = f(x, w) & (x, w) \in \mathcal{C} \\ x^+ = g(x, w) & (x, w) \in \mathcal{D} \end{cases} \quad (1.1)$$

où $x \in \mathbb{R}^n$ est l'état du système, $w \in \mathbb{R}^{n_w}$ est un signal exogène, $\mathcal{C} \subset \mathbb{R}^n \times \mathbb{R}^{n_w}$ est l'ensemble du flux, $\mathcal{D} \subset \mathbb{R}^n \times \mathbb{R}^{n_w}$ est l'ensemble du saut, $f : \mathcal{C} \mapsto \mathbb{R}^n$ et $g : \mathcal{D} \mapsto \mathbb{R}^n$ sont des fonctions continues, appelées *dynamique du flux* et *dynamique du saut*, respectivement. Pour raccourcir la terminologie par la suite, le comportement dû à la dynamique du flux est dénommé simplement *flux*. Le comportement dû à la dynamique du saut est dénommé *saut* (ou *reset*)

1.3 Le domaine temporel hybride et les solutions

Pour le système hybride (1.1), les solutions sont définies en fonction du temps ordinaire t , qui considère la quantité de flux, et d'une variable discrète i , qui tient compte des sauts.

Définition 1.1. (*Domaine temporel hybride*) Un sous-ensemble E en $\mathbb{R}_{\geq 0} \times \mathbb{Z}_{\geq 0}$ est un domaine temporel hybride compact si

$$E = \bigcup_{i=0}^{J-1} ([t_i, t_{i+1}], i) \quad (1.2)$$

pour quelque suite finie d'instants temporels $0 = t_0 \leq t_1 \leq t_2 \leq \dots \leq t_J$. Il est un domaine temporel hybride si $\forall (T, J) \in E$, $E \cap ([0, T] \times \{0, 1, \dots, J\})$ est un domaine temporel hybride compact. \diamond

Sur la notion de domaine temporel hybride, nous pouvons introduire le concept d'arc hybride, comme dans la définition suivante.

Définition 1.2. (*Arc hybride*) Une fonction $\phi : E \mapsto \mathbb{R}^n$ est un arc hybride si E est un domaine temporel hybride et si pour chaque $j \in \mathbb{Z}_{\geq 0}$, la fonction $t \mapsto \phi(t, j)$ est localement absolument continue sur l'intervalle $I^j = \{t : (t, j) \in E\}$. \diamond

La définition de fonction absolument continue se trouve dans [55, pag. 119].

Supposons que ϕ représente un arc hybride, nous notons son domaine temporel hybride comme $\text{dom}(\phi)$.

Il est utile de distinguer certains types d'arcs hybrides en fonction de leurs domaines. Cependant la liste suivante présente seulement les arcs d'intérêt pour ce mémoire. Une liste plus exhaustive se trouve dans [19, Définition 1.7].

Définition 1.3. (*Types d'arcs hybrides*) Un arc hybride ϕ est dit :

- **non-trivial** si $\text{dom}(\phi)$ contient au moins deux points ;
- **complet** si $\text{dom}(\phi)$ est non-borné ;
- **Zénon** s'il est complet et $\sup_t \text{dom}(\phi) < \infty$;
- **continu** si non-trivial et $\text{dom}(\phi) \subset \mathbb{R}_{\geq 0} \times \{0\}$;
- **compact** si $\text{dom}(\phi)$ est compact.

\diamond

Pour un système hybride (1.1), ses solutions sont des arcs hybrides qui satisfont certaines conditions, comme précisé dans la définition suivante.

Définition 1.4. (*Solution d'un système hybride*) Un arc hybride ϕ est une solution du système hybride (1.1), si $\phi(0, 0) \in \bar{\mathcal{C}} \cup \mathcal{D}$ et¹ :

(S1) pour tout $j \in \mathbb{Z}_{\geq 0}$ tel que $I^j = \{t : (t, j) \in \text{dom}(\phi)\}$ a l'intérieur non vide

$$\begin{aligned} \phi(t, j) &\in \mathcal{C} && \text{for all } t \in \text{int}(I^j), \\ \dot{\phi}(t, j) &= f(\phi(t, j)) && \text{for almost all } t \in \text{dom}(\phi); \end{aligned} \quad (1.3)$$

(S2) pour tout $(t, j) \in \text{dom}(\phi)$ tel que $(t, j + 1) \in \text{dom}(\phi)$,

$$\begin{aligned} \phi(t, j) &\in \mathcal{D}, \\ \phi(t, j + 1) &= g(\phi(t, j)). \end{aligned} \quad (1.4)$$

\diamond

1. Puisque $\phi = (x, w)$, nous exigeons que $\text{dom}(x) = \text{dom}(w)$, d'après [46].

1.4 Stabilité asymptotique et exponentielle

En général, un système hybride (1.1) converge vers un ensemble plutôt que vers un point d'équilibre. Dans ce mémoire, nous ne considérons que les ensembles compacts (pour des définitions plus génériques le lecteur est renvoyé vers [31]).

Notons que le système hybride peut présenter également un type de solution que l'on dit être maximale et non complète [30, 31]. Cependant, les systèmes hybrides traités dans cette thèse ne présentent que des solutions complètes et donc nous pouvons utiliser les définitions suivantes pour la stabilité et l'attractivité.

Définition 1.5. (*Stabilité asymptotique globale*) *Considérons un système hybride (1.1) avec $w = 0$, un ensemble compact $\mathcal{A} \subset \mathbb{R}^n$ est dit :*

- *stable pour (1.1) : si pour chaque $\epsilon > 0$ il existe un $\delta > 0$ tel que toute solution x de (1.1) avec $|x(0, 0)|_{\mathcal{A}} \leq \delta$ satisfait $|x(t, j)|_{\mathcal{A}} \leq \epsilon$ pour tout $(t, j) \in \text{dom}(x)$;*
- *attractive pour (1.1) : si toute solution x de (1.1) satisfait $\lim_{t+j \rightarrow \infty} |x(t, j)|_{\mathcal{A}} = 0$, où $(t, j) \in \text{dom}(x)$;*
- *globalement asymptotiquement stable (GAS) pour (1.1) : s'il est stable et attractive pour (1.1).*

◇

Définition 1.6. (*Stabilité exponentielle globale*) *Considérons un système hybride (1.1) avec $w = 0$, un ensemble compact $\mathcal{A} \subset \mathbb{R}^n$ est dit globalement exponentiellement stable (GES) s'il existe k et λ réels et strictement positifs tels que chaque solution x satisfait*

$$|x(t, j)|_{\mathcal{A}} \leq k \exp(-\lambda(t + j)) |x(0, 0)|_{\mathcal{A}}, \quad (1.5)$$

pour tout $(t, j) \in \text{dom}(x)$.

◇

1.5 Temps de maintien

Dans les chapitres suivants, nous utilisons une régularisation temporelle dite *temps de maintien* (ou *variable de dwell-time*) représentée comme

$$\begin{aligned} \dot{\tau} &= 1 - dz\left(\frac{\tau}{\rho}\right) & \tau \in [0, \rho] \\ \tau^+ &= 0 & \tau \in [\rho, 2\rho], \end{aligned} \quad (1.6)$$

où $\rho > 0$ est dit paramètre temporel du temps de maintien. Notons que l'ensemble $[0, 2\rho]$ est invariant pour (1.6).

Définition 1.7. (*Condition de temps de maintien*) *Le temps de maintien (1.6) garantit*

$$\rho + t - s \geq \rho(j - k), \quad (1.7)$$

pour chaque paire d'instantanés hybrides $(t, j), (s, k) \in \text{dom}(\tau)$, $(t, j) \geq (s, k)$.

◇

La condition (1.7) (aussi appelée propriété de dwell-time) est un cas particulier de [12, Proposition 1.1]. Notons que si (1.1) satisfait (1.7) alors chaque solution maximale (x, w) de (1.1) a un domaine hybride $E = \text{dom}(x)$ qui est non-borné dans le temps ordinaire t [31]. Par conséquent, il n'existe pas de solution Zénon lorsqu'une condition de temps de maintien est satisfaite.

Remarque 1.1. Dans cette thèse, nous comptons sur l'architecture du temps de maintien définie dans (1.6). Cependant, tous les résultats présentés ici sont valides aussi quand (1.6) est remplacée par tout autre dynamique de temps de maintien qui satisfait (1.7), avec la réserve que l'ensemble invariant du τ change en conséquence. ★

1.6 Taux de convergence en t

Définition 1.8. (*Taux de convergence en t*) Soit un ensemble compact $\mathcal{A} \subset \mathbb{R}^n$ et $w = 0$, le système hybride (1.1) a un taux de convergence en t (ou t -decay rate) $\lambda > 0$ s'il existe un réel k strictement positif tel que chaque solution x satisfait

$$|x(t, j)|_{\mathcal{A}} \leq k \exp(-\lambda t) |x(0, 0)|_{\mathcal{A}}, \quad (1.8)$$

pour tout $(t, j) \in \text{dom}(x)$. ◇

Notons que si le système hybride (1.1) satisfait (1.7), le taux de convergence en t (1.8) implique la stabilité exponentielle globale de (1.1) dans le sens de la théorie hybride, c'est-à-dire comme dans (1.5).

1.7 La norme t - \mathcal{L}_2 et la stabilité t - \mathcal{L}_2

Définition 1.9. Soit un signal hybride w défini sur $\text{dom}(w) \subset \mathbb{R}_{\geq 0} \times \mathbb{Z}_{\geq 0}$, la norme t - \mathcal{L}_2 de w est donnée par

$$\|w\|_{2t} = \left(\sum_{j \in \text{dom}_j(w)} \int_{t_j}^{t_{j+1}} |w(t, j)|^2 dt \right)^{\frac{1}{2}}, \quad (1.9)$$

où t_{j+1} est ∞ si $(j+1) \notin \text{dom}_j(w)$, avec $\text{dom}_j(w) = \{j \in \mathbb{Z}_{\geq 0} : (t, j) \in \text{dom}(w) \text{ pour } t \geq 0\}$. ◇

La définition (1.9) correspond à la norme \mathcal{L}_2 à temps continu du signal à temps continu $t \mapsto w_t(t)$, obtenu en projetant le signal hybride $(t, j) \mapsto w(t, j)$ sur le temps ordinaire. Lorsque le signal hybride w ne fait que du flux, c'est-à-dire $\text{dom}(w) = [0, +\infty) \times \{0\}$, alors (1.9) correspond à la norme \mathcal{L}_2 classique en temps continu. Notons que (1.9) n'est pas une norme, parce qu'un signal w avec une valeur non-nulle au départ et qui saute en zéro à $(t, j+1) = (0, 1)$ satisfait $\|w\|_{2t} = 0$ (pour en savoir plus sur les normes hybrides voir dans [9, 45]). Néanmoins, nous appelons (1.9) *norme* en raison de l'intuition qu'il généralise la norme à temps continu.

Définition 1.10. Un signal hybride w , avec $\text{dom}(w) \subset \mathbb{R}_{\geq 0} \times \mathbb{Z}_{\geq 0}$, est dit $w \in t$ - \mathcal{L}_2 si $\|w\|_{2t} < \infty$. ◇

Définition 1.11. Supposons un ensemble $\mathcal{A} \subset \mathbb{R}^n$ globalement asymptotiquement stable pour (1.1) et $z = h(x, w)$ avec $h(\cdot, \cdot)$ continue en ses arguments. Le système (1.1) est dit à gain t - \mathcal{L}_2 fini de w à z avec le gain $\gamma > 0$ si toute solution de (1.1) de départ de \mathcal{A} satisfait

$$\|z\|_{2t} \leq \gamma \|w\|_{2t} \quad (1.10)$$

pour tout $w \in t$ - \mathcal{L}_2 . ◇

Selon la définition ci-dessus, nous considérons z comme *sortie de prestation* du système (1.1).

1.8 Conclusion

Nous avons présenté différentes définitions et notions de la littérature, utiles pour la compréhension de ce manuscrit. Nous avons défini le système hybride et ses composantes, ainsi que les notions de stabilité utilisées par la suite. De plus, des indices de performance ont été présentés dans les Sections 1.6 et 1.7. Notons que ces indices sont définis en fonction du temps ordinaire t et cela nous permet de faire des comparaisons avec des systèmes à temps continu. Il est important de souligner qu'en général les indices de performance à temps continu ne peuvent pas être appliqués dans le cadre des systèmes hybrides. Cependant, dans ce mémoire, nous considérons seulement des systèmes hybrides pour lesquels ces indices peuvent être définis sans questions.

Analyse d'une classe de systèmes hybrides

Contents

2.1	Introduction	11
2.2	Classe de systèmes hybrides	12
2.2.1	Relaxation de la région de saut et son inflation ϵ	13
2.3	Stabilité $t\text{-}\mathcal{L}_2$	13
2.3.1	Formulation LMI	15
2.4	Conclusion	16

Dans ce chapitre nous présentons une classe de systèmes hybrides et des outils pour l'analyse de la stabilité $t\text{-}\mathcal{L}_2$. Nous commençons par exposer la motivation et les intérêts des résultats dans la Section 2.1. Dans la Section 2.2, le modèle hybride général et quelques propriétés sont discutés. La Section 2.2.1 présente le problème d'analyse que nous résolvons. La Section 2.3 présente le résultat principal basé sur une fonction de Lyapunov générique et la Section 2.3.1 fournit la formulation LMI du résultat.

2.1 Introduction

Les systèmes dynamiques hybrides présentent des caractéristiques soit à temps continu soit à temps discret et leurs solutions peuvent couvrir une large gamme de comportements. Dans [31], est exposé une étude exhaustive sur l'existence et les propriétés des solutions avec la présentation des outils d'analyse basés sur des conditions de Lyapunov. Néanmoins, le problème de tenir compte de toutes les solutions devient encore plus difficile à chaque fois qu'un indice de performance doit être établi. Dans ce cadre, les travaux [48] présentent des conditions d'analyse de la stabilité $t\text{-}\mathcal{L}_2$ pour une classe de systèmes hybrides. Même en [66], une étude rigoureuse sur les systèmes de contrôle hybrides avec un contrôleur de type FORE est disponible.

Dans ce chapitre, nous considérons la même classe de systèmes hybrides que [48] mais nous relaxons les conditions de stabilité. Nous soulignons que la plupart des systèmes hybrides dans la littérature résultant de l'interconnexion d'un système linéaire avec un contrôleur dont l'état peut être modifié avec une loi de saut, sont inclus dans la classe de systèmes hybrides abordée dans [48] et dans ce chapitre. Enfin, la plupart des systèmes de contrôle hybrides étudiés dans ce mémoire appartiennent également à cette classe.

2.2 Classe de systèmes hybrides

Les résultats d'analyse que nous présentons sont valables pour la classe suivante de systèmes hybrides

$$\begin{cases} \dot{x} = Ax + Bw \\ \dot{\tau} = 1 - dz\left(\frac{\tau}{\rho}\right) & (x, \tau) \in \mathcal{C} \\ \begin{cases} x^+ = Gx \\ \tau^+ = 0 \end{cases} & (x, \tau) \in \mathcal{D} \\ z = C_z x + D_{zw} w \\ y = Cx + D_w w \end{cases} \quad (2.1a)$$

où $x \in \mathbb{R}^n$ est l'état, $\tau \in [0, 2\rho]$ avec $\rho > 0$ est la temporisation à travers le temps de maintien, $w \in \mathbb{R}^{n_w}$ est un signal exogène, $z \in \mathbb{R}^{n_z}$ est la sortie de performance, $y \in \mathbb{R}^{n_y}$ est la sortie mesurée, \mathcal{C} et \mathcal{D} sont

$$\mathcal{C} = \{(x, \tau) : x \in \mathcal{F} \text{ or } \tau \in [0, \rho]\} = \{(x, \tau) : x \in \mathcal{F}\} \cup \{(x, \tau) : \tau \in [0, \rho]\}, \quad (2.1b)$$

$$\mathcal{D} = \{(x, \tau) : x \in \mathcal{J} \text{ and } \tau \in [\rho, 2\rho]\} = \{(x, \tau) : x \in \mathcal{J}\} \cap \{(x, \tau) : \tau \in [\rho, 2\rho]\}, \quad (2.1c)$$

avec \mathcal{F} et \mathcal{J} des cônes symétriques qui dépendent de la matrice $M = M^\top$ selon

$$\mathcal{F} = \left\{ x \in \mathbb{R}^n : x^\top M x \leq 0 \right\}, \quad (2.1d)$$

$$\mathcal{J} = \left\{ x \in \mathbb{R}^n : x^\top M x \geq 0 \right\}. \quad (2.1e)$$

Puisque $\mathcal{C} \cup \mathcal{D}$ est invariant et aucune divergence à temps fini n'est possible à cause de la dynamique du flux linéaire, toutes les solutions maximales sont complètes et nous parlons de stabilité asymptotique au lieu de stabilité pre-asymptotique [30, 31]¹. En ce qui suit, les intervalles du flux sont représentés comme $[t_i, t_{i+1}]$ avec $i \in \mathbb{Z}_{\geq 0}$, où t_i et t_{i+1} sont les instants de saut (pour plus de détails, consulter le Chapitre 1).

La variable temporelle τ présente la même dynamique que dans la Section 1.5. Donc la composante τ des ensembles \mathcal{C} et \mathcal{D} garantit la *condition de temps de maintien* (1.7), alors que la composante x de \mathcal{C} et \mathcal{D} est projetée sur l'ensemble du flux \mathcal{F} et l'ensemble du saut \mathcal{J} . Pour plus de détails sur les ensemble \mathcal{F} et \mathcal{J} , le lecteur est renvoyé à [19].

Remarque 2.1. Le système hybride (2.1) satisfait les propriétés suivantes :

- i. $t_{i+1} - t_i \geq \rho$, pour tout $i \in \mathbb{Z}_{\geq 1}$. Plus précisément, si $t_{i+1} - t_i > \rho$, $i \in \mathbb{Z}_{\geq 1}$, alors $x(t, i) \in \mathcal{F}$ pour tout $t \in [t_i + \rho, t_{i+1}]$;
- ii. seulement dans l'intervalle $[t_0, t_1]$, nous avons $t_1 - t_0 \geq \rho - \tau(t_0, 0)$ et donc il est possible que $t_1 - t_0 \leq \rho$ (par exemple $t_1 = t_0$ si $\tau(t_0, 0) \geq \rho$). Néanmoins, $x(t, 0) \in \mathcal{F}$ pour tout $t \in [\max\{t_0, t_0 + \rho - \tau(t_0, 0)\}, t_1]$;
- iii. il peut y avoir du flux quand $x \in \mathcal{J}$ à cause du temps de maintien :
 - si $x \in \mathcal{J}$ et $\tau < \rho$, alors le système fait du flux ;
 - si $x \in \mathcal{F}$ et $\tau < \rho$, alors le système doit faire du flux et pourrait rentrer dans \mathcal{J} avant que $\tau \geq \rho$.
- iv. si $x \in \mathcal{F} \cap \mathcal{J}$ et $\tau = \rho$, la solution peut soit sauter soit faire du flux ;

1. Notons que (2.1a) et $\mathcal{C} \cup \mathcal{D} = \mathbb{R}^n \times [0, 2\rho]$ satisfont les [30, 31, Basic Assumptions], donc les solutions existent pour toute condition initiale $(x, \tau) = \mathbb{R}^n \times [0, 2\rho]$.

v. la linéarité des equations à temps discret et à temps continu (2.1a) et la forme conique de \mathcal{F} et \mathcal{J} permettent de conclure sur l'homogénéité de l'état x du système (2.1).

★

Notons que les points i et ii de la Remarque 2.1 dépendent de la propriété de dwell-time (1.7).

2.2.1 Relaxation de la région de saut et son inflation ϵ

Dans ce chapitre, nous voulons offrir des conditions suffisantes pour établir des bornes $t\text{-}\mathcal{L}_2$ pour le système (2.1), en utilisant une fonction de Lyapunov définie seulement dans le sous-état x . Même comme dans [48], nous voulons établir s'il existe un ensemble non-vide du paramètre temporel, ρ , du temps de maintien, qui garantit la stabilité du système (2.1), comme formellement indiqué dans le problème suivant.

Problème 2.1. *Considérons un système (2.1) avec $A, B, G, M, C_z, D_{zw}, C$ et D_w connus. Notre but est de fournir des conditions suffisantes basées sur une fonction de Lyapunov $x \mapsto V(x)$ pour établir s'il existe un paramètre temporel $\rho > 0$ tel que :*

- l'ensemble $\mathcal{A} := \{0\} \times [0, 2\rho] \subset \mathbb{R}^n \times [0, 2\rho]$ est globalement asymptotiquement stable pour (2.1) avec $w = 0$;
- une estimation du gain $t\text{-}\mathcal{L}_2$ de (2.1) de w à z est donnée.

○

Puisque le temps de maintien influence la composante x des trajectoires du système seulement à travers les ensembles \mathcal{C} et \mathcal{D} , nous voulons décrire les trajectoires du système (2.1) en utilisant une fonction de Lyapunov $x \mapsto V(x)$ (au lieu de $(x, \tau) \mapsto W(x, \tau)$), en tenant compte des effets du temps de maintien. Plus précisément, nous voulons certifier l'existence du paramètre $\rho > 0$ pour le système (2.1), qui garantit la prestation $t\text{-}\mathcal{L}_2$. La motivation principale pour ce type de problème (traité aussi dans [48]) est de fournir des conditions convexes d'analyse qui peuvent être vérifiées en utilisant les outils SDP. Quand les conditions sont obtenues en utilisant une fonction $x \mapsto V(x)$, une version convexe peut être trouvée en choisissant $V(x)$ quadratique. En général, la même approche ne peut pas être suivie quand une fonction de Lyapunov $(x, \tau) \mapsto W(x, \tau)$ est utilisée, parce que le temps de maintien est pris en compte par des fonctions exponentielles.

Pour faire face aux effets du temps de maintien dans la Remarque 2.1, nous introduisons les ensembles coniques supplémentaires

$$\tilde{\mathcal{F}} = \left\{ x \in \mathbb{R}^n : x^\top \tilde{M} x \leq 0 \right\}, \quad (2.2)$$

$$\tilde{\mathcal{F}}_\epsilon = \left\{ x \in \mathbb{R}^n : x^\top \tilde{M} x - \epsilon x^\top x \leq 0 \right\}, \quad (2.3)$$

avec $\tilde{M} = \tilde{M}^\top \in \mathbb{R}^{n \times n}$ et $\epsilon > 0$. Notons que (2.3) est l'inflation ϵ de (2.2), donc nous obtenons que $\tilde{\mathcal{F}} \subset \tilde{\mathcal{F}}_\epsilon$.

2.3 Stabilité $t\text{-}\mathcal{L}_2$

Théorème 2.1. *Considérons un système (2.1) et les définitions dans (2.2) et (2.3). S'il existe une fonction continûment différentiable $V : \mathbb{R}^n \rightarrow \mathbb{R}_{\geq 0}$, une matrice \tilde{M} et un scalaire ϵ strictement positif tels que l'ensemble $\tilde{\mathcal{F}}_\epsilon$ dans (2.3) satisfait $\mathcal{F} \subset \tilde{\mathcal{F}}_\epsilon$ et des scalaires $a_1, a_2, a_3, a_4, a_5, \bar{\gamma}$ réels*

strictement positifs et un scalaire non-négatif ρ satisfaisant

$$a_1|x|^2 \leq V(x) \leq a_2|x|^2, \quad \forall x \in \mathbb{R}^n, \quad (2.4a)$$

$$\langle \nabla V(x), Ax + Bw \rangle + a_3V(x) + \frac{1}{\gamma}z^\top z - \bar{\gamma}w^\top w < 0, \quad \forall x \in \tilde{\mathcal{F}}_\epsilon, \forall w \in \mathbb{R}^{n_w}, x \neq 0, \quad (2.4b)$$

$$V(Gx) \leq \exp(a_3\rho)V(x), \quad \forall x \in \mathcal{J} \quad (2.4c)$$

$$Gx \in \tilde{\mathcal{F}}, \quad \forall x \in \mathcal{J} \quad (2.4d)$$

$$\langle \nabla V(x), Ax + Bw \rangle \leq a_4V(x) + a_5|x||w|, \quad \forall x \in \mathbb{R}^n, \forall w \in \mathbb{R}^{n_w}, \quad (2.4e)$$

alors pour chaque γ satisfaisant

$$\gamma \geq \bar{\gamma} \exp\left(\frac{a_3\rho}{2}\right), \quad \gamma > \sqrt{2}|D_{zw}|, \quad (2.5)$$

il existe $\bar{\rho} > 0$ tel que pour chaque $\rho \in (\rho, \bar{\rho})$:

- 1) l'ensemble $\mathcal{A} = \{0\} \times [0, 2\rho]$ est globalement asymptotiquement stable pour le système hybride (2.1) avec $w = 0$. Plus précisément, il existe $\rho_1^* := \varphi_e^{-1}\left(\frac{\epsilon}{|2(\tilde{M} - \epsilon I)A|}\right)$ où \tilde{M} définit l'ensemble $\tilde{\mathcal{F}}$ dans (2.2) et $\varphi_e(s) := s \exp(2|A|s)$, tel que $\bar{\rho} = \rho_1^*$ garantissant la propriété de stabilité ;
- 2) le gain t - \mathcal{L}_2 de w à z est plus petit que ou égal à γ , c'est-à-dire (1.10) est vrai pour toute solution de (2.1) avec condition initiale $\xi(0, 0) = (x(0, 0), \tau(0, 0)) \in \{0\} \times [0, 2\rho]$ et pour tout $w \in t$ - \mathcal{L}_2 . Plus précisément, $\bar{\rho}$ est définie comme $\bar{\rho} := \min\{\rho_2^*, \rho_3^*\}$, où ρ_2^* et ρ_3^* sont définis de la façon suivante :

$$\rho_2^* := \varphi_1^{-1}(\gamma^2 - 2|D_{zw}|^2), \quad \rho_3^* := \varphi_2^{-1}\left(\frac{\epsilon}{a_2}\right) \quad (2.6a)$$

$$\varphi_1(s) := \kappa_1(s) + \kappa_2(s) + \frac{2|C_z|^2 s}{a_1}(1 + \kappa_1(s) + \kappa_2(s)) \quad (2.6b)$$

$$\varphi_2(s) := L_1 \frac{s}{a_1}(1 + \kappa_1(s) + \kappa_2(s)) + L_2 \sqrt{\frac{s}{a_1}(1 + \kappa_1(s) + \kappa_2(s))} \quad (2.6c)$$

$$\kappa_1(s) := \exp\left(\frac{\bar{a}_4}{2}s\right) \kappa(s) + \frac{4a_1\bar{a}_4}{\bar{a}_5^2} \kappa^2(s) \quad (2.6d)$$

$$\kappa_2(s) := \exp\left(\frac{\bar{a}_4}{2}s\right) \kappa(s) + \kappa^2(s) \quad (2.6e)$$

$$\kappa(s) := \frac{\bar{a}_5}{2} \sqrt{\frac{\exp(\bar{a}_4 s) - 1}{a_1 \bar{a}_4}} \quad (2.6f)$$

$$L_1 := 2|(\tilde{M} - \epsilon I)A|, \quad L_2 := 2|(\tilde{M} - \epsilon I)B| \quad (2.6g)$$

$$\bar{a}_4 := a_4 + a_3, \quad \bar{a}_5 := a_5 \exp(a_3\rho) \quad (2.6h)$$

où \tilde{M} définit l'ensemble $\tilde{\mathcal{F}}$ dans (2.2).

Donc en sélectionnant $\bar{\rho} := \min\{\rho_1^*, \rho_2^*, \rho_3^*\}$, les points 1 et 2 sont garantis. \square

Démonstration du Théorème 2.1. Pour la démonstration de ce résultat le lecteur peut consulter [19]. \blacksquare

Le Théorème 2.1 généralise les résultats donnés dans [48] en introduisant les nouveautés suivantes :

- la matrice D_{zw} peut être non nulle. En particulier, la condition (2.5) garantit que ρ_2^* existe, quand $D_{zw} \neq 0$. Dans [48, 57] cette matrice était égale à zéro ;
- la valeur de la fonction de Lyapunov $x \mapsto V(x)$ peut augmenter pendant les sauts. En sélectionnant $\underline{\rho}$ avec une valeur positive dans (2.4c), nous permettons l'augmentation de $V(x)$, compensée par une décroissance pendant le flux [31, Proposition 3.29] ;
- la condition [48, Assumption 1] (c'est-à-dire $Gx \in \mathcal{F}$ pour tout $x \in \mathcal{J}$) est remplacée par la condition (2.4d) qui utilise l'ensemble $\tilde{\mathcal{F}}$, défini dans (2.2). Plus précisément, l'utilisation de l'ensemble $\tilde{\mathcal{F}}$ et son inflation $\tilde{\mathcal{F}}_\epsilon$ donnent plus de flexibilité puisqu'en général $\tilde{\mathcal{F}}$ peut couvrir une région plus large que \mathcal{F} à condition que \mathcal{F} soit contenu dans $\tilde{\mathcal{F}}_\epsilon$. Notons que la condition [48, Assumption 1] est un cas particulier du Théorème 2.1 et peut être retrouvée en sélectionnant $\tilde{\mathcal{F}} \equiv \mathcal{F}$.

Remarque 2.2. Le Théorème 2.1 ne garantit pas que l'ensemble des ρ (c'est-à-dire $(\underline{\rho}, \bar{\rho})$) soit non-vidé. En particulier, ρ_1^* , ρ_2^* et ρ_3^* sont strictement positifs (et donc $\bar{\rho} > 0$) et si $\underline{\rho} = 0$, l'ensemble des ρ est certainement non-vidé. En même temps, quand $\underline{\rho}$ est positif, il n'est pas garanti a priori que $\underline{\rho} < \bar{\rho}$ et donc si $\underline{\rho} > \bar{\rho}$, l'ensemble $(\underline{\rho}, \bar{\rho})$ est vidé. ★

Remarque 2.3. Propriétés importantes du Théorème 2.1 :

1. si $\tilde{\mathcal{F}} \equiv \mathcal{F}$, $\underline{\rho} = 0$ et $D_{zw} = 0$, le point 2 du Théorème 2.1 correspond à [48, Theorem 1]. Dans ce cas, [48, Theorem 1] peut être considéré comme un corollaire du point 2 du Théorème 2.1 ;
2. la deuxième condition dans (2.5) est nécessaire pour le point 2 du Théorème 2.1 afin de garantir $\rho_2^* > 0$. Si $D_{zw} = 0$ alors (2.5) implique $\gamma = \bar{\gamma}$. Autrement si $D_{zw} \neq 0$, il faut vérifier la deuxième condition dans (2.5) avec $\gamma = \bar{\gamma}$. Si elle n'est pas satisfaite il faut sélectionner une valeur de γ plus grande pour garantir (2.5) et pour que l'ensemble $(\underline{\rho}, \bar{\rho})$ soit non vidé ;
3. considérons $\tilde{\mathcal{F}}_\epsilon$ avec $\epsilon = \infty$ (c'est-à-dire $\tilde{\mathcal{F}}_\epsilon \equiv \mathbb{R}^n$), alors (2.4b) est valide globalement et même si $D_{zw} \neq 0$, la condition (2.5) n'est pas nécessaire et $\gamma = \bar{\gamma}$. En particulier, puisque (2.4b) est valide globalement, la démonstration du Théorème 2.1 peut être modifiée de sorte que les conditions (2.4d) et (2.4e) ne sont plus nécessaires et l'ensemble $(\underline{\rho}, \bar{\rho})$ est toujours non vidé ;
4. le point 1 du Théorème 2.1 établit la stabilité asymptotique de l'ensemble $\{0\} \times [0, 2\rho]$. Effectivement, pour obtenir la stabilité exponentielle, un terme supplémentaire dans (2.4a) est nécessaire. Plus précisément, le terme $a_3V(x)$ dans (2.4a) est nécessaire pour compenser l'augmentation éventuelle pendant les sauts qui dépend de $\underline{\rho}$. Néanmoins, si nous pouvons introduire un terme $(a_3 + \zeta)V(x)$ dans (2.4b), avec $\zeta > 0$ (voir [39, Lemma 4.3]), alors $\{0\} \times [0, 2\rho]$ est globalement asymptotiquement stable pour (2.1) même si $\underline{\rho} \neq 0$. En même temps, quand $\underline{\rho} = 0$ le terme $a_3V(x)$ dans (2.4b) ne doit compenser aucune augmentation et le point 1 du Théorème 2.1 établit déjà la stabilité *exponentielle* globale de l'ensemble $\{0\} \times [0, 2\rho]$.

★

2.3.1 Formulation LMI

Proposition 2.1. Considérons le système (2.1). S'il existe des matrices $P = P^\top > 0$, $\tilde{M} = \tilde{M}^\top$, des scalaires non négatifs $\underline{\rho}$, τ_F , τ_C , $\tau_R \in \mathbb{R}_{\geq 0}$ et des scalaires positifs ϵ , $\bar{\gamma}$, a_3 tels que

$$\begin{pmatrix} A^\top P + PA + a_3P - (\tilde{M} - \epsilon I) & PB & C_z^\top \\ B^\top P & -\bar{\gamma}I & D_{zw}^\top \\ C_z & D_{zw} & -\bar{\gamma}I \end{pmatrix} < 0, \quad (2.7a)$$

$$G^\top PG - \exp(a_3 \underline{\rho})P + \tau_R M \leq 0, \quad (2.7b)$$

$$\tilde{M} - \tau_F M \leq \epsilon I, \quad (2.7c)$$

$$G^\top \tilde{M} G + \tau_C M \leq 0. \quad (2.7d)$$

Alors pour un γ satisfaisant (2.5), il existe $\bar{\rho} > 0$ tel que pour un $\rho \in (\underline{\rho}, \bar{\rho})$:

- 1) l'ensemble $\{0\} \times [0, 2\rho]$ est globalement exponentiellement stable pour (2.1) avec $w = 0$;
- 2) le gain $t\text{-}\mathcal{L}_2$ de w à z est plus petit que ou égal à γ , pour tout $w \in t\text{-}\mathcal{L}_2$.

□

Démonstration de la Proposition 2.1. La démonstration est obtenue en montrant que toutes les conditions du Théorème 2.1 sont satisfaites. Pour plus de détails voir [19]. ■

La Proposition 2.1 particularise le Théorème 2.1 pour le cas où la fonction de Lyapunov $x \mapsto V(x)$ est quadratique. Donc la Remarque 2.2 est encore valide.

Pour l'analyse d'un système (2.1) (voir le Problème 2.1), les conditions (2.7) sont linéaires exception faite pour a_3 et $\underline{\rho}$. En particulier, le terme $a_3 P$ dans (2.7a) et le terme exponentiel dans (2.7b) nécessitent que a_3 et $\underline{\rho}$ soient fixés. Néanmoins, le minimum de $\bar{\gamma}$ ou le maximum de ϵ peut toujours être estimé.

Remarque 2.4. De la même manière que [48, Theorem 1] est un corollaire du point 2 du Théorème 2.1, la [48, Proposition 1] est un corollaire de la Proposition 2.1. Plus précisément, quand $\tilde{M} = \tau_F M$ et $\underline{\rho} = 0$ alors :

- à cause de la nature quadratique de $V(x)$ et de l'inégalité stricte dans (2.7b), il existe un scalaire strictement positif qui garantit (2.4b) ;
- dans (2.7b), $\underline{\rho} = 0$ implique $\exp(a_3 \underline{\rho}) = 1$ pour tout a_3 ;
- (2.7c) est satisfaite pour tout $\epsilon > 0$;
- (2.7d) remplace [48, Assumption 1].

Quand $\tilde{M} \leq \tau_F M$ et $\underline{\rho} = 0$, (2.7) peuvent être résolues avec $a_3 = \epsilon = 0$. Plus précisément les termes $a_3 P$ et ϵI peuvent être introduits a posteriori en exploitant l'inégalité stricte dans (2.7a) et la nature quadratique de $V(x)$. ★

Remarque 2.5. 1. Si $\tilde{M} = 0$, alors (2.7a) a une validité globale. Donc selon le point 3 de la Remarque 2.3, la condition (2.5) n'est plus nécessaire, aussi comme (2.7c) et (2.7d).

2. A partir de la Remarque 2.4, la Proposition 2.1 établit la stabilité exponentielle globale pour n'importe quel choix de $\underline{\rho} \geq 0$. Nous rappelons que ce n'était pas le cas pour le Théorème 2.1. ★

2.4 Conclusion

Dans ce chapitre, nous avons présenté des conditions suffisantes pour évaluer la stabilité $t\text{-}\mathcal{L}_2$ pour une classe de systèmes hybrides. Par rapport à la littérature, les résultats présentés généralisent ceux développés dans [48]. En particulier, nos résultats peuvent être appliqués à une classe plus large que ceux de [48], grâce à l'introduction de l'ensemble $\tilde{\mathcal{F}}$. De plus, l'augmentation de la fonction de Lyapunov pendant les sauts est consentie et cela réduit les problèmes numériques quand des outils SDP sont utilisés.

Architectures des contrôleurs hybrides

Contents

3.1	Introduction	17
3.2	Aspects préliminaires	18
3.3	Boucles hybrides à retour d'état	19
3.3.1	Première architecture	19
3.3.2	Deuxième architecture	20
3.4	Commentaires et remarques	21
3.5	Simulations	21
3.5.1	Un servomoteur	22
3.5.2	Un moteur en CC	22
3.6	Conclusion	23

Dans ce chapitre, nous présentons deux stratégies de contrôle hybride. Après une courte introduction dans la Section 3.1, l'architecture générale des contrôleurs est présentée dans la Section 3.2. La Section 3.3 contient le problème général de commande. Les Sections 3.3.1 et 3.3.2 présentent les deux résultats principaux et quelques simulations numériques sont donnés dans la Section 3.5.

3.1 Introduction

Récemment, un des principaux axes de recherche de la commande est basé sur la conception de contrôleurs hybrides pour les systèmes à temps continu linéaires. Dans ce chapitre, nous nous concentrons sur les contrôleurs hybrides dont l'état peut être choisi selon une loi de saut. Dans ce contexte, [3, 4] montrent que ce type de systèmes hybrides (dits aussi systèmes à reset) peut garantir simultanément plusieurs spécifications de design qui ne peuvent pas être satisfaites avec un contrôleur linéaire classique.

L'une des principales architectures des contrôleurs hybrides utilisée dans la littérature est le contrôleur de type FORE. Cependant, aucune technique de synthèse n'a pas été proposée, même si nous mentionnons les travaux présentés dans [47, 48, 66] qui ont fourni des résultats intéressants. A part le contrôleur FORE, des architectures différentes de contrôleurs hybrides ont été présentées dans [32, 52]. [32] propose une architecture de contrôleur hybride dont les ensembles du flux et du saut sont à base temporelle. Cette stratégie garantit la stabilité et réduit le dépassement de la sortie du système. Néanmoins, la technique n'est pas facile à mettre en œuvre et ne fournit pas des outils de synthèse convexes. D'autre part, [52] propose deux nouvelles architectures hybrides pour lesquelles des outils de synthèse optimale sont disponibles (voir [53, 54]).

Dans ce chapitre, nous étendons les architectures des contrôleurs hybrides présentées dans [52] afin d'obtenir des systèmes de contrôle hybrides, qui correspondent à la représentation donnée dans (2.1). Cela va nous permettre d'utiliser les résultats présentés dans le Chapitre 2 pour pouvoir mener l'analyse de la stabilité et également de rechercher des nouvelles stratégies de synthèse.

3.2 Aspects préliminaires

Considérons un système linéaire à temps continu \mathcal{P}

$$\begin{aligned} \dot{x}_p &= \bar{A}_p x_p + \bar{B}_p u \\ y &= \bar{C}_p x_p + \bar{D}_p u \end{aligned} \quad (3.1)$$

où $x_p \in \mathbb{R}^{n_p}$ est l'état, $u \in \mathbb{R}^{n_u}$ est l'entrée de contrôle, $y \in \mathbb{R}^{n_y}$ est la sortie mesurée.

Hypothèse 3.1. L'état x_p et la sortie y du système \mathcal{P} sont connus. ◦

L'Hypothèse 3.1 est nécessaire parce que les boucles hybrides présentées dans ce chapitre (c'est-à-dire la dynamique du saut et les ensembles du flux et du saut) dépendent de l'état x_p du système \mathcal{P} . En même temps, la dynamique du flux du contrôleur peut être considérée comme une boucle linéaire en fonction de la sortie y du système. Pour la suite, nous appelons ce type de schéma *boucle hybride à retour d'état*. Plus précisément, nous utilisons le contrôleur hybride suivant

$$\begin{cases} \dot{x}_c = \bar{A}_c x_c + \bar{B}_c y \\ \dot{\tau} = 1 - \text{dz} \left(\frac{\tau}{\rho} \right) & (x_p, x_c, \tau) \in \mathcal{C} \\ \begin{cases} x_c^+ = K_p x_p \\ \tau^+ = 0 \end{cases} & (x_p, x_c, \tau) \in \mathcal{D} \\ u = \bar{C}_c x_c + \bar{D}_c y \end{cases} \quad (3.2a)$$

où $x_c \in \mathbb{R}^{n_c}$ est l'état, $\tau \in [0, 2\rho]$ est le temps de maintien et \mathcal{C} et \mathcal{D} sont

$$\begin{aligned} \mathcal{C} &= \{(x_p, x_c, \tau) : (x_p, x_c) \in \mathcal{F} \text{ or } \tau \in [0, \rho]\} \\ &= \{(x_p, x_c, \tau) : (x_p, x_c) \in \mathcal{F}\} \cup \{(x_p, x_c, \tau) : \tau \in [0, \rho]\}, \end{aligned} \quad (3.2b)$$

$$\begin{aligned} \mathcal{D} &= \{(x_p, x_c, \tau) : (x_p, x_c) \in \mathcal{J} \text{ and } \tau \in [\rho, 2\rho]\} \\ &= \{(x_p, x_c, \tau) : (x_p, x_c) \in \mathcal{J}\} \cap \{(x_p, x_c, \tau) : \tau \in [\rho, 2\rho]\}, \end{aligned} \quad (3.2c)$$

avec \mathcal{F} et \mathcal{J} cônes symétriques définis par la matrice $M = M^\top$

$$\mathcal{F} = \left\{ (x_p, x_c) : \begin{bmatrix} x_p \\ x_c \end{bmatrix}^\top M \begin{bmatrix} x_p \\ x_c \end{bmatrix} \leq 0 \right\}, \quad (3.2d)$$

$$\mathcal{J} = \left\{ (x_p, x_c) : \begin{bmatrix} x_p \\ x_c \end{bmatrix}^\top M \begin{bmatrix} x_p \\ x_c \end{bmatrix} \geq 0 \right\}. \quad (3.2e)$$

Hypothèse 3.2. L'interconnexion de (3.1) et (3.2) est bien posée, c'est-à-dire la matrice $(I - \bar{D}_p \bar{D}_c)$ n'est pas singulière. ◦

Sous l'Hypothèse 3.2, l'interconnexion entre (3.1) et (3.2) donne le système hybride suivant

$$\begin{cases} \begin{cases} \begin{bmatrix} \dot{x}_p \\ \dot{x}_c \end{bmatrix} = \begin{bmatrix} A_p & B_p \\ B_c & A_c \end{bmatrix} x := Ax \\ \dot{\tau} = 1 - dz\left(\frac{\tau}{\rho}\right) \end{cases} & (x, \tau) \in \mathcal{C} \\ \begin{cases} x^+ = \begin{bmatrix} I & 0 \\ K_p & 0 \end{bmatrix} x := Gx \\ \tau^+ = 0 \\ y = [C_p \ C_c] x := Cx \end{cases} & (x, \tau) \in \mathcal{D} \end{cases} \quad (3.3)$$

avec $x := [x_p^\top \ x_c^\top]^\top \in \mathbb{R}^{n:=n_p+n_c}$ et

$$\begin{pmatrix} A_p & B_p \\ B_c & A_c \\ C_p & C_c \end{pmatrix} := \begin{pmatrix} \bar{A}_p + \bar{B}_p \bar{D}_c (I - \bar{D}_p \bar{D}_c)^{-1} \bar{C}_p & \bar{B}_p \bar{C}_c + \bar{B}_p \bar{D}_c (I - \bar{D}_p \bar{D}_c)^{-1} \bar{D}_p \bar{C}_c \\ \bar{B}_c (I - \bar{D}_p \bar{D}_c)^{-1} \bar{C}_p & \bar{A}_c + \bar{B}_c (I - \bar{D}_p \bar{D}_c)^{-1} \bar{D}_p \bar{C}_c \\ (I - \bar{D}_p \bar{D}_c)^{-1} \bar{C}_p & (I - \bar{D}_p \bar{D}_c)^{-1} \bar{D}_p \bar{C}_c \end{pmatrix}. \quad (3.4)$$

Notons que (3.3) a la même structure que (2.1) (avec $B = 0$, $C_z = 0$, $D_{zw} = 0$ et $D_w = 0$).

3.3 Boucles hybrides à retour d'état

Nous voulons établir des conditions suffisantes pour que le contrôleur \mathcal{H}_c stabilise le système \mathcal{P} . Plus précisément, le but de ce chapitre est d'augmenter une boucle linéaire classique à temps continu (pas nécessairement stable) avec une boucle hybride à retour d'état de sorte que la propriété de stabilité exponentielle soit garantie. L'écriture formelle de notre objectif est donnée dans le problème qui suit.

Problème 3.1. *Considérons un système (3.1) sous l'Hypothèse 3.1 et les matrices \bar{A}_c , \bar{B}_c , \bar{C}_c et \bar{D}_c du contrôleur (3.2) tels que l'Hypothèse 3.2 soit satisfaite. Notre but est de concevoir la partie hybride à retour d'état de (3.2), c'est-à-dire la matrice $M = M^\top \in \mathbb{R}^{n \times n}$, le gain $K_p \in \mathbb{R}^{n_c \times n_p}$ et $\rho > 0$ tels que l'ensemble $\mathcal{A} := \{0\} \times [0, 2\rho] \subset \mathbb{R}^n \times [0, 2\rho]$ est globalement exponentiellement stable pour le système (3.3)-(3.4). \circ*

3.3.1 Première architecture

Théorème 3.1. *Considérons un système (3.1) et un contrôleur (3.2) sous les Hypothèses 3.1 et 3.2 et supposons que $P = P^\top := \begin{bmatrix} P_p & P_{pc} \\ P_{pc}^\top & P_c \end{bmatrix} > 0$ satisfait*

$$\Xi := \text{He} \left(\bar{P}_p (A_p + B_p K_p) + \frac{\alpha}{2} \bar{P}_p \right) < 0, \quad (3.5)$$

avec

$$\bar{P}_p := P_p - P_{pc} P_c^{-1} P_{pc}^\top > 0, \quad K_p := -P_c^{-1} P_{pc}^\top, \quad (3.6)$$

pour $\alpha > 0$. Alors il existe $\bar{\rho} > 0$ tel que pour tout $\rho \in (0, \bar{\rho})$, et $\tilde{\alpha} \in (0, \alpha]$, le contrôleur hybride (3.2) avec

$$M := \text{He} \left(PA + \frac{\tilde{\alpha}}{2} P \right), \quad (3.7)$$

résout le Problème 3.1, c'est-à-dire l'ensemble $\mathcal{A} := \{0\} \times [0, 2\rho]$ est globalement exponentiellement stable (3.3)-(3.4) avec M définie comme dans (3.7). \square

Démonstration de Théorème 3.1 La démonstration est obtenue en montrant que les conditions pour le point 1 de la Proposition 2.1 sont garanties et peut être trouvée dans [19]. \blacksquare

Le Théorème 3.1 est une extension des résultats présentés dans [52]. En particulier, le contrôleur (3.2) du Théorème 3.1 est issu de l'augmentation du contrôleur hybride donné dans [52] avec un temps de maintien et établit stabilité exponentielle globale au lieu de stabilité asymptotique globale.

Nous remarquons que la stabilité est obtenue à travers les sauts, puisque la matrice de la dynamique de flux A peut, en général, être non Hurwitz.

3.3.2 Deuxième architecture

Théorème 3.2. Considérons un système (3.1) et un contrôleur (3.2) sous les Hypothèses 3.1 et 3.2 et supposons que $\bar{P}_p = \bar{P}_p^\top > 0$, $K_p \in \mathbb{R}^{n_c \times n_p}$ satisfont (3.5) pour $\alpha > 0$. Alors pour chaque $\tilde{\alpha} \in (0, \alpha]$, il existe $\mu > 0$ tel que

$$\chi := \text{He} \left(\bar{P}_p(A_p + B_p K_p) + \frac{\tilde{\alpha}}{2} \bar{P}_p + \frac{\mu}{2} K_p^\top K_p \right) < 0, \quad (3.8)$$

et pour chaque μ satisfaisant (3.8), il existe $\bar{\rho} > 0$ tel que pour tout $\rho \in (0, \bar{\rho})$ le contrôleur hybride (3.2) avec

$$M := \text{He} \left(\begin{bmatrix} \bar{P}_p A_p + \frac{\tilde{\alpha}}{2} \bar{P}_p & \bar{P}_p B_p \\ 0 & \frac{\mu}{2} I \end{bmatrix} \right), \quad (3.9)$$

résout le Problème 3.1, c'est-à-dire l'ensemble $\mathcal{A} := \{0\} \times [0, 2\rho]$ est globalement exponentiellement stable pour le système (3.3)-(3.4) avec M définie dans (3.9). De plus, toute solution $\xi = (x_p, x_c, \tau)$ de (3.3), (3.4) avec M dans (3.9), et condition initiale $\xi(0, 0) = (x_p(0, 0), x_c(0, 0), \tau(0, 0)) \in \mathbb{R}^{n_p} \times \{0\} \times [0, 2\rho]$, satisfait

$$|x_p(t, j)| \leq K \exp\left(-\frac{\tilde{\alpha}}{2}t\right) |x_p(0, 0)|, \quad \forall (t, j) \in \text{dom}(\xi), \quad (3.10)$$

où $K := \frac{\lambda_{\max}(\bar{P}_p)}{\lambda_{\min}(\bar{P}_p)} \exp((\tilde{\alpha} + 2|A|)\frac{\rho}{2})$ et $\bar{\rho} := \varphi^{-1}\left(-\frac{\lambda_{\max}(\chi)}{|2MA|I + K_p^\top K_p}\right)$, où $\varphi(s) := s \exp(2|A|s)$. \square

Démonstration du Théorème 3.2. La démonstration peut être trouvée dans [19]. \blacksquare

Remarque 3.1. Le Théorème 3.2 garantit la stabilité exponentielle globale de l'ensemble \mathcal{A} . Néanmoins, la borne (3.10) est valide pour toute solution $\xi = (x_p, x_c, \tau)$ de (3.3)-(3.4) du Théorème 3.2, avec une condition initiale $\xi(0, 0) = (x_p(0, 0), x_c(0, 0), \tau(0, 0))$ satisfaisant $x_c(0, 0) = 0$. \star

Remarque 3.2. Le gain K dans la borne (3.10) tient compte de l'augmentation de la fonction de Lyapunov due au premier intervalle du flux qui dépend de la variable temporelle (voir la Remarque 2.1). La borne (3.10) peut devenir moins conservative si nous exprimons la dépendance de

K par rapport à $\tau(0,0)$. Plus précisément, la démonstration du Théorème 3.2 peut être modifiée de sorte que le gain K dans (3.10) devienne $\tilde{K}(\tau(0,0))$, défini comme

$$\tilde{K}(\tau(0,0)) := \frac{\lambda_{\max}(\bar{P}_p)}{\lambda_{\min}(\bar{P}_p)} \exp\left(\left(\tilde{\alpha} + 2|A|\right) \frac{\max\{0, \rho - \tau(0,0)\}}{2}\right), \quad (3.11)$$

avec $\tau(0,0) \in [0, 2\rho]$. Notons que $\tilde{K}(\tau(0,0)) \leq K$. ★

Remarque 3.3. Le taux de convergence en t dans (3.10) dépend de $\tilde{\alpha} > 0$, qui est sélectionné dans \mathcal{F} et \mathcal{J} , à travers la matrice M définie dans (3.9). Notons que $\tilde{\alpha} \in (0, \alpha]$, avec $\alpha > 0$ qui garantit (3.5). ★

3.4 Commentaires et remarques

Remarque 3.4. Les Théorèmes 3.1 et 3.2 généralisent les résultats présentés dans [52, 53]. Parmi leur similarités avec [52, 53], nous mentionnons :

- a. les ensemble du flux et du saut, \mathcal{F} et \mathcal{J} respectivement, sont définis selon une fonction de type Lyapunov. En particulier, le Théorème 3.1 utilise les mêmes ensembles que [52, Proposition 1], alors que le Théorème 3.2 utilise des ensembles légèrement modifiés par rapport à [53, Theorem 1] (voir aussi [52, Proposition 2]).
- b. la loi de saut est telle que :
 - i. la fonction de type Lyapunov utilisée dans \mathcal{F} et \mathcal{J} n'augmente pas pendant les sauts ;
 - ii. la fonction de type Lyapunov utilisée dans \mathcal{F} et \mathcal{J} décroît après chaque saut.
- c. la condition (3.5) doit toujours être satisfaite ;
- d. les resets (ou les sauts) garantissent la stabilité.

Parmi les différences entre les Théorèmes 3.1 et 3.2 et les résultats dans [52, 53], nous mentionnons :

- e. les Théorèmes 3.1 et 3.2 établissent stabilité exponentielle globale et en plus le Théorème 3.2 garantit le taux de convergence en t dans la direction x_p . [52, 53] établissent seulement la stabilité asymptotique globale ;
- f. les Théorèmes 3.1 et 3.2 font référence au contrôleur hybride (3.2), qui contient un temps de maintien, alors que [52, 53] n'utilisent pas des variables de temporisation ;
- g. les Théorèmes 3.1 et 3.2 sont démontrés en utilisant des fonctions de Lyapunov lisses qui garantissent la robustesse (voir [11]). ★

La condition (3.5) qui doit être satisfaite dans les Théorèmes 3.1 et 3.2 rappelle la condition classique pour le contrôle statique à retour de sortie [2, 6, 14, 29]. Donc la condition (3.5) peut être résolue avec une formulation convexe (pour plus de détails consulter [19, Simulations §3.5]).

3.5 Simulations

Nous allons présenter des simulations qui utilisent les stratégies de contrôle décrites dans les Théorèmes 3.1 et 3.2. En tenant compte de la formulation du Problème 3.1, nous supposons que la matrice A de (3.3) est donnée et qu'elle n'est pas nécessairement stable. Nous utilisons la synthèse optimale présentée dans [53] pour concevoir une boucle de régulation hybride qui garantit une réduction du dépassement de la sortie du système. Pour plus de détails, consulter [19].

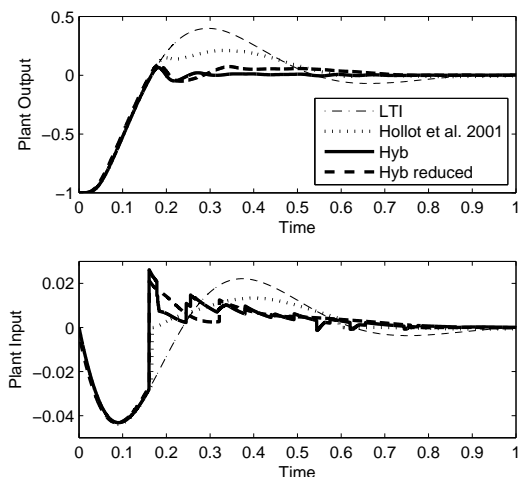


FIGURE 3.1 – Comparaison entre la commande linéaire, un contrôleur FORE proposé dans [36], le contrôleur hybride (3.2) du Théorème 3.1 (appelé *Hyb*) et le contrôleur hybride (3.2) du Théorème 3.1 issu d’un modèle d’ordre réduit (appelé *Hyb reduced*).

3.5.1 Un servomoteur

Considérons l’exemple donné dans [15, 36] où la réduction du dépassement de la sortie ne peut pas être obtenue avec un contrôleur linéaire à temps continu à cause des autres spécifications imposées.

La Figure 3.1 compare plusieurs boucles de régulation connues dans la littérature. Notons que le contrôleur appelé *Hyb reduced* vient du Théorème 3.1 et est obtenu en utilisant la technique de synthèse présentée dans [54] sur un modèle réduit du système, de sorte que la mesure de l’état du système n’est plus nécessaire. Toutes les boucles de contrôle utilisent le même contrôleur à temps continu et les boucles hybrides utilisent un état de plus pour la partie hybride.

La Figure 3.1 montre que la commande hybride peut réduire le dépassement de la sortie du système. Le contrôleur *Hyb* réduit le dépassement par rapport à [36], mais utilise la mesure de l’état complet du système. Cependant, le contrôleur *Hyb reduced* maintient un petit dépassement par rapport à [36], même sans avoir accès à la mesure de l’état du système. Il reconstruit l’état du modèle réduit à partir des signaux de régulation.

3.5.2 Un moteur en CC

Considérons un moteur électrique en curenent continu pour le positionnement d’un poids.

La Figure 3.2 compare le comportement de la boucle linéaire à retour de sortie avec la même boucle linéaire augmentée par une boucle hybride selon le Théorème 3.2 et en utilisant encore une fois la technique de synthèse de [54] pour la réduction du dépassement. Les réponses montrent que les sauts de l’état du contrôleur peuvent effectivement réduire le dépassement de la sortie, conformément à l’exemple précédent.

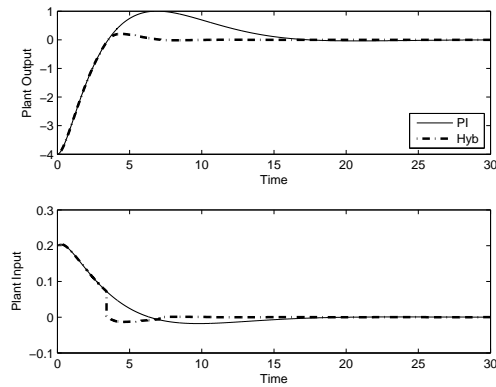


FIGURE 3.2 – Moteur en CC contrôlé à travers la technique du Théorème 3.2.

3.6 Conclusion

Dans ce chapitre, deux stratégies de synthèse d'un contrôleur hybride ont été proposées. Ces deux architectures de contrôle généralisent celles présentées dans [52, 53] en introduisant le temps de maintien (ou dwell-time). Cette variable donne un degré de liberté de plus et permet d'utiliser les résultats du Chapitre 2. Les simulations montrent que ces architectures peuvent réduire le dépassement de la sortie du système. De plus le Théorème 3.2 donne une borne pour le taux de convergence en t , qui sera utilisée pour la synthèse multi-objectif du Chapitre 5. Le problème principal de ces architectures est leur dépendance de la connaissance de l'état du système. Le chapitre suivant est dédié à la résolution de ce problème.

Architectures des contrôleurs hybrides avec estimation d'état

Contents

4.1	Introduction	25
4.2	Aspects préliminaires	26
4.3	Boucle hybride à retour de sortie avec temps de maintien	26
4.3.1	Définition du problème	26
4.3.2	Première architecture	28
4.3.3	Deuxième architecture	28
4.3.4	Commentaires et remarques	29
4.3.5	Simulations	30
4.4	Boucle hybride à retour de sortie sans temps de maintien	31
4.4.1	Définition du problème	31
4.4.2	Stabilité asymptotique pratique	33
4.4.3	Simulations	34
4.5	Conclusion	34

Dans ce chapitre, nous présentons des systèmes hybrides à retour de sortie qui utilisent un observateur pour obtenir une estimation de l'état du système. Les Sections 4.1 introduisent les motivations et quelques difficultés liées à l'introduction d'un observateur dans une boucle hybride. La Section 4.3 étend les résultats du chapitre précédent. Dans la Section 4.4 un système hybride à retour de sortie sans temps de maintien est discuté. Tous les résultats présentés dans ce chapitre ont été publiés dans [21, 22].

4.1 Introduction

Les résultats développés dans le Chapitre 3 peuvent garantir des propriétés désirables comme la stabilité exponentielle et la réduction du dépassement. Néanmoins, comme dans [52–54], la nécessité de connaître l'état rend ces architectures inéligibles pour des applications pratiques, malgré les stratégies de synthèse optimales disponibles.

Pour cette raison, les résultats de ce chapitre étendent ceux du Chapitre 3 au cas d'une *boucle hybride à retour de sortie* où le contrôleur hybride ne dépend que de la sortie du système.

4.2 Aspects préliminaires

L'idée pour étendre les résultats du Chapitre 3 au cas du retour de sortie est d'utiliser un observateur de Luenberger pour reconstruire l'état du système. Encore une fois nous considérons le système \mathcal{P} introduit dans (3.1) sans l'hypothèse que l'état soit disponible à travers des mesures.

Nous utilisons un observateur de Luenberger \mathcal{O} (voir [42]), défini comme

$$\begin{aligned}\dot{\hat{x}}_p &= \bar{A}_p \hat{x}_p + \bar{B}_p u + L(y - \hat{y}) := A_e \hat{x}_p + B_e u + Ly \\ \hat{y} &= \bar{C}_p \hat{x}_p + \bar{D}_p u\end{aligned}\quad (4.1)$$

où $\hat{x}_p \in \mathbb{R}^{n_p}$ est l'estimation de l'état, $u \in \mathbb{R}^{n_u}$ est l'entrée de contrôle, $\hat{y} \in \mathbb{R}^{n_y}$ est l'estimation de la sortie, $A_e := \bar{A}_p - L\bar{C}_p$ et $B_e := \bar{B}_p - L\bar{D}_p$.

Hypothèse 4.1. Le gain L est tel que la matrice $A_e := \bar{A}_p - L\bar{C}_p$ est Hurwitz. \circ

Remarque 4.1. Considérons l'erreur d'estimation définie par $e := x_p - \hat{x}_p$ (inconnue puisque x_p n'est pas disponible à travers les mesures). A partir de (3.1) et (4.1) nous obtenons que $x_p^+ = x_p$ et $\hat{x}_p^+ = \hat{x}_p$, ce qui implique $e^+ = e$ (c'est-à-dire que l'erreur ne change pas pendant les sauts). Au contraire, pendant le flux nous avons $\dot{e} = A_e e$ où A_e est Hurwitz grâce à l'Hypothèse 4.1 (c'est-à-dire que l'erreur converge vers l'origine pendant le flux). En conséquence, pour garantir la convergence de l'erreur vers l'origine, toute solution Zénon doit être supprimée. \star

Dans la suite nous discuterons deux stratégies pour supprimer toute solution Zénon.

Remarque 4.2. Le signal $\eta := y - \hat{y}$ est disponible à travers les mesures et, en absence du bruit, retourne quelques informations sur l'erreur d'estimation. Plus précisément, à partir de (3.1) et (4.1), nous avons $\eta = \bar{C}_p e$. Puisque l'introduction de l'observateur dans la boucle de contrôle introduit des effets indésirables pendant le transitoire, cette information supplémentaire sera utilisée pour réduire ces effets. \star

4.3 Boucle hybride à retour de sortie avec temps de maintien

4.3.1 Définition du problème

Nous utilisons l'architecture de contrôle hybride \mathcal{H}_{co} suivante

$$\begin{cases} \begin{cases} \begin{bmatrix} \dot{\hat{x}}_p \\ \dot{\hat{x}}_c \end{bmatrix} = \begin{bmatrix} A_e & B_e \bar{C}_c \\ 0 & \bar{A}_c \end{bmatrix} \begin{bmatrix} \hat{x}_p \\ x_c \end{bmatrix} + \begin{bmatrix} B_e \bar{D}_c + L \\ \bar{B}_c \end{bmatrix} y \\ \dot{\tau} = 1 - dz\left(\frac{\tau}{\rho}\right) \end{cases} & (\hat{x}_p, x_c, e, \tau) \in \mathcal{C} \\ \begin{cases} \begin{bmatrix} \hat{x}_p^+ \\ x_c^+ \end{bmatrix} = \begin{bmatrix} I & 0 \\ K_p & 0 \end{bmatrix} \begin{bmatrix} \hat{x}_p \\ x_c \end{bmatrix} + \begin{bmatrix} 0 \\ K_y \end{bmatrix} \eta \\ \tau^+ = 0 \end{cases} & (\hat{x}_p, x_c, e, \tau) \in \mathcal{D} \\ u = \begin{bmatrix} 0 & \bar{C}_c \end{bmatrix} \begin{bmatrix} \hat{x}_p \\ x_c \end{bmatrix} + \bar{D}_c y \end{cases} \end{cases} \quad (4.2a)$$

où $\hat{x}_p \in \mathbb{R}^{n_p}$ est l'état de l'observateur, $x_c \in \mathbb{R}^{n_c}$ est l'état des sauts, $\tau \in [0, 2\rho]$ est la variable temporelle, A_e et B_e sont définies comme dans (4.1) (voir aussi l'Hypothèse 4.1) et $\eta \in \mathbb{R}^{n_y}$ est

défini dans la Remarque 4.2, les ensembles \mathcal{C} et \mathcal{D} sont

$$\begin{aligned}\mathcal{C} &= \{(\hat{x}_p, x_c, e, \tau) : (\hat{x}_p, x_c, e) \in \mathcal{F} \text{ or } \tau \in [0, \rho]\} \\ &= \{(\hat{x}_p, x_c, e, \tau) : (\hat{x}_p, x_c, e) \in \mathcal{F}\} \cup \{(\hat{x}_p, x_c, e, \tau) : \tau \in [0, \rho]\},\end{aligned}\quad (4.2b)$$

$$\begin{aligned}\mathcal{D} &= \{(\hat{x}_p, x_c, e, \tau) : (\hat{x}_p, x_c, e) \in \mathcal{J} \text{ and } \tau \in [\rho, 2\rho]\} \\ &= \{(\hat{x}_p, x_c, e, \tau) : (\hat{x}_p, x_c, e) \in \mathcal{J}\} \cap \{(\hat{x}_p, x_c, e, \tau) : \tau \in [\rho, 2\rho]\},\end{aligned}\quad (4.2c)$$

avec \mathcal{F} et \mathcal{J} des cônes symétriques définis par la matrice $\bar{M} = \bar{M}^\top$

$$\mathcal{F} = \left\{ (\hat{x}_p, x_c, e) \in \mathbb{R}^n : \begin{bmatrix} \hat{x}_p \\ x_c \\ e \end{bmatrix}^\top \underbrace{\begin{bmatrix} I & 0 & 0 \\ 0 & I & 0 \\ 0 & 0 & \bar{C}_p \end{bmatrix}^\top \bar{M} \begin{bmatrix} I & 0 & 0 \\ 0 & I & 0 \\ 0 & 0 & \bar{C}_p \end{bmatrix}}_M \begin{bmatrix} \hat{x}_p \\ x_c \\ e \end{bmatrix} \leq 0 \right\}, \quad (4.2d)$$

$$\mathcal{J} = \left\{ (\hat{x}_p, x_c, e) \in \mathbb{R}^n : \begin{bmatrix} \hat{x}_p \\ x_c \\ e \end{bmatrix}^\top \underbrace{\begin{bmatrix} I & 0 & 0 \\ 0 & I & 0 \\ 0 & 0 & \bar{C}_p \end{bmatrix}^\top \bar{M} \begin{bmatrix} I & 0 & 0 \\ 0 & I & 0 \\ 0 & 0 & \bar{C}_p \end{bmatrix}}_M \begin{bmatrix} \hat{x}_p \\ x_c \\ e \end{bmatrix} \geq 0 \right\}. \quad (4.2e)$$

Notons que l'information de l'observateur est utilisée par la boucle hybride et non pas par la dynamique du flux. De plus, quand $e = 0$ alors $\eta = 0$ et (4.2) devient égal à l'architecture (3.2) du chapitre précédent.

Sous l'Hypothèse 3.2, l'interconnexion entre (3.1) et (4.2) mène au système hybride suivant

$$\begin{cases} \begin{cases} \begin{bmatrix} \dot{\hat{x}}_p \\ \dot{x}_c \\ \dot{e} \end{bmatrix} = \begin{bmatrix} A_p & B_p & B_o \\ B_c & A_c & B_c \\ 0 & 0 & A_e \end{bmatrix} x := Ax & (x, \tau) \in \mathcal{C} \\ \dot{\tau} = 1 - dz\left(\frac{\tau}{\rho}\right) \end{cases} \\ \begin{cases} x^+ = \begin{bmatrix} I & 0 & 0 \\ K_p & 0 & K_y \bar{C}_p \\ 0 & 0 & I \end{bmatrix} x := Gx & (x, \tau) \in \mathcal{D} \\ \tau^+ = 0 \\ y = [C_p \ C_c \ C_p] x := Cx \end{cases} \end{cases} \quad (4.3)$$

avec $x := [\hat{x}_p^\top \ x_c^\top \ e^\top]^\top \in \mathbb{R}^{n:=2n_p+n_c}$, $B_o := L\bar{C}_p + \bar{B}_p\bar{D}_c(I - \bar{D}_p\bar{D}_c)^{-1}\bar{C}_p$ et A_p, B_p, A_c, B_c, C_p et C_c définis dans (3.4) et les ensembles du flux et du saut définis comme dans (4.2b) et (4.2c).

Notons que dans ce type d'architecture les solutions Zénon sont supprimées à travers l'utilisation du temps de maintien qui garantit la condition de temps de maintien (1.7) (voir la Remarque 4.1).

Problème 4.1. *Considérons un système (3.1) et les matrices $\bar{A}_c, \bar{B}_c, \bar{C}_c, \bar{D}_c$ et L du contrôleur (4.2) tels que les Hypothèses 4.1 et 3.2 soient satisfaites. Notre but est de concevoir la partie hybride à retour de sortie de (4.2), c'est-à-dire la matrice $\bar{M} = \bar{M}^\top \in \mathbb{R}^{(n_p+n_c+n_y) \times (n_p+n_c+n_y)}$, les gains $K_p \in \mathbb{R}^{n_c \times n_p}$, $K_y \in \mathbb{R}^{n_c \times n_y}$ et $\rho > 0$ tels que l'ensemble $\mathcal{A} := \{0\} \times [0, 2\rho] \subset \mathbb{R}^n \times [0, 2\rho]$ est globalement exponentiellement stable pour le système (4.3). \circ*

4.3.2 Première architecture

Théorème 4.1. Considérons un système (3.1) et un contrôleur (4.2) sous les Hypothèses 4.1 et 3.2, quatre paramètres K_y, K_x, K_c et K_η et supposons que $P = P^\top := \begin{bmatrix} P_p & P_{pc} \\ P_{pc}^\top & P_c \end{bmatrix} > 0$ satisfait (3.5) et (3.6) pour $\alpha > 0$. Alors il existe $\bar{\rho} > 0$ tel que pour tout $\rho \in (0, \bar{\rho})$ et $\tilde{\alpha} \in (0, \alpha]$, le contrôleur hybride (4.2) avec

$$\bar{M} := \text{He} \left(\frac{P \begin{bmatrix} A_p & B_p \\ B_c & A_c \end{bmatrix} + \frac{\tilde{\alpha}}{2} P}{\begin{array}{cc|c} & & K_x \\ & & K_c \\ 0 & 0 & K_\eta \end{array}} \right), \quad (4.4)$$

résout le Problème 4.1, c'est-à-dire l'ensemble $\mathcal{A} := 0 \times [0, 2\rho]$ est globalement asymptotiquement stable pour le système hybride (4.3) avec \bar{M} définie comme dans (4.4). \square

Démonstration de Théorème 4.1. La démonstration complète peut être trouvée dans [19]. \blacksquare

Le Théorème 4.1 a quelques points communs avec le Théorème 3.1. Les conditions (3.5) et (3.6) sont utilisées par les deux résultats et l'élément (1, 1) de la matrice \bar{M} en (4.4) correspond à M dans le Théorème 3.1. En même temps, le Théorème 4.1 présente des nouveaux gains dus à la présence de l'état e .

Pour plus de détails sur les solutions de ce système à retour de sortie par rapport aux systèmes à retour d'état étudiés dans [52–54], le lecteur peut consulter [19, Proposition 4.1].

Nous introduisons aussi le corollaire suivant.

Corollaire 4.1. Considérons un système (3.1) et un contrôleur (4.2) sous les Hypothèses 4.1 et 3.2, avec K_y, K_x, K_c, K_η matrices nulles et supposons que $P = P^\top := \begin{bmatrix} P_p & P_{pc} \\ P_{pc}^\top & P_c \end{bmatrix} > 0$ satisfait (3.5) et (3.6) pour $\alpha > 0$. Alors il existe $\bar{\rho} > 0$ tel que pour tout $\rho \in (0, \bar{\rho})$ et $\tilde{\alpha} \in (0, \alpha]$, le contrôleur hybride (4.2) avec \bar{M} définie comme dans (4.4) résout le Problème 4.1, c'est-à-dire l'ensemble $\mathcal{A} := 0 \times [0, 2\rho]$ est globalement exponentiellement stable pour le système hybride (4.3) avec \bar{M} définie comme dans (4.4). \square

4.3.3 Deuxième architecture

Théorème 4.2. Considérons un système (3.1) et un contrôleur (4.2) sous les Hypothèses 4.1 et 3.2, cinq paramètres $\mu > 0, K_y, K_x, K_c, K_\eta$ et supposons que $\bar{P}_p = \bar{P}_p^\top > 0, K_p \in \mathbb{R}^{n_c \times n_p}$ satisfont (3.5) pour $\alpha > 0$. Alors il existe $\bar{\rho} > 0$ tel que pour tout $\rho \in (0, \bar{\rho})$ et $\tilde{\alpha} \in (0, \alpha]$, le contrôleur hybride (4.2) avec

$$\bar{M} := \text{He} \left(\frac{\begin{bmatrix} \bar{P}_p A_p + \frac{\tilde{\alpha}}{2} \bar{P}_p & \bar{P}_p B_p \\ 0 & \frac{\mu}{2} I \end{bmatrix}}{\begin{array}{cc|c} & & K_x \\ & & K_c \\ 0 & 0 & K_\eta \end{array}} \right), \quad (4.5)$$

résout le Problème 4.1, c'est-à-dire l'ensemble $\mathcal{A} := 0 \times [0, 2\rho]$ est globalement exponentiellement stable pour le système hybride (4.3) avec \bar{M} définie comme dans (4.5). \square

Démonstration du Théorème 4.2. La démonstration complète du théorème peut être trouvée dans [19]. \blacksquare

Même si le Théorème 4.2 est une généralisation du Théorème 3.2, il ne donne aucune borne de convergence exponentielle, à cause de la présence de l'observateur. De plus, des nouveaux gains sont introduits, liés au nouveau état e , exactement comme pour le Théorème 4.1 (voir la Remarque 4.2).

Comme dans la section précédente, nous présentons le corollaire suivant.

Corollaire 4.2. Considérons un système (3.1) et un contrôleur (4.2) sous les Hypothèses 4.1 et 3.2, un paramètre $\mu > 0$ et K_y, K_x, K_c, K_η matrices nulles et supposons que $\bar{P}_p = \bar{P}_p^\top > 0$, $K_p \in \mathbb{R}^{n_c \times n_p}$ satisfont (3.5) pour $\alpha > 0$. Alors il existe $\bar{\rho} > 0$ tel que pour tout $\rho \in (0, \bar{\rho})$ et $\tilde{\alpha} \in (0, \alpha]$, le contrôleur hybride (4.2) avec \bar{M} définie comme dans (4.5) résout le Problème 4.1, c'est-à-dire l'ensemble $\mathcal{A} := 0 \times [0, 2\rho]$ est globalement exponentiellement stable pour le système hybride (4.3) avec \bar{M} définie comme dans (4.5). \square

4.3.4 Commentaires et remarques

Les Théorèmes 4.1 et 4.2 sont la version à retour de sortie des Théorèmes 3.1 et 3.2. Plus précisément, sous les mêmes conditions des Théorèmes 3.1 et 3.2, respectivement, et en ajoutant un observateur de Luenberger qui satisfait l'Hypothèse 4.1, les Théorèmes 4.1 et 4.2 présentent deux systèmes de contrôle hybride à retour de sortie. Notons que le gain L (voir l'Hypothèse 4.1) garantit la convergence à zéro de e et, en plus, les gains K_y, K_x, K_c, K_η sont introduits pour réduire les effets indésirables dus à la présence de l'observateur (voir la Remarque 4.2). Malheureusement, une méthode pour choisir ces derniers gains n'est pas disponible en ce moment, même si la remarque suivante clarifie quelques aspects.

Pour plus de détails sur les solutions des systèmes à retour de sortie par rapport aux systèmes à retour d'état, le lecteur peut consulter [19, Proposition 4.2].

Remarque 4.3. Selon les Théorèmes 4.1 et 4.2 les matrices K_y, K_x, K_c, K_η peuvent être sélectionnées de façon complètement arbitraire. Notons que toutes ces matrices sont multipliées par η qui, selon la Remarque 4.2 et en absence de bruit, est égal à $\eta = \bar{C}_p e$. Donc nous avons que $\lim_{t+j \rightarrow \infty} e(t, j) = 0$ implique $\lim_{t+j \rightarrow \infty} \eta(t, j) = 0$ et les matrices K_y, K_x, K_c, K_η sont sans effet quand e est proche de zéro. Néanmoins, pendant le transitoire, ces matrices peuvent améliorer le comportement du système :

- le gain K_η peut être choisi négatif et large pour inhiber les sauts quand η (et en quelque mesure aussi l'erreur d'estimation) est grand. Cela est raisonnable, puisque les sauts dépendent de l'état estimé \hat{x}_p et les sauts peuvent être imprécis si e est grand ;
- le gain K_y peut améliorer la dynamique du saut quand l'erreur e est grande et peut être réglé en regardant ses effets sur la réponse du système (trial and error) ;
- les effets des gains K_x, K_c ne sont pas encore claires.

★

La Remarque 3.4 encore s'applique aux Théorèmes 4.1 et 4.2, exception faite pour le point b, qui est vrai seulement quand $e = 0$.

Toutes les considérations données dans la Section 3.4 sur la condition (3.5) sont encore valides. Cela justifie aussi la possibilité d'utiliser la synthèse garantissant la réduction du dépassement

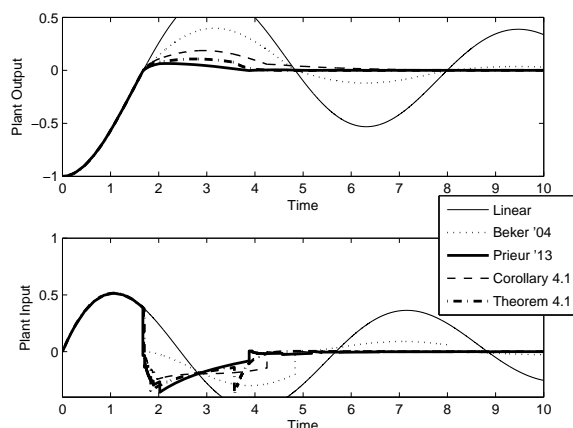


FIGURE 4.1 – Comparaison entre un système linéaire, le système hybride avec un contrôleur de type FORE de [3], le système hybride à retour d'état de [54] et les systèmes hybrides à retour de sortie (4.3) issus du Corollaire 4.1 et du Théorème 4.1, respectivement.

présentée dans [54].

Notons que les systèmes de contrôle considérés dans les Théorèmes 4.1 et 4.2 satisfont la représentation donnée dans (2.1). Donc les résultats du Chapitre 2 peuvent être utilisés.

Tous les commentaires concernant les Théorèmes 4.1 et 4.2 s'appliquent aussi à leurs corollaires. L'intérêt des corollaires est que l'implémentation des contrôleurs est plus simple puisque moins de paramètres doivent être choisis.

4.3.5 Simulations

Dans cette section, nous présentons quelques simulations pour montrer le comportement des systèmes de contrôle développés. Comme dans le chapitre précédent (et aussi dans la littérature), nous supposons que la dynamique du flux du contrôleur est donnée (et ne stabilise pas nécessairement la boucle) et nous obtenons la partie hybride en utilisant la stratégie de synthèse qui garantit la réduction du dépassement donnée dans [54]. Nous allons présenter les détails les plus importants, pour plus d'informations consulter [19].

4.3.5.1 Un système avec un intégrateur

La Figure 4.1 montre que les effets indésirables dus à la présence de l'observateur produisent un dépassement plus grand par rapport au cas du système hybride à retour d'état de [54]. Notons qu'en utilisant les gains K_y , K_x , K_c et K_{eta} le système du Théorème 4.1 peut compenser ces effets. Le système hybride avec un contrôleur FORE de [3] présente un dépassement plus grand par rapport aux autres systèmes hybrides, même s'il améliore la réponse par rapport au cas linéaire.

4.3.5.2 Un moteur en CC

Nous présentons seulement le second cas où la synthèse de l'observateur et de la boucle hybride est faite sur un modèle réduit du système.

La Figure 4.2 montre que les comportements des systèmes hybrides sont très similaires même si l'erreur d'estimation est non nulle. Dans tous les cas il est possible de voir une amélioration de

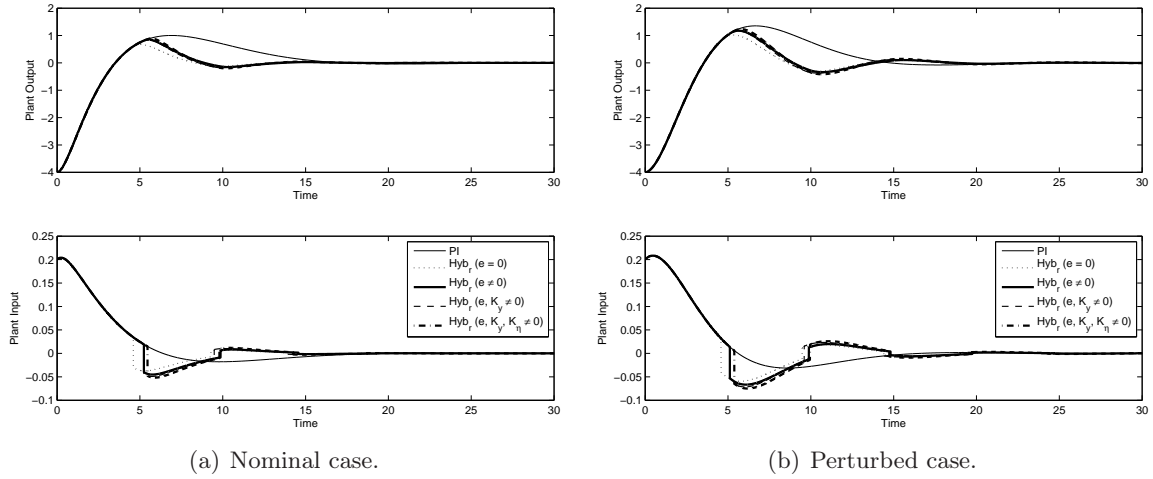


FIGURE 4.2 – Reduced order observer, case 2.

la réponse et du dépassement par rapport au cas linéaire. Notons que dans toutes ces simulations la partie temps continu du contrôleur (même pour le cas linéaire) est la même.

4.4 Boucle hybride à retour de sortie sans temps de maintien

4.4.1 Définition du problème

Nous utilisons l'architecture de contrôle hybride suivante

$$\begin{cases} \begin{bmatrix} \dot{\hat{x}}_p \\ \dot{x}_c \end{bmatrix} = \begin{bmatrix} A_e & B_e \bar{C}_c \\ 0 & \bar{A}_c \end{bmatrix} \begin{bmatrix} \hat{x}_p \\ x_c \end{bmatrix} + \begin{bmatrix} B_e \bar{D}_c + L \\ \bar{B}_c \end{bmatrix} y & (\hat{x}_p, x_c, e) \in \mathcal{C} \\ \begin{bmatrix} \hat{x}_p^+ \\ x_c^+ \end{bmatrix} = \begin{bmatrix} I & 0 \\ K_p & 0 \end{bmatrix} \begin{bmatrix} \hat{x}_p \\ x_c \end{bmatrix} + \begin{bmatrix} 0 \\ K_y \end{bmatrix} \eta & (\hat{x}_p, x_c, e) \in \mathcal{D} \\ u = [0 \ \bar{C}_c] \begin{bmatrix} \hat{x}_p \\ x_c \end{bmatrix} + \bar{D}_c y \end{cases} \quad (4.6a)$$

où $\hat{x}_p \in \mathbb{R}^{n_p}$ est l'état de l'observateur, $x_c \in \mathbb{R}^{n_c}$ est l'état des sauts, A_e , B_e et $\eta \in \mathbb{R}^{n_y}$ sont définis dans l'Hypothèse 4.1 et dans la Remarque 4.2, et les ensembles \mathcal{C} et \mathcal{D} sont

$$\begin{aligned} \mathcal{C} &= \{(\hat{x}_p, x_c, e) : (\hat{x}_p, x_c, e) \in \mathcal{F} \text{ or } (\hat{x}_p, x_c, e) \in \mathcal{F}_\rho\} \\ &= \{(\hat{x}_p, x_c, e) : (\hat{x}_p, x_c, e) \in \mathcal{F}\} \cup \{(\hat{x}_p, x_c, e) : (\hat{x}_p, x_c, e) \in \mathcal{F}_\rho\}, \end{aligned} \quad (4.6b)$$

$$\begin{aligned} \mathcal{D} &= \{(\hat{x}_p, x_c, e) : (\hat{x}_p, x_c, e) \in \mathcal{J} \text{ and } (\hat{x}_p, x_c, e) \in \mathcal{J}_\rho\} \\ &= \{(\hat{x}_p, x_c, e) : (\hat{x}_p, x_c, e) \in \mathcal{J}\} \cap \{(\hat{x}_p, x_c, e) : (\hat{x}_p, x_c, e) \in \mathcal{J}_\rho\}, \end{aligned} \quad (4.6c)$$

avec

$$\mathcal{F}_\rho = \left\{ (\hat{x}_p, x_c, e) \in \mathbb{R}^n : \begin{bmatrix} \hat{x}_p \\ x_c \\ e \end{bmatrix}^\top \underbrace{\begin{bmatrix} I & 0 & 0 \\ 0 & I & 0 \\ 0 & 0 & \bar{C}_p \end{bmatrix}^\top \bar{M}_\rho \begin{bmatrix} I & 0 & 0 \\ 0 & I & 0 \\ 0 & 0 & \bar{C}_p \end{bmatrix}}_{M_\rho} \begin{bmatrix} \hat{x}_p \\ x_c \\ e \end{bmatrix} \leq \rho \right\}, \quad (4.6d)$$

$$\mathcal{J}_\rho = \left\{ (\hat{x}_p, x_c, e) \in \mathbb{R}^n : \begin{bmatrix} \hat{x}_p \\ x_c \\ e \end{bmatrix}^\top \overbrace{\begin{bmatrix} I & 0 & 0 \\ 0 & I & 0 \\ 0 & 0 & \bar{C}_p \end{bmatrix}^\top \bar{M}_\rho \begin{bmatrix} I & 0 & 0 \\ 0 & I & 0 \\ 0 & 0 & \bar{C}_p \end{bmatrix}} \begin{bmatrix} \hat{x}_p \\ x_c \\ e \end{bmatrix} \geq \rho \right\}, \quad (4.6e)$$

où $\bar{M}_\rho = \bar{M}_\rho^\top > 0$, $\rho > 0$ et les ensembles \mathcal{F} et \mathcal{J} sont des cônes symétriques définis à travers la matrice $\bar{M} = \bar{M}^\top$ comme

$$\mathcal{F} = \left\{ (\hat{x}_p, x_c, e) \in \mathbb{R}^n : \begin{bmatrix} \hat{x}_p \\ x_c \\ e \end{bmatrix}^\top \underbrace{\begin{bmatrix} I & 0 & 0 \\ 0 & I & 0 \\ 0 & 0 & \bar{C}_p \end{bmatrix}^\top \bar{M} \begin{bmatrix} I & 0 & 0 \\ 0 & I & 0 \\ 0 & 0 & \bar{C}_p \end{bmatrix}}_M \begin{bmatrix} \hat{x}_p \\ x_c \\ e \end{bmatrix} \leq 0 \right\}, \quad (4.6f)$$

$$\mathcal{J} = \left\{ (\hat{x}_p, x_c, e) \in \mathbb{R}^n : \begin{bmatrix} \hat{x}_p \\ x_c \\ e \end{bmatrix}^\top \overbrace{\begin{bmatrix} I & 0 & 0 \\ 0 & I & 0 \\ 0 & 0 & \bar{C}_p \end{bmatrix}^\top \bar{M} \begin{bmatrix} I & 0 & 0 \\ 0 & I & 0 \\ 0 & 0 & \bar{C}_p \end{bmatrix}} \begin{bmatrix} \hat{x}_p \\ x_c \\ e \end{bmatrix} \geq 0 \right\}. \quad (4.6g)$$

Notons que l'information de l'observateur est utilisée par la boucle hybride et non pas par la dynamique du flux.

Sous l'Hypothèse 3.2, l'interconnexion entre (3.1) et (4.6) mène au système hybride suivant

$$\begin{cases} \begin{bmatrix} \dot{\hat{x}}_p \\ \dot{\hat{x}}_c \\ \dot{e} \end{bmatrix} = \begin{bmatrix} A_p & B_p & B_o \\ B_c & A_c & B_c \\ 0 & 0 & A_e \end{bmatrix} x := Ax & x \in \mathcal{C} \\ x^+ = \begin{bmatrix} I & 0 & 0 \\ K_p & 0 & K_y \bar{C}_p \\ 0 & 0 & I \end{bmatrix} x := Gx & x \in \mathcal{D} \\ y = [C_p \ C_c \ C_p] x := Cx \end{cases} \quad (4.7)$$

avec $x := [\hat{x}_p^\top \ x_c^\top \ e^\top]^\top \in \mathbb{R}^{n:=2n_p+n_c}$, $B_o := L\bar{C}_p + \bar{B}_p\bar{D}_c(I - \bar{D}_p\bar{D}_c)^{-1}\bar{C}_p$ et A_p, B_p, A_c, B_c, C_p et C_c définis dans (3.4) et les ensembles du flux et du saut définis dans (4.6b) et (4.6c).

Notons que (4.7) n'utilise pas une variable temporelle et, de plus, les ensembles \mathcal{C} et \mathcal{D} sont différents par rapport à ceux présentés dans le Chapitre 2. Donc les résultats du Chapitre 2 ne peuvent pas être appliqués.

Problème 4.2. *Considérons un système (3.1) et les matrices $\bar{A}_c, \bar{B}_c, \bar{C}_c, \bar{D}_c$ et L du contrôleur (4.6) tels que les Hypothèses 4.1 et 3.2 sont satisfaites. Notre but est de concevoir la partie hybride à retour de sortie de (4.6), c'est-à-dire les matrices $\bar{M} = \bar{M}^\top \in \mathbb{R}^{(n_p+n_c+n_y) \times (n_p+n_c+n_y)}$ et $\bar{M}_\rho = \bar{M}_\rho^\top \in \mathbb{R}^{(n_p+n_c+n_y) \times (n_p+n_c+n_y)}$, les gains $K_p \in \mathbb{R}^{n_c \times n_p}$ et $K_y \in \mathbb{R}^{n_c \times n_y}$ et $\rho > 0$ tels que l'origine du système (4.7) est pratiquement globalement asymptotiquement stable, c'est-à-dire l'ensemble $\mathcal{A} := \left\{ (\hat{x}_p, x_c) : \begin{bmatrix} \hat{x}_p \\ x_c \end{bmatrix}^\top P \begin{bmatrix} \hat{x}_p \\ x_c \end{bmatrix} \leq \rho \right\} \times \{0\} \subset \mathbb{R}^{n_p+n_c} \times \mathbb{R}^{n_p}$ est globalement asymptotiquement stable pour le système (4.7), où ρ peut être sélectionné arbitrairement petit (mais plus grand que zéro). \circ*

Pour plus de détails sur la *stabilité asymptotique pratique* consulter [13, 19]).

4.4.2 Stabilité asymptotique pratique

Théorème 4.3. Considérons le système (3.1) et le contrôleur (4.6) sous les Hypothèses 4.1 et 3.2 et supposons que $P = P^\top := \begin{bmatrix} \hat{P}_p & P_{pc} \\ P_{pc}^\top & P_c \end{bmatrix} > 0$ satisfait (3.5) et (3.6) pour $\alpha > 0$. Alors pour tout $\tilde{\alpha} \in (0, \alpha]$ et $K_y \in \mathbb{R}^{n_c \times q}$, le contrôleur hybride (4.6) avec $\rho > 0$ et

$$\bar{M} = \text{He} \left(\tilde{P} \begin{bmatrix} A_p & B_p & -B_p K_y \\ B_c & A_c & 0 \\ 0 & 0 & 0 \end{bmatrix} + \frac{\tilde{\alpha}}{2} \hat{P} \right), \quad (4.8a)$$

$$\bar{M}_\rho = \hat{P}, \quad (4.8b)$$

où

$$\hat{P} = \begin{bmatrix} I & 0 & 0 \\ 0 & I & -K_y \end{bmatrix}^\top P \begin{bmatrix} I & 0 & 0 \\ 0 & I & -K_y \end{bmatrix}, \quad (4.9)$$

résout le Problème 4.2, c'est-à-dire l'ensemble $\mathcal{A} := \left\{ (\hat{x}_p, x_c) : \begin{bmatrix} \hat{x}_p \\ x_c \end{bmatrix}^\top P \begin{bmatrix} \hat{x}_p \\ x_c \end{bmatrix} \leq \rho \right\} \times \{0\}$ est globalement asymptotiquement stable pour le système (4.7), où ρ peut être arbitrairement petit. \square

Démonstration du Théorème 4.3. La démonstration complète du théorème peut être trouvée dans [19]. \blacksquare

Le Théorème 4.3 généralise la boucle hybride à retour d'état de [52] au cas à retour de sortie. Le Théorème 4.3 garantit stabilité asymptotique pratique globale où le paramètre $\rho > 0$ n'a aucune contrainte et peut être choisi proche de zéro. Notons que l'ensemble \mathcal{A} correspond à l'ensemble \mathcal{F}_ρ qui dépend de ρ .

Le Théorème 4.3 garantit la convergence de l'erreur d'estimation vers l'origine en supprimant toutes les solutions Zénon (voir la Remarque 4.1), sans utiliser aucune variable temporelle. En particulier, une condition de temps de maintien est garantie en combinant les éléments suivants :

- i. les equations dynamiques du flux et du saut sont linéaires ;
- ii. les sauts sont à l'intérieur de l'ensemble du flux ;
- iii. les ensembles (4.6b) et (4.6c) sont faits de sorte qu'une petite région autour de l'origine (c'est-à-dire \mathcal{F}_ρ) est enlevée de l'ensemble du saut (voir aussi [24]).

Parmi les similarités avec [52], nous mentionnons :

- a. les ensembles \mathcal{F} et \mathcal{J} sont les mêmes, exception faite pour une région arbitrairement petite autour de l'origine ;
- b. la dynamique du saut :
 - i. garantit que la fonction de type Lyapunov dans \mathcal{F} et \mathcal{J} n'augmente pas pendant les sauts ;
 - ii. garantit que la fonction de type Lyapunov dans \mathcal{F} et \mathcal{J} décroît après chaque saut ;
- c. si $e = 0$ la fonction de type Lyapunov dans \mathcal{F} et \mathcal{J} n'augmente pas pendant le flux ;
- d. la condition (3.5) doit être satisfaite ;
- e. la stabilité est obtenue à travers les sauts.

4.4.3 Simulations

Considérons le même exemple que dans la Section 4.3.5.1, où la synthèse de la boucle hybride a été faite avec la synthèse de [54] pour la réduction du dépassement.

La Figure 4.3 montre que le contrôleur du Théorème 4.3 avec $K_y = 0$ donne un dépassement plus grand que la boucle hybride à retour d'état de [54], mais plus petit que le contrôleur FORE de [3]. Le même contrôleur réglé avec $K_y = -2$ montre une diminution du dépassement, même si le signal de contrôle est beaucoup plus grand, et donne une vitesse de convergence plus grande bien que superflue dans ce cas où seulement le dépassement était exigé.

4.5 Conclusion

Nous avons présenté quelques boucles hybrides à retour de sortie qui utilisent un observateur de Luenberger pour obtenir une estimation de l'état du système. Dans ce cas, pour garantir la convergence de l'erreur d'estimation, la suppression des solutions de type Zénon est exigée. Les architectures de contrôle issues des Théorèmes 4.1 et 4.2 et leurs corollaires utilisent un temps de maintien pour supprimer les solutions de type Zénon. Au contraire, le Théorème 4.3 garantit la condition de temps de maintien en imposant une structure sur les ensembles du flux et du saut et sur la loi de saut. Quelques simulations montrent que les deux philosophies peuvent donner des systèmes hybrides capables de réduire le dépassement.

Parmi les différences principales entre les deux approches, nous mentionnons que les Théorèmes 4.1 et 4.2 et leurs corollaires établissent stabilité exponentielle globale alors que le Théorème 4.3 établit la stabilité asymptotique pratique. De plus, les Théorèmes 4.1 et 4.2 semblaient avoir plus de flexibilité due à un plus grand ensemble de paramètres à régler.

Parmi les similarités, notons que tous les résultats de ce chapitre dépendent de la condition (3.5) qui est strictement liée aux fonctions de type Lyapunov utilisées dans les ensembles du flux et du saut, \mathcal{F} et \mathcal{J} .

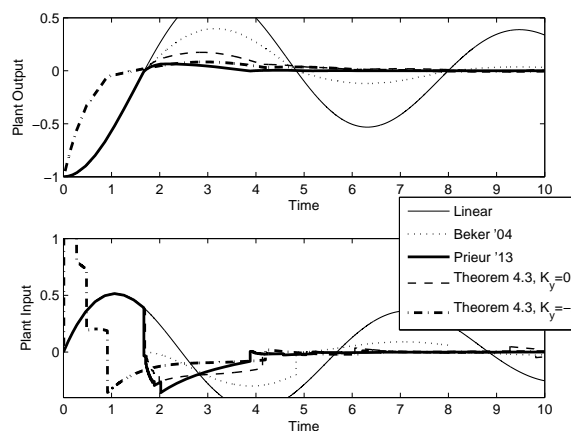


FIGURE 4.3 – Comparaison entre un système linéaire, le système hybride avec un contrôleur de type FORE de [3], le système hybride à retour d'état de [54] et deux systèmes hybrides à retour de sortie (4.7) issus du Théorème 4.3 avec $K_y = 0$ et $K_y = -2$, respectivement.

Synthèse d'un contrôleur hybride multi-objectif

Contents

5.1	Introduction	35
5.2	Synthèse convexe d'un contrôleur hybride	36
5.2.1	Aspects préliminaires et définition du problème	36
5.2.2	Synthèse convexe multi-objectif	37
5.3	Commentaires sur la boucle hybride à retour de sortie	39
5.4	Simulations	39
5.4.1	Un avion F-8	39
5.5	Conclusion	40

Dans ce chapitre nous présentons une méthode de synthèse convexe d'un contrôleur hybride. La Section 5.1 fournit quelques motivations pour cette étude. La Section 5.2 donne le résultat principal et quelques propriétés de synthèse. La Section 5.3 contient quelques commentaires par rapport à la boucle hybride à retour de sortie. Enfin un exemple de simulation conclut le chapitre. Les résultats suivants ont été publiés dans [20].

5.1 Introduction

Dans les Chapitres 3 et 4, nous avons présenté des systèmes de contrôle issus de l'interconnexion d'un contrôleur hybride et un système linéaire qui garantissent la stabilité de la boucle fermée. Nous avons fait l'hypothèse que la dynamique du flux (et aussi la partie à temps continu du contrôleur hybride) était donnée, de sorte que seule la boucle hybride était conçue pour garantir la stabilité et la réduction du dépassement.

Le fait que la dynamique à temps continu est fixée limite le potentiel du contrôleur hybride puisque seul un sous-ensemble des paramètres peut être réglé. Le problème de concevoir un contrôleur hybride complet (c'est-à-dire les dynamiques du flux et du saut et les ensembles du flux et du saut) est compliqué. La difficulté principale est d'obtenir des conditions convexes pour la synthèse. Dans la littérature, la seule méthode de synthèse d'un contrôleur hybride pour un système linéaire peut être trouvée dans [57], où une synthèse optimale par rapport au gain t - \mathcal{L}_2 est proposée. Malheureusement, les résultats donnés dans [57] sont préliminaires et quelques aspects ont besoin de plus de clarifications.

Dans ce chapitre, nous proposons des conditions convexes pour le design d'un contrôleur hybride multi-objectif pour un système linéaire à temps continu. En particulier, la synthèse est multi-objectif par rapport aux indices de prestation suivants :

- le taux de convergence en t (voir la Définition 1.8) ;
- le gain t - \mathcal{L}_2 (voir la Définition 1.9).

L'idée principale est d'utiliser l'architecture présentée dans la Section 3.3.2 et le résultat de la Proposition 2.1 et les combiner à travers un changement de coordonnées, pour obtenir une stratégie de synthèse multi-objectif d'un contrôleur hybride complet.

5.2 Synthèse convexe d'un contrôleur hybride

5.2.1 Aspects préliminaires et définition du problème

Considérons un système \mathcal{P}

$$\begin{aligned} \dot{x}_p &= \bar{A}_p x_p + \bar{B}_p u + \bar{B}_w w \\ z &= \bar{C}_z x_p + \bar{D}_z u + \bar{D}_{zw} w \\ y &= \bar{C}_p x_p + \bar{D}_p u + \bar{D}_w w \end{aligned} \quad (5.1)$$

où $x_p \in \mathbb{R}^{n_p}$ est l'état, $u \in \mathbb{R}^{n_u}$ est l'entrée de contrôle, $y \in \mathbb{R}^{n_y}$ est la sortie mesurée, $w \in \mathbb{R}^{n_w}$ est un signal exogène et $z \in \mathbb{R}^{n_z}$ est la sortie de performance.

Hypothèse 5.1. Le système (5.1) est tel que $\bar{D}_p = 0$. ◦

Notons que l'Hypothèse 5.1 est utile pour simplifier le développement mais elle n'est pas restrictive. Au cas où \mathcal{P} a $\bar{D}_p \neq 0$, nous pouvons toujours définir $\bar{y} := y - \bar{D}_p u$ et utiliser \bar{y} comme nouvelle sortie mesurée.

L'architecture du contrôleur hybride \mathcal{H}_c est

$$\begin{cases} \dot{x}_c = \bar{A}_c x_c + \bar{B}_c y \\ \dot{\tau} = 1 - \text{dz} \left(\frac{\tau}{\rho} \right) & (x_p, x_c, \tau) \in \mathcal{C} \\ \begin{cases} x_c^+ = K_p x_p \\ \tau^+ = 0 \end{cases} & (x_p, x_c, \tau) \in \mathcal{D} \\ u = \bar{C}_c x_c + \bar{D}_c y \end{cases} \quad (5.2a)$$

où $x_c \in \mathbb{R}^{n_c}$ est l'état, $\tau \in [0, 2\rho]$ avec $\rho > 0$ est le temps de maintien et \mathcal{C} et \mathcal{D} sont

$$\begin{aligned} \mathcal{C} &= \{(x_p, x_c, \tau) : (x_p, x_c) \in \mathcal{F} \text{ or } \tau \in [0, \rho]\} \\ &= \{(x_p, x_c, \tau) : (x_p, x_c) \in \mathcal{F}\} \cup \{(x_p, x_c, \tau) : \tau \in [0, \rho]\}, \end{aligned} \quad (5.2b)$$

$$\begin{aligned} \mathcal{D} &= \{(x_p, x_c, \tau) : (x_p, x_c) \in \mathcal{J} \text{ and } \tau \in [\rho, 2\rho]\} \\ &= \{(x_p, x_c, \tau) : (x_p, x_c) \in \mathcal{J}\} \cap \{(x_p, x_c, \tau) : \tau \in [\rho, 2\rho]\}, \end{aligned} \quad (5.2c)$$

avec \mathcal{F} et \mathcal{J} des cônes symétriques définis selon

$$\mathcal{F} = \left\{ (x_p, x_c) : \begin{bmatrix} x_p \\ x_c \end{bmatrix}^\top M \begin{bmatrix} x_p \\ x_c \end{bmatrix} \leq 0 \right\} \quad (5.2d)$$

$$= \left\{ (x_p, x_c) : \begin{bmatrix} x_p \\ x_c \end{bmatrix}^\top \text{He} \left(\begin{bmatrix} \bar{P}_p A_p + \frac{\tilde{\alpha}}{2} \bar{P}_p & \bar{P}_p B_p \\ 0 & \frac{\mu}{2} I \end{bmatrix} \right) \begin{bmatrix} x_p \\ x_c \end{bmatrix} \leq 0 \right\}, \quad (5.2e)$$

$$\mathcal{J} = \left\{ (x_p, x_c) : \begin{bmatrix} x_p \\ x_c \end{bmatrix}^\top M \begin{bmatrix} x_p \\ x_c \end{bmatrix} \geq 0 \right\} \quad (5.2f)$$

$$= \left\{ (x_p, x_c) : \begin{bmatrix} x_p \\ x_c \end{bmatrix}^\top \text{He} \left(\begin{bmatrix} \bar{P}_p A_p + \frac{\tilde{\alpha}}{2} \bar{P}_p & \bar{P}_p B_p \\ 0 & \frac{\mu}{2} I \end{bmatrix} \right) \begin{bmatrix} x_p \\ x_c \end{bmatrix} \geq 0 \right\}, \quad (5.2g)$$

où A_p et B_p sont définis par la suite (voir (5.3)).

Notons que le contrôleur (5.2) a exactement la même structure que celui du Théorème 3.2. Donc l'Hypothèse 3.1 est maintenue.

L'interconnexion de (5.1) et (5.2) mène au système hybride (2.1) avec $x = [x_p^\top x_c^\top]^\top \in \mathbb{R}^{n:=n_p+n_c}$,

$$\left(\begin{array}{c|c} A & B \\ \hline G & - \\ \hline C_z & D_{zw} \\ \hline C_p & D_{pw} \end{array} \right) = \left(\begin{array}{cc|c} A_p & B_p & B_{pw} \\ \hline B_c & A_c & B_{cw} \\ \hline G & & - \\ \hline C_z & & D_{zw} \\ \hline C_p & & D_{pw} \end{array} \right) = \left(\begin{array}{cc|cc} \bar{A}_p + \bar{B}_p \bar{D}_c \bar{C}_p & \bar{B}_p \bar{C}_p & \bar{B}_w + \bar{B}_p \bar{D}_c \bar{D}_w & \\ \hline \bar{B}_c \bar{C}_p & \bar{A}_c & \bar{B}_c \bar{D}_w & \\ \hline I & 0 & - & \\ \hline K_p & 0 & - & \\ \hline \bar{C}_z + \bar{D}_z \bar{D}_c \bar{C}_p & \bar{D}_z \bar{C}_c & \bar{D}_{zw} + \bar{D}_z \bar{D}_c \bar{D}_w & \\ \hline \bar{C}_p & 0 & \bar{D}_w & \end{array} \right) \quad (5.3)$$

et les ensembles \mathcal{F} et \mathcal{J} définies dans (5.2d) et (5.2f) respectivement. Par la suite ce système hybride sera appelé : système (2.1), (5.3).

Problème 5.1. *Considérons le système \mathcal{P} dans (5.1) sous les Hypothèses 3.1 et 5.1 et le contrôleur hybride \mathcal{H}_c défini dans (5.2). Notre but est de concevoir les matrices \bar{A}_c , \bar{B}_c , \bar{C}_c , \bar{D}_c , K_p , \bar{P}_p , et les scalaires positifs $\tilde{\alpha}$ et μ tels qu'il existe $\bar{\rho} > 0$ tel que pour tout $\rho \in (0, \bar{\rho})$ les propriétés suivantes sont satisfaites :*

- i. **Taux de convergence en t :** *l'ensemble $\{0\} \times [0, 2\rho]$ est globalement exponentiellement stable pour le système (2.1), (5.3) avec $w = 0$. De plus, le taux de convergence en t est égal à $\tilde{\alpha}/2$ pour la composante x_p des solutions $\xi = (x, \tau)$ du système (2.1), (5.3) ;*
- ii. **\mathcal{H}_∞ spécification :** *pour tout $w \in t\text{-}\mathcal{L}_2$, le gain $t\text{-}\mathcal{L}_2$ du système (2.1), (5.3) de w à z est plus petit que ou égal à γ .*

◦

5.2.2 Synthèse convexe multi-objectif

Théorème 5.1. *Considérons (5.1) sous les Hypothèses 3.1 et 5.1, et supposons qu'il existe $Y = Y^\top \in \mathbb{R}^{n_p \times n_p}$, $W = W^\top \in \mathbb{R}^{n_p \times n_p}$, $\hat{A} \in \mathbb{R}^{n_p \times n_p}$, $\hat{B} \in \mathbb{R}^{n_p \times n_y}$, $\hat{C} \in \mathbb{R}^{n_u \times n_p}$, $\hat{D} \in \mathbb{R}^{n_u \times n_y}$ et des scalaires positifs γ et α tels que*

$$\begin{bmatrix} Y & I \\ I & W \end{bmatrix} > 0, \quad (5.4a)$$

$$\text{He} \left(\begin{array}{cc|cc} \bar{A}_p Y + \bar{B}_p \hat{C} & \bar{A}_p + \bar{B}_p \hat{D} \hat{C}_p & \bar{B}_w + \bar{B}_p \hat{D} \hat{D}_w & Y \bar{C}_z^\top + \hat{C}^\top \bar{D}_z^\top \\ \hline \hat{A} & W \bar{A}_p + \hat{B} \hat{C}_p & W \bar{B}_w + \hat{B} \hat{D}_w & \bar{C}_z^\top + \hat{C}_p^\top \hat{D}^\top \bar{D}_z^\top \\ \hline 0 & 0 & -\frac{\gamma}{2} I & \bar{D}_{zw}^\top + \bar{D}_w^\top \hat{D}^\top \bar{D}_z^\top \\ \hline 0 & 0 & 0 & -\frac{\gamma}{2} I \end{array} \right) < 0, \quad (5.4b)$$

$$\text{He} \left(\bar{A}_p Y + \bar{B}_p \hat{C} + \frac{\alpha}{2} Y \right) < 0. \quad (5.4c)$$

Pour n'importe quelle solution de (5.4), définissons

$$\begin{aligned} \bar{D}_c &= \hat{D}, \\ \bar{C}_c &= (\hat{C} - \bar{D}_c \bar{C}_p Y)(Y - W^{-1})^{-1}, \\ \bar{B}_c &= -W^{-1} \hat{B} + \bar{B}_p \bar{D}_c, \\ \bar{A}_c &= -W^{-1} (\hat{A} + W \bar{B}_c \bar{C}_p Y - W \bar{B}_p \bar{C}_c (Y - W^{-1}) - W(\bar{A}_p + \bar{B}_p \bar{D}_c \bar{C}_p) Y)(Y - W^{-1})^{-1}, \\ \bar{P}_p &= Y^{-1}, \\ K_p &= (Y - W^{-1}) Y^{-1}. \end{aligned} \quad (5.5)$$

Alors pour chaque $\tilde{\alpha}$ satisfaisant $0 < \tilde{\alpha} \leq \alpha$, il existe $\mu > 0$ tel que (3.8) est satisfaite. De plus, pour chaque $\mu > 0$ satisfaisant (3.8), il existe $\bar{\rho} > 0$ tel que pour tout $\rho \in (0, \bar{\rho})$ le contrôleur hybride (5.2) garantit que pour le système (2.1), (5.3) :

- i. l'ensemble $\{0\} \times [0, 2\rho]$ est globalement exponentiellement stable. De plus le taux de convergence en t de la composante x_p de la solution ξ du système (2.1), (5.3) est égal à $\tilde{\alpha}/2$ (voir (3.10)) pour toutes les solutions avec $x_c(0, 0) = 0$;
- ii. le gain $t\text{-}\mathcal{L}_2$ de w à z est plus petit que ou égal à γ , pour tout $w \in t\text{-}\mathcal{L}_2$.

□

Démonstration du Théorème 5.1. La démonstration complète du théorème peut être trouvée dans [19]. ■

Le Théorème 5.1 fournit une procédure convexe pour concevoir un contrôleur hybride qui résout le Problème 5.1. Plus précisément, les conditions (5.4a) et (5.4b) sont linéaires dans leurs variables, alors que (5.4c) est un problème aux valeurs propres généralisées si α est une variable (voir [7]) et linéaire si α est fixé. Notons que la synthèse est faite en trois étapes :

1. résolution de (5.4) dans leurs variables ;
2. utilisation de (5.5) pour définir le contrôleur hybride selon (5.2) ;
3. résolution de (3.8) dans la seule variable restante $\mu > 0$.

La synthèse présentée dans le Théorème 5.1 fournit un contrôleur hybride (5.2) qui est multi-objectif par rapport au taux de convergence en t et au gain $t\text{-}\mathcal{L}_2$. Plus particulièrement, le taux de convergence en t est certifié à travers (3.10) (voir les Remarques 3.1 et 3.2) et dépend de α et $\tilde{\alpha}$ (voir la Remarque 3.3). En même temps, le gain $t\text{-}\mathcal{L}_2$ de w à z est plus petit que ou égal à γ défini comme dans (5.4b).

Le problème d'optimisation dans le Théorème 5.1 peut être résolu soit en minimisant le gain $t\text{-}\mathcal{L}_2$, γ , et en fixant le paramètre α , soit en maximisant α et en résolvant le problème aux valeurs propres généralisées. Pour cette raison, nous ne parlons pas de contrôleur hybride multi-objectif optimal par rapport aux deux indices de prestation, mais de contrôleur hybride multi-objectif optimal par rapport à un indice de prestation, étant fixé l'autre. Notons que la synthèse donne un contrôleur avec le même ordre que le système, c'est-à-dire $n_p = n_c$.

5.3 Commentaires sur la boucle hybride à retour de sortie

Le Théorème 5.1 propose une stratégie de synthèse d'un contrôleur hybride à retour d'état et donc l'Hypothèse 3.1 est nécessaire. Néanmoins, l'extension du résultat du Théorème 5.1 au cas de la boucle hybride à retour de sortie à travers les résultats du Chapitre 4 n'a pas encore été obtenue.

L'idée est de faire une synthèse en deux étapes en augmentant le contrôleur hybride à retour d'état du Théorème 5.1 avec les stratégies du Théorème 4.2 (ou du Corollaire 4.2). Malheureusement, le cas à retour de sortie ne peut pas être multi-objectif puisque le Théorème 4.2 (et le Corollaire 4.2) ne garantit aucun taux de convergence en t . Donc la synthèse à retour de sortie peut être optimale par rapport au seul gain $t\text{-}\mathcal{L}_2$. Dans ce cadre, le Corollaire 4.2 peut être directement utilisé en faisant tout simplement la synthèse *a posteriori* du gain L . Par contre le Théorème 4.2 a besoin de plus d'attention pour faire l'extension à retour de sortie et pour plus de détails le lecteur est renvoyé vers [19].

Nous remarquons que l'introduction de l'observateur réduit la prestation $t\text{-}\mathcal{L}_2$ obtenue avec la technique du Théorème 5.1 et donc, la certification du gain $t\text{-}\mathcal{L}_2$ doit être faite *a posteriori* en utilisant les résultats d'analyse donnés dans le Chapitre 2.

5.4 Simulations

Nous présentons la synthèse du Théorème 5.1 et une comparaison avec la synthèse linéaire (voir [19, Appendice 5.4.2] ou [58]). Pour simplicité nous proposons une synthèse convexe en imposant la même vitesse de convergence pour le cas hybride et le cas linéaire (c'est-à-dire $\alpha = \alpha_L$) et minimisant le gain $t\text{-}\mathcal{L}_2$. Pour le cas hybride nous présentons aussi le cas à retour de sortie et nous indiquons avec SF la boucle hybride à retour d'état (state feedback) et avec OF la boucle hybride à retour de sortie (output feedback).

5.4.1 Un avion F-8

Nous présentons un exemple d'un avion F-8 à deux entrées et deux sorties utilisé dans [38]. Pour plus de détails, consulter [19].

La Figure 5.1 montre les valeurs de γ linéaires et hybrides obtenues à partir de différentes valeurs de $\alpha_L = \alpha$. Notons que le cas hybride présente des valeurs de γ beaucoup plus petites que celles du cas linéaire (où "linear b.r.l." représente les valeurs de γ obtenues en faisant l'analyse linéaire *a posteriori* selon le lemme borné réel [16]).

Plus précisément, au cas où $\alpha = \alpha_L = 1.01$ nous avons un contrôleur linéaire avec un gain \mathcal{L}_2 égal à $\gamma = 68.00357$, un contrôleur hybride à retour d'état (SF) avec un gain $t\text{-}\mathcal{L}_2$ égal à $\gamma = 1.07906$ et un contrôleur hybride à retour de sortie avec un gain $t\text{-}\mathcal{L}_2$ égal à $\gamma_o = 2139.94263$.

Les Figures 5.2(a) et 5.3(a) (et leurs détails dans les Figures 5.2(b) et 5.3(b)) montrent, pour le cas sans perturbation, que la boucle hybride à retour d'état (SF) a un comportement désirable alors que la boucle linéaire oscille et présente des piques plus grands que la boucle hybride à retour de sortie (OF).

Les Figures 5.4(a) et 5.5(a) (et leurs détails dans les Figures 5.4(b) et 5.5(b)) montrent qu'en présence d'une perturbation $w \in \mathcal{L}_2$, la boucle hybride à retour d'état (SF) a encore un comportement désirable et même la boucle hybride à retour de sortie a un comportement meilleur que du

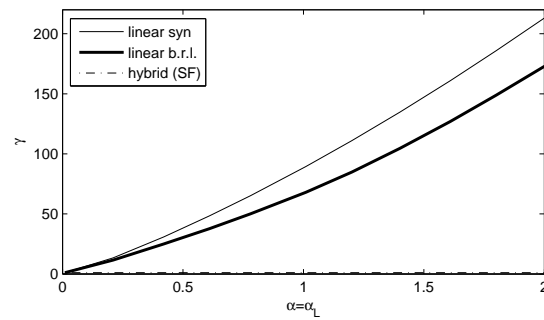
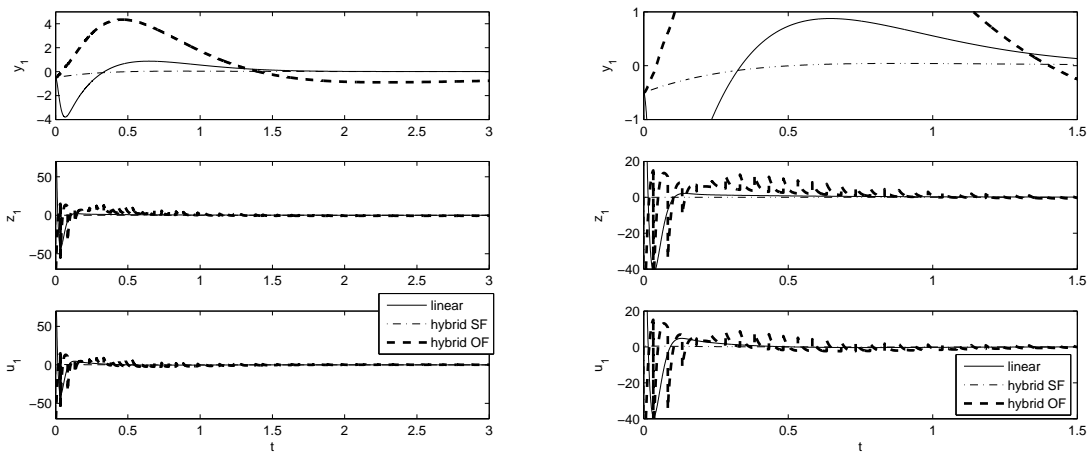


FIGURE 5.1 – Valeurs de γ en fonction de $\alpha = \alpha_L$ pour le cas linéaire et pour le cas hybride à retour d'état.

cas linéaire.

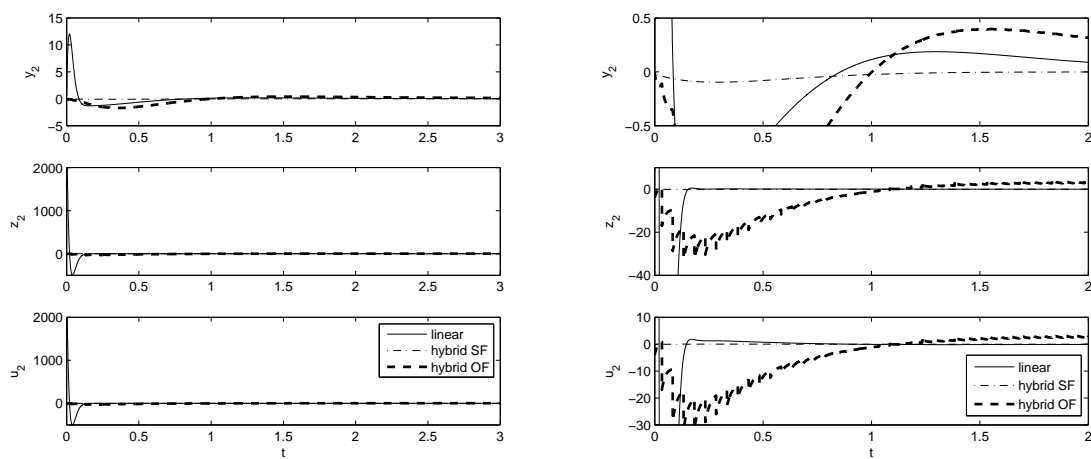
5.5 Conclusion

Une stratégie de synthèse convexe d'un contrôleur hybride multi-objectif par rapport au taux de convergence en t et au gain $t\text{-}\mathcal{L}_2$ a été présentée. Nous avons même présenté les difficultés liées à l'extension des résultats à une boucle hybride à retour de sortie qui représente encore un challenge pour laquelle n'est pas disponible une synthèse convexe. Enfin parmi des simulations nous avons montré que le contrôleur hybride présente un comportement meilleur que celui obtenu avec un contrôleur linéaire. Le cas avec la boucle hybride à retour de sortie présente un comportement plus désirable que cela du contrôleur linéaire même si la certification du gain $t\text{-}\mathcal{L}_2$ est beaucoup pire que pour le cas linéaire. Une possible solution à ce problème peut être dans les gains du Théorème 4.2 qui doivent encore être étudiés.



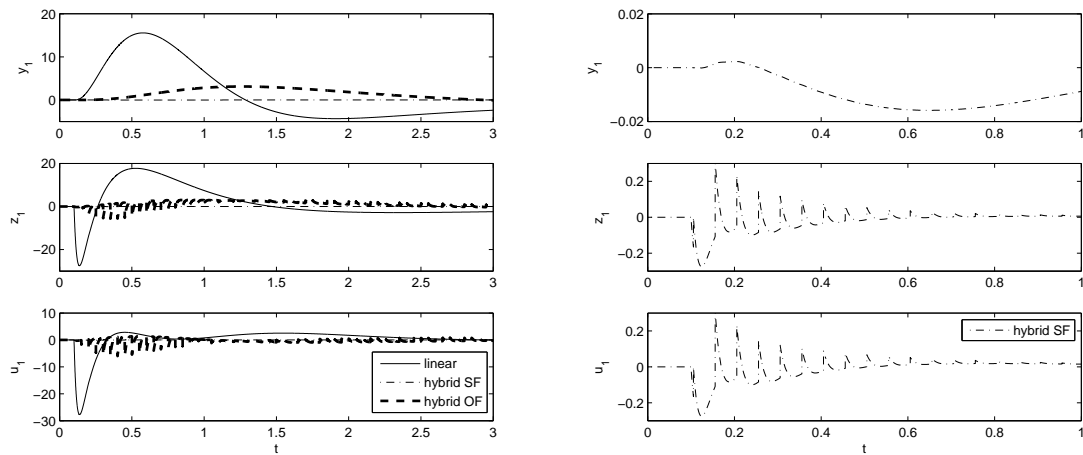
(a) Contrôleurs hybrides et linéaire avec $\alpha = \alpha_L = 1$ (sans perturbation).
 (b) Zoom de la Figure 5.2(a) (sans perturbation).

FIGURE 5.2 – Comparaison entre la boucle linéaire, la boucle hybride à retour d'état (SF) et la boucle hybride à retour de sortie (OF). Signaux y_1 , z_1 et u_1 .



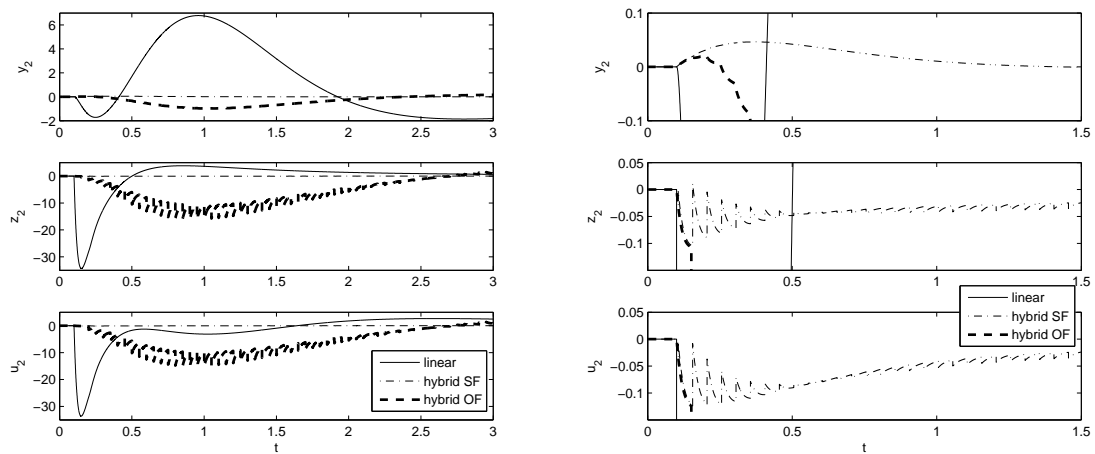
(a) Contrôleurs hybrides et linéaire avec $\alpha = \alpha_L = 1$ (sans perturbation).
 (b) Zoom de la Figure 5.3(a) (sans perturbation).

FIGURE 5.3 – Comparaison entre la boucle linéaire, la boucle hybride à retour d'état (SF) et la boucle hybride à retour de sortie (OF). Signaux y_2 , z_2 et u_2 .



(a) Contrôleurs hybrides et linéaire avec $\alpha = \alpha_L = 1$ (condition initiale nulle). (b) Zoom de la Figure 5.4(a) (condition initiale nulle).

FIGURE 5.4 – Comparaison entre la boucle linéaire, la boucle hybride à retour d'état (SF) et la boucle hybride à retour de sortie (OF). Signaux y_1 , z_1 et u_1 .



(a) Contrôleurs hybrides et linéaire avec $\alpha = \alpha_L = 1$ (condition initiale nulle). (b) Zoom de la Figure 5.5(a) (condition initiale nulle).

FIGURE 5.5 – Comparaison entre la boucle linéaire, la boucle hybride à retour d'état (SF) et la boucle hybride à retour de sortie (OF). Signaux y_2 , z_2 et u_2 .

Conclusion générale

Cette partie en français présente de manière succincte une partie des résultats les plus importants de la version anglaise [19]. Bien que ce tome en français est auto-contenu, les démonstrations des résultats et quelques détails sur l'implémentation des résultats numériques ont été omis et peuvent être trouvés de façon détaillée sur le tome en anglais [19]. Par la suite de cette conclusion générale nous résumons les étapes de nos études et donnons quelques idées pour les travaux futurs.

Dans un premier temps nous avons présenté des conditions d'analyse basées sur une fonction de Lyapunov pour établir une certification du gain t - \mathcal{L}_2 pour une classe de systèmes hybrides. En plus, nous avons obtenu des conditions LMI qui peuvent être résolues de manière efficace à travers les outils de la programmation convexe. Notons que dans tous les cas les conditions présentées généralisent les résultats publiés dans [48].

Les résultats d'analyse du Chapitre 2 ne peuvent pas être directement étendus à la synthèse d'un contrôleur hybride pour un système à temps continu, à cause du fait que les conditions obtenues ne sont plus convexes. La difficulté principale vient de la généralité des architectures des contrôleurs hybrides, même pour des ensembles coniques et des équations linéaires. Pour simplifier le problème, une structure doit être imposée pour le contrôleur hybride, par exemple comme pour l'architecture FORE. Dans ce cas, les contrôleurs hybrides présentés dans le Chapitre 3 représentent une alternative intéressante. Le fait d'utiliser une fonction de type Lyapunov pour définir les ensembles du flux et du saut permet d'obtenir des lois de saut qui garantissent la décroissance de cette fonction au long des trajectoires du système (et donc qui garantissent la stabilité). Ces conditions imposent une certaine structure au problème de synthèse et réduisent les degrés de liberté, mais, en même temps, simplifient le développement des stratégies convexes, comme illustré dans [53, 54].

Les contrôleurs présentés dans le Chapitre 3 exigent la connaissance de l'état complet du système, ce qui représente une limitation quant à leur utilisation dans la pratique. Le Chapitre 4 propose une solution pour dépasser cette limitation, basée sur l'utilisation d'un observateur de Luenberger. Les résultats obtenus présentent des avantages par rapport à la réduction du dépassement de la sortie du système, même si le prix à payer est un contrôleur d'ordre plus élevé et l'absence des garanties sur le taux de convergence en t .

Le Chapitre 5 associe les résultats génériques du Chapitre 2 et les contrôleurs hybrides structurés du Chapitre 3 pour présenter la synthèse convexe multi-objectif d'un contrôleur hybride qui prend en compte le gain t - \mathcal{L}_2 et le taux de convergence en t . Les résultats du Chapitre 5 montrent que les contrôleurs hybrides pourraient représenter un grand avancement dans le domaine du contrôle multi-objectif. Même si les résultats sont donnés pour le cas du retour d'état, l'étude donne également quelques résultats préliminaires pour le cas plus compliqué du retour de sortie hybride.

Les résultats donnés dans le Chapitre 4 ne sont pas encore applicables à la synthèse multi-objectif illustrée dans le Chapitre 5. Seule la plus simple des schémas hybrides à retour de sortie est utilisée pour les simulations, dont les paramètres sont obtenus sans utiliser une stratégie de synthèse optimale. Dans ce cas, l'analyse montre qu'à la fois le gain t - \mathcal{L}_2 et le taux de convergence

en t sont moins performants. Cependant, les simulations montrent également que le schéma de contrôle hybride quasi-multi-objectif¹ à retour de sortie pourrait donner des meilleurs résultats que le cas optimal multi-objectif linéaire.

Comme travaux futurs nous mentionnons les études sur la prise en compte des saturations des actionneurs. Les simulations montrent souvent que, pour les contrôleurs hybrides, les pics obtenus sont moins grands que les contrôleurs linéaires classiques (même dans le cas des du retour de sortie hybride). Il semble alors naturel de se poser des questions sur le comportement des contrôleurs hybrides en présence des saturations. Pour ce cas nous avons développé des conditions d'analyse de la stabilité, qui prennent la forme des inégalités matricielles si une fonction de Lyapunov quadratique est considérée. Cependant, de manière similaire à [62], nous obtenons des LMI pour des résultats globaux et des BMI pour les résultats régionaux à cause du fait que les ensembles du flux et du saut doivent être pris en compte, ce qui empêche l'utilisation des changements de coordonnées de la théorie classique. En imposant une structure sur la fonction de Lyapunov nous avons développé des conditions suffisantes pour le design d'un contrôleur anti-windup pour une classe de schémas de contrôle hybride. Ce résultat préliminaire peut être trouvé dans [23].

1. L'attribue *quasi* est utilisé pour renforcer l'idée que l'observateur est choisi *a posteriori* sans avoir un critère de choix optimal.

Bibliographie

- [1] K.J. Åström. Limitations on Control System Performance. *European Journal of Control*, 6(1) :2–20, 2000.
- [2] R. Bambang, E. Shimemura, and K. Uchida. Mixed $\mathcal{H}_2/\mathcal{H}_\infty$ control with pole placement : state feedback case. In *Proceedings of the 1993 American Control Conference*, pages 2777–2779, San Francisco, CA, 1993.
- [3] O. Beker, C. Hollot, and Y. Chait. Fundamental Properties of Reset Control Systems. *Automatica*, 40(6) :905–915, 2004.
- [4] O. Beker, C.V. Hollot, and Y. Chait. Plant with an Integrator : an Example of Reset Control Overcoming Limitations of Linear Feedback. *IEEE Transactions on Automatic Control*, 46(11) :1797–1799, November 2001.
- [5] H.W. Bode. *Network Analysis and Feedback Amplifier Design*. Van Nostrand, New York, NY, USA, 1945.
- [6] S.P. Boyd, L. El Ghaoui, E. Feron, and V. Balakrishnan. *Linear Matrix Inequalities in System and Control Theory*. Society for Industrial and Applied Mathematics, 1994.
- [7] S.P. Boyd and L. Vandenberghe. *Convex Optimization*. Cambridge University Press, New York, NY, USA, 2004.
- [8] R.W. Brockett. Asymptotic Stability and Feedback Stabilization. In *Differential Geometric Control Theory.*, volume 27 of *Progress in Mathematics.*, pages 181–191. Birkhäuser, 1983.
- [9] C. Cai and A.R. Teel. Characterizations of Input-to-state Stability for Hybrid Systems. *Systems & Control Letters*, 58(1) :47–53, 2009.
- [10] C. Cai, A.R. Teel, and R. Goebel. Converse Lyapunov Theorems and Robust Asymptotic Stability for Hybrid Systems. In *Proceedings of the 2005 American Control Conference*, pages 12–17, Portland (OR), USA, June 2005.
- [11] C. Cai, A.R. Teel, and R. Goebel. Smooth Lyapunov Functions for Hybrid Systems, Part I : Existence is Equivalent to Robustness. *IEEE Transactions on Automatic Control*, 52(7) :1264–1277, 2007.
- [12] C. Cai, A.R. Teel, and R. Goebel. Smooth Lyapunov Functions for Hybrid Systems, Part II : (Pre)Asymptotically Stable Compact Sets. *IEEE Transactions on Automatic Control*, 53(3) :734–748, 2008.
- [13] A. Chaillet and A. Loria. Uniform Semiglobal Practical Asymptotic Stability for Non-Autonomous Cascaded Systems and Applications. *Automatica*, 44(2) :337–347, 2008.
- [14] B.M. Chen, Z. Lin, and Y. Shamash. *Linear Systems Theory : a Structural Decomposition Approach*. Birkhäuser, Boston, 2004.
- [15] Q. Chen. *Reset Control Systems : Stability, Performance and Application*. PhD thesis, University of Massachusetts, Amherst (MA), USA, 2000.
- [16] M. Chilali and P. Gahinet. H_∞ Design with Pole Placement Constraints : an LMI Approach. *IEEE Transactions on Automatic Control*, 41 :358–367, 1996.
- [17] M. Claeys, D. Arzelier, D. Henrion, and J.-B. Lasserre. Moment LMI approach to LTV impulsive control. In *Proceedings of the 52nd IEEE Conference on Decision and Control*, December 2013, to appear.

- [18] J.-M. Coron, L. Praly, and A.R. Teel. Feedback Stabilization of Nonlinear Systems : Sufficient Conditions and Lyapunov and Input-Output Techniques. In *Trends in Control : A European Perspective*, pages 293–348. Springer, 1995.
- [19] F. Fichera. *Lyapunov techniques for a class of hybrid systems and reset controller syntheses for continuous-time plants*. PhD thesis, ISAE, France, 2013.
- [20] F. Fichera, C. Prieur, S. Tarbouriech, and L. Zaccarian. A Convex Hybrid \mathcal{H}_∞ Synthesis with Guaranteed Convergence Rate. In *Proceedings of the 51st Conference on Decision and Control*, pages 4217–4222, Maui (HI), USA, 2012.
- [21] F. Fichera, C. Prieur, S. Tarbouriech, and L. Zaccarian. Improving the Performance of Linear Systems by Adding a Hybrid Loop : the Output Feedback Case. In *Proceedings of the 2012 American Control Conference*, pages 3192–3197, Montreal, Canada, 2012.
- [22] F. Fichera, C. Prieur, S. Tarbouriech, and L. Zaccarian. Using Luenberger Observers and Dwell-time Logic for Feedback Hybrid Loops in Continuous-time Control Systems. *International Journal of Robust and Nonlinear Control*, 23 :1065–1086, 2013.
- [23] F. Fichera, C. Prieur, S. Tarbouriech, and L. Zaccarian. In *Static Anti-windup Scheme for a Class of Homogeneous Dwell-time Hybrid Controllers.*, Zurich, Switzerland, 2013, to appear.
- [24] F. Forni, S. Galeani, D. Nešić, and L. Zaccarian. Lazy Sensors for the Scheduling of Measurements Samples Transmission in Linear Closed Loops Over Networks. In *Proceedings of the 49th IEEE Conference on Decision and Control*, pages 6469–6474, Atlanta (GA), USA, December 2010.
- [25] B.A. Francis. *A Course in H_∞ Control Theory*. 88, 1987.
- [26] G. Franklin, J.D. Powell, and A. Emami-Naeini. *Feedback Control of Dynamic Systems, 6Ed*. Prentice Hall, 2009.
- [27] J.S. Freudenberg and D.P. Looze. Right Half Plane Poles and Zeros and Design Trade-offs in Feedback Systems. *IEEE Transactions on Automatic Control*, 30(6) :555–565, 1985.
- [28] J.S. Freudenberg and D.P. Looze. A Sensitivity Trade-off for Plants with Time Delay. *IEEE Transactions on Automatic Control*, 32(2) :99–104, 1987.
- [29] J. Geromel, P. Peres, and J. Bernussou. On a Convex Parameter Space Method for Linear Control Design of Uncertain Systems. *SIAM Journal on Control and Optimization*, 29(2) :381–402, 1991.
- [30] R. Goebel, R.G. Sanfelice, and A.R. Teel. Hybrid Dynamical Systems. *IEEE Control Systems Magazine*, 29(2) :28–93, April 2009.
- [31] R. Goebel, R.G. Sanfelice, and A.R. Teel. *Hybrid Dynamical Systems : Modeling, Stability and Robustness*. Princeton University Press, 2012.
- [32] Y. Guo, W. Gui, C. Yang, and L. Xie. Stability analysis and design of reset control systems with discrete-time triggering conditions. *Automatica*, 48(3) :528–535, 2012.
- [33] J.P. Hespanha, D. Liberzon, and A.S. Morse. Hysteresis-based Switching Algorithms for Supervisory. *Automatica*, 39(2) :263–272, 2004.
- [34] J.P. Hespanha and A.S. Morse. Stabilization of Nonholonomic Integrators via Logic-based Switching. *Automatica*, 35(3) :385–393, 1999.
- [35] J.P. Hespanha and A.S. Morse. Switching Between Stabilizing Controllers. *Automatica*, 38 :1905–1971, 2002.

- [36] C. Hollot, O. Beker, Y. Chait, and Q. Chen. On Establishing Classic Performance Measures for Reset Control Systems. In *Perspectives in Robust Control.*, volume 268 of *Lecture Notes in Control and Information Sciences.*, pages 123–147. Springer London, 2001.
- [37] M. Jungers and J. Daafouz. Guaranteed Cost Certification for Discrete-Time Linear Switched Systems With a Dwell Time. *IEEE Transactions on Automatic Control*, 58(3) :768–772, 2013.
- [38] P. Kapasouris, M. Athans, and G. Stein. Design of Feedback Control Systems for Stable Plants with Saturating Actuators. In *Proceedings of the 27th IEEE Conference on Decision and Control*, pages 469–479, Austin, TX, 1988.
- [39] H.K. Khalil. *Nonlinear Systems*. Prentice Hall, PTR, 2002.
- [40] M. Krstić, I. Kanellakopoulos, and P.V. Kokotović. *Nonlinear and Adaptive Control Design*, volume 8. John Wiley & Sons New York, 1995.
- [41] D. Liberzon. *Switching in Systems and Control*. Birkhäuser, 2003.
- [42] D.G. Luenberger. Observers for Multivariable Systems. *IEEE Transactions on Automatic Control*, 11(2) :190–197, 1966.
- [43] A.M. Lyapunov. The General Problem of the Stability of Motion. *International Journal of Control*, 55(3) :531–534, 1992.
- [44] R.H. Middleton. Trade-offs in Linear Control System Design. *Automatica*, 27(2) :281–292, 1991.
- [45] D. Nešić, A.R. Teel, G. Valmorbida, and L. Zaccarian. On Finite Gain \mathcal{L}_p Stability for Hybrid Systems. In *4th IFAC Conference on Analysis and Design of Hybrid Systems (ADHS)*, pages 418–423, Eindhoven, The Netherlands, June 2012.
- [46] D. Nešić, A.R. Teel, G. Valmorbida, and L. Zaccarian. Finite-Gain \mathcal{L}_p Stability for Hybrid Dynamical Systems. *Automatica*, 2013, on-line.
- [47] D. Nešić, A.R. Teel, and L. Zaccarian. Stability and Performance of SISO Control Systems with First Order Reset Elements. *IEEE Transactions on Automatic Control*, 56(11) :2567–2582, 2011.
- [48] D. Nešić, L. Zaccarian, and A.R. Teel. Stability Properties of Reset Systems. *Automatica*, 44(8) :2019–2026, 2008.
- [49] C. De Persis and F. Mazenc. Stability of Quantized Time-delay Nonlinear Systems : a Lyapunov–Krasowskii-functional Approach. *Mathematics of Control, Signals, and Systems*, 21(4) :337–370, 2010.
- [50] F.R. Poursafei, J.P. Hespanha, and G. Stewart. Quadratic Optimization for Controller Initialization in Multivariable Switching Systems. In *Proceedings of the 2010 American Control Conference*, pages 2511–2516, Baltimore, Maryland, USA, June 2010.
- [51] C. Prieur. Asymptotic Controllability and Robust Asymptotic Stabilizability. *SIAM Journal on Control and Optimization*, 43(5) :1888–1912, 2005.
- [52] C. Prieur, S. Tarbouriech, and L. Zaccarian. Guaranteed Stability for Nonlinear Systems by Means of a Hybrid Loop. In *Proceedings of the 8th IFAC Symposium on Nonlinear Control Systems (NOLCOS)*, pages 72–77, Bologna, Italy, September 2010.
- [53] C. Prieur, S. Tarbouriech, and L. Zaccarian. Improving the Performance of Linear Systems by adding a Hybrid Loop. In *18th IFAC World Congress*, pages 6301–6306, Milano, Italy, September 2011.
- [54] C. Prieur, S. Tarbouriech, and L. Zaccarian. Lyapunov-based hybrid loops for stability and performance of continuous-time control systems. *Automatica*, 49(2) :577–584, 2013.

-
- [55] H.L. Royden and P. Fitzpatrick. *Real Analysis*, volume 4. Prentice Hall New York, 1988.
- [56] E.P. Ryan. On Brockett's Condition for Smooth Stabilizability and its Necessity in a Context of Nonsmooth Feedback. *SIAM Journal on Control and Optimization*, 32(6) :1597–1604, 1994.
- [57] A. Satoh. State Feedback Synthesis of Linear Reset Control with \mathcal{L}_2 Performance Bound via LMI Approach. In *IFAC 18th World Congress*, pages 5860–5865, Milan, Italy, 2011.
- [58] C. Scherer, P. Gahinet, and M. Chilali. Multiobjective Output-feedback Control via LMI Optimization. *IEEE Transactions on Automatic Control*, 42(7) :896–911, 1997.
- [59] G.N. Silva and R.B. Vinter. Measure Driven Differential Inclusions. *Journal of Mathematical Analysis and Applications*, 202(3) :727–746, 1996.
- [60] G. Stein. Respect the Unstable. *IEEE Control Systems*, 23(4) :12–25, 2003.
- [61] D.D. Swonder. Control of Systems Subject to Sudden Change in Character. *Proceedings of the IEEE*, 64(8) :1219–1225, 1976.
- [62] S. Tarbouriech, T. Loquen, and C. Prieur. Anti-windup Strategy for Reset Control Systems. *International Journal of Robust and Nonlinear Control*, 21(10) :1159–1177, 2011.
- [63] A.R. Teel, R.M. Murray, and G.C. Walsh. Non-holonomic Control Systems : from Steering to Stabilization with Sinusoids. *International Journal of Control*, 62(4) :849–870, 1995.
- [64] T. Yang. *Impulsive Control Theory*, volume 272. Springer, 2001.
- [65] L. Zaccarian, D. Nešić, and A.R. Teel. First Order Reset Elements and the Clegg Integrator Revisited. In *Proceedings of the 2005 American Control Conference*, pages 563–568, vol. 1, Portland (OR), USA, June 2005.
- [66] L. Zaccarian, D. Nešić, and A.R. Teel. Analytical and Numerical Lyapunov Functions for SISO Linear Control Systems with First-order Reset Elements. *International Journal of Robust and Nonlinear Control*, 21 :1134–1158, 2011.